

Spring 5-13-2017

Divergent Responses of Larval and Juvenile Blue Mussels to Low Salinity Exposure

Melissa A. May

University of Maine, melissa.may@maine.edu

Follow this and additional works at: <http://digitalcommons.library.umaine.edu/etd>

 Part of the [Cellular and Molecular Physiology Commons](#), [Integrative Biology Commons](#), [Marine Biology Commons](#), [Molecular Biology Commons](#), and the [Other Genetics and Genomics Commons](#)

Recommended Citation

May, Melissa A., "Divergent Responses of Larval and Juvenile Blue Mussels to Low Salinity Exposure" (2017). *Electronic Theses and Dissertations*. 2650.

<http://digitalcommons.library.umaine.edu/etd/2650>

This Open-Access Dissertation is brought to you for free and open access by DigitalCommons@UMaine. It has been accepted for inclusion in Electronic Theses and Dissertations by an authorized administrator of DigitalCommons@UMaine.

**DIVERGENT RESPONSES OF LARVAL AND JUVENILE BLUE MUSSELS TO
LOW SALINITY EXPOSURE**

By

Melissa A. May

B.S. Northern Arizona University, 2004

M.S. University of San Diego, 2008

A DISSERTATION

Submitted in Partial Fulfillment of the

Requirements for the Degree of

Doctor of Philosophy

(in Marine Biology)

The Graduate School

The University of Maine

May 2017

Advisory Committee:

Paul Rawson, Associate Professor of Marine Sciences, Advisor

Sara Lindsay, Associate Professor of Marine Sciences

Malcolm Shick, Professor Emeritus of Zoology and Oceanography

Rebecca Van Beneden, Professor of Biochemistry and Marine Sciences

Nikki Adams, Professor of Biological Sciences, California Polytechnic State

University

© 2017 Melissa A. May

All Rights Reserved

**DIVERGENT RESPONSES OF LARVAL AND JUVENILE BLUE MUSSELS TO
LOW SALINITY EXPOSURE**

By Melissa A. May

Dissertation Advisor: Dr. Paul Rawson

An Abstract of the Dissertation Presented
in Partial Fulfillment of the Requirements for the
Degree of Doctor of Philosophy
(in Marine Biology)
May 2017

In this study, we compared the osmotic stress response of larval and juvenile blue mussels (*Mytilus edulis*) at the transcriptomic, metabolomic, and whole organism levels. Blue mussels inhabit coastal areas, where they face climate-induced reductions in nearshore salinity. Despite their ecological and economic importance, scientists do not fully understand the underlying transcriptomic and cellular mechanisms of the osmotic stress response in blue mussels or how the ability to respond to stress changes throughout development. Blue mussels spend the first weeks of life developing through several larval stages in the plankton. These early life history stages are more vulnerable to environmental stress than juvenile or adult mussels, yet these stages are grossly understudied. Thus, an increased knowledge of how mussels at all developmental stages cope with low salinity is imperative for predicting how climate change will affect the distribution of *M. edulis*.

In a series of experiments, we evaluated adjustments of molecular, cellular, and physiological processes in larval and juvenile blue mussels during short-term, low salinity exposure to elucidate stage-specific divergence in the osmotic stress response.

We found that larval mussels differ from juveniles in the composition of their metabolome and in the differential expression of genes involved in the stress response. These differences in the larval response to low salinity exposure likely play a role in the increased susceptibility of these stages to stress and suggest that larvae may need to expend more energy relative to juvenile or adult mussels to mount a response.

Additionally, we evaluated the effects of larval stress on later developmental stages and found that larval stress carries through metamorphosis and yields smaller juvenile mussels, potentially affecting the subsequent growth and size distributions of adult mussels. While larval exposure to low salinity generally had negative impacts on juvenile growth, there was evidence the previous exposure to stress may condition juvenile mussels for future low salinity events, depending on the timing of exposure. More studies on larval tolerance and the impacts of larval stress on juvenile fitness will be necessary for making accurate predictions of the effects of climate change on *M. edulis* distribution and abundance.

ACKNOWLEDGMENTS

I have been incredibly blessed in the tremendous support I have received during my time at the University of Maine. I am extremely grateful for the many people contributed to my research projects, provided moral support, and offered their friendship. The work detailed in this dissertation could not be completed without many of these people, while others helped to make this daunting and difficult process a little more bearable. So, thank you!

Above all, I would like to express my gratitude to my Ph.D. advisor, Paul Rawson. Most graduate students are not fortunate enough to have an advisor that is a great as you have been, Paul. Thank you for mentoring me, for always advocating for me, for treating me with respect, and for being an overall good human. I appreciate the help and advice you have given me over the past 6 years as well as the time you put aside to make sure that I was making progress, that I had the tools I needed to succeed, and even to pick me up for school when I needed a ride. It has been a pleasure to work with you (and for you), so thank you for letting me be your graduate student.

I am exceptionally lucky to not only have this level of support from my advisor, but from my entire advisory committee, Sara Lindsay, Becky Van Beneden, Malcolm Shick, and Nikki Adams. You have all been incredibly helpful and encouraging throughout this process and I have learned a great deal from each of you. Sara, thank you for always being available for my questions or if I needed to talk, for letting me use your equipment, and for helping take care of my cats. Becky, thank you for letting me use your lab, your equipment, and your lab supplies, for letting me TA for you, for taking me to Zumba®, and for everything you do for the graduate students. Malcolm, thank you for

teaching me physiology, for leading by example of how to be a dedicated and enthusiastic instructor, for providing comments and insight for my work, and for sticking around long enough to be on my committee. And last, but not least, Nikki; thank you for agreeing to be on my committee (even though we had never met!), for being available to talk about my research, and for helping make my transition to San Luis Obispo easier. Words cannot express how grateful I am to you all for providing your assistance and knowledge throughout this process and for facilitating my success.

I would also like to thank many of the faculty and staff at the University of Maine who have helped me complete portions of this dissertation. Karl Bishop, thank you for taking the time to train me to use NMR, for helping me run samples, for your help analyzing and writing parts of this dissertation, and for always being willing to make my project better. Thanks to the Chemistry Department for allowing me to use their NMR equipment and Dave Labrecque for training me and for helping me fix the problems I encountered running my NMR experiments. Thank you, Seth Tyler and Kelly Edwards, for training me in microscopy and for providing me with supplies, equipment, and advice for many of my projects. Mary Tyler, thank you for training me in histology and for allowing me to use your lab, your stains, and your equipment – you are a wonderful human. Thanks to Benildo de los Reyes for helping me analyze my microarray data and Bob Cashion for teaching me how to do protein modeling. Thanks to Remi Gratacap, Bill Halteman, and Keith Evans for their advice on statistical analyses and Michelle Goode, Clarissa Henry, and Remy Babich for their advice on *in situ* hybridizations. And, Maura Thomas and Irv Kornfield, thank you for giving me lab equipment in a pinch and for always being helpful and encouraging.

Many of my larval experiments were conducted at the Darling Marine Center and would not have been possible without the help of the DMC faculty, staff, and students. Thank you to the hatchery staff, Mick Devin, Dave Cheney, and Tyler Hild, for helping rear larvae and providing algae for my larval cultures. I would also like to thank Larry Mayer, Mary Jane Perry, Kathleen Thornton, Rhian Waller, and Mike Horst, who generously allowed me to use their lab equipment and space. Thank you to Linda Healy and Tim Miller for helping me coordinate logistics of working at the DMC and for providing support during my stay. And, finally, thank you to Alison Culkin, Antonia Barela, and Steven Wilkinson for sitting in a cold room with me for hours on end to help run my experiments.

Numerous other people have assisted me, academically, financially, or mentally during my time at the University of Maine. Thank you to the School of Marine Sciences and the Graduate Student Government for providing support for my research. Thank you Jody Feero and Sue Thibodeau for your help – the department would not run and graduate students would be lost without you! Thanks to David Cox and Patty Singer for their support processing my many orders and sequencing my samples. And thanks to all the other members of the faculty, especially Mark Wells and WGE, for your encouragement, support, and comradery. Thank you to my lab members, including Erin Macro, Katelyn Hunt, Courtney Norman, Karen Pianka, Tyler Carrier, Samantha Holmes, Samantha Silverbrand, Emily Miller, Hanna Deon, Cheyenne Adams, and Lauren Rice, for keeping me sane and making me laugh. I would also like to thank Cynthia Riginos and Brent Lockwood for providing me with sequence information and Chris Langdon, Travis Oja, Blaine Schoolfield, and Catalina Sea Ranch for sending me mussels.

There were many people throughout my academic career that have helped me get to this point. Thank you, Xavier College Preparatory, for providing me with a fantastic education and for teaching us that it was okay to be strong, confident, and intelligent women. Thank you, Mr. Austin, for teaching me how to write. Thanks to Steve Shuster for showing me how interesting invertebrates can be, for mentoring me and for providing me with opportunities throughout my undergraduate career. Thank you to my master's thesis committee—Jim Sumich, Hugh Ellis, and Mary Sue Lowry—for furthering my education and helping to training me to become a good scientist. And thank you Pete Raimondi, Jonathon Stillman, and Anne Todgham for allowing me to work in your labs and for giving me advice that helped me get into this Ph.D. program.

I am also fortunate to have a strong support group of community members, graduate students, and friends that have been an important part of my graduate experience. Many thanks to my water polo team and my CrossFit Black Bear family for keeping me active and allowing me to have fun, even when my stress levels were high. Thanks to Bob Cutler at Family Dog for all of the large iced coffees and food and Thai Kitchen for always delivering my Thai food with a smile. Thank you to all of the graduate students for good conversations and company, and extra thanks to Ali Chase, Karen Stamieszkin, and Megan Switzer for being great friends. Thanks to my friends in New England who have treated me like family and helped make the transition to the East Coast a little easier – Christine Veazey and Al Fletcher, Kelly Gardner and Arthur Dickey (and family), Amber Michaud, and the entire Roy family. Thank you to my lifelong friends, Dawn Durante, Sarah Coble, Ashley Donovan, Neal Skapura, Valerie Fong, Adam Boroian, and Christine Burchfield for being fantastic people who came to

visit or let me visit them and for listening to me talk about my graduate school woes for the past six years – I love you all. Christopher Roy, thank you for helping run my experiments, for letting me be part of your family, and for the support and encouragement you have given me over the past six years.

None of this would have been possible without the love and support of my family. Thank you to my mom and dad for providing me with any opportunity they could to further my education and my interest in marine science. Mom, I also appreciate you flying to New Orleans to watch me give a talk at a conference and for visiting me in Maine. Thank you to my aunts and uncles who sent me gifts (Sport and Shy) or who took me in on holidays and fed me (Colleen and Will) and thank you to my wonderful grandma, Jeanne, for taking care of me when I am at home and for always being interested in my research and my progress in school. And, finally, I would like to thank my best friend and my sister; Steph, you know why.

TABLE OF CONTENTS

ACKNOWLEDGEMENTS	iii
LIST OF TABLES	xiii
LIST OF FIGURES	xv
LIST OF EQUATIONS	xviii
LIST OF ABBREVIATIONS.....	xix
Chapter	
1. INTRODUCTION	1
1.1. Background and Rationale.....	1
1.2. Project Overview	5
2. CARRYOVER EFFECTS FROM LARVAL EXPOSURE TO REDUCED SALINITY ON GROWTH OF JUVENILE BLUE MUSSELS (<i>MYTILUS EDULIS</i>)	7
2.1 Abstract.....	7
2.2 Introduction.....	8
2.3 Methods.....	10
2.3.1. Mussel Collection and Larval Culture	10
2.3.2. Acute Exposure to Low Salinity	12
2.3.3. Juvenile Repeated-Exposure Experiment	13
2.3.4. Size Measurements and Data Analysis	14

4. COMPARING CELLULAR RESPONSES OF LARVAL AND JUVENILE BLUE MUSSELS (<i>MYTILUS EDULIS</i>) TO LOW SALINITY EXPOSURE.....	73
4.1 Abstract.....	73
4.2 Introduction.....	74
4.3 Methods.....	77
4.3.1 Preliminary Microarray Study	77
4.3.2 Marker Development	82
4.3.3 Salinity Experiments on Juveniles	83
4.3.4 Salinity Experiments on Larvae.....	84
4.3.5 Ammonia Measurements	85
4.3.6 Gene Expression Studies Using qPCR	86
4.3.7 Data Analysis	89
4.4 Results.....	89
4.4.1. Microarray Analysis.....	89
4.4.2. qPCR-based Analysis of <i>BHMT</i> and <i>TAUT</i> Expression.....	90
4.4.3. NH ₃ Excretion and O ₂ Consumption	93
4.5 Discussion.....	101
4.5.1. Transcriptional Response to Low Salinity.....	102
4.5.2. Organismal Response to Low Salinity.....	106
5. UNDERSTANDING THE ROLE OF CALMODULIN AND OTHER CALMODULIN-LIKE GENES IN THE ACUTE HYPOOSMOTIC STRESS RESPONSE OF THE BLUE MUSSEL, <i>MYTILUS EDULIS</i>	111
5.1 Abstract.....	111

5.2 Introduction.....	112
5.3 Methods.....	115
5.3.1 Sequencing and Marker Development.....	115
5.3.2 Salinity Challenge Experiments.....	116
5.3.3 Gene Expression Studies.....	117
5.3.4 <i>In Situ</i> Hybridizations	117
5.3.5 Data Analysis	122
5.4 Results.....	123
5.4.1 Structural Analysis of <i>CaM</i> and <i>CAML</i> Genes.....	123
5.4.2 Baseline Expression of <i>CaM</i> and <i>CAML</i> Genes	127
5.4.3 <i>CaM</i> and <i>CAML</i> Expression During Hypoosmotic Exposure	133
5.5 Discussion.....	142
6. ORNITHINE METABOLISM AND THE OSMOTIC STRESS RESPONSE: A COMPARATIVE STUDY OF CONGENERIC SPECIES.....	149
6.1 Abstract.....	149
6.2 Introduction.....	150
6.3 Methods.....	153
6.3.1 Hyposalinity Experiments.....	153
6.3.2 Hypersalinity Experiments.....	155
6.3.3 Gene Expression Studies.....	155
6.3.4 Ornithine Aminotransferase Activity Assays	157
6.3.5 Data Analysis	158
6.4 Results.....	159

6.4.1.	Regulation of Ornithine in Hyposaline-Challenged <i>M. edulis</i>	159
6.4.2.	Ornithine Regulation in Congeners Exposed to Low Salinity.....	164
6.4.3.	Ornithine Regulation During Hypersalinity Exposure	167
6.5	Discussion.....	170
7.	SUMMARY AND CONCLUSIONS	176
	REFERENCES	179
	APPENDICES	198
	Appendix A. Supplemental Material for Chapter 2	198
	Appendix B. Supplemental Material for Gene Expression Studies.....	201
	Appendix C. Preliminary Hypoosmotic Stress Experiments	243
	BIOGRAPHY OF THE AUTHOR.....	256

LIST OF TABLES

Table 2.1.	ANOVA results for larval exposure on size at metamorphosis.....	19
Table. 2.2.	ANOVA results for veliger exposure on juvenile shell area	21
Table 2.3.	ANOVA results for veliger exposure on specific growth rate.....	25
Table 2.4.	ANOVA results for pediveliger exposure on juvenile shell area	27
Table 2.5.	ANOVA results for pediveliger exposure on specific growth rate.....	31
Table 3.1.	Chemical shifts of key osmolytes detected by 1D ¹ H NMR.....	46
Table 3.2.	Table of common metabolites identified in <i>Mytilus edulis</i>	49
Table 3.3.	Relative concentrations of free amino acids in larval mussels	55
Table 3.4.	Concentrations of FAAs in the tissues of juvenile mussels	57
Table 3.5.	FAA concentrations in larval <i>M. edulis</i> during low salinity exposure	59
Table 4.1.	Information on primers used for qPCR.....	88
Table 4.2.	<i>BHMT</i> ANOVA results.....	92
Table 4.3.	<i>TAUT</i> ANOVA results	95
Table 5.1.	Primer sets used in the <i>CaM</i> and <i>CAML</i> qPCR assays	118
Table 5.2.	Primer sets used to target genes for <i>in situ</i> hybridizations.....	120
Table 6.1.	Primer sets used in the <i>OAT</i> and <i>ODC</i> qPCR assays.....	156
Table A.1.	Supplemental table containing complete dataset for peaks identified in <i>M. edulis</i>	198
Table B.1.	Differentially expressed genes in salinity challenged <i>M. edulis</i> and <i>M. trossulus</i> from the 2009 microarray study	208
Table B.2.	Table of primers developed for <i>BHMT</i> and <i>TAUT</i>	225
Table B.3.	Table of primers developed for <i>40S</i>	226

Table B.4.	Table of primers developed for <i>OAT</i>	227
Table B.5.	Table of primers developed for <i>ODC</i>	228
Table B.6.	Table of primers developed for <i>CaM</i> , <i>CAML1</i> , and <i>CAML2</i>	229
Table B.7.	Sequencing and qPCR primers for <i>DPT</i> , <i>SCBP</i> , and <i>TCTEX</i>	233
Table C.1.	Preliminary data on concentrations of FAAs in veliger mussels during low salinity treatment	254
Table C.2.	Preliminary data on concentrations of FAAs in pediveliger mussels during low salinity treatment	255

LIST OF FIGURES

Figure 1.1	Life cycle of <i>M. edulis</i>	4
Figure 2.1.	Photomicrograph of a juvenile <i>M. edulis</i>	15
Figure 2.2.	Effects of low salinity treatment on size at metamorphosis	18
Figure 2.3.	Effects of veliger low-salinity exposure on size at 35 dpm	20
Figure 2.4.	Veliger-exposed size at metamorphosis versus at 35 dpm	22
Figure 2.5.	Effects of veliger low-salinity exposure on the specific growth rate.....	24
Figure 2.6.	Effects of pediveliger low-salinity exposure on size at 35 dpm	26
Figure 2.7.	Pediveliger-exposed size at metamorphosis versus 35 dpm	28
Figure 2.8.	Effects of pediveliger low-salinity exposure on specific growth rate.....	29
Figure 3.1.	Representative 2D-TOCSY spectrum	50
Figure 3.2.	Representative ¹ H NMR spectra	51
Figure 3.3.	Relative concentrations of six intracellular osmolytes	54
Figure 4.1.	Differentially expressed genes potentially involved in cell volume regulation	81
Figure 4.2.	<i>BHMT</i> expression in <i>M. edulis</i> during low salinity exposure	91
Figure 4.3.	<i>TAUT</i> expression in <i>M. edulis</i> during low salinity exposure	94
Figure 4.4.	NH ₃ excretion in juvenile mussels during low salinity exposure	97
Figure 4.5.	O ₂ consumption in juvenile mussels during low salinity exposure	98
Figure 4.6.	Ammonia excretion in veligers exposed to low salinity	99
Figure 4.7.	Ammonia excretion in pediveligers exposed to low salinity	100
Figure 5.1.	Comparison of <i>M. edulis</i> and human calmodulin	124
Figure 5.2.	Multiple sequence alignment of Mytilid <i>CaM</i>	125

Figure 5.3	Multiple sequence alignment of invertebrate calmodulins	126
Figure 5.4.	Comparison of <i>M. edulis</i> CaM and CAML1 predicted proteins.....	128
Figure 5.5.	Comparison of <i>M. edulis</i> CaM and CAML2 predicted proteins.....	129
Figure 5.6.	Visualization of <i>CaM</i> expression in the gills of <i>M. edulis</i>	130
Figure 5.7.	Visualization of <i>CAML1</i> in <i>M. edulis</i> gill tissue.....	131
Figure 5.8.	Visualization of <i>CAML2</i> in <i>M. edulis</i> gill tissue.....	132
Figure 5.9.	Baseline <i>CaM</i> expression in <i>M. edulis</i>	134
Figure 5.10.	Baseline <i>CAML1</i> expression in juvenile mussels	135
Figure 5.11.	Baseline <i>CAML2</i> expression in <i>M. edulis</i>	136
Figure 5.12.	<i>CaM</i> expression in <i>M. edulis</i> during low-salinity exposure	137
Figure 5.13.	<i>CAML1</i> expression in <i>M. edulis</i> during low-salinity exposure.....	139
Figure 5.14	<i>CAML2</i> expression in <i>M. edulis</i> during low-salinity exposure.....	141
Figure 6.1.	Overview of ornithine metabolism	152
Figure 6.2.	<i>OAT</i> expression in hyposalinity-challenged <i>M. edulis</i>	160
Figure 6.3.	<i>ODC</i> expression in <i>M. edulis</i> during low-salinity exposure.....	161
Figure 6.4.	Ornithine aminotransferase activity in <i>M. edulis</i>	162
Figure 6.5.	<i>OAT</i> expression in the gill of congeneric mussels exposed to low salinity.....	165
Figure 6.6.	<i>ODC</i> expression in the gill of congeneric mussels exposed to low salinity.....	166
Figure 6.7.	<i>OAT</i> expression in the gill of congeneric mussels exposed to high salinity.....	168

Figure 6.8.	<i>ODC</i> expression in the gill of congeneric mussels exposed to high salinity.....	169
Figure B.1.	Multiple sequence alignment of <i>BHMT</i> in bivalves	230
Figure B.2.	<i>BHMT</i> sequence information from <i>M. edulis</i>	231
Figure B.3.	Position of <i>TAUT</i> qPCR primers in the <i>M. galloprovincialis</i> coding sequence.....	232
Figure B.4.	<i>40S Ribosomal Protein</i> coding sequence from <i>M. californianus</i>	234
Figure B.5.	Sequence information for <i>OAT</i> from <i>M. edulis</i>	235
Figure B.6.	<i>ODC</i> sequencing primers in the <i>M. edulis</i> coding sequence	236
Figure B.7.	Position of <i>CaM</i> primers in the <i>M. edulis</i> coding sequence	237
Figure B.8.	Position of <i>CAML1</i> primers in the <i>M. edulis</i> coding sequence.....	238
Figure B.9.	Position of <i>CAML2</i> primers in the <i>M. edulis</i> coding sequence.....	239
Figure B.10.	Partial nucleotide and amino acid sequence for <i>DPT</i> in <i>M. edulis</i>	240
Figure B.11.	Partial nucleotide and amino acid sequence for <i>SCBP</i> in <i>M. edulis</i>	241
Figure B.12.	Partial nucleotide and amino acid sequence for <i>TCTEX</i> in <i>M. edulis</i>	242
Figure C.1.	Preliminary <i>BHMT</i> gene expression results.....	246
Figure C.2.	Preliminary <i>TAUT</i> gene expression results.....	247
Figure C.3.	Preliminary <i>OAT</i> gene expression results	248
Figure C.4.	Preliminary <i>ODC</i> gene expression results	249
Figure C.5.	Preliminary <i>CaM</i> gene expression results.....	250
Figure C.6.	Preliminary <i>CAML1</i> gene expression in the gill of juvenile mussels	251
Figure C.7.	Preliminary <i>CAML2</i> gene expression results.....	252
Figure C.8.	Preliminary <i>ICLN</i> gene expression results.....	253

LISTS OF EQUATIONS

Equation 1.	Specific Growth Rate.....	16
Equation 2.	Relative Quantification of Metabolites.....	45

LIST OF ABBREVIATIONS

18S	18 S ribosomal RNA gene
40S	40 S Small ribosomal subunit gene
AFDW	Ash-free dry weight
ANOVA	Analysis of variance
ARNA	Aminoallyl UTP–modified RNA
BHMT	Betaine-homocysteine <i>S</i> -methyltransferase gene
BLAST	Basic Local Alignment Search Tool
BP	Base pairs
BSA	Bovine serum albumin
CAM	Calmodulin gene
CAML1	Calmodulin-like 1 gene
CAML2	Calmodulin-like 2 gene
CDNA	Complementary DNA
CT	Cycle threshold
DIG	Digoxigenin
DPF	Days post-fertilization
DPM	Days post-metamorphosis
DPT	Dermatopontin
EF1A	Elongation-factor 1a gene
EST	Expressed sequence tag
ETOH	Ethanol
FAA	Free amino acid

GDH	Glutamate dehydrogenase
HPLC	High-performance liquid chromatography
ICLN	Chloride Nucleotide-Sensitive Channel 1A gene
NMR	Nuclear magnetic resonance spectroscopy
OAT	Ornithine aminotransferase gene
ODC	Ornithine decarboxylase gene
PCR	Polymerase chain reaction
QPCR	Real-time, quantitative PCR
RACE	Rapid amplification of cDNA ends
RNA	Ribonucleic acid
RFU	Relative fluorescence unit
P5C	Pyrroline-5-carboxylic acid
PBS	Phosphate buffered saline solution
PBS-T	Phosphate buffered saline solution with TWEEN
SCBP	Sarcoplasmic calcium binding protein
SE	Standard error of the mean
TAUT	Taurine transporter gene
TCTEX	T-complex testis-expressed gene
TM	Annealing or melt temperature
TOCSY	Total correlation spectroscopy
TSP	Trimethylsilylpropanoic acid
TUB	α -tubulin gene
UV-FSW	Ultra-violet sterilized, filtered seawater

CHAPTER 1

INTRODUCTION

1.1. Background and Rationale

Physiologists have traditionally studied organismal adaptations in form and function with respect to challenges posed by the environment. However, with the accelerating pace of global climate change there is a critical need for studies investigating whether species possess the innate physiological and genetic capacity to acclimate and adapt to long-term changes in the environment (Osovitz and Hofmann 2007, Jones et al. 2010, Somero 2011). Among marine species, those inhabiting the intertidal zone are particularly at risk from climate-change variability; due to the inherent high-stress nature of the habitat, intertidal species are already living under conditions close to their physiological limits (Tomanek and Helmuth 2002) and may become climate-change losers (Somero 2010).

Most climate change studies have focused on the physiology of marine organisms in response to increasing ocean temperatures or to ocean acidification (Somero 2011). Another less studied threat is shifting ocean salinity. Studies have documented a freshening of water in the upper 700 m of the ocean in the past 50 years, caused by anthropogenic activity (Antonov et al. 2002, Pierce et al. 2012). This freshening is expected to continue (Durack et al. 2012) and future changes in the hydrological cycle will undoubtedly lead to widespread variability in sea surface salinity. Understanding the capacity of marine organisms to respond to shifts in salinity will therefore be an important component in assessing the ability of species to adapt to climate change.

Four species of mytilid mussels, *Mytilus californianus*, *M. edulis*, *M. galloprovincialis*, and *M. trossulus* (Koehn 1991), are dominant members of coastal communities in North America where they have a profound impact on intertidal and subtidal community structure (Arribas et al. 2014). Mussels are keystone species; their dense aggregations offer essential refuges for small marine invertebrates leading to increased species diversity along coastlines (Tsuchiya and Nishihira 1985, Petes et al. 2008). They are also an important prey species for many organisms, including shore birds, sea stars, lobsters (Seed 1969), and humans, who value mussels for their economic importance. Additionally, blue mussels serve as bioindicators for detection of pollutants and trace metals in coastal systems (Phillips and Segar 1986).

Variation in salinity plays an important role in structuring the distribution of mussel species (Gardner and Thompson 2001). For example, *M. californianus* is a relatively stenohaline species restricted to open coast habitats on the Pacific coast of North America (Suchanek 1979), whereas *M. trossulus* is considered the most euryhaline of the congeners and can be found in habitats with highly variable salinities (Qiu et al. 2002, Braby and Somero 2006, Gardner and Thompson 2001). Thus, shifts in weather patterns due to climate change and associated changes in sea-surface salinities in coastal regions are likely to cause widespread shifts in the geographic range of Mytilid mussels and consequently altering community structure and function (Tsuchiya and Nishihira 1985) In addition, abrupt or prolonged changes in salinity are known to reduce growth (Qiu et al. 2002, Westerborn et al. 2002, Riisgård et al. 2012) and immune function (Bussell et al. 2008) in mussels. Species-specific differences in tolerance among mussel

congeners provides a unique opportunity to evaluate the evolutionary underpinnings of the response to low salinity stress.

Blue mussels have a complex life history, consisting of a benthic adult stage and a series of planktonic larval stages (Figure 1.1). Mytilid larvae spend a minimum of 3 w in the plankton before settling into adult mussel beds (Widdows 1991), though the duration of larval development can be increased if metamorphosis is delayed due to unfavorable environmental conditions (Bayne 1965). Mortality in mussel larvae is inherently high and increases considerably when larvae are stressed and larval duration is increased (Bayne 1965, Young 1990, Widdows 1991). Several studies have shown that larval stages are more sensitive than juvenile or adult mussels to changing environments (Hrs-Brenko and Calabrese 1969, Qiu et al. 2002, Gazeau et al. 2010, Rayssac et al. 2010), possibly resulting from high-energy demands for growth (Sprung 1984) or increased surface-area to volume ratio (Manahan 1983). Despite the importance of larval settlement to sustaining populations and, thereby dictating the distributions of adult mussels, little research has addressed the genetic and attendant physiological capacity of larvae to tolerate various environmental stressors.

Blue mussels, like many other marine invertebrates, are osmoconformers, meaning they remain isosmotic to seawater (Costa and Pritchard 1978, Davenport 1979). When fluctuations in environmental salinity occur, mussels mount an osmotic stress response (Kültz 2005) to prevent cellular damage from changes in their cell volume and salt concentration (Bowlus and Somero 1979, Yancey et al. 1982). Several studies have evaluated the physiological responses of adult blue mussels to low salinity exposure, although only a few have attempted to uncover the molecular underpinnings responsible

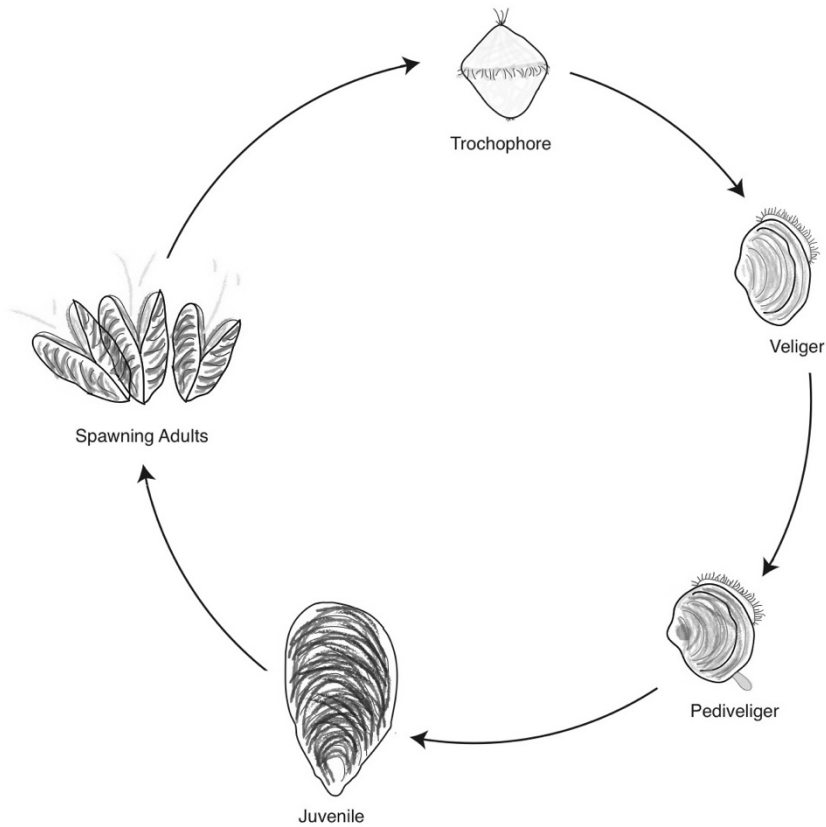


Figure 1.1. Life cycle of *M. edulis*. Adult blue mussels are sessile marine invertebrates that reproduce through broadcast spawning. Gametes are released into the water column and fertilization is external. Within 24 h, embryos have developed to a ciliated trochophore stage, which transitions to the veliger stage and the larva begins to secrete the larval shell and develop the velum. The veliger is the longest of the larval stages, lasting 2 – 3 w, and is a period of marked growth. Eventually, a mussel larva develops a pedal organ and transitions into a pediveliger, the final larval stage. Upon contact with a suitable substrate, the pediveliger can settle and undergo metamorphosis, marking the final transition back into the benthos as a juvenile.

for these physiological changes (Evans and Somero 2010, Lockwood and Somero 2011, Tomanek et al. 2012). Even less is known about the genetics and physiology of larval mussels and their ability to mount an osmotic stress response.

1.2. Project Overview

The purpose of this study was to broaden our understanding of the osmotic stress response in *M. edulis*, by evaluating how aspects of the response differ across developmental stages and among tissue types in juvenile mussels. We examined these responses at the organismal, cellular, and molecular levels and an important aspect of our research was a consideration of how the response changes as a function of the duration of exposure. Although this research focused on *Mytilus edulis*, as it is the predominant mussel species in the Gulf of Maine, inclusion of the congeners *M. trossulus* and *M. galloprovincialis* in portions of this study has allowed us to put some of our findings into an evolutionary context. Our goal was to provide insight into the regulation of gene expression during osmotic stress, how changes in expression may affect the responses observed at different levels of organization, and how these processes may vary among life history stages and different tissues.

This research included a series of experiments in which we evaluated 1) the effects of larval exposure to low salinity on post-metamorphic size and growth, 2) stage- and tissue- specific metabolite compositions and changes in organic osmolytes during hypoosmotic exposure, 3) the relationship between patterns of gene expression and cellular-level changes in low salinity-challenged mussels, 4) the role of important cellular signaling genes (calmodulin) in the hypoosmotic stress response, and 5) the catabolism of ornithine during low salinity exposure in closely related mussel species. These studies

highlight important differences in the physiology and transcriptome observed in early developmental stages and juveniles as well as the complexity of the osmotic stress response in blue mussels.

CHAPTER 2

CARRYOVER EFFECTS FROM LARVAL EXPOSURE TO REDUCED SALINITY ON GROWTH OF JUVENILE BLUE MUSSELS (*MYTILUS EDULIS*)

2.1. Abstract

Among species with complex life histories, larval experience can have a profound impact on the phenotype of later developmental stages. Although exposure to low salinity is known to negatively impact both larval and juvenile blue mussels (*Mytilus edulis*), the carryover effects of low salinity experienced by mussel larvae on juvenile performance is unknown. To test if the effects of exposure to hypoosmotic conditions has an impact on mussel phenotypes across metamorphosis, we compared the size at metamorphosis and the size and growth at 35 d post-metamorphosis (dpm) for mussels that experienced short-term, hypoosmotic treatment at two different larval stages. Additionally, we looked at the effect of repeated low-salinity exposure across developmental stages on the size and growth of juvenile mussels. Exposed veligers showed significant reductions in size and growth rate, while pediveligers from the treatment group showed significant reductions in growth, but not in size at 35 dpm, compared to control animals. We also found that growth was negatively impacted for mussels that experienced repeated exposure as both veligers and juveniles; in contrast, there was a positive effect on growth in mussels exposed as pediveligers and juveniles. Our data indicate that stress from low

salinity exposure carries over to later developmental stages in *M. edulis*, but that the response to stress may vary depending on when the larval exposure occurs.

2.2. Introduction

The distribution of marine species depends heavily on their tolerance to abiotic stressors. Changes to the physical environment associated with global climate change, including increased sea temperature, decreased pH, and altered salinity (Doney et al. 2012), have heightened the need for studies on the ability of species to respond to increased stress associated with climate variability and to acclimate to a changing environment (Somero 2010). Beyond simply documenting how species cope with environmental stress, several studies have shown that previous exposure to stress is an important factor influencing the subsequent stress response (e.g., Bertram and Strathmann 1998, Maltby 1999, Buckley et al. 2001, O'Connor et al. 2014). For species having complex life history strategies, such as many marine invertebrates, exposure to stressors early in development may carry-over into other developmental stages and impact the fitness, growth, or survival of the animal (Padilla and Miner 2006, Pechenik 2006). A better understanding of such legacy or carryover effects is critical for predicting how the response of individual species to climate change will affect their distribution and abundance.

Blue mussels (*Mytilus edulis*) are important constituents of intertidal and subtidal communities in temperate and subarctic regions. They are considered ecosystem engineers (Arribas et al. 2014) because they increase habitat complexity and reduce stress for other inhabitants, and are prey for many other marine species. In coastal areas, salinity fluctuation is a primary stressor experienced by *M. edulis* (Gardner and

Thompson 2001). Given that changes in global climate are projected to increase the frequency and severity of salinity fluctuations nearshore (Antonov et al. 2002, Durack et al. 2012), the ability to tolerate salinity stress is an increasingly critical factor affecting whether mussel populations will persist. The persistence of mussel populations, however, depends on their tolerance to salinity stress not only as adults but throughout development because exposure during larval stages will impact the fitness of juveniles that are recruiting back into the mussel beds (Grosberg and Levitan 1992). While studies have examined the effects of chronic low salinity on larval (Bayne 1965, Hrs. Brenko and Calabrese 1969, His et al. 1989, Qiu et al. 2002) and post-metamorphic (Bøhle 1972, Almada-Villela 1984, Gardner and Thompson 2001, Riisgård et al. 2012, Landes et al. 2015) growth and survival, to our knowledge, none have tested the carryover effects of low salinity exposure during larval development in blue mussels.

The role that larval experience may play in dictating the phenotype of post-metamorphic individuals is not well understood (Marshall and Morgan 2011). In many instances, stress experienced at early life history stages has negatively impacted post-metamorphic success (see Pechenik 2006 for a review), although there are also instances in which previously experienced stress benefits the individual (Bacon 1971, Qiu and Qian 1999, Parker et al. 2015). Only one study has looked at carryover effects in blue mussels (Phillips 2002), so we know very little about how stress experienced during development influences post-metamorphic fitness or alters the response to repeated stress in *M. edulis*.

The goal of this study was to evaluate how the exposure of larvae to acute, low-salinity conditions (as would be experienced during a flood event) affects juvenile performance and tolerance to the same stressor. We used larval and juvenile size

(measured as shell area), as well as juvenile growth rate, as proxies for carryover effects across metamorphosis. Additionally, we examined the influence of larval stress on later developmental stages to see if juvenile growth was further impacted by repeated stress. Finally, we compared these responses using two different larval phases, the veliger and pediveliger, to see if expression of carryover effects depends on when during larval development the stress occurs.

Low salinity stress stunts both larval (Bayne 1965, Hrs-Brenko and Calabrese 1969, Innes and Haley 1977) and post-metamorphic (Bøhle 1972, Almada-Villela 1984, Riisgård et al. 2012, Landes et al. 2015) growth in blue mussels. Therefore, we expected that mussel larvae exposed to low salinity would show reductions in larval growth that would carryover through metamorphosis and yield smaller juveniles. Similarly, we hypothesized that individuals subjected to repeated exposure to short-term, low salinity across life history stages would show greater reductions in growth than mussels that were not treated or that did not experience repeated exposure. We expected that the overall effect of low salinity exposure on size would be similar in mussels treated as veligers to those treated as pediveligers, but that there would be slight variations in the response due to differences in the metabolic demands of the two larval stages (Sprung 1984).

2.3. Methods

2.3.1. Mussel Collection and Larval Culture

Adult *Mytilus edulis* were collected from the intertidal zone at Pemaquid Point (Bristol, ME) and from a subtidal population on the underside of the dock at the Darling Marine Center (Walpole, ME) on June 7, 2015. The mussels were held overnight in a refrigerator (4 °C) and the following day were induced to spawn by exposing them to

cyclic thermal shock (Helm et al. 2004). Briefly, animals were placed at 14 °C in 1 µm filtered, UV-sterilized seawater (UV-FSW), allowed to warm slowly to 21 °C, and quickly reimmersed in 14 °C UV-FSW. This “thermal shock” protocol was continued until individual mussels began to spawn. Five replicate groups of embryos were produced; each replicate was constructed using the eggs from four females fertilized with the sperm from two males, thus ensuring that each replicate contained distinct, but genetically heterogeneous populations of larvae.

Embryos developed overnight at ambient conditions (13.5 °C, 32 ppt UV-FSW) in 20 l buckets and were transferred as trochophores into 350 l larval tanks at densities ranging from 100–500 individuals·ml⁻¹. Larvae were maintained in tanks with UV-FSW supplemented with probiotic bacteria (Dr. Tim’s Aquatics, LLC) that was gently aerated to ensure proper mixing and to prevent larvae from settling. Once larvae had transitioned to the feeding D-stage (at approximately 2 d post-fertilization, dpf), they were fed daily mixtures of *Monochrysis* sp., *Chaetoceros muelleri*, *C. calcitrans*, *Tetraselmis chuii* and *Isochrysis galbana* (clone T-Iso). As the larvae grew, food rations were adjusted following the guidelines for larval bivalve culture in Helm et al. (2004). Every other day, the water in each of the five larval tanks was changed, the larval density was estimated, and shell lengths were measured on a small subsample of larvae. Water changes were conducted using a 48 µm sieve to ensure that smaller individuals would be retained in the cultures so the size variation in our larval populations would be representative of natural size variability.

2.3.2. Acute Exposure to Low Salinity

To test the effects of larval stress on post-metamorphic growth, we exposed larvae to short-term hypoosmotic conditions in two separate experiments. In the first experiment the treatment was applied to larvae at the veliger stage (14 dpf) when larvae had developed the velum and an umbo on the shell (Stafford 1906). A subset of approximately 100,000 veligers was removed from each stock culture and placed in individual 1 l beakers containing ambient, UV-FSW (controls). A second subset of 100,000 veligers was sampled from each stock culture and placed in five separate beakers containing a low salinity treatment (20 ppt) made by mixing RO water and UV-FSW. All beakers were kept at the same density (10 individuals·ml⁻¹) and fed. After 24 h the larvae from the five control and five low-salinity treatment beakers were restocked into separate 350 l tanks at 13.5 °C and 32 ppt (as detailed in the section above). Due to space limitations, we could only stock one tank with the larvae from the five control beakers and one tank with the larvae from the five experimental beakers. Thus, while larvae sampled from each stock tank were independently exposed to control and hyposaline conditions, they were pooled for the remainder of larval development. After pooling, however, the tanks were kept at the same densities, received water from same source following water changes, and were fed algae from the same source; the only factor differentiating the two tanks was the 24 h exposure to water of different salinity. In the second experiment, the larvae were treated at the pediveliger stage (26 dpf), indicated by the development of a large pedal organ (Bayne 1965). Again, roughly 100,000 pediveligers were removed from each stock culture and placed into either a control or treatment beaker for 24 h, as previously described. Following the treatment, the

pediveligers were restocked in separate larval tanks at ambient conditions and permitted to continue development.

Mussel larvae had become competent at 32 dpf. Individual racks consisting of eight settlement plates (15 x 9 cm PVC plates with an affixed Scotch-Brite® Scour Pad) were placed into each of the treatment tanks that contained veliger-control, veliger-treated, pediveliger-control, or pediveliger-treated larvae. The water in each tank was vigorously bubbled to promote the settlement of larvae on the plates rather than on the sides of the tanks. Visual observations of the tanks (i.e., absence of swimming larvae) and the absence of larvae on a sieve during water changes indicated that most larvae had settled and undergone metamorphosis. The settlement plates were then transferred to the University of Maine in Orono, ME, where the juvenile mussels were kept on the settlement plates in a recirculating seawater system for the duration of the experiment. Plates from each treatment were placed into separate tanks filled with artificial seawater (15 °C, 32 ppt, Instant Ocean®) and each tank was fed 0.5×10^9 cells·d⁻¹ of Shellfish Diet 1800 (Reed Maricultlure, Inc.).

2.3.3. Juvenile Repeated-Exposure Experiment

To test whether low-salinity exposure during early life history stages affects the response of the juvenile mussel to the same conditions, we exposed a subset of juveniles at 7 d post-metamorphosis (dpm) to acute hypoosmotic conditions. Four plates from each of the four larval treatments were randomly selected and placed into containers containing ambient (15 °C, 32 ppt) or low salinity (15 °C, 20 ppt) seawater. After 24 h, plates were placed back into the recirculating system where they were maintained for an additional 28 d. This secondary treatment yielded four different treatment combinations

for each of the two larval experiments: mussels that had never been exposed, mussels that were exposed only as juveniles, those that were exposed only as larvae, and those that were exposed as both larvae and juveniles.

On August 12, 2015 (35 dpm), the scour pads were removed from the settlement plates, with the animals intact, and fixed in 70 % ethanol. Post-fixation, the pads were placed into an 80 μm sieve and gently rinsed to remove the attached mussels. Samples were stained in Rose Bengal and juveniles with intact gill filaments (indicating that they were healthy and had developed normally up to the point of fixation; see Fig. 1), were imaged using an Olympus SZ-PT stereomicroscope with an ocular-mounted HDR-CX150 Sony Handycam. All images were taken at 40X.

2.3.4. Size Measurements and Data Analysis

The larval shell of *M. edulis* is composed entirely of aragonite, while the juvenile shell contains a mixture of calcite and aragonite (Fuller and Lutz 1988). The transition from the larval shell, the prodissoconch II, to the dissoconch or the juvenile shell occurs at metamorphosis (Bayne 1965) and the two shell types are easily distinguished (Figure 2.1). We used the line demarking the transition between the two shells to estimate the size at metamorphosis. Additionally, we measured the size of individuals at 35 dpm and used the two measures to estimate the specific growth rate over the first 35 dpm. Growth in mussels is often measured as a change in the length of the shell (Widdows 1991). However, the axis along which the shell elongates changes between pre- and post-metamorphic mussels. Thus, to get a better estimate of the size of each mussel, we recorded the two-dimensional area of the shell in mm^2 . The areas (A) of the larval and juvenile shell for an individual were measured using the “magnetic lasso” tool in Adobe

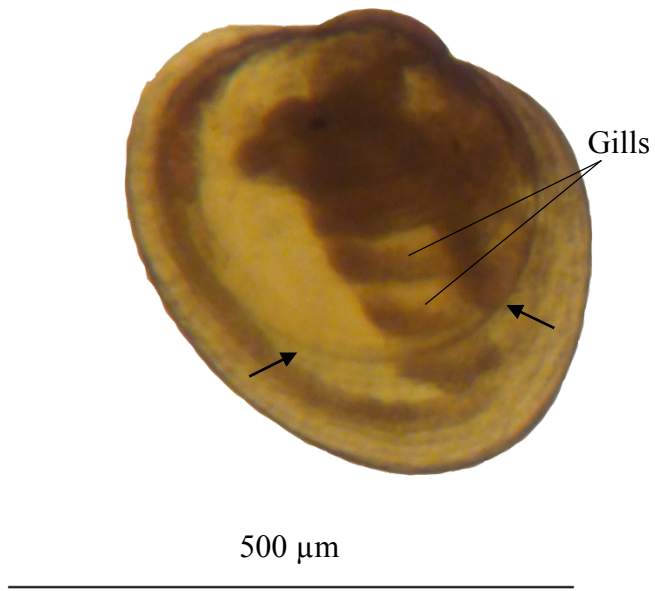


Figure 2.1. Photomicrograph of a juvenile *M. edulis*. The larval shell is distinguished from the juvenile shell by change in color and texture; a ridge that demarcates the boundary of the two shell layers and is highlighted by the arrows. The gills (labeled) are an indication of the health of individual larvae at the time of fixation; only juveniles with clearly evident gills and pronounced ridge between the larval and juvenile shells were analyzed in this study.

Photoshop. The area of the shell was calculated as the number of pixels within the highlighted region calibrated to a stage micrometer imaged at 40X. The larval and juvenile areas were then used to calculate the specific growth rate (μ , d^{-1}), a commonly used metric for growth in studies of mussels (Bayne 1965, Gardner and Thompson 2001, Riisgård et al. 2012), using the equation:

$$\mu = \ln \left(\frac{A_j}{A_l} \right) t^{-1} \quad [1]$$

where A_j is the area of the juvenile shell, A_l is the area of the larval shell, and t is the number of days from metamorphosis to the end of the experiment (modified from Fisher 1921). Only images in which the larval shell was clearly discernable were used in this analysis.

All statistical analyses were conducted using SPSS Statistics 22.0 (IBM Corporation). Our analyses focused on variation among larvae on replicate plates post-settlement. The effects of larval exposure to low-salinity on the area of the larval shell at metamorphosis were tested using a two-factor, nested ANOVA with variability among settlement plates nested within larval treatment (low-salinity versus control for each of the veliger and pediveliger experiments). This analysis allowed us to test whether larvae on different replicate plates had consistent shell areas at the time of settlement. We tested the effects of larval and juvenile salinity exposures on the size of the juvenile mussel (shell area at 35 dpm) and on the growth of the mussel following metamorphosis (specific growth rate) using three-factor, nested ANOVA. In these models, larval and juvenile treatments were the main effects, with settlement plate nested within the larval by juvenile treatment interaction term, and settlement plate treated as a random term. For each model, hypotheses were tested using a Type III Sum of Squares model with an

overall model-wide $\alpha = 0.05$. In the veliger experiment, one plate was excluded from all analyses because only one juvenile mussel was recovered from this plate.

2.4. Results

Throughout larval development, larvae in all treatment groups actively swam and showed no outward signs of stress. We did not observe any differences in the timing of metamorphosis among any of the four treatment groups, although we could not monitor individuals post-settlement because they settled within the fibers of the scour pads. We did not directly measure survivorship within treatment groups, however, we observed differences in the number of individuals found on the settlement plates at the end of the experiment, which may indicate variation in survival. We collected only 155 individuals that had survived the veliger experiment, while we recovered 775 individuals from the settlement plates of the pediveliger experiment. However, we observed no difference in either experiment between the numbers of individuals found on the control versus the salinity challenged plates, suggesting that any variation in survival was attributable to handling effects rather than salinity treatment.

2.4.1. Veliger Salinity Experiment

We observed a significant reduction in the area of the shell at metamorphosis for veligers that were exposed to acute hypoosmotic conditions (Figure 2.2) compared to veligers held under control conditions (Table 2.1). The small size at metamorphosis carried over to the juvenile stage in mussels that had been subjected to short-term hypoosmotic exposure at the veliger stage. Shell area in mussels treated as veligers was significantly reduced relative to shell area for mussels that had not been exposed as larvae (Figure 2.3). In the veliger experiment, neither juvenile treatment nor the interaction of

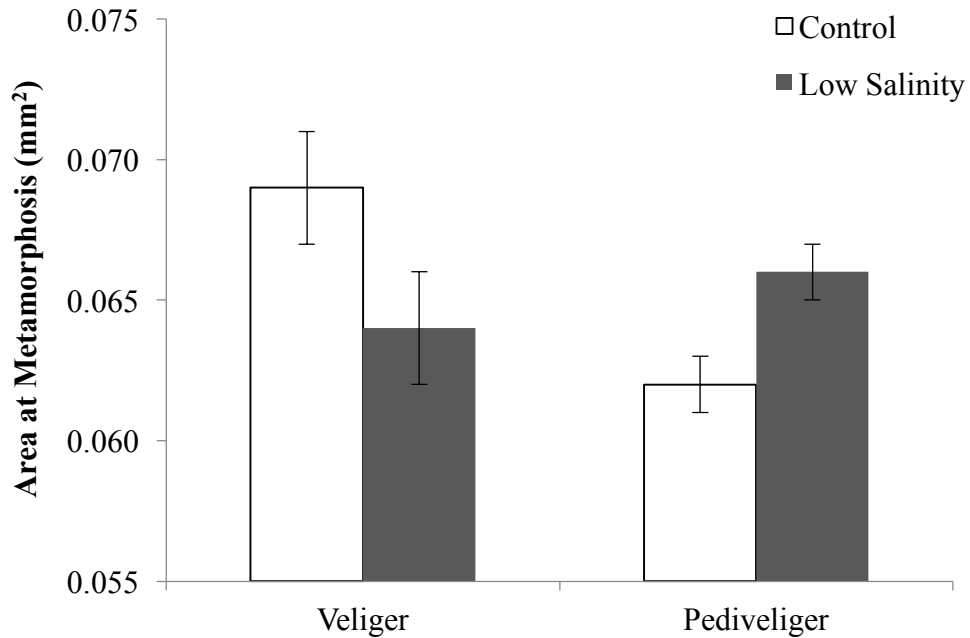


Figure 2.2. Effects of low salinity treatment on size at metamorphosis. The size at metamorphosis was calculated as the marginal mean shell area ($\text{mm}^2 \pm \text{SE}$), for veliger (left) and pediveliger mussels (right). Veliger larvae that experienced acute hypoosmotic exposure (grey bars, at left; $n = 84$) were significantly smaller at metamorphosis than the controls (open bar; $n = 70$; $F = 5.221$, $df = 1$, $p = 0.034$), while exposed pediveligers ($n = 360$) were significantly larger than the controls at metamorphosis (at right; $F = 17.909$, $df = 1$, $p = 0.001$; $n = 410$).

	Source	df	MS	<i>F</i>	<i>p</i>
Veliger	Larval treatment	1	0.001	5.221	0.034
	Plate (larval treatment)	13	0.000	1.095	0.368
	Error	139	0.000		
Pediveliger	Larval treatment	1	0.003	17.909	0.001
	Plate (larval treatment)	14	0.000	1.653	0.061
	Error	754	0.000		

Table 2.1. ANOVA results for larval exposure on size at metamorphosis. We ran a nested, two-factor ANOVA examining the effect of 24 h hyposaline exposure (larval treatment) on the total area of the larval shell for larvae stressed as veligers (top) and pediveligers (bottom). The effects of treatment on size at metamorphosis and the nested effect of settlement plate within treatment are included for both models.

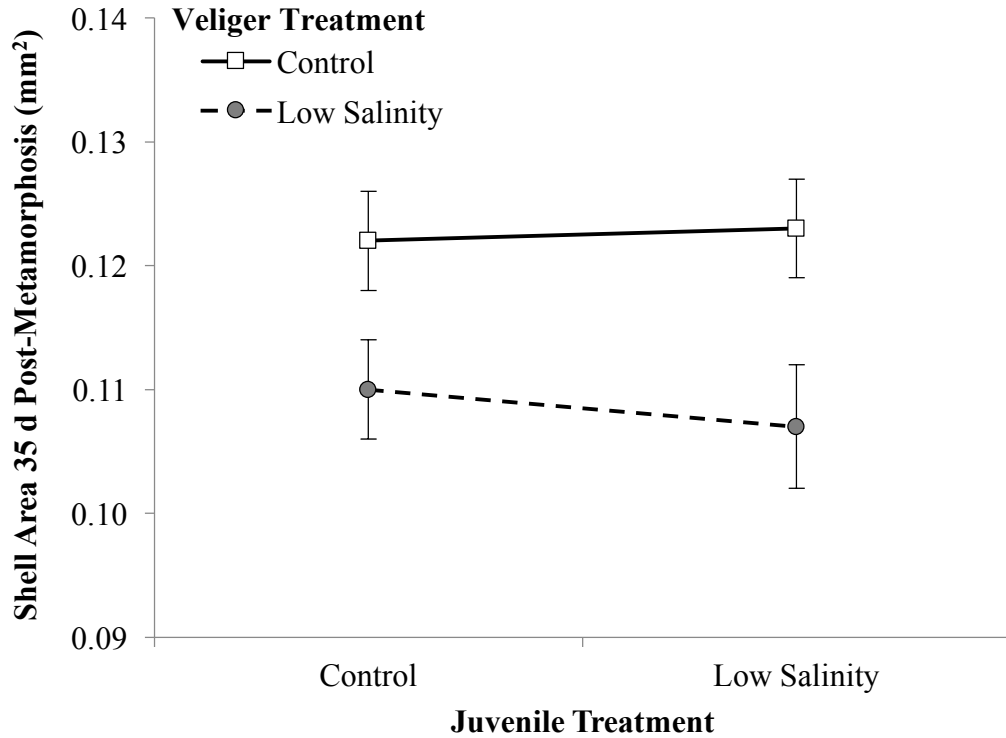


Figure 2.3. Effects of veliger low-salinity exposure on size at 35 dpm. The plot shows mean juvenile shell area at 35 dpm ($\text{mm}^2 \pm \text{SE}$) for mussels exposed to control (solid line) or low salinity (dashed line) treatments as veligers and exposed again to either control (left) or low salinity (right) conditions at 7 d post-metamorphosis. There was no effect of juvenile treatment on the mean size of juvenile mussels, but there was a significant decrease in size for mussels that had been exposed to hypoosmotic conditions as veligers relative to the control groups ($F = 7.595$, $df = 1$, $p = 0.016$).

Source	df	MS	<i>F</i>	<i>p</i>
Larval treatment	1	0.006	7.595	0.016
Juvenile treatment	1	7.43 x 10 ⁻⁵	0.101	0.756
Larval x juvenile treatment	1	0.000	0.181	0.677
Plate (larval, juvenile treatment)	11	0.001	1.425	0.168
Error	139	0.001		

Table 2.2. ANOVA results for veliger exposure on juvenile shell area. We ran a three-factor, nested ANOVA examining the salinity effects of veliger exposure on juvenile shell area. The ANOVA model includes the main effects of low-salinity exposure during the veliger stage (larval treatment), salinity exposure at 7 dpm (juvenile treatment), the interaction of the main effects, and the nested effect of settlement plate on the area of the juvenile shell at 35 dpm.

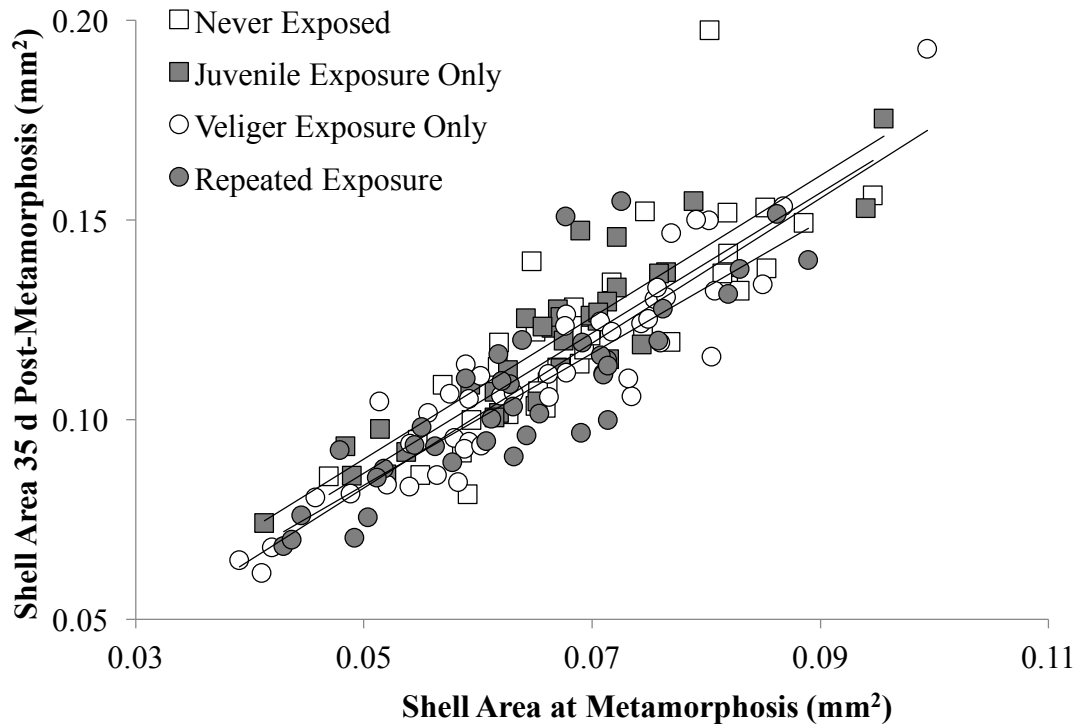


Figure 2.4. Veliger-exposed size at metamorphosis versus at 35 dpm. There is a strong correlation between size at metamorphosis and size 35 dpm for each of the treatment blocks, which include mussels that were never exposed (open squares; $y = 1.7575x - 0.0013$, $r^2 = 0.65$), mussels that were exposed 7 dpm (gray squares; $y = 1.7744x + 0.0014$, $r^2 = 0.84$), mussels exposed only as veligers (open circles; $y = 1.8132x - 0.0078$, $r^2 = 0.86$), and those exposed both as veligers and 7 dpm (gray circles; $y = 1.6513x + 0.001$, $r^2 = 0.73$).

larval and juvenile treatment had a significant effect on juvenile shell area (Table 2.2). However, mussels that experienced exposure at both larval and juvenile stages were the smallest at 35 dpm (Figure 2.3).

We observed a strong correlation between the size of the mussel at metamorphosis and at 35 dpm (Figure 2.4), which suggests that there was no compensatory growth by smaller mussels. Therefore, any reduction in size associated with larval stress persists through metamorphosis and yields smaller juveniles. As such, the growth rate of juveniles that had been exposed as veligers was reduced compared to the controls (Figure 2.5), although this effect was not significant (Table 2.3). There was no significant effect from juvenile treatment on the specific growth rate of juveniles stressed as veligers nor a significant interaction effect between larval and juvenile treatments on specific growth rates.

2.4.2. Pediveliger Salinity Experiment

Pediveligers that were exposed to acute hypoosmotic conditions had significantly larger shell areas at metamorphosis than the control group (Table 2.1), which is the opposite of what we observed in the veliger experiment (Figure 2.2). We also observed a significant increase in the area of juvenile mussels that had been treated as pediveligers relative to the control group (Figure 2.6). Contrary to what we observed in mussels treated as veligers, those that were exposed at both the pediveliger stage and 7 dpm had the largest shell area at 35 dpm, while those exposed only as juveniles were the smallest. However, the effects from juvenile treatment, the interaction of larval and juvenile treatment, and the effect from settlement plate were not significant (Table 2.4).

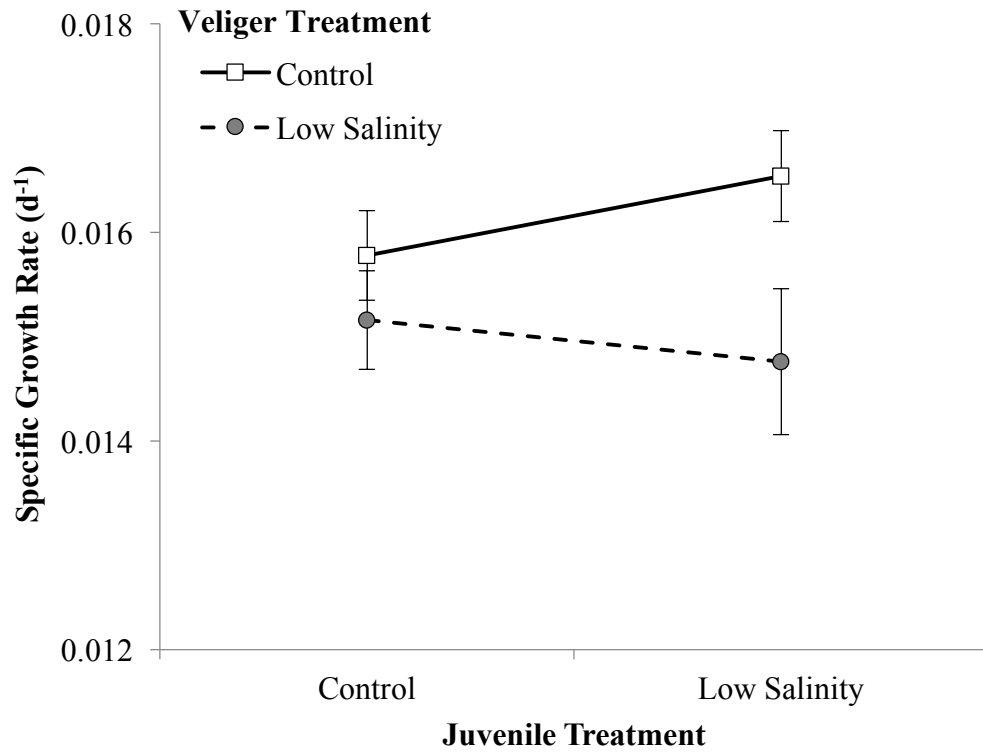


Figure 2.5. Effects of veliger low-salinity exposure on the specific growth rate. The marginal mean specific growth over a 35-d period (d^{-1} , \pm SE) are shown for mussels exposed to control (solid line) or low salinity (dashed line) conditions as veligers and to control (left) or treatment (right) conditions as 7 dpm juveniles. Mussels exposed as veligers showed reduced specific growth rates compared to the control groups, although there were no significant effects of either larval or juvenile treatment on the specific growth rate.

Source	df	MS	<i>F</i>	<i>p</i>
Larval treatment	1	4.15 x 10 ⁻⁵	3.214	0.097
Juvenile treatment	1	7.92 x 10 ⁻⁷	0.062	0.808
Larval x juvenile treatment	1	1.29 x 10 ⁻⁵	0.783	0.393
Plate (larval, juvenile treatment)	11	1.41 x 10 ⁻⁵	2.243	0.015
Error	139	6.29 x 10 ⁻⁶		

Table 2.3. ANOVA results for veliger exposure on specific growth rate. We ran a three-factor, nested ANOVA examining the effects of low salinity exposure during the veliger stage on specific growth rate. The ANOVA model includes the main effects of salinity exposure during the veliger stage (larval treatment), salinity exposure at 7 dpm (juvenile treatment), the interaction of the main effects, and the nested effect of settlement plate on the specific growth rate over 35 dpm.

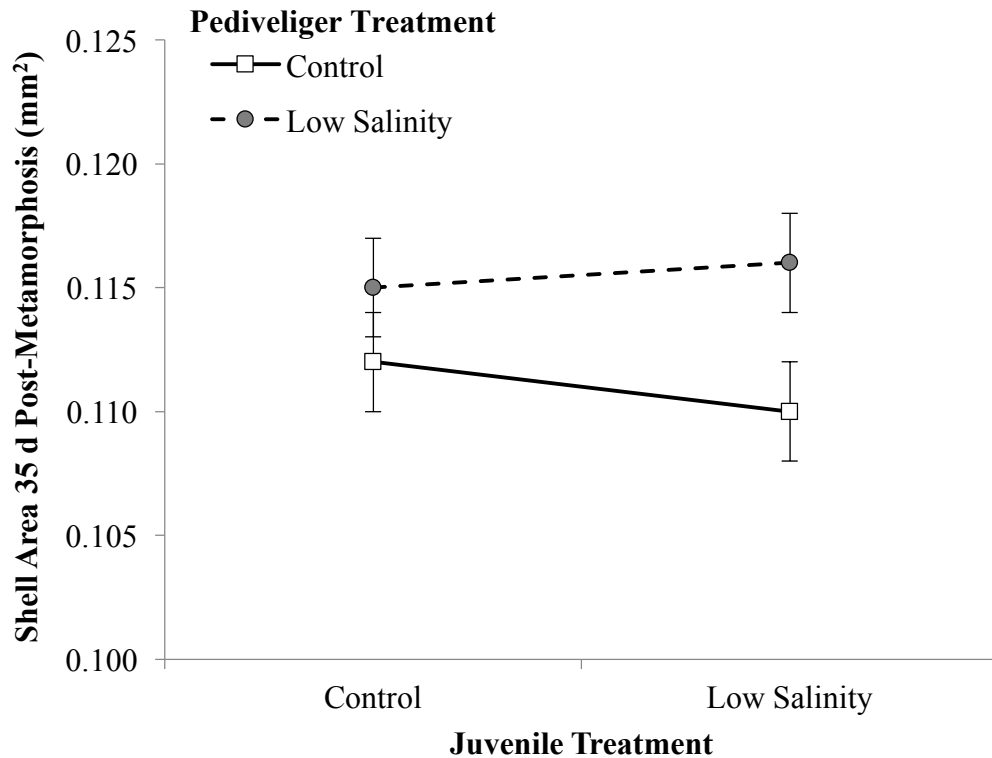


Figure 2.6. Effects of pediveliger low-salinity exposure on size at 35 dpm. The plot shows the marginal means for juvenile shell area (mm² ± SE) for mussels exposed to control (solid line) or low salinity (dashed line) treatments as pediveligers and exposed again to either control (left) or low salinity (right) conditions at 7 dpm. There was no effect of juvenile treatment on the mean size of juvenile mussels, but there was a significant increase in size for mussels that had been exposed to hypoosmotic exposure as pediveligers relative to the control groups ($F = 8.086$, $df = 1$, $p = 0.012$).

Source	df	MS	<i>F</i>	<i>p</i>
Larval treatment	1	0.004	8.086	0.012
Juvenile treatment	1	9.97 x 10 ⁻⁷	0.002	0.963
Larval x juvenile treatment	1	0.000	0.639	0.436
Plate (larval, juvenile treatment)	12	0.000	0.908	0.538
Error	754	0.000		

Table 2.4. ANOVA results for pediveliger exposure on juvenile shell area. We ran a three-factor, nested ANOVA examining the effects of low salinity exposure during the pediveliger stage on juvenile shell area. The ANOVA model includes the main effects of salinity exposure during the pediveliger stage (larval treatment), salinity exposure at 7 dpm (juvenile treatment), the interaction of the main effects, and the nested effect of settlement plate on the area of the juvenile shell at 35 dpm.

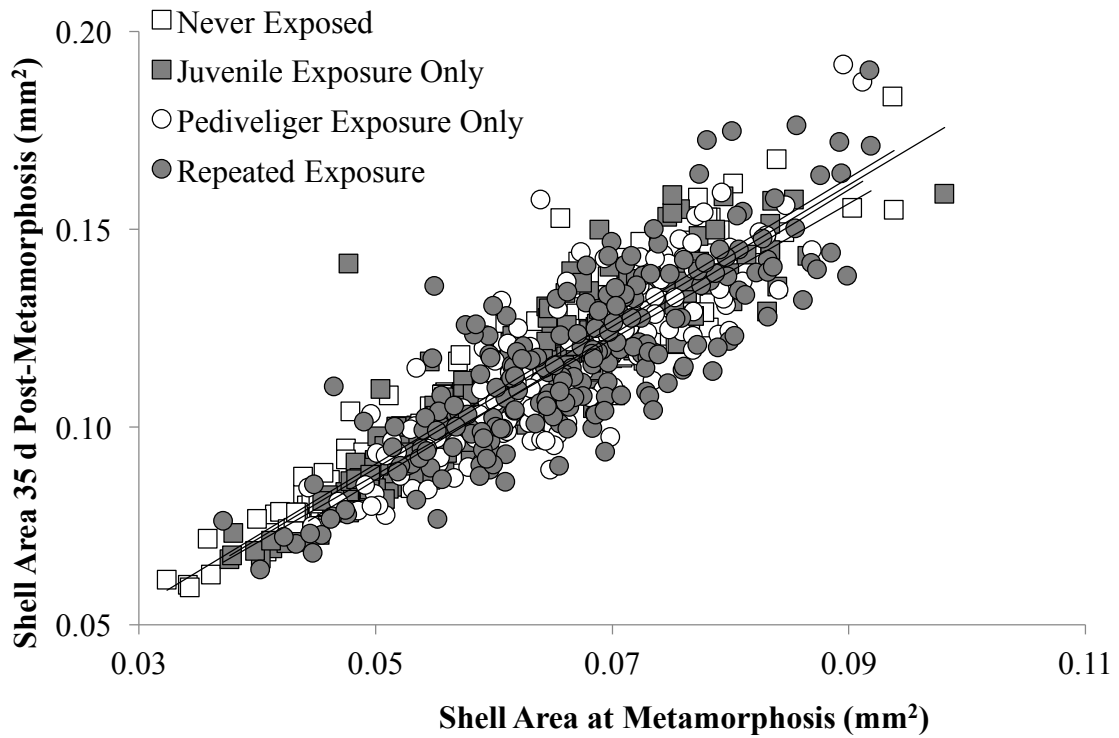


Figure 2.7. Pediveliger-exposed size at metamorphosis versus 35 dpm. There is a strong correlation between size at metamorphosis and size 35 dpm for each of the treatment blocks, which include mussels that were never exposed (open squares; $y = 1.809x + 0.002$, $r^2 = 0.88$), mussels that were exposed 7 dpm (gray squares; $y = 1.7913x - 0.4 \times 10^{-5}$, $r^2 = 0.83$), mussels exposed only as pediveligers (open circles; $y = 1.8336x - 0.0051$, $r^2 = 0.71$), and those exposed both as pediveligers and 7 dpm (gray circles; $y = 1.7155x + 0.0022$, $r^2 = 0.69$).

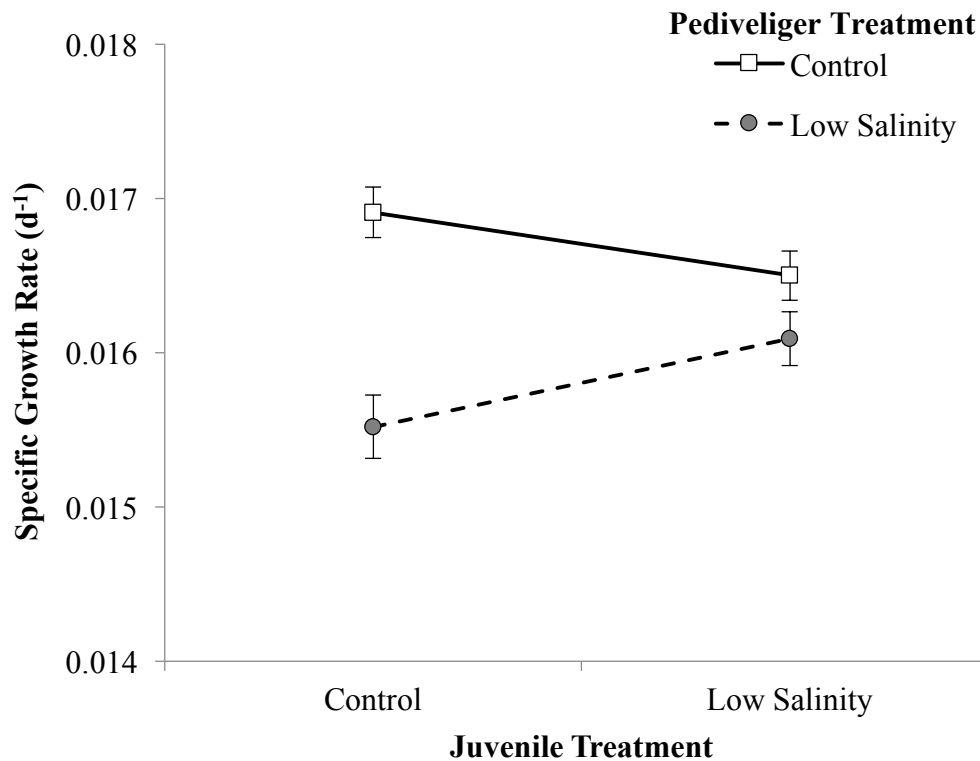


Figure 2.8. Effects of pediveliger low-salinity exposure on specific growth rate. The marginal mean specific growth rate in the 35 dpm (in $d^{-1} \pm SE$) for mussels that were exposed to control (solid line) or low salinity (dashed line) as pediveligers and control (left) or low salinity (right) as 7 d post-metamorphic juveniles. There was no significant effect of larval or juvenile treatment on the specific growth of mussels, although mussels exposed to low salinity as pediveligers showed significant reductions in growth rates relative to the control groups.

Similar to what we observed in the veliger experiment, there was a strong correlation between the area at metamorphosis and the area 35 dpm in the pediveliger-treated groups (Figure 2.7). Despite this, mussels that were treated as pediveligers had lower specific growth rates than the control groups (Figure 2.8). Mussels that were never exposed had higher growth rates than those exposed at the pediveliger or juvenile stage, and those treated as both pediveligers and juveniles grew faster than those stressed only as larvae. However, these trends were not significant, due to the high variance among settlement plates within treatment, which masked any treatment-level or interaction effects in this experiment (Table 2.5).

2.5. Discussion

This is the first study to our knowledge that documents carryover effects from reduced salinity in blue mussels. Mussels that were treated at the veliger stage were significantly smaller than control mussels despite that the larval stress was applied at 14 dpf and for only a 24 h duration (Figure 2.2). This effect was consistent across settlement plates. At similar rearing temperatures, Hrs-Brenko and Calabrese (1969) reported that mean length of *Mytilus edulis* early-veliger larvae was reduced 66.5 % after prolonged (16–17 d) exposure to 20 ppt seawater. We detected smaller reductions in overall size of the shell (7.3 %), though our animals were only exposed to 20 ppt for 24 h and the differences in size between treatment groups would likely become more divergent with prolonged exposure. The mean size at 35 dpm and specific growth-rate of juveniles were also reduced in mussels briefly exposed as veligers (Figure 2.3 and Figure 2.5, respectively), demonstrating that the effect of larval experience persists through metamorphosis. Phillips (2002) reported similar findings in that larval diet influenced

Source	df	MS	<i>F</i>	<i>p</i>
Larval treatment	1	0.000	2.386	0.148
Juvenile treatment	1	1.11 x 10 ⁻⁶	0.020	0.890
Larval x juvenile treatment	1	4.00 x 10 ⁻⁵	0.718	0.413
Plate (larval, juvenile treatment)	12	6.18 x 10 ⁻⁵	11.581	< 0.001
Error	754	5.33 x 10 ⁻⁶		

Table 2.5. ANOVA results for pediveliger exposure on specific growth rate. We ran a three-factor, nested ANOVA examining the effects of low salinity exposure on the specific growth on pediveliger- and juvenile-treated mussels. The effects of pediveliger treatment and juvenile treatment on the specific growth rate over 35 dpm, their interaction, and the nested effect of settlement plate within each of the treatments are displayed.

post-metamorphic size in a congener, *M. galloprovincialis*, and other studies have found low-salinity stress reduces juvenile growth in the marine invertebrates, such as *Capitella* sp. (Pechenik et al. 2001), *Amphibalanus improvius* (Nasrolahi et al. 2012), and *Crepidula fornicata* (Bashevkin and Pechenik 2015).

The effects of reduced salinity experienced by pediveligers on juvenile size were inconsistent with the effects we observed in our veliger-stress experiment. Mussels stressed as pediveligers had larger shell area at metamorphosis (Figure 2.2) and at 35 dpm (Figure 2.6) than those in the control groups. This trend toward an increase in size in pediveliger-stressed mussels is likely an artifact resulting from unexpectedly small size at metamorphosis in the control group (Figure 2.2, open bar on the right) and could have resulted from early settlement of larger individuals in the control tanks. However, the larvae in each tank were monitored daily and we found no evidence of differential settlement. Innes and Haley (1977) found a genetic basis for variation in growth for blue mussel larvae when larvae were exposed to salinity stress, yet both the treatment and control groups in our pediveliger and veliger experiments were drawn from the same pool of larvae and thus variation in size at metamorphosis in this experiment was unlikely to be genetically-based. Regardless, the smaller mussels at metamorphosis under ambient conditions confounds our analysis of the effects of salinity stress on size at this stage.

Despite the small size of control animals, the overall growth rate of mussels treated as pediveligers was lower than in the controls (Figure 2.8, solid versus the dashed lines). While the size of juvenile mussels at 35 dpm is correlated to the size at metamorphosis (Figure 2.7), mussels that experienced stress as pediveligers on average grew slower than those that were unstressed as larvae. This is consistent with what we observed in mussels

exposed as veligers and supports our hypothesis that larval stress carries through metamorphosis and negatively impacts post-metamorphic growth.

Within each of our larval studies, we also looked at the interaction of a repeated, hyposaline exposure on the growth of juvenile mussels. In some cases, studies on other marine invertebrates have shown that previous experience may either help to increase tolerance at other life history stages (Bacon 1971, Qiu and Qian 1999, Parker et al. 2015) or may further reduce juvenile performance (Emlet and Sadro 2006, Hettinger et al. 2012, Nasrolahi et al. 2012) depending on the stressor. We found that the effects of repeated hypoosmotic exposure on juvenile growth was stage-specific but also dependent on the metric used to assess the effects of stress (size versus growth).

We hypothesized that repeated exposure to low salinity would cause reductions in the overall growth and size of mussels compared to those that were unexposed or only exposed to salinity stress once. Qiu et al. (2002) found that mussel larvae are more sensitive to low salinity stress than juveniles, so we also expected that exposure during larval development would have a greater impact on the growth and size of juveniles compared to exposure experienced post-metamorphosis. In the veliger experiment, the smallest mussels at 35 dpm were those that experienced repeated exposure to low salinity. Mussels that were exposed only as veligers were smaller than both groups of mussels that were never exposed and those exposed only as juveniles, as we expected (Figure 2.3). These trends were also reflected in the growth rate, but to a lesser extent (Figure 2.5). The largest and fastest growing mussels from our veliger experiment were those that were exposed to acute, low salinity conditions only at 7 dpm. These findings

suggest that the response to low salinity stress varies for pre- and post-metamorphic blue mussels.

The effects of repeated exposure on pediveliger-treated mussels differed from the veliger experiment. With respect to size at 35 dpm, mussels that were not exposed to larval stress were the smallest of any treatment group, which makes comparisons to mussels that did experience larval stress more difficult. If we evaluate only mussels in the treatment groups, those that received repeated exposure (i.e., as pediveligers and 7 dpm) were slightly larger than those that were only exposed at the pediveliger stage (Figure 2.6). This trend is also reflected in the specific growth measurements (Figure 2.8). While unexpected, these findings are similar to what has been reported in other marine invertebrates (Bacon 1975, Qiu and Qian 1999, Fischer and Phillips 2014), where previous exposure may help to condition the individual and perhaps even increase the capacity to respond to the stress when experienced at later life-history stages. Unlike the mussel response in the veliger experiment, mussels in the pediveliger experiment that were treated only as juveniles were smaller and had lower growth rates than mussels that were never exposed to hyposaline conditions.

Our results indicate that the *timing* of stress experienced in early life stages is an important determinant of the response of post-metamorphic mussels, as indicated by variation in the size and growth of the treatment groups from each experiment. This finding is not surprising when considering the physiology of each larval stage. For example, veligers have the highest mass-specific metabolic rate of any larval phase and show marked increases in size-specific growth (Sprung and Widdows 1986), while pediveligers are energetically preparing to undergo metamorphosis (Sprung 1984). One

might then expect that when actively growing veligers are exposed to a stressor that may limit feeding or energy allocated towards growth, the residual effects from this stress would be more pronounced than when the same stress is experienced at later larval phase.

Mussels that are exposed to low salinity as veligers are smaller than those exposed as pediveligers. At the time of metamorphosis pediveligers from the treatment group are, on average, 3.1 % larger than those treated as veligers (Figure 2.2) and 4.5 % larger 35 dpm (Figure 2.6). The specific growth rate of the treated pediveligers is 9.0 % higher than the treated veligers, suggesting that veligers may be more susceptible than pediveligers to low salinity stress. We also observed some evidence that the mussels from the veliger experiment experienced higher mortality than those from the pediveliger experiment, as our sample sizes in the latter study were 4-5x higher than those in the former. However, the experimental design prohibited direct measurement of survival, so these findings should be interpreted with caution. Nonetheless, our study is the first to suggest that veliger and pediveliger mussel larvae differ in their ability to tolerate low salinity exposure.

Mussel larvae spend the majority of their development in the veliger stage which, depending on environmental conditions, can last many weeks (Bayne 1965, Widdows 1991). The growth of mussels during this stage is critical for developing adequate nutritional stores to undergo metamorphosis (Crisp 1976). Thus, any event, such as a flood event, that would negatively impact larval growth will have an effect on recruitment success. In this study, veligers that were exposed to acute, low salinity were smaller at metamorphosis and had reduced growth compared to other treatments. This reduction in growth is likely the result of decreased filtration rates and nutritional status

that accompanies osmotic stress (Bøhle 1972), which Phillips (2002, 2006) showed was critical to juvenile success. On the other hand, Martel et al. (2014) found that smaller size at metamorphosis was correlated to an increase in settlement success and may be an indication of an ecological tradeoff to cope with non-lethal stress. However, this is contrary to what we observed and to what has been reported in similar studies on the effects of salinity stress on successful larval development in barnacles (Qiu and Qian 1999, Qiu et al. 2002). In either case, because size at metamorphosis is correlated with juvenile size (this study and Phillips 2002), short-term exposure of veligers to osmotic stress may shift the size structure of persisting populations towards smaller individuals, as is commonly observed in populations adapted to low salinity (Riisgård et al. 2012, Landes et al. 2015).

The exposure of larval mussels to salinity stress may also have implications for the resilience of local mussel populations if, as our data from pediveligers suggest, the mussels are better equipped to deal with repeated exposure. Other studies have observed epigenetic modifications following exposure to stress, including significant changes in the levels of protein phosphorylation in adults of blue mussel congeners during acute osmotic shock (Evans and Somero 2010) and in other bivalves during larval exposure to elevated CO₂ (Dineshram et al. 2013), which may help prepare young mussels for the natural fluctuations in salinity that they will encounter in intertidal systems. Other types of epigenetic modifications, such as DNA methylation, have been reported in the honeybee *Apis mellifera*, where the developmental fate of the animal is mediated by DNA methylation patterns triggered by larval diet (Cameron et al. 2013). The role of DNA methylation or other post-translational modifications has not been studied in larval

mussels, but it is possible that these changes would persist through metamorphosis and condition mussels for future stressful events. If present, these molecular mechanisms may help blue mussels cope with a rapidly changing environment (Somero 2010). Further studies should be conducted to better understand how early life experiences may alter the gene expression of later developmental stages.

CHAPTER 3

NUCLEAR MAGNETIC RESONANCE SPECTROSCOPY (NMR) PROFILING OF METABOLITES IN LARVAL AND JUVENILE BLUE MUSSELS (*MYTILUS EDULIS*) UNDER AMBIENT AND LOW SALINITY CONDITIONS

3.1 Abstract

NMR-based studies can provide important foundational information on the metabolic baselines of understudied species. We used 1D ^1H nuclear magnetic resonance spectroscopy (NMR) and 2D total correlation spectroscopy (TOCSY) to describe baseline metabolite pools in larval and juvenile blue mussels under ambient conditions and to quantify changes in the abundance of common osmolytes in larval and juvenile blue mussels during low salinity exposure. Blue mussels (*Mytilus edulis*) are ecologically and economically important marine invertebrates whose populations are at risk due to climate-change induced variation in their environment, such as decreased coastal salinity. Blue mussels are osmoconformers and use components of the metabolite pools (free amino acids) to help maintain osmotic balance and cellular function during low salinity exposure. Metabolite studies in species such as blue mussels can help improve our understanding of the physiology, as well as the capacity of the study organism to respond to environmental stress. Furthermore, NMR-based metabolomic studies provide an easy and inexpensive tool to evaluate changes in metabolites that may occur among different tissue types or across developmental stages. Mussels have a complex life history and little is known about the capacity of blue mussel larvae to regulate metabolites during osmotic

stress. We found evidence for stage- and tissue-specific differences in the baseline metabolic profiles of blue mussels, which likely reflect variation in the function and morphology of each larval stage or tissue type. These differences impacted the utilization of various osmolytes during low salinity exposure within the different stages and tissues, again likely stemming from innate physiological differences of these samples. This study highlights the importance of foundational metabolomic studies that include multiple tissue types and developmental stages to adequately evaluate organismal responses to stress and better place these findings in a broader ecological context.

3.2 Introduction

The blue mussel (*Mytilus edulis*) is an important marine species that is commonly found in intertidal and subtidal habitats of the temperate and sub-boreal regions of the North Atlantic. From an ecological perspective, *M. edulis* is considered a foundational species, as it provides habitat and structure within coastal ecosystems (Arribas et al. 2014). Additionally, mussels are of importance because they are commercially fished and cultured and used in environmental monitoring programs (Goldberg 1975). Thus, any factor that threatens the health of mussel populations also poses a risk for other species within the community and impacts the quality of mussels as food sources or as bioindicators. Given their ecological and economic significance and the increasing pace of environmental change, there is substantial interest in the physiological tolerances of *M. edulis* and the effects of environmental stress on the persistence of blue mussel populations (e.g., Tuffnail et al. 2009, Ellis et al. 2014, Lesser 2016).

To adequately understand the capacity for species to respond to environmental stress, there is a critical need for foundational metabolomic studies that provide the

baselines for future comparisons. While some studies have presented data on the metabolomic signatures of unstressed mussels (Hines et al. 2007, Jones et al. 2008, Tuffnail et al. 2009), these studies have often focused on a single tissue and did not address the naturally occurring variation in the metabolome among tissue types. In addition, mussels have a complex life cycle that includes a protracted planktonic period of larval development so that studies on adult mussels are only representative of the physiological state of post-metamorphic, benthic stages. The energetic demands of larvae differ from post-metamorphic mussels, as they must obtain adequate energy stores to reach competency and undergo metamorphosis (Sprung 1984, Sprung and Widdows 1986). Thus, a comprehensive metabolomic study of species with complex life-histories, like *M. edulis*, must also account for developmental changes in physiology.

Ontogenetic variation in the metabolome may also impact the ability of mussels to respond to osmotic stress. Adult mussels selectively retain free amino acids (FAA), which function as osmolytes, within their metabolite pools as a means of intracellular osmotic regulation (Lange 1963, Bowlus and Somero 1979, Yancey et al. 1982, Somero 1986). Variation in the composition and utilization of FAA pools in response to osmotic stress have been widely studied in many marine bivalves (e.g. Shumway et al. 1977, Davenport 1979, Livingstone et al. 1979, Deaton et al. 1985, Neufeld and Wright 1996). However, there have been no studies to date that have looked broadly at the metabolic changes that occur across developmental stages or across tissues in juvenile mussels when subjected to osmotic stress. Bivalve larvae differ from juveniles in their uptake and metabolism of FAAs (Manahan 1983, Welborn and Manahan 1995), so it is likely that

the larval response to changes in environmental salinity differs from that of juvenile and adult mussels.

Nuclear magnetic resonance spectroscopy (NMR) is a commonly used tool for studying the metabolic profiles of bivalve molluscs (Hines et al. 2007, Jones et al. 2008, Tuffnail et al. 2009, Tikunov et al. 2010, Capello et al. 2013, Ellis et al. 2014). NMR is relatively inexpensive, rapidly generates extensive, quantitative metabolomic data, and can be used to detect the presence of solutes in low concentrations or in small samples. We capitalized on these advantages to study the ontogenetic variation in the metabolome of mussels during control and low salinity treatment. We used NMR spectroscopy to examine the baseline composition of the metabolome, with attention to the composition of the FAA pools, in larval (veliger and pediveliger stages) and juvenile blue mussels reared under ambient conditions. Additionally, we monitored changes in the FAA pools of hypoosmotically challenged larval and juvenile mussels to assess how ontogenetic variation in the metabolome affects the ability of mussels to respond. This study provides important physiological baseline data on *M. edulis* that are integral to understanding the cellular changes that occur during hypoosmotic stress.

3.3. Methods

3.3.1 Sample Collection

The larval *Mytilus edulis* used in this study were cultured at the Darling Marine Center Hatchery in Walpole, ME, under at a standard temperature and salinity (13.5 °C, 32 ppt). Briefly, adult mussels were induced to spawn by exposure to cyclic thermal shock in June 2015 (see Section 2.3.1), and their gametes were used to create five genetically-distinct replicate pools of larvae (2 males and 4 females per pool). The larval

cultures were fed daily a mixture of *Monochrysis* sp., *Chaetoceros muelleri*, *C. calcitrans*, *Tetraselmis chuii*, and *Isochrysis galbana* (clone T-Iso), per the recommendations for bivalve aquaculture (Helm et al. 2004). At 14 d post-fertilization (dpf), when the larvae had developed to the veliger stage, a subsample of approximately 100,000 larvae was removed from each replicate tank and placed into a 1 l beaker containing either control (32 ppt) or low salinity (20 ppt) UV-sterilized, filtered seawater (UV-FSW; 13.5 °C). Larvae were held in the control or low salinity treatments for 24, 48, or 72 h (n = 5 replicates each time point). We conducted water changes every 24 h and starved the larvae for the 24 h prior to sampling. At the end of each treatment, the larvae were isolated on a 48- μ m sieve, transferred to a sterile 1.5 ml Eppendorf tube, flash frozen in liquid N₂, and stored at -80 °C until analysis. At 26 dpf when the remaining larvae had transitioned to the pediveliger stage, another subsample containing approximately 100,000 pediveligers was placed into 1 l beakers containing control (32 ppt) or low salinity (20 ppt) UV-FSW (13.5 °C). As before, the pediveligers were sieved, flash frozen, and stored at -80 °C. Unfortunately, prior to 26 dpf, there was high mortality in one of the larval replicate tanks so only four replicates were taken at the pediveliger stage.

Juvenile *M. edulis* (26–45 mm in length) were collected from a subtidal population at the Darling Marine Center and transported to the University of Maine, Orono, ME, in September 2015. The mussels were held in a recirculating tank containing artificial seawater (Instant Ocean®) and fed a daily ration of Shellfish Diet 1800 (Reed Mariculture, Inc.). Following a 3-wk acclimation to 15 °C and 32 ppt, the mussels were placed in 1 l beakers containing control (32 ppt) or low (20 ppt) salinity artificial

seawater for 24, 48, or 72 h. As with the larval experiments, the water was changed daily and all mussels were starved for 24 h prior to sampling for metabolic profiling. At the end of each exposure, juvenile mussels were sacrificed ($n = 5$) and the gill, mantle edge, and posterior adductor muscle of each were dissected out; the tissues were flash frozen in liquid N_2 upon dissection and stored at $-80\text{ }^\circ\text{C}$. To avoid gamete-specific differences in the metabolic signatures (Hines et al. 2007) for the mussels used in this study, we avoided using the gametogenic portion of mantle. The gonad of mussels forms in the visceral mass but during reproductive periods it extends significantly into the mantle (Newell 1989), so we sampled tissues from young mussels that did not show signs of gonad production.

3.3.2 NMR Spectroscopy

The larval and juvenile tissue samples were processed to examine the metabolic profile of each sample using ^1H nuclear magnetic resonance spectroscopy (NMR). A small section of each tissue or a subset of each larval sample was placed into a pre-weighed, sterile, 1.5 ml tube. The tissue was dried overnight at room temperature in a SavantTM SpeedVacTM Concentrator (Thermo ScientificTM). The dried samples were ground using a mortar and pestle and the dry weight of each sample was measured. Metabolites were extracted by adding $30\text{ ml}\cdot\text{g}^{-1}$ dry weight of 2:1 acetonitrile-water mixture to the sample and vortexed to mix (Lin et al. 2007). Samples were spun at 13,000 g for 10 m at $4\text{ }^\circ\text{C}$ and the supernatant, containing the extracted metabolites, was removed and stored at $-80\text{ }^\circ\text{C}$. We used 100 μl of the supernatant from each to standardize across samples; each 100 μl sub-sample was dried in the SpeedVacTM, resuspended in 500 ml deuterium (D_2O), and dried again to remove residual water. Two

D₂O exchanges were conducted before the samples were redissolved in 500 ml D₂O containing 2 mM trimethylsilylpropanoic acid (TSP) and 1.96 mM maleic acid, which were used as internal reference standards for relative quantification. The extracts were then transferred into Wilmad® 5 mm glass NMR tubes and stored at 4 °C until analysis.

Samples were run on a 400 MHz Varian Inova NMR Spectrometer at room temperature. We acquired data using the instrument's default parameters, modified to include a 5000 Hz spectral width, 13.5 μs pulse width, 1 Hz exponential line broadening, and 64 transients. The transmitter was offset to the D₂O peak and chemical shifts were referenced to TSP (0 ppm). Standards containing the amino acids betaine, glycine, taurine, proline, glutamate, and ornithine were also run under the same specifications to aid in the identification of common metabolites.

A representative sample from each larval stage or tissue type was analyzed using 2D total correlation spectroscopy (TOCSY) to observe the coupling patterns of the components within each sample. These data provided structural information that helped verify the presence of amino acids and other metabolites in the corresponding 1D NMR data. The 2D spectra were obtained on the Varian 400 NMR Spectrometer at 30 °C. We acquired the 2D NMR using a 2.8 s recycle delay, a 30 μs pulse width, 1 Hz line broadening, and 64 transients over 512 t₁ increments, for a total of 2048 t₂ data points.

3.3.3 Data Analysis

The 1D NMR spectra were processed using ACD/NMR Processor Academic Edition Software. Data were Fourier transformed with a backward linear prediction for the first 2 points and then baseline corrected, phased, and calibrated to the TSP peak prior to analysis. For relative quantification, we manually selected and integrated the peaks for

TSP, alanine, β -alanine, taurine, glycine, betaine, homarine, and maleic acid (Table 3.1). For each compound of interest, we calculated the concentration following the method of Bharti and Roy (2012):

$$M_i = \left(\frac{I_i}{H_i} / \frac{I_s}{H_s} \right) * M_s \quad [2]$$

where M is the relative concentration, I is the integral of the peak(s), and H is the number of protons contributing to the signal for the peak of interest (i) relative to the maleic acid standard (s). The concentrations for the metabolites of interest were then standardized to the mean TSP concentration and adjusted for dry weight, to yield the relative concentration in $\mu\text{mole g}^{-1}$ dry tissue weight.

To make direct comparisons of the metabolites quantified from the larval and juvenile samples, we adjusted the dry weights for the larval samples to account for the mass contributed by the larval shell. For this analysis, we prepared Whatman GF/C™ Glass Microfiber filters (25 mm diameter) by soaking in reverse osmosis (RO) water for 1 h and drying them overnight at 65 °C. The filters were then ashed at 350 °C overnight in a Thermo Isotemp® Muffle Furnace and weighed. We placed a subset of larvae from each larval sample onto a filter and rinsed using 10 ml of 0.5 M ammonium formate to remove any residual salts from the seawater. The prepared samples were dried overnight at 65 °C and weighed (total dry weight), prior to ashing at 350 °C overnight to determine the ash-free dry weight (AFDW). The ratio of AFDW relative to dry weight was used to determine the proportion of the dry weight accounted for by the tissue (and not shell). The amino acid concentrations for each of the larval samples were then scaled by this proportion.

Compound	Shift (ppm)	Type	H
TSP	0	s	9
Alanine	1.46	d	3
β -Alanine	2.54	t	2
Taurine	3.43	t	2
Glycine	3.55	s	2
Betaine	3.91	s	2
Homarine	4.36	s	2
Maleic Acid	6.32	s	2

Table 3.1. Chemical shifts of key osmolytes detected by 1D ^1H NMR. We calculated the concentration of six amino acids and amino-acid derivatives relative to our two internal standards, TSP and maleic acid. The type of each peak exhibited by each compound is also indicated, where s = singlet, d = doublet, and t = triplet, as well as the number of protons (H) contributing to the signal.

The 2D NMR spectra were processed using SpinWorks 3.1 NMR data processor. We Fourier transformed the data using complex forward linear prediction, predicting from 2,048 to 4,096 points in the F2 dimension and from 512 to 2,048 points in the F1 dimension. Spectra were baseline corrected, phased, and calibrated to the TSP peak at 0 ppm. The coupling partners were recorded for each peak from the representative veliger, pediveliger, gill, mantle, and adductor samples and put into an Excel spreadsheet. The identification of metabolites was completed manually through reference to the primary literature and the Human Metabolome Database (Wishart et al. 2013).

Metabolic baselines were determined by analyzing the solute concentrations for larval and juvenile mussels from our 24 h control groups using ^1H NMR spectroscopy. To test for tissue-specific or stage-specific differences in the relative quantities of key metabolites such as alanine, taurine, glycine, betaine, and homarine, we ran a one-way ANOVA in SPSS Statistics 22.0 (IBM Corporation). For the juvenile samples, we tested the tissue-type as a fixed-factor, main effect using a Type III Sum of Squares model with $\alpha = 0.05$. To test for differences between larval stages, we used a one-way ANOVA with larval stage as a fixed-factor and tested stage as a main effect against a Type III Sum of Squares model. Two replicates of the baseline veliger samples were removed from analysis because of errors during extraction.

We also investigated temporal variation for the five most abundant metabolites contributing to the FAA pool under hypoosmotic conditions, glycine, alanine, taurine, betaine, and homarine. To test for the effects of low-salinity exposure on the concentrations of alanine, β -alanine, betaine, glycine, homarine, and taurine we used a series of two-factor ANOVAs. In each model, the effects of treatment (low and control

salinity) and length of exposure (24, 48 or 72 h) were fixed-factor, main effects. We included an interaction term and tested against a Type III Sum of Squares model with $\alpha = 0.05$. Four cases were excluded from analysis because of sample loss during preparation.

3.4. Results

3.4.1. Baseline Metabolic Profiles

We detected 99 distinct metabolite signatures using NMR on extracts from two larval stages and from the gill, mantle, and adductor tissues of juvenile *Mytilus edulis*. We confirmed the identity of 16 of these 99 metabolites (Table 3.2) using information obtained from the 2D TOCSY scans (Figure 3.1). Interestingly, only 9 of the 16 identified metabolites were common to both larval stages and all three tissues of the juvenile mussels: alanine, aspartate, betaine, glycine, homarine, hypotaurine, isoleucine, taurine, and threonine (Table 3.2, metabolites 1–9). Arginine, β -alanine, glutamate, glutamine, leucine, lysine, as well as four unknown metabolites, were found in larval and juvenile mussels, but were not always present in both larval stages or samples from all three tissues of the juveniles (metabolites 10–19, Table 3.2). Among these metabolites are amino acids and other amino acid derivatives that appear to be the major constituents of the *M. edulis* intracellular FAA pool, regardless of developmental stage.

We found several metabolites, however, whose presence or relative concentration varied across developmental stages. We observed 2 prominent peaks at 2.92 and 2.96 ppm that were present in the veliger and pediveliger samples, but were not detected in any of the juvenile samples (Figure 3.2a). These compounds likely comprise a large portion of the metabolite pool in larvae, but could not be identified with information

No	Metabolite	Chemical shift (multiplicity)
Common to all samples		
1	Alanine	1.46 (d), 3.77 (t)
2	Aspartate	2.68 (dd), 2.82 (dd), 3.87 (dd)
3	Betaine	3.26 (s), 3.91 (s)
4	Glycine	3.55 (s)
5	Homarine	4.36 (s), 7.96 (m), 8.03 (d), 8.53 (m), 8.69 (d)
6	Hypotaurine	2.63 (t), 3.36 (t)
7	Isoleucine	0.98 (m), 1.03 (m)
8	Taurine	3.25 (t), 3.43 (t)
9	Threonine	1.32 (d), 3.58 (d), 4.25 (t)
Common to larvae and juveniles		
10	Arginine	1.73 (m), 1.93 (m), 3.23 (m), 3.76 (m)
11	β -Alanine	2.56 (t), 3.18 (t)
12	Glutamate	2.05 (m), 2.14 (m), 2.38 (m), 3.76 (m)
13	Glutamine	2.14 (m), 2.42 (m), 3.76
14	Leucine	0.96 (t), 1.72 (m)
15	Lysine	1.73 (m), 1.88 (m), 3.02 (t)
16	Unknown #2 ¹	1.24 (s)
17	Unknown Metabolite	0.87 (m)
18	Unknown Metabolite	3.66 (m), 4.28 (d)
19	Unknown Metabolite	3.75 (d), 4.27 (t)
Larvae-specific		
20	Unknown Metabolite	2.92 (s)
21	Unknown Metabolite	2.96 (s)
22	Lactic acid	1.32 (d), 4.12 (m)
Juvenile-specific		
23	Unknown #1 ¹	1.09 (s)
24	Unknown Metabolite	2.25 (s)
25	Unknown Metabolite	2.56 (s)
26	Unknown Metabolite	3.11 (s), 3.28 (s)

¹Listed by identity from Tikunov et al. (2010)

Table 3.2. Table of common metabolites identified in *Mytilus edulis*. For each compound, the chemical shift (in ppm) and the type of peak are listed, where s = singlet, d = doublet, dd = doublet of doublets, t = triplet, and m = multiplet. The table is divided into metabolites that were common to all sample types (veliger, pediveliger, gill, mantle, and adductor), those common to larvae and juveniles (but not all juvenile tissues), those found in both larval stages, but not in juveniles (larvae-specific), and those found only in the juvenile samples (juvenile-specific). The numbers in the first column correspond the peak numbers in Figure 3.2.

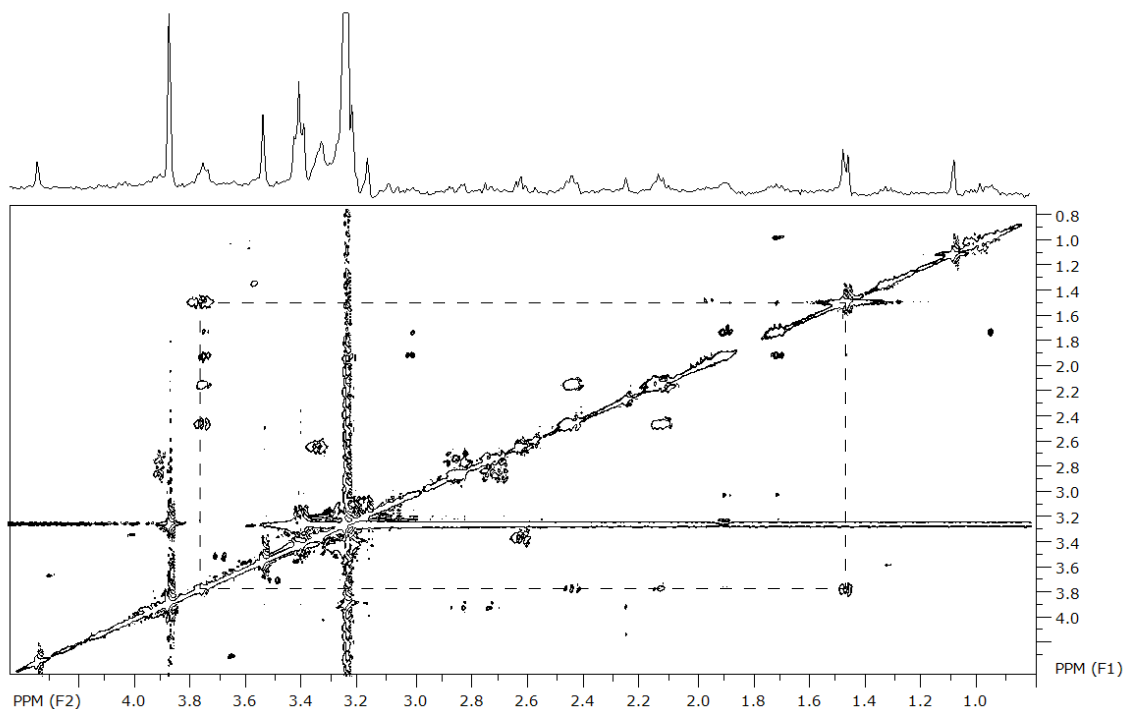


Figure 3.1. Representative 2D-TOCSY spectrum. Each peak in the 1D spectrum corresponds to a peak along the diagonal over 0–5 ppm, referenced to the chemical shift of TSP (0 ppm). The box on the 2D plot connects the cross-peaks contributed by the resonances of the hydrogen atoms within alanine, where there is a doublet at 1.46 ppm and a triplet at 3.77 ppm. These coupling patterns are used to verify the identity of the compounds in Table 3.2; the complete list of all coupling partners generated from the TOCSY experiments is provided in Table A.1.

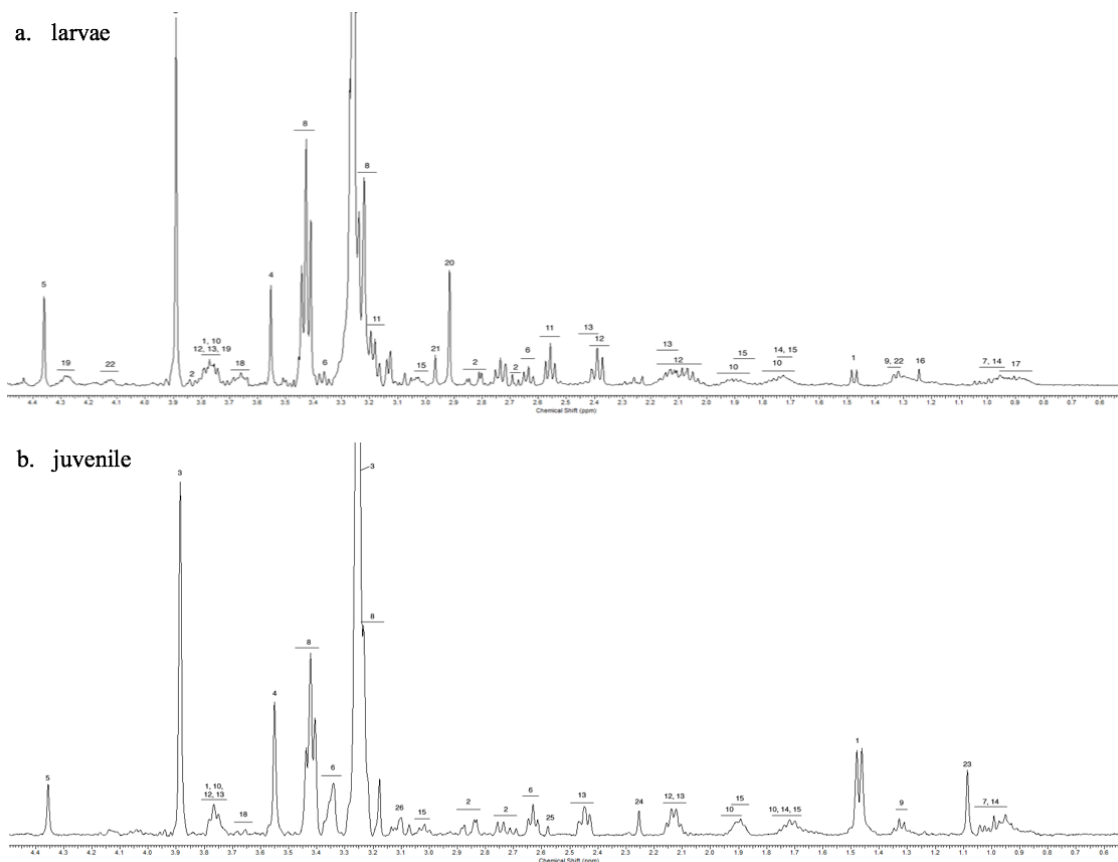


Figure 3.2. Representative ^1H NMR spectra. The 1D spectra for larval (a) and juvenile (b) mussels are shown over the 0–4.5 ppm range, where the chemical shifts for most of the metabolites we detected are found. The numbers above each peak correspond to the metabolites listed in Table 3.2. Spectra are referenced to the chemical shift of TSP (0 ppm).

present in the literature or online databases. Lactic acid also appeared to be specific to larvae, although, the chemical shift of lactic acid overlaps with that of threonine (and other metabolites at 1.32 ppm). Thus, it is possible that lactic acid was present in the juvenile samples, but that the concentrations were too low to see the long-range coupling protons at 4.12 ppm. In addition to the larval-specific metabolites, we observed four unknown metabolites at 1.09, 2.25, 2.56, and 3.11 ppm only in the juvenile samples (Figure 3.2b). The intensity of the peaks was high in some tissues, suggesting there are tissue-specific variations in concentration for these metabolites in post-metamorphic mussels.

While we observed the presence of stage-specific and tissue-specific metabolites, we could not determine the identity of most of the metabolites we detected (Table A.1). There were 13 metabolites found only in veligers and an additional 13 found only in pediveligers. In juvenile mussels, we observed 15 metabolites that were unique to the gill, 9 that were found only in the mantle tissue, and 12 in the adductor muscle. Surprisingly, we did not observe β -alanine or another metabolite, identified as “Unknown #2” by Tikunov et al. (2010), in the mantle of juvenile *M. edulis* even though these metabolites were present in our other samples. Similarly, unknown metabolite #18 (Table 3.2) was absent from the adductor muscle, but present in the gill and mantle tissue, as well as in veliger and pediveliger larvae. Other metabolites were detected in our pediveliger samples and samples from juvenile tissues, but not in profiles from veliger larvae (Table A.1). In contrast, we did not detect any metabolites common to veligers and juveniles but missing in the pediveliger profiles.

We used our 1D NMR data to investigate changes in the relative concentrations of six metabolites, alanine, β -alanine, betaine, glycine, homarine, and taurine, in more detail. These compounds play an important role in the FAA pool of mussels (Shumway et al. 1977, Davenport 1979, Livingstone et al. 1979, Deaton et al. 1985, Neufeld and Wright 1996), with taurine, betaine, and glycine being the most abundant (Figure 3.3). The composition of the FAA pools of veliger and pediveliger larvae were similar, although the concentrations of these metabolites in pediveligers tended to be higher than what we measured in veligers. However, there were no significant differences in the concentrations of these six metabolites among the two larval stages (Table 3.3).

We also measured the concentrations of these metabolites in the gill, mantle, and adductor muscle from juvenile mussels. In juveniles, the FAA pools were dominated by taurine and betaine, and to a lesser extent, glycine and alanine (Figure 3.3). Surprisingly, we observed tissue-specific differences in the concentrations of many of these solutes. The alanine content in the gill was significantly lower than the concentrations in the mantle and adductor muscle ($F_{2,12} = 4.988$, $p = 0.027$). Glycine abundance was significantly higher in the adductor than in the gill or the mantle ($F_{2,12} = 5.24$, $p = 0.023$); a similar pattern was observed for the variation in homarine ($F_{2,12} = 9.544$, $p = 0.003$). There was no variation in the abundance of taurine ($F_{2,12} = 1.701$, $p = 0.224$) or betaine ($F_{2,12} = 1.967$, $p = 0.182$) among the tissues of juvenile mussels.

The concentrations of metabolites measured in the larvae varied from those in the tissue samples of juveniles, suggesting stage-specific differences in the composition of FAA pools in blue mussels (Figure 3.3). Pediveligers had higher concentrations of taurine and betaine than any other stage or tissue and both larval samples had higher

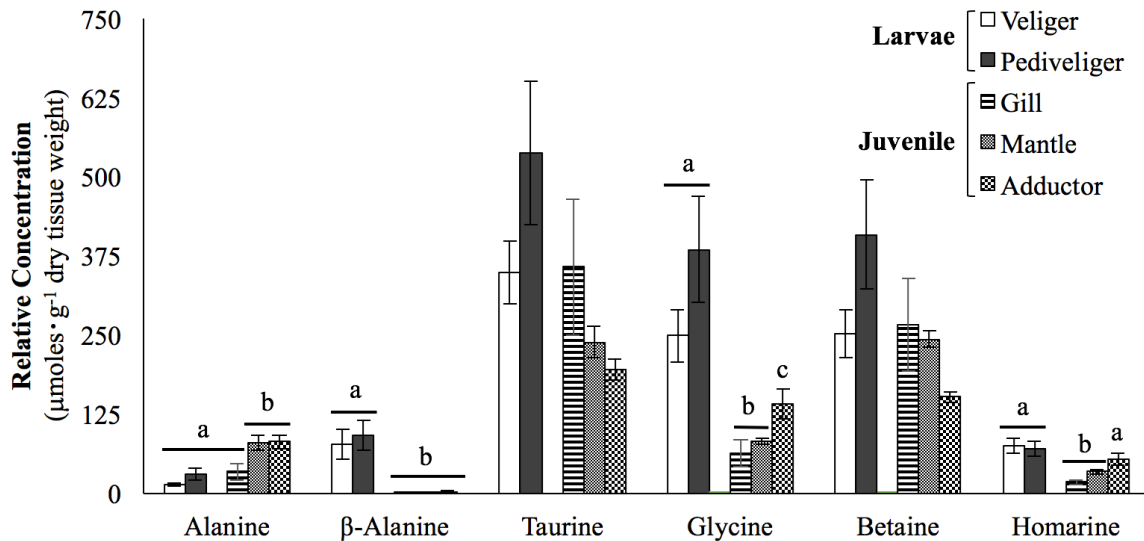


Figure 3.3. Relative concentrations of six intracellular osmolytes. The mean (\pm SE) concentrations of alanine, β -alanine, taurine, glycine, betaine, and homarine are shown for larval and juvenile mussels. Larval samples were analyzed for both veliger- (white bars; $n = 3$) and pediveliger-staged (black bars; $n = 4$) larvae, while data from the gill (horizontal-lined pattern), mantle (checked pattern), and adductor muscle (diamond pattern) were obtained from the tissues of individual juveniles ($n = 5$). Letters denote significant differences between the samples ($\alpha = 0.05$).

	Veliger	Pediveliger	$F_{1,5}$	p
Alanine	13.5 ± 2.6	29.3 ± 9.3	1.953	0.221
β-Alanine	77.9 ± 23.5	91.1 ± 23.3	0.151	0.713
Betaine	251.9 ± 36.7	408.7 ± 87.1	2.125	0.205
Glycine	248.4 ± 42.1	384.6 ± 83.9	1.671	0.253
Homarine	75.2 ± 12.4	70.0 ± 11.8	0.088	0.778
Taurine	349.5 ± 49.8	537.5 ± 114.2	1.796	0.241

Table 3.3. Relative concentrations of free amino acids in larval mussels. Stage-specific variation in the mean concentration of six metabolites ($\mu\text{mole g}^{-1}$ dry tissue weight \pm SE) is presented for veligers ($n = 3$) and pediveligers ($n = 4$). For each metabolite, the F statistic and associated p-value from a one-way ANOVA testing the significance of the difference in means among larval stages are provided.

concentrations of glycine and homarine than we observed in the tissues of juvenile mussels. The accumulation of β -alanine also appeared to be stage-specific as the concentrations were so low in the juvenile tissue samples that they could not be reliably quantified. Alanine was the only FAA that we observed in higher abundance in the juvenile samples relative to the larval samples, although this trend was restricted to the mantle and adductor tissues.

3.4.2. Metabolite Concentrations During Hypoosmotic Exposure

There was a general trend of decreasing concentration for the five predominant amino acids—taurine, betaine, glycine, homarine, and glycine—in the gill, mantle, and adductor muscle of juvenile *M. edulis* when the mussels were exposed to low salinity treatment (Table 3.4). We observed a significant decrease in glycine concentration in the gill and mantle tissues; for these tissues, there was a 72 % and 35 % drop in glycine concentration over the first 24 h of exposure, respectively. In addition to glycine, we also observed a significant decrease in the concentration of alanine in the adductor muscle; for both glycine and alanine the largest drop in concentration in the adductor muscle (39–49 %) occurred after 48–72 h of exposure to low salinity conditions.

Duration of exposure had a significant effect on the concentration of glycine ($F_{2,24} = 4.746$, $p = 0.018$), betaine ($F_{2,24} = 4.198$, $p = 0.027$), and homarine ($F_{2,24} = 4.129$, $p = 0.029$) in the gill tissue. However, this effect was driven by a decline in the concentration of these metabolites in the control mussels at 48 h and not resulting from low salinity exposure. This trend was also observed in the mantle tissue, with significant effects from the length of exposure on the concentrations of taurine ($F_{2,24} = 10.278$, $p = 0.001$),

	Duration of Exposure (h)						F
	24		48		72		
	30 ppt	20 ppt	30 ppt	20 ppt	30 ppt	20 ppt	
Gill							
Taurine	357.3 ± 239.7	345.3 ± 36.6	188.4 ± 98.0	343.2 ± 46.9	423.0 ± 97.2	359.6 ± 45.0	0.38
Betaine	266.2 ± 163.2	277.0 ± 50.3	152.0 ± 79.4	275.3 ± 61.3	345.4 ± 60.2	306.1 ± 45.2	1.00
Glycine	62.8 ± 45.4	17.6 ± 6.0	23.0 ± 6.8	14.8 ± 5.5	74.7 ± 25.9	22.7 ± 11.3	18.7*
Homarine	17.4 ± 8.3	13.3 ± 3.9	12.8 ± 10.1	7.7 ± 4.1	21.2 ± 6.7	16.3 ± 4.0	3.76
Alanine	34.2 ± 30.3	22.2 ± 7.7	20.4 ± 9.9	23.5 ± 7.8	24.7 ± 6.8	24.0 ± 10.0	0.56
Mantle							
Taurine	238.2 ± 54.9	224.6 ± 27.7	119.3 ± 50.4	200.3 ± 61.8	277.5 ± 29.1	220.3 ± 45.1	0.04
Betaine	243.3 ± 30.2	243.0 ± 50.9	149.2 ± 57.0	266.2 ± 65.2	315.6 ± 77.2	255.3 ± 72.9	0.71
Glycine	81.5 ± 10.3	52.9 ± 13.5	31.6 ± 10.1	37.5 ± 38.1	89.4 ± 17.1	37.8 ± 23.9	10.2*
Homarine	34.2 ± 7.0	29.6 ± 7.6	25.0 ± 15.3	27.3 ± 13.7	42.8 ± 13.0	39.0 ± 15.8	0.19
Alanine	80.4 ± 25.5	73.1 ± 23.6	43.9 ± 22.2	58.8 ± 65.0	63.3 ± 29.7	53.9 ± 53.0	0.00
Adductor							
Taurine	195.6 ± 38.1	216.3 ± 54.1	270.0 ± 24.3	263.8 ± 36.3	295.6 ± 51.0	198.1 ± 33.6	3.44
Betaine	151.7 ± 20.3	177.7 ± 77.7	192.8 ± 39.6	213.7 ± 61.4	224.6 ± 74.0	158.6 ± 29.3	0.10
Glycine	141.6 ± 51.7	137.4 ± 16.9	208.9 ± 77.0	110.3 ± 36.7	211.3 ± 48.6	100.7 ± 53.0	14.8*
Homarine	53.4 ± 19.7	57.8 ± 22.5	62.8 ± 23.7	48.3 ± 14.7	79.1 ± 13.1	65.4 ± 40.6	0.81
Alanine	80.8 ± 24.3	66.1 ± 16.4	95.5 ± 38.9	58.6 ± 24.9	124.8 ± 40.7	63.3 ± 13.1	11.4*

Table 3.4. Concentrations of FAAAs in the tissues of juvenile mussels. The mean concentrations ($\mu\text{moles}\cdot\text{g}^{-1}$ dry weight \pm SE) of

alanine, betaine, glycine, homarine, and taurine, measured using NMR spectroscopy, are listed for the gill, mantle margin, and

adductor mussel of juvenile *M. edulis*. We estimated the concentrations for mussels held under control (30 ppt) or a low-salinity (20

ppt) conditions for 24, 48, or 72 h. The column at right (*F*) indicates the F-statistic for the main effect of salinity treatment in a two-

way ANOVA for each tissue by metabolite combination. An asterisk indicates metabolites for which the concentration in low salinity

treatments was significantly different than in control mussels with $p < 0.05$.

glycine ($F_{2,24} = 7.100$, $p = 0.004$), betaine ($F_{2,24} = 4.053$, $p = 0.030$), and homarine ($F_{2,24} = 3.506$, $p = 0.046$). In the mantle, there was a significant interaction between treatment and length of exposure on the concentrations of taurine ($F_{2,24} = 5.756$, $p = 0.009$), glycine ($F_{2,24} = 4.655$, $p = 0.020$), and betaine ($F_{2,24} = 5.440$, $p = 0.011$). For the adductor muscle samples, we detected a significant effect of the length of exposure ($F_{2,24} = 5.789$, $p = 0.009$) and the interaction between treatment and length of exposure ($F_{2,24} = 5.752$, $p = 0.009$) on the concentrations of taurine. The taurine content in the control groups increased from 24 to 72 h, while the concentration of taurine in the treatment groups was similar to the controls until 72 h when it dropped by roughly 33 %.

In addition to taurine, betaine, homarine, glycine, and alanine, we monitored changes in the concentration of β -alanine in larval mussels, which was more abundant in veliger and pediveliger mussels compared to juveniles (Figure 3.3). Veliger and pediveliger larvae that were exposed to low salinity had decreased concentrations of all six osmolytes at all time points tested (Table 3.5). In the both veliger and pediveliger larvae, glycine and β -alanine concentrations were significantly reduced in the low salinity treatment groups. There was no evidence for either a duration of exposure or an interaction between salinity treatment and duration of exposure on the concentrations of FAAs in veliger mussels. In contrast, in the pediveligers there was a significant effect of the length of exposure on the concentrations of β -alanine ($F_{2,18} = 4.750$, $p = 0.025$), glycine ($F_{2,18} = 5.671$, $p = 0.012$), betaine ($F_{2,18} = 3.733$, $p = 0.044$), and homarine ($F_{2,18} = 4.311$, $p = 0.030$). We observed a decrease in the concentrations of all six osmolytes, regardless of treatment, at 72 h compared to 24 h in the pediveligers.

Veliger	Duration of Exposure (h)						F
	24		48		72		
	30 ppt	20 ppt	30 ppt	20 ppt	30 ppt	20 ppt	
Taurine	349.5 ± 86.2	309.9 ± 27.4	293.5 ± 131.9	244.1 ± 60.6	283.1 ± 61.9	272.0 ± 65.1	1.12
Betaine	251.9 ± 60.6	207.8 ± 9.7	231.5 ± 102.3	168.3 ± 47.0	218.2 ± 62.0	205.0 ± 55.9	3.15
Glycine	248.4 ± 72.9	82.4 ± 11.3	232.5 ± 121.6	61.6 ± 24.1	183.9 ± 49.6	59.6 ± 19.1	39.6*
β-alanine	77.9 ± 40.7	38.7 ± 10.3	67.8 ± 37.9	38.6 ± 13.6	70.2 ± 29.8	44.0 ± 25.7	9.59*
Homarine	75.2 ± 21.4	54.6 ± 5.2	52.3 ± 26.1	48.6 ± 11.4	56.6 ± 17.4	49.5 ± 13.0	2.55
Alanine	13.5 ± 4.5	12.8 ± 2.7	17.1 ± 9.4	10.9 ± 5.9	14.4 ± 7.3	11.9 ± 7.6	1.38
Pediveliger							
Taurine	537.5 ± 228.3	450.0 ± 207.0	359.8 ± 174.5	365.3 ± 158.1	298.7 ± 71.9	297.3 ± 51.0	3.07
Betaine	408.7 ± 174.2	307.3 ± 136.4	269.0 ± 115.3	249.2 ± 91.1	228.0 ± 62.2	188.2 ± 15.9	1.39
Glycine	384.6 ± 167.9	122.9 ± 60.8	220.6 ± 106.2	72.1 ± 22.8	174.5 ± 53.0	48.5 ± 5.3	24.7*
β-alanine	91.1 ± 46.6	54.1 ± 38.1	55.6 ± 20.8	29.6 ± 21.6	37.6 ± 16.2	25.0 ± 2.8	4.75*
Homarine	70.0 ± 23.6	57.8 ± 25.0	46.6 ± 16.9	49.4 ± 18.4	41.3 ± 16.2	32.0 ± 4.2	0.66
Alanine	29.3 ± 18.6	18.7 ± 16.5	20.4 ± 7.5	16.5 ± 3.9	10.0 ± 3.4	9.5 ± 3.3	1.27

Table 3.5. FAA concentrations in larval *M. edulis* during low salinity exposure. The mean concentration of alanine, β-alanine,

betaine, glycine, homarine, and taurine ($\mu\text{moles}\cdot\text{g}^{-1}$ dry tissue weight \pm SE) are shown for veligers and pediveligers under control (30 ppt) and low salinity (20 ppt) conditions. The column at right (*F*) indicates the F-statistic for the main effect of salinity treatment in a two-way ANOVA for each stage by metabolite combination. An asterisk indicates metabolites for which the concentration in low salinity treatments was significantly different than in control larvae with $p < 0.05$.

3.5. Discussion

Our ^1H NMR-based metabolite study in *Mytilus edulis* resolved 99 metabolites in two larval stages and three tissues sampled from juvenile mussels (Table A.1). Overall, we were successful in positively identifying 22 metabolites (Table 3.2), which is comparable to what has been identified in other metabolomic studies of blue mussels, such as Tuffnail et al. (2009) and Ellis et al. (2014). However, only 50 % of the 32 total metabolites identified across all three studies were observed in more than one study. These 16 metabolites have also been reported in NMR-based studies of *M. galloprovincialis* (Hines et al. 2007, Jones et al. 2008, Cappello et al. 2013) and oysters (Tukinov et al. 2010).

The difference in the metabolites detected by each study is likely to have a methodological basis. For example, Lin et al. (2007) demonstrated that solvents differ in their extraction efficiency for certain amino acids; Ellis et al. (2014) used a methanol/chloroform mixture, while we used an acetonitrile/water extraction. Furthermore, our studies also varied in the methods that were used to identify metabolites. Tuffnail et al. (2009) only used information from 1D NMR referenced to other published research to identify metabolites in their study, while Ellis et al. (2014) ran homonuclear J-resolved (JRES) 2D spectroscopy experiments. We used 2D TOCSY experiments, which generally have higher resolution and provide more structural information that can be used to confidently identify metabolites (Dona et al. 2016). Further, analysis of our 1D spectra suggested the presence of many of the metabolites found in the other two studies; even so we were unable to confirm these findings using the data generated from the TOCSY studies and spectral information available from Wishart et al. (2013). Differences in the

metabolites reported may also be related to functional characteristics of the type or portion of the tissue (i.e. gametogenic versus mantle edge) used in each study.

Regardless of the reason for the discrepancies among studies, the metabolite data we collected from *M. edulis* using NMR spectroscopy indicate there are striking differences in the metabolite pools across developmental stages and among tissues of post-metamorphic mussels acclimated to ambient conditions (13.5 °C, 30 ppt). Of the 99 metabolites that were detected in our study, only 9 were common among both larval samples and within the three tissues we sampled from juvenile blue mussels (Table 3.2). An additional 10 metabolites were present in larval and juvenile mussels, but were not detected in one or more stages or tissues. However, the prevalence of these metabolites (many of which are osmolytes) among tissues and throughout development reveals their importance to cellular function in *M. edulis*.

3.5.1. Composition of FAA Pools in Juvenile Mussels

A primary goal of our project was to document stage- and tissue-specific differences in the abundance of free amino acids (FAA). FAAs typically function as osmolytes in marine invertebrates, in addition to maintaining a stable intracellular environment (Lewis 1952) and serving as stores for protein synthesis or energy metabolism (Somero 1986). A number of studies have examined variation in the FAA pools of post-metamorphic *M. edulis* (e.g., Shumway et al. 1977, Livingstone et al. 1979, Deaton et al. 1985); our inclusion of more tissue types and larval stages complements and builds on their foundation.

In juvenile mussels, we found that taurine and betaine were the most prevalent organic osmolytes found, regardless of tissue type (Figure 3.3). Taurine and betaine act as

counterbalancing solutes and promote cellular stability (Bowlus and Somero 1979, Yancey 2005), so relatively high concentrations of these metabolites are important to the maintenance of cellular function in both stressed and unstressed mussels. Furthermore, these solutes are not synthesized by post-metamorphic mussels and must be taken up from the environment or obtained through the diet (Bishop et al. 1983), so retention at high concentrations is likely to be energetically advantageous and osmotically important. Taurine is often cited as the most abundant osmolyte in blue mussels, and overall, the concentration of taurine in the tissues we examined were similar to that observed in previous studies of the adductor muscle (Bricteux-Grégoire et al. 1964, Shumway et al. 1977) and digestive gland (Livingstone et al. 1979) of *M. edulis*. Although Lange (1963) claimed that the concentrations of taurine were 50 % higher in the adductor muscle than the gill or mantle, we did not observe significant differences in taurine concentration among tissues (Table 3.3). Several studies suggest that taurine constitutes 28–83 % of the FAA pool (Lange 1963, Livingstone et al. 1979, Wright and Secomb 1986, Wright et al. 1987, Rice and Stephens 1988); however, betaine was not measured in those studies. In all three tissue types that we studied, we detected similar concentrations of taurine and betaine, which Bricteux-Grégoire et al. (1964) had also reported in the adductor muscle of *M. edulis*. Our findings suggest that taurine and betaine are important osmolytes in *M. edulis* and that previous studies, such as those of Wright et al. (1992) and Deaton (2001), may have overestimated the contribution of taurine and underestimated the contribution of betaine to FAA pools.

We observed significant differences in the concentration of glycine among three tissues of juvenile mussels (Figure 3.3). Glycine is a common osmolyte found in mussels.

High concentrations of this metabolite do not affect enzyme stability (Bowlus and Somero 1979, Yancey et al. 1982), it is naturally abundant in seawater (Stephens and Schinske 1961, Crawford and Webb 1968, Péquignat 1973), and it is synthesized via multiple metabolic pathways (Manahan 1983). The concentrations of glycine we observed in the adductor are comparable to that reported in Shumway et al. (1977). Our results are consistent with Zandee et al. (1980), who found that concentrations of glycine in the adductor are higher than in the gill or mantle in *M. edulis*, and with Wright et al. (1987) who reported low concentrations of glycine in the gill and mantle tissue of *M. californianus*. Wright et al. (1987), however, found that the glycine content of the mantle was roughly 4-fold higher than in the gill, whereas in our study, the difference in glycine concentration between these two tissues was on the order of 30 %. Tukinov et al. (2010) and Ellis et al. (2014) also reported differences in the amount of glycine among tissue blocks of oysters and in the mantle of male and female *M. edulis*, respectively, which both authors attributed to glycine's role in energy metabolism via oxidation or conversion to pyruvate. Overall, variation in glycine content among the tissues of *M. edulis* is likely a reflection in different aerobic metabolic demands of the tissue.

The concentrations of alanine also differed among tissue types in our study, with the alanine content of the adductor and mantle approximately 2-fold higher than that of the gill (Figure 3.3). The concentration of alanine in the adductor muscle reported by Shumway et al. (1977) was 25 % of what we found. Although Wright et al. (1987) did not find any differences in the alanine concentrations in the gill and mantle of *M. edulis*, Rice and Stephens (1988) observed that alanine concentrations in the gill were 10-fold higher than the mantle and 50-fold higher than in the adductor, which is the opposite of

what we found. Combined, these results suggest that concentrations of alanine are likely highly variable and context-specific and likely reflect tissue-specific metabolism. Alanine is an end-product of anaerobic metabolism (De Zwaan and Wijsman 1976), and accumulations of alanine have also been associated with prolonged starvation in mussels (Bayne 1973).

We also detected homarine (*N*-methyl picolinic acid), a compound that is typically considered a metabolic byproduct in marine invertebrates (Gasteiger et al. 1960). Although not commonly studied in bivalves, studies in crustaceans suggest that homarine is derived from glycine and may be involved in methylation reactions to create betaine (Netherton and Gurin 1982) or may itself function as an osmolyte (Nishitani et al. 1995). The concentrations of homarine were highest in the adductor muscle and lowest in the gill (Figure 3.3). Given the gill is one of the first tissues to respond to osmotic stress (Silva and Wright 1992), our observation suggests that homarine does not play a leading role in osmoregulation. Instead, because glycine concentrations were also high in the adductor, we propose that homarine variation reflects differences in betaine metabolism among the tissues we sampled.

In addition to tissue-specific differences in the FAA pools, we also observed numerous tissue-specific metabolites (Table A.1), likely resulting from the specific metabolic demands of a particular tissue type. For instance, the gill had the highest diversity of solutes among the tissues included in our study; 42 % of all metabolites we catalogued were detected in this tissue type. In mussels, the gill functions in osmoregulation (Rice and Stephens 1988) and maintenance of intracellular FAA pools (Wright et al. 1987), so it is perhaps not surprising that we observed a high number of

metabolites in the gill. At the same time, many of the FAAs we quantified were in lower concentrations in the gill. This tissue-specific variation may stem from leakage of the amino acids out of the gill (Wright et al. 1987), given that the gill is more permeable than mantle or adductor muscle, or from differences in metabolism to meet tissue-specific cellular energy demands.

Variation in the baseline composition of the metabolite pool was also observed in the mantle margin, which functions in secretion of the shell (Wilbur and Saleuddin 1983). With the exception of alanine, the concentrations of all amino acids within the mantle were intermediate to those in the gill and mantle. Wilbur and Saleuddin (1983) suggest alanine is associated with the production of succinate to sequester H^+ created as a byproduct from secretion of the bicarbonate shell, so the increased levels of alanine observed in this tissue may result from processes associated with biomineralization.

Surprisingly, we also detected cysteine-*S*-sulfate (Table A.1) in the mantle, an intermediate in the biosynthesis of taurine from cysteine (Bishop et al. 1983). Taurine is normally obtained from the diet, though low levels of biosynthesis are possible (Bishop et al. 1983). The levels of taurine in the mantle were lower than that of betaine, so this may be a mechanism used to increase intracellular concentrations when uptake from the environment is not adequate.

Our data from the posterior adductor muscle suggest that under ambient conditions, the tissue utilized anaerobic metabolism. Alanine, which is created during anaerobiosis (De Zwaan and Wisjman 1976), was significantly increased in the adductor compared to the gill. We also detected citric acid in the adductor (Table A.1), which accumulates as the TCA cycle slows (Bishop et al. 1983). Shick et al. (1986) found

increases in anaerobic end products, including alanine, were related to valve movements in mussels recovering from aerial exposure. Given that the adductor regulates opening and closing of the valves (Lowy 1953), our results suggest that anaerobic pathways are likely an important mechanism for generating energy in this tissue under baseline conditions. These findings are further supported by the increased glycine content and decreased taurine in the adductor (Figure 3.3), which Zandee et al. (1980) suggested results from negative nitrogen balance, which may result from increased amino acid catabolism during stress.

3.5.2. Composition of Larval FAA Pools

The composition of the FAA pools in larvae are relatively similar to those we observed in juvenile mussels (Table 3.3). In both veliger and pediveliger larvae, taurine, betaine, and glycine were the most abundant metabolites identified and accounted for over 80 % of the total quantified. Previous studies suggest that taurine constitutes approximately 70 % of the FAA pool of bivalve larvae (Manahan 1989, Widdows 1991). In contrast, we found that taurine accounts for approximately 40 % of the baseline FAA concentrations in veliger and pediveliger larvae and that the concentration of taurine was only 30 % higher than those of betaine and glycine. Although we were not able to measure the concentration of all metabolites found within larval mussels, our study suggests that taurine abundance is lower than previously reported and that glycine and betaine are also found in high abundance. The concentrations of taurine and betaine were notably higher in the pediveligers than in the veligers or juvenile tissues (Figure 3.3). We attribute this to higher rates of taurine biosynthesis at this stage, because larvae, unlike

post-metamorphic mussels, obtain taurine through *de novo* synthesis (Welborn and Manahan 1995).

Glycine concentrations in the larval samples were over 40 % higher than what has reported for any of the tissues of the juvenile mussels (Figure 3.3). Manahan (1983) found that the uptake of glycine, which could be used as an energy source, was quicker in bivalve larvae was quicker than in juveniles. Considering the metabolic demands for growth in veliger and pediveliger larvae, it would be advantageous for larvae to retain high intracellular levels of glycine. *M. edulis* larvae are also capable of taking up alanine rapidly from the environment and incorporating it into protein (Manahan 1983), so the low levels of alanine we observed in our larval samples may reflect the transfer of alanine out of the FAA pool into proteins.

Interestingly, we only observed appreciable concentrations of β -alanine in mussel larvae. β -alanine can act to stabilize proteins (Bowlus and Somero 1979), is important for redox balance (Yancey 2005), and often serves as an osmolyte in a variety of marine invertebrates (Kasschau et al. 1984, Yancey 2005). Given these functions, it is surprising that we did not detect β -alanine in the juvenile samples. Livingstone et al. (1979) reported that β -alanine made up only 0.3 % of the total FAA pool in the digestive gland of *M. edulis*, while in larvae, we found it was more abundant and accounted for more than 7 % of the metabolites quantified. The presence of β -alanine is shown to block uptake of taurine in the gill of *M. californianus* (Neufeld and Wright 1995). Thus, we interpret the higher concentrations of β -alanine in larvae as further evidence of high levels of taurine synthesis, rather than uptake, in the larval stages.

To our knowledge, this is the first NMR-based metabolomic study to examine the composition of FAA pools in blue mussel larvae. We observed numerous metabolites that were unique to veliger and pediveliger larvae, including two unknown metabolites at 2.92 and 2.96 ppm. The intensity of these peaks was comparable to that of glycine or homarine, so it is likely that these unknown metabolites are important functional components of mytilid larvae. Unfortunately, both peaks had a single resonance and did not appear to have any coupling partners, so determining their identity using online databases was not possible. We also identified other metabolic signatures that were unique to each larval stage (Table A.1), but again, the identities of these metabolites are unknown. As veligers, mussels invest substantial amounts of energy into tissue growth and deposition of the larval shell (prodossoconch II; Sprung 1984), so it is likely that many of these metabolites are byproducts of energy metabolism or shell secretion. Pediveligers, on the other hand, are preparing for metamorphosis (Sprung 1984), are rapidly increasing in size (Widdows 1991), and have developed a pedal organ. The unidentified solutes found with pediveliger may reflect metabolic differences associated with the developmental maturation, tissue growth, or the abundance of neurotransmitters.

3.5.3. Effects of Low Salinity on FAA Pools

In both larval and juvenile mussels, changes in the free amino acid pools during hypoosmotic exposure resulted from large decreases in glycine content (Tables 3.4 and 3.5). Previous studies on the fluxes of free amino acids from the tissues of low salinity-challenged *M. edulis* have reported the utilization of various FAAs, although these studies differed in the tissue sampled, duration of exposure, and how the low salinity treatment was applied. The role of glycine during the salinity response in blue mussels

has been evaluated in other studies (Bricteux-Grégoire et al. 1964, Gilles 1972, Shumway et al. 1977, Livingstone, et al. 1979, Deaton et al. 1985), although glycine has received less attention compared to taurine. In studies of larval blue mussels, we found that the glycine content began to decrease after 6 h of exposure to low salinity (Tables C.1 and C.2); this decrease persisted in all stages and tissues through 72 h (Tables 3.4 and 3.5). As mentioned above, glycine is an important osmolyte and its prevalence in the cell, along with low energy content, makes loss during hypoosmotic stress relatively energetically inexpensive. Glycine concentrations vary seasonally in blue mussels, which Kluytmans et al. (1980) suggested was due to its incorporation into pyruvate via serine as a means of generating cellular energy. It is likely serving a similar role during hypoosmotic exposure.

The changes in the concentrations of betaine or taurine we noted for larval and juvenile blue mussels during low salinity exposure were not statistically significant. Bricteux-Grégoire et al. (1964) observed decreases in betaine and taurine in the adductor muscle after 48 or 72 h of exposure, while other authors have reported that changes in the intracellular concentrations of taurine in *M. edulis* only begin after prolonged exposure (weeks) to low salinity (Gilles 1972, Hoyaux et al. 1976, Livingstone et al. 1979). Losses of taurine and betaine are likely energetically expensive and both metabolites may provide a benefit to the cell during osmotic stress (Bowlus and Somero 1979, Huxtable 1992), so loss of these osmolytes only occurs during longer exposures when the mussel is experiencing higher levels of stress.

The adductor muscle responds differently compared to the gill and mantle tissue with respect to variation in the concentrations of glycine, betaine, and taurine. These

tissues vary in their permeability (Wright et al. 1987), in the number of solute transporters found within each of the tissues (Rice and Stephens 1988), and in the indirect effects of osmolytes on cellular function (Yancey 2005). For instance, Babarro and Fernández-Reiriz (2006) speculated that taurine plays a role in mucus formation on the gills, which may explain why variation in taurine concentrations was reduced in the gill relative to the adductor muscle. We observed a significant decrease in the concentration of alanine along with glycine in the adductor muscle, whereas only glycine changed significantly in the gill and mantle tissues of juvenile mussels during low salinity exposure (Table 3.4). The adductor mussel had the highest concentrations of alanine, which likely results from anaerobic metabolism within this tissue, making it more readily available as an osmolyte. In any case, it is apparent that tissue-specific differences in the flux of osmolyte concentrations are not necessarily reflective of the whole organism.

This is the first study to evaluate changes in the FAA pools of larval mussels under hypoosmotic conditions. In addition to glycine loss, there was a decrease in the concentration of β -alanine in larval mussels during low salinity exposure (Table 3.5). Although the presence of β -alanine in FAA pools of *M. edulis* was reported by Livingstone et al. (1979), to our knowledge, decreases in β -alanine during low salinity exposure have not previously been observed. As discussed above, we did not observe appreciable concentrations in β -alanine in juvenile mussels, indicating that this response is unique to larval mussels. In bivalves, β -alanine is synthesized from aspartate or from the polyamine spermine (Meng et al. 2013) making it relatively easy to replace following low salinity exposure. As with the tissue-specific differences in the utilization of FAAs,

the flux of β -alanine likely stems from differences in larval metabolism that lead to its accumulation in cells.

We also observed stage-specific differences in the response of other components of the FAA pools in larval mussels compared to juveniles. For instance, the magnitude of the glycine flux was much larger than what we observed in juvenile mussels. In salinity-treated veligers and pediveligers, there was a roughly 70 % decrease in glycine compared to its 50 % decrease in the adductor and mantle tissues of juvenile mussels. Larvae have higher rates of leakage than juvenile mussels because of their increased surface area to volume ratio (Manahan 1983), which increases the likelihood of FAA loss to the environment relative to juveniles. Larvae also expend considerable amounts of energy on growth (Sprung and Widdows 1986), which may be accounted for by increased energy metabolism though glycine (Kluytmans et al. 1980).

Changes in the taurine concentrations in treatment versus control groups also varied developmentally and was greater in larvae after 24 and 48 h of exposure to low salinity, but not at 72 h. In larval bivalves, taurine is synthesized *de novo* (Welborn and Manahan 1995), but in post-metamorphic mussels it must be obtained from the diet (Allen and Awapara 1960, Bishop et al. 1985). Thus, it is surprising from an energetic standpoint that larvae would have greater decreases in taurine relative to juveniles. However, the dietary need for taurine increases with age in *C. gigas* larvae (Welborn and Manahan 1995), so it is possible that increases in metabolism during stress contribute to a greater taurine loss in larvae. Relative to juvenile mussels, the high energy demands of larvae may lead to increased susceptibility to hypoosmotic stress.

This study contributes to our understanding of the metabolic baselines of veliger and pediveliger larvae and highlights important biochemical differences in the FAA pools of various tissues of post-metamorphic *M. edulis*. We found variations in the composition and utilization of FAAs within larval and juvenile mussels, which provides insight into the role of these metabolites in energy metabolism and maintaining osmotic balance within the cell. Furthermore, many of the metabolites measured in this study function as osmolytes, so understanding their distribution and abundance across tissues and life-history can improve our understanding on the capacity of different developmental stages to respond to salinity and other environmental stressors.

Variation in the baseline concentrations of these osmolytes among various tissues and developmental stages likely plays a role in the observed responses to hypoosmotic stress. Larval mussels—which vary from post-metamorphic mussels in form, function, lifestyle, and habitat—showed differences in their utilization of osmolytes during low salinity exposure. A better understanding of the larval metabolome, as well as their ability to regulate FAA pools provides insight into why larval mussels are more susceptible to hypoosmotic stress than juvenile or adult mussels (Qiu et al. 2002). Similarly, tissue-specific variations in the utilization of metabolites during low salinity treatment in juveniles reflected variation in the function of these tissues, which helps improve our understanding of the osmotic stress response in post-metamorphic mussels. Together, these observations highlight the importance of foundational metabolomic studies that include multiple tissue types and developmental stages to adequately evaluate organismal responses to stress and better place their findings in a broader ecological context.

CHAPTER 4

COMPARING CELLULAR RESPONSES OF LARVAL AND JUVENILE BLUE MUSSELS (*MYTILUS EDULIS*) TO LOW SALINITY EXPOSURE

4.1 Abstract

Blue mussels (*Mytilus edulis*) live in coastal estuarine and marine habitats that may be threatened by decreases in nearshore salinity associated with global climate change. Mussels are osmoconformers and exposure to low salinity conditions triggers an organismal response that may be mediated by changes in transcription. Previous studies have evaluated the tissue-level responses to osmotic stress in *M. edulis* or transcriptomic responses in blue mussel congeners, but there has not yet been an attempt to monitor changes in the levels of gene expression in osmotically challenged *M. edulis* or to link patterns of expression to cellular-level responses. Using a combination of techniques, we evaluated transcriptomic responses of juvenile *M. edulis* during short-term low-salinity treatment, while also monitoring changes in O₂ consumption and NH₃ excretion. We expanded this study to include two larval stages (veliger and pediveliger), since blue mussels have a complex life history and little is known about how larval mussels respond to low salinity. We found tissue- and stage-specific responses in the expression of genes that may be involved in regulation of the FAA pools—betaine-homocysteine *S*-methyltransferase (*BHMT*) and the taurine transporter (*TAUT*)—though it is possible that transcription of these genes is related to retention of the counterbalancing osmolytes, betaine and taurine. These results, along with variation at the organismal level, suggest

that the response to osmotic stress in *M. edulis* is highly dependent on tissue- and stage-specific differences in metabolism and morphology.

4.2 Introduction

Blue mussels in the *Mytilus edulis* species-complex are marine and estuarine invertebrates that inhabit coastal areas in North America and Europe. These species are osmoconformers and respond to decreases in environmental salinity by reducing the concentrations of intracellular ions and osmolytes to maintain an osmotic pressure equilibrated to the environment (Costa and Pritchard 1978, Davenport 1979). Fluctuations in nearshore coastal salinity are projected to increase in frequency and severity as a consequence of global climate change (Antonov et al. 2002, Durack et al. 2012), potentially threatening the persistence of local mussel populations. The species within the *Mytilus* complex, *M. edulis*, *M. trossulus*, and *M. galloprovincialis* (Koehn 1991), differ in their tolerance to low and fluctuating salinity (Gardner and Thomson 2001, Qiu et al. 2002, Braby and Somero 2006) and have been the subjects of comparative studies to better understand species-specific differences in low-salinity resilience. A deeper understanding of the blue mussels' capacity to cope with altered salinity will be important for predicting how mussel abundance and distribution may shift with changing climate.

The response to hypoosmotic exposure in blue mussels can be measured at multiple levels of organization (Pierce 1982). In mussels, the changes at the organismal level include altered behavior (i.e. valve closure; Davenport 1979) and increases in O₂ consumption (Stickle and Sabourin 1979) and NH₃ excretion (Bishop 1976, Livingstone et al. 1979). At the cellular-level, mussels decrease the concentration of free amino acids

(FAA), including methylamines, amino acids, and amino acid derivatives (Bowlus and Somero 1979). Organic osmolytes such as these are utilized during periods of decreased salinity because they can be lost without altering the pH or inorganic ionic balance and, therefore, help to maintain function of the cell (Somero 1986, Yancey et al. 1982). These cellular-level responses, including amino acid transport and catabolism, are mediated by changes in gene expression (Burg et al. 1996, Kültz 2005, Lockwood and Somero 2011). Several studies have evaluated the organismal and cellular-level responses in mytilids (e.g., Bricteux-Grégoire et al. 1964, Shumway et al. 1977, Davenport 1979, Livingstone et al. 1979, Neufeld and Wright 1996), yet only one to date by Lockwood and Somero (2011) has studied transcriptomic responses of blue mussels during low salinity exposure. Their study, however, did not include *M. edulis*. In the western North Atlantic, *M. edulis* is one of the predominant mussel species where its range overlaps with that of *M. trossulus* (Koehn 1991, Rawson et al. 2001); these species are important members of intertidal and subtidal communities throughout the region (Arribas et al. 2014).

To improve our understanding of the underlying molecular mechanisms of the osmotic stress response in blue mussels, we compared the transcriptomic responses of *M. edulis* and *M. trossulus* during hyposaline exposure. Using an oligonucleotide microarray-based approach, we identified differentially expressed genes in *M. edulis* and *M. trossulus* at a salinity where the two species begin to show divergence in their tolerance (Qui et al. 2002). Blue mussels are considered ‘non-model’ species due to the lack of detailed genomic information. As Kültz et al. (2007) have discussed, this places constraint on efforts to clearly annotate transcriptomic data and ascribe function to differentially expressed genes. Thus, we used the microarray data to identify and further

study candidate genes involved in amino acid metabolism and transport of two important osmolytes, betaine and taurine. Using real-time quantitative polymerase chain reaction (qPCR), we monitored the expression of betaine-homocysteine *S*-methyltransferase (*BHMT*, which codes for an enzyme involved in betaine metabolism) and taurine transporter (*TAUT*) in salinity challenged *M. edulis*. In this study, we link patterns of gene expression of *BHMT* and *TAUT* to changes we observed on the cellular and organismal level by monitoring changes in the FAA pools using nuclear magnetic resonance spectroscopy (NMR; see Chapter 3), as well as O₂ consumption and NH₃ excretion.

A full understanding of a species' ability to respond to environmental change must consider how the capacity varies throughout development. Blue mussels have a complex life history and spend several weeks or more developing through a series of larval stages in the plankton before settling, metamorphosing, and becoming benthic juveniles. Studies of blue mussel larvae suggest that they are more sensitive to low salinity exposure than post-metamorphic mussels (Hrs-Brenko and Calabrese 1969, Qiu et al. 2001) and there is evidence that low salinity tolerance among larvae is genetically regulated (Innes and Haley 1977). Furthermore, mussel larvae differ from juvenile mussels in their uptake and transport of amino acids (Manahan 1983, Welborn and Manahan 1995), which likely impacts larval tolerance to low salinity. However, to our knowledge, there have not been any studies that evaluate transcriptomic or cellular-level responses of *M. edulis* larvae to hypoosmotic stress.

Transcriptomic studies on mussel larvae are relatively rare; in one, Mitta et al. (2000) showed that the larvae of *M. galloprovincialis* lack expression of antimicrobial

peptides commonly expressed by post-metamorphic mussels. Their results suggest that in *M. galloprovincialis*, the capacity to express certain genes varies among early life history stages. To our knowledge, however, there have not been any studies that evaluated transcriptomic or cellular-level responses of the larvae of any blue mussel species when exposed to hypoosmotic stress. We conducted a series of experiments using veliger and pediveliger larvae to compare patterns of *BHMT* and *TAUT* expression to those of juvenile mussels exposed to low salinity treatment. These studies expand our understanding of the osmotic stress response in blue mussels and particularly improve our knowledge on how these responses vary across life history stages.

4.3 Methods

4.3.1 Preliminary Microarray Study

We conducted a microarray-based study to evaluate temporal patterns of gene expression in response to low salinity for *M. edulis* and *M. trossulus*. Mussels (50–60 mm shell length) were collected from floating docks at the Darling Marine Center, Walpole, ME (*M. edulis*), and Newport Harbor, Newport, OR (*M. trossulus*), and transported to and held in recirculating seawater tanks the University of Maine, Orono, ME. After a 3-w acclimation to common garden conditions of 16 °C and 30 ppt, experimental mussels were exposed to a gradual decrease in salinity to 20 ppt over an 8 h period by adding distilled water, while control mussels were kept at 30 ppt. Four mussels from each species were sampled from the experimental treatments after 5 h when the salinity reached 24 ppt, after 8 h when the salinity reached 20 ppt, and after 32 and 56 h (i.e., 24 and 48 h after the salinity had reached 20 ppt). An identical number of mussels were

sampled from the control conditions at the same time points. At sampling, gill tissue from each individual was dissected, flash frozen in liquid N₂, and stored at -80 °C.

Total RNA was extracted from gill tissue of each specimen using a RNeasy Kit (QIAGEN); each isolation included on-column digestion of DNA following the manufacturer's recommendations. Total RNA for each mussel was quality checked and concentration determined using a Bioanalyzer and RNA 6000 Nano Kit (Agilent Technologies). The isolated RNA was used to probe a microarray containing long oligo (60-mer) probes corresponding to stress-induced expressed sequence tags (ESTs) from *M. californianus* and *M. galloprovincialis*. The development of this microarray has been described in Gracey et al. (2008). Briefly, the microarray is a 105,000-feature microarray that was *in situ* synthesized by Agilent Technologies and includes 44,524 unique probes representing 12,961 and 1,688 ESTs from *M. californianus* and *M. galloprovincialis*, respectively. The baseline ESTs used in developing the microarray were isolated by Suppression Subtractive Hybridization enrichment for transcripts expressed under several different types of environmental stress. We used a reference hybridization protocol to probe the microarray, as per Lockwood and Somero (2011), to reduce problems associated in transcript binding due to the heterologous nature of the microarray relative to the test RNAs. Due to time and funding constraints, we did not use individual RNAs in our experiment, but pooled RNAs from all 4 individuals of each species sampled from each time by treatment (control versus low salinity) combination.

For the reference design, we first created reference RNAs to co-hybridize on the microarray chip with RNA preps of interest to control for slide-to-slide variation in hybridization to a heterologous array. The reference RNAs for both species were

constructed by combining approximately 700 ng total RNA from mussels sampled from the low salinity treatment at 8, 32, and 56 h and mussels sampled from the control treatment at 5, 32 and 56 h. We generated double stranded complementary DNA (cDNA) from 1 μ g reference total RNA using the Ambion Aminoallyl MessageAmpII Kit (Thermo Fisher Scientific, Inc.). Each reference RNA preparation was “spiked” with control RNA supplied by Agilent for hybridization to test probes included on the microarray chip. For each sample, we added 1 μ g total RNA to cDNA reactions to create 16 sets of double stranded cDNA “spiked” with a second control RNA supplied by Agilent. The cDNAs were purified by spin-column, frozen overnight, and then used in amplified RNA reactions to produce aminoallyl UTP–modified RNA (aRNA).

The aRNA from reference (555 nm emission) and experimental samples (647 nm emission) were labeled with Alex Fluor fluorescent dyes (Life Technologies™) with 555 nm and 647 nm emission spectra, respectively. Dye incorporation was assessed on a NanoDrop 2000 UV-Vis Spectrophotometer; 750 ng of labeled aRNAs from reference and experimental samples were then competitively hybridized to the microarray. For *M. edulis* we conducted eight total hybridizations that included aRNA from the four low salinity treatments (aRNA from pooled samples at 5, 8, 32, 56 h) and four control treatments from the same time points, each co-hybridized with the reference aRNA for *M. edulis*. An identical set-up was used for the eight *M. trossulus* hybridizations. Each hybridization slide contained two copies of the microarray and the low salinity and control hybridizations for each time point were conducted simultaneously on the same slide. All hybridization and washing steps followed protocols from Agilent.

Post-hybridization, the slides were scanned with an AXON GenePix® 4000B Microarray Scanner (Molecular Devices, LLC). As per Lockwood and Somero (2011), the signal intensities for each spot were extracted and LOWESS normalized within each slide using Feature Extraction Software 9.5.3.1 (FES; Agilent Technologies). Only spots that FES indicated had good hybridization among all samples were included in further analysis. Due to low signal quality, the hybridization data for the *M. edulis* control RNA at the 5 h time point had to be discarded.

The microarray data were analyzed using Microsoft Access to look for ESTs whose relative expression differed in *M. edulis* compared to *M. trossulus* after 8 or 32 h of low-salinity exposure. We limited our analysis to ESTs where the FES detected a good hybridization signal for 3 or more of the probes (array oligos). For these ESTs, we calculated the median value of the raw expression values; the median values for each treatment were \log_2 transformed and the treatment groups were normalized to the controls. Data were imported into TM4's MultiExperiment Viewer (MeV; Saeed et al. 2003) for cluster analysis and genes were clustered using a Pearson Correlation, with 2000 iterations and $\alpha = 0.05$. Each cluster was sorted again using K-means Clustering to identify subsets of genes having similar expression patterns. We identified ESTs from each cluster and performed a functional analysis of the ESTs using Blast2GO (Conesa et al. 2005). Finally, we searched the dataset for groups of ESTs having similar expression patterns over time and treatment that may highlight differences in the response of low salinity between *M. edulis* and *M. trossulus* (Table B.1).

Analysis of our microarray data indicated that the taurine transporter gene (*TAUT*) and the gene coding for betaine-homocysteine *S*-methyltransferase (*BHMT*) were

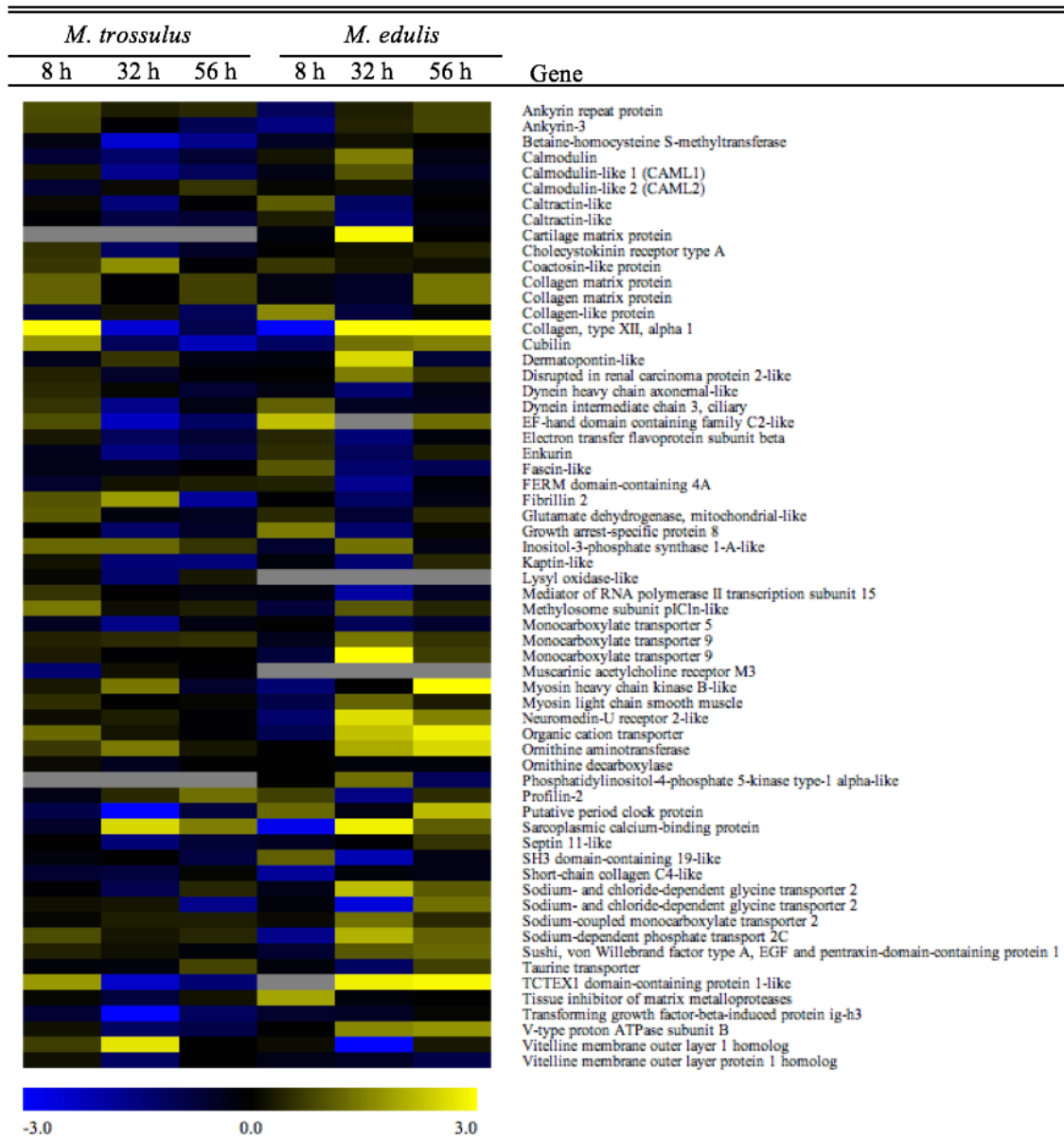


Figure 4.1. Differentially expressed genes potentially involved in cell volume regulation. Expression values are coded by color for *M. trossulus* (left) and *M. edulis* (right) exposed to 8, 32, and 56 h of low salinity, where yellow indicates an upregulation and blue a downregulation of the gene in the gill tissue. Gene annotations were determined in Blast2GO by sequence homology of the corresponding EST to online databases.

differentially expressed among the gill tissues of *M. edulis* and *M. trossulus* exposed to low salinity conditions for 32 h (Figure 4.1). We found a strong downregulation (> 2-fold) of *BHMT* in *M. trossulus* during prolonged low-salinity exposure and no change in expression in *M. edulis*. Expression of *TAUT* showed the opposite pattern and was downregulated 1-fold in salinity treated *M. edulis* at 32 h, while its expression did not vary between the treatment and control groups in *M. trossulus*.

4.3.2 Marker Development

To validate the patterns of expression for *BHMT* and *TAUT* we observed in the microarray data, we developed gene-specific primers to monitor patterns of expression during low salinity exposure using real-time, quantitative polymerase chain reaction (qPCR). Primers were initially created using information from the *M. californianus* EST database to generate sequences from *M. edulis* and *M. trossulus* for the genes of interest by amplification using polymerase chain reaction (PCR). We developed species-specific primer sets for the two target genes, *BHMT* and *TAUT*, and four potential reference genes (see below). More details on the primer and assay development for each of the genes used in this study and sequence information for *M. edulis*, are provided in Appendix B.

We selected two reference genes to use for normalization in our qPCR assay by evaluating the stability of potential genes using the Excel add-on NormFinder (Anderson et al. 2004). Our analysis included elongation factor 1a (*EF1a*), α -tubulin (*TUB*), and 18S ribosomal RNA (*18S*), which have been used as normalizing genes in qPCR studies in mytilids (Caponera and Rawson 2008, Cubero-Leon et al. 2012, Lacroix et al. 2014), as well as 40S small ribosomal subunit (*40S*), which was designed in our lab (Appendix B). qPCR data from multiple treatments, lengths of exposure, stage and/or tissue were chosen

and the C_t values were \log_2 linearized for analysis in NormFinder. *40S* and *EF1a* were the best combination of genes found by the NormFinder algorithm, with a stability value of 0.211, and were therefore selected as normalizing genes for our qPCR studies.

4.3.3 Salinity Experiments on Juveniles

We examined how blue mussels responded at three levels of organization by sampling tissues for gene expression studies and for analysis of intracellular FAA concentrations (see Chapter 3), and by monitoring oxygen (O_2) consumption and ammonia (NH_3) excretion over the course of a 72-h exposure to low salinity. Juvenile *M. edulis* (25–45 mm length) were collected from the underside of the dock at the Darling Marine Center (Walpole, ME) and acclimatized to control conditions in a recirculating system (13.5 °C, 30 ppt) at the University of Maine, Orono, ME. Mussels were fed approximately a 4 % daily ration of Shellfish Diet 1800 (Reed Mariculture, Inc.) of estimated dry tissue weight during the acclimatization period.

Following acclimation, juvenile mussels were placed into 1 l beakers containing filtered, artificial seawater at control (30 ppt) or low (20 ppt) salinities for 1, 2, 4, 24, 48, or 72 h (13.5 °C, $n = 5$). We conducted daily water changes for mussels in the 48 and 72 h exposures and starved all animals for 24 h prior to sampling. At 1 h prior to sampling, the mussels were placed into 35-ml, acid-washed glass chambers containing either 20 or 30 ppt seawater. The chambers were sealed and 2 ml of water was periodically removed through the septa using a syringe. Each water sample was injected into a water cooled (13.5 °C), Microcell Respirometer (Strathkelvin Instruments Model MC100) in which O_2 concentration was measured by a Clark-type microcathode oxygen electrode (Strathkelvin Instruments Model 1302) connected to a Strathkelvin Instruments 782

Oxygen Meter. After the 1 h incubation, 15 ml of water was sampled from each chamber and stored at 4 °C for determination of NH₃ production (described below). The mussels were then dissected and the gill, mantle margin, and posterior adductor muscle were removed, flash frozen in liquid N₂, and stored at -80 °C.

4.3.4 Salinity Experiments on Larvae

We conducted parallel experiments with veliger and pediveliger larvae. Larval *M. edulis* from a controlled spawn conducted in June 2015 at the Darling Marine Center's Hatchery in Walpole, ME, were reared in five replicate tanks from fertilization onward at 13.5 °C and 32 ppt (details of rearing densities and feeding methods are provided in Section 2.3.1). At 14-d post-fertilization (dpf), the larvae had developed to the veliger stage and a subset of approximately 100,000 larvae was removed from each replicate tank and placed into a 1 l beaker containing either control (32 ppt) or low-salinity (20 ppt) UV-sterilized, filtered seawater (UV-FSW; 13.5 °C). One set of veligers from each tank was exposed to the control conditions and one set to treatment conditions for 1, 2, 4, 24, 48, or 72 h (thus, n = 5 for each time point by treatment combination). We conducted daily water changes for the larvae in the 48 and 72 h exposures and starved the larvae for 24 h prior to sampling.

One hour prior to the end of each incubation (i.e., 0, 1, 3, 23, 47, and 71 h), a smaller subset of approximately 10,000 larvae from each experimental and control beaker was placed into 35 ml, acid-washed, glass containers (n = 5) containing either 20 or 32 ppt and the chambers were sealed. We attempted to measure larval O₂ consumption during these incubations using the NeoFox-GT FOSPOR Red-Eye® Oxygen Sensing System (Ocean Optics, Inc.), but due to difficulties calibrating the system to the

chambers, the data were excluded from analysis. Following the 1 h incubation, the larvae and water were placed into a sterile, 50 ml centrifuge tube and gently spun down. An uncontaminated water sample was removed from each and used for NH_3 determinations (described in Section 4.3.5). The remaining larval samples from each chamber were frozen at $-20\text{ }^\circ\text{C}$ and processed later to determine weights of the larvae. At the same time (i.e., end of treatment), the contents of each beaker were sieved onto an $80\text{ }\mu\text{m}$ sieve and the larvae were transferred to a sterile, 1.5 ml Eppendorf tube and flash frozen in liquid N_2 . All samples were stored at $-80\text{ }^\circ\text{C}$. This experimental protocol was repeated using pediveliger larvae at 26 dpf. Unfortunately, one of our larval cultures crashed following our veliger experiments, so the pediveliger experiments were conducted using the remaining, healthy cultures ($n = 4$).

4.3.5 Ammonia Measurements

For the larval samples, NH_3 concentration was determined using a modification of the salicylate-hypochlorite method described by Bower and Holm-Hansen (1980). For each sample, we added $300\text{ }\mu\text{l}$ of the salicylate-catalyst solution and $500\text{ }\mu\text{l}$ of the alkaline-hypochlorite solution to 5 ml of seawater. The reactions were incubated in the dark at room temperature for 1 h and absorbance read on a CARY 50 Scan UV-Vis spectrophotometer at 640 nm. The concentrations of $\text{NH}_3\text{-N}$ were determined by comparison to an ammonia-nitrogen standard curve incubated in parallel to the samples.

The production of NH_3 in our low salinity experiment on juveniles was determined using the phenolhypochlorite method described by Solórzano (1969). Briefly, we mixed 1 ml of the water from each experimental chamber with $40\text{ }\mu\text{l}$ 10 % phenol-alcohol solution, $40\text{ }\mu\text{l}$ of 0.5 % sodium nitroprusside, and $100\text{ }\mu\text{l}$ of the oxidizing

solution (20 % Chlorox® bleach, 80 % alkaline-citrate solution). The reactions were incubated in the dark at room temperature for 1–3 h and absorbance was read at 630 nm on a Beckman DU 600 Series UV/VIS spectrophotometer. Concentrations of NH₃-N were determined by comparison to a standard curve incubated in parallel to the samples.

Ammonia production was calculated as $\mu\text{g NH}_3\text{-N}\cdot\text{h}^{-1}\cdot\text{g}^{-1}$ dry tissue weight. The dry weight of each juvenile mussel was estimated using the measured dry weight of the mussel's tissue, adjusted to account for the tissues that had been dissected out. The larval dry weights were measured by transferring the larvae onto a clean, 25 mm Whatman GF/C™ Glass Microfiber filters. The larval samples were rinsed with 10 ml of 0.5 M ammonium formate to remove any residual salts from the seawater and dried overnight at 65 °C. We then determined the ash free dry weight (AFDW) of the larvae by drying samples overnight in a muffle furnace at 350 °C. The dry tissue weight of the larvae was calculated by removing the proportion of the dry weight contributed by the shell or the difference between the dry weight and AFDW.

4.3.6 Gene Expression Studies Using qPCR

We monitored stage-specific expression of *TAUT* and *BHMT* during a 72-h exposure to low salinity using qPCR. Total RNA was purified from approximately 50 mg of wet tissue weight using PureLink® RNA Mini Kit (Life Technologies™) following the manufacturer's protocol, but with the following modifications. We pipetted 600 μl of the Lysis Buffer with 1 % β -mercaptoethanol into a 2-ml flat-bottom tube and added a section of the tissue or a pooled sample of roughly 50,000 larvae. The samples were homogenized in the buffer for 10 s using a RNase-free Tissue Tearor (Biospec Products, Inc.); the sample was centrifuged at 13.2 g for 5 m (4 °C) to pellet cell debris. RNA

concentrations were determined by measuring the absorbance at 260 and 280 nm on a NanoDrop 2000 UV-Vis Spectrophotometer. The RNA samples were stored at -80 °C. We constructed double-stranded cDNA strands from the RNA extracts using a iScript™ cDNA Synthesis Kit (Bio-Rad Laboratories, Inc.). Each reaction included 50 ng of total RNA and followed the manufacturer's protocol. To confirm successful production of cDNA, we amplified a portion of the α -tubulin gene using regular PCR and 1 μ l of each cDNA reaction.

For the qPCR assays, we set up 15 μ l reactions in 96 well PCR plates; each well contained 7.5 μ l iTaq™ Universal SYBR Green Supermix (Bio-Rad Laboratories, Inc.), 300 nM of the forward and reverse primers (see Table 4.1), 2 μ g of cDNA, and nuclease-free water. We ran the assays for two normalizing genes (*40S* and *EF1a*) and both of our target genes (*BHMT* and *TAUT*) using three technical replicates for each sample in each assay. The qPCR reactions were run on a CFX96 Touch™ Real-Time PCR Detection System (Bio-Rad Laboratories, Inc.). The cycling protocol involves of 3 m at 95 °C, 40 cycles of 10 s at 95 °C, 20 s at 60 °C, and 30 s at 72 °C, an additional 60 s at 95 °C, followed by a melt-curve analysis. Our melt-curve analysis was performed by running 30 s cycles beginning at 60 °C and increasing by 1 °C until reaching 95 °C. Each plate included the qPCR reactions for 10 cDNA templates (i.e., the control and treatment samples from one time point; n = 5 each), a no-template control for each gene, and a normalizing control, consisting of pooled cDNA amplified with α -tubulin to ensure that there was limited variability in C_t values for a common sample among plates across experiments. Following qPCR amplification, we set the threshold for every plate to 250 RFU (relative fluorescence units) in the CFX Manager software (Bio-Rad Laboratories,

Gene Name	Symbol	Function	Primer	Sequence (5' to 3')	Size (bp)	T _m (°C)
40S Ribosomal Subunit	<i>40S</i>	Normalizing Gene	40S RBP-F5 40S RBP-R4	TACCGCTGACAGTCTTGGTG ACATCCACGGACTGACTTCC	193	56.8
Elongation Factor 1 α	<i>EF1a</i>	Normalizing Gene	EF1a Q1F EF1a Q1R	ACCCAAAGGAGCCAAAAGTT TGTC AACGATACCAGCATCC	211	54.8
α -Tubulin	<i>TUB</i>	Normalizing Gene	TUB FOR TUB REV	ATTGCAACCATCAAGACCAAG CATACCTTCTCCGACGTACCA	246	53.7
Taurine Transporter	<i>TAUT</i>	Target	TAUT FOR5 TAUT REV4	GGCGATCTTCACTCCCCCTTTT GAACTTAAGGCCAATATCCAACC	142	53.8
Betaine-Homocysteine S-Methyltransferase	<i>BHMT</i>	Target	BHMT Q1F BHMT REV2	CGTCGTCTTGAAGAGGCTGG TGC GAAC TGT CGAATGTCTGAAC	252	57.5

Table 4.1. Information on primers used for qPCR. We used three genes, 40S ribosomal subunit (*40S*), elongation factor 1 α (*EF1a*), and α -tubulin (*TUB*), to normalize the expression of taurine transporter (*TAUT*) and betaine-homocysteine S-methyltransferase 2 (*BHMT*). For each gene, the forward and reverse primers are listed by name with the corresponding oligonucleotide sequence in the 5' to 3' orientation. The product size amplified using our qPCR primers (in base pairs, bp), as well as the annealing temperature for the primer set (T_m), are also listed.

Inc.) and exported the data into an Excel Spreadsheet. Changes in *BHMT* and *TAUT* expression were analyzed using the ΔC_t method as described in Bustin et al. (2009), normalized to *40S* and *EF1a*.

4.3.7. Data Analysis

We examined the temporal variation in *BHMT* and *TAUT* expression as a function of low salinity treatment using two-factor ANOVA on the ΔC_t values. For each larval stage (veliger and pediveliger larvae) and juvenile tissue sample (gill, mantle, and adductor muscle), individual ANOVA models included salinity treatment and duration of exposure as main effects, and their interaction. The hypotheses that gene expression varied over time and treatment were tested using Type III Sum of Squares with an overall model-wide $\alpha = 0.05$. Similarly, two-way ANOVA was used to assess the effects of low salinity exposure on NH_3 excretion (all stages) and O_2 consumption (for juveniles only). These analyses were conducted using SPSS Statistics 22.0 (IBM Corporation).

4.4 Results

4.4.1. Microarray Analysis

We identified more than 60 transcripts potentially involved in cell volume regulation (based on Blast2Go annotation) that exhibited divergent patterns of expression in the gills of *M. edulis* and *M. trossulus* mussels after prolonged exposure to reduced salinity. For example, after 32 h at 20 ppt, several ESTs corresponding to transporter genes were more highly upregulated in *M. edulis* compared to *M. trossulus* (Figure 4.1; lower right). Overall, however, the differences in gene expression for this subset of genes among the two species were subtle, with few genes showing greater than 1- or 2-fold change in expression across the three time points analyzed. For *BHMT*, the microarray

analysis suggest that it was downregulated after 32 and 56 h of low salinity exposure in *M. trossulus* while the expression of *BHMT* was relatively unchanged in *M. edulis*. In contrast, the microarray results suggested that *TAUT* was downregulated to a greater degree in *M. edulis* compared to *M. trossulus* at 32 h post-exposure.

4.4.2. qPCR-based Analysis of *BHMT* and *TAUT* Expression

Our qPCR-based analysis of *BHMT* expression in *M. edulis* indicated that this gene was predominantly downregulated at all three life history stages and in all tissues of the juveniles during 24–72 h exposure to low salinity (Figure 4.2). Overall, salinity treatment, length of exposure, and their interaction had no significant effect on *BHMT* expression (Table 4.2). One notable exception was in the gill, where the decrease in salinity resulted in an approximately 20 % reduction in *BHMT* expression that was statistically significant. Although there was no significant effect of length of exposure on *BHMT* expression among the three tissues we sampled from juvenile mussels, expression in the mantle and gill tissues showed the greatest degree of downregulation after 48 h of exposure.

The expression of *BHMT* in the larval samples was also generally downregulated but, for the most part, the changes due to exposure to low salinity, the length of exposure, or their interaction were not statistically significant (Table 4.2). In the veligers, there was almost no change in expression between control and treatment animals at 24 and 72 h (Figure 4.2a) and a slight, but non-significant, downregulation at 48 h. In pediveligers, there was no effect of treatment on expression, but we observed a significant effect on the duration of exposure on *BHMT* expression. This effect appears to have been driven by changes in the raw C_t values in both the control and treatment groups, which decreased

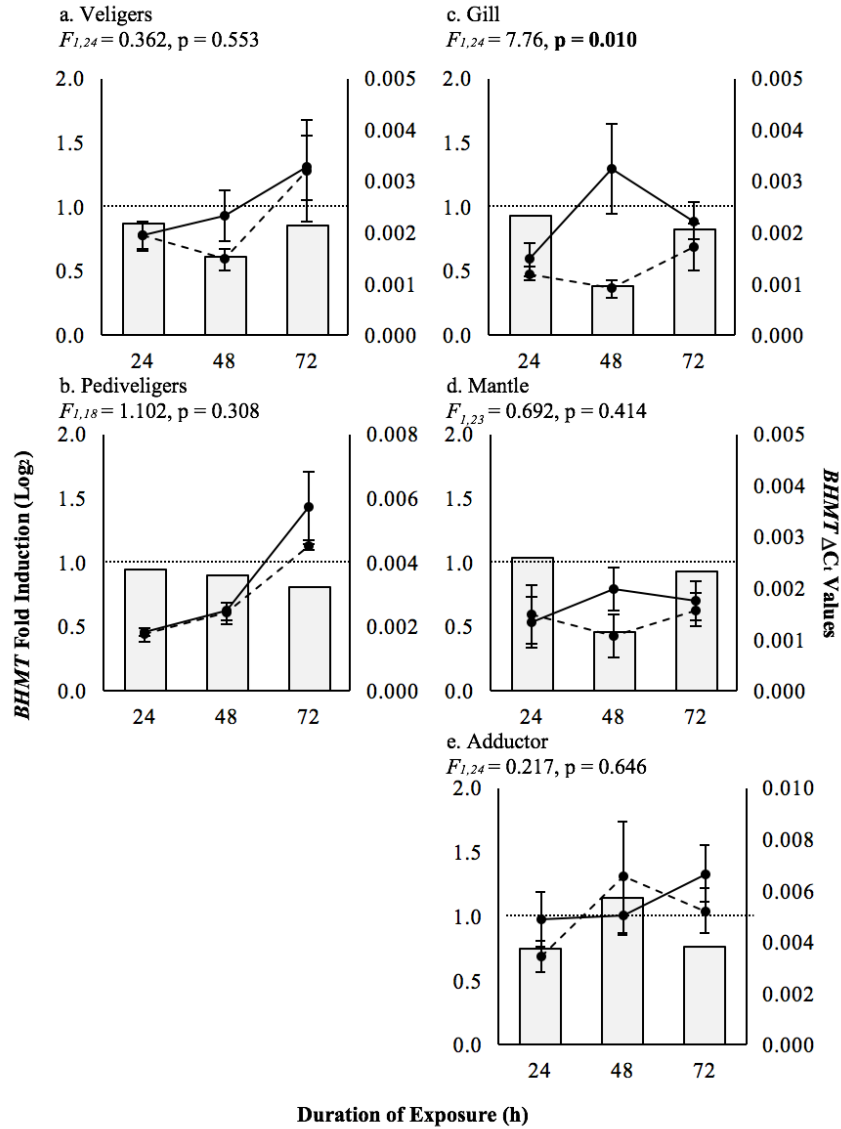


Figure 4.2. *BHMT* expression in *M. edulis* during low salinity exposure. Our qPCR results are plotted as the $\Delta\Delta C_t$ (fold induction, bars) and the mean ΔC_t (\pm SE) for control (solid line) and low salinity (dashed line) treated veligers (a), pediveligers (b), and the gill (c), mantle (d), and adductor (e) tissues of juvenile mussels. The fold induction shows the \log_2 expression of the treatment groups relative to the control, thus, a value of 1 (dotted line) indicates that there was no difference in expression between. *BHMT* expression was significantly downregulated in the gill tissue (a) but not in the other samples.

Stage	Tissue	Source	df	MS	F	P
Veliger		Tissue type	1	6.75 x 10 ⁻⁷	0.362	0.553
		Duration of exposure	2	5.72 x 10 ⁻⁶	3.074	0.065
		Tissue type x Exposure duration	2	5.49 x 10 ⁻⁷	0.295	0.747
		Error	24	1.86 x 10 ⁻⁶		
Pediveliger		Tissue type	1	1.13 x 10 ⁻⁶	1.102	0.308
		Duration of exposure	2	2.48 x 10 ⁻⁵	24.239	< 0.001
		Tissue type x Exposure duration	2	8.25 x 10 ⁻⁷	0.807	0.461
		Error	18	1.02 x 10 ⁻⁶		
Gill		Tissue type	1	8.11 x 10 ⁻⁶	7.776	0.010
		Duration of exposure	2	1.57 x 10 ⁻⁶	1.502	0.243
		Tissue type x Exposure duration	2	3.20 x 10 ⁻⁶	3.067	0.065
		Error	24	1.04 x 10 ⁻⁶		
Juvenile	Mantle	Tissue type	1	6.48 x 10 ⁻⁷	0.692	0.414
		Duration of exposure	2	1.85 x 10 ⁻⁷	0.197	0.822
		Tissue type x Exposure duration	2	7.23 x 10 ⁻⁷	0.772	0.474
		Error	23	9.37 x 10 ⁻⁷		
Adductor		Tissue type	1	1.54 x 10 ⁻⁶	0.217	0.646
		Duration of exposure	2	9.42 x 10 ⁻⁶	1.326	0.284
		Tissue type x Exposure duration	2	7.30 x 10 ⁻⁶	1.028	0.373
		Error	24	7.11 x 10 ⁻⁶		

Table 4.2. *BHMT* ANOVA results. The two-factor ANOVA tested the effects of low salinity treatment and duration of exposure on *BHMT* expression for veliger and pediveliger larvae and the gill, mantle, and adductor tissues of juvenile *M. edulis*.

from the 24 to 72 h samples by 2 cycles, indicating that the expression of the gene, regardless of treatment, was upregulated at 72 h compared to the earlier time points.

We observed a much larger degree of tissue- and stage-specific variation in the expression of *TAUT* (Figure 4.3). Expression of this gene increased by about 20 % in the gill and nearly 50 % in the adductor muscle, but decreased by 40 % in the mantle after 24 h of exposure to low salinity. Interestingly, *TAUT* expression in the adductor muscle remained elevated at 48 h but decreased to control levels by 72 h post-exposure. However, as with *BMHT* expression, salinity treatment, length of exposure, and their interaction had no significant effect on *TAUT* expression in the juvenile adductor muscle and mantle tissues (Table 4.3). Expression in gill tissue was the notable exception, where the 20 %, on average, increase in expression in the low salinity treatment across all time points was statistically significant.

The two larval stages showed differential patterns of *TAUT* expression when exposed to low salinity (Figure 4.3). In veliger mussels, there was a significant upregulation of *TAUT* (approximately 36 %) during low-salinity exposure relative to the control groups. In contrast, *TAUT* was downregulated during low salinity exposure in pediveligers, although the effects of treatment on expression were not significant. As with the expression of *BHMT*, we observed a significant effect of the duration of exposure on *TAUT* expression among pediveliger larvae (Table 4.3), where there was more gene product at 72 h compared to 24 or 48 h (Figure 4.3b).

4.4.3. NH₃ excretion and O₂ consumption

Ammonia excretion increased in mussels exposed to low salinity at all stages of development. Among juvenile mussels, the effect of salinity treatment on excretion was

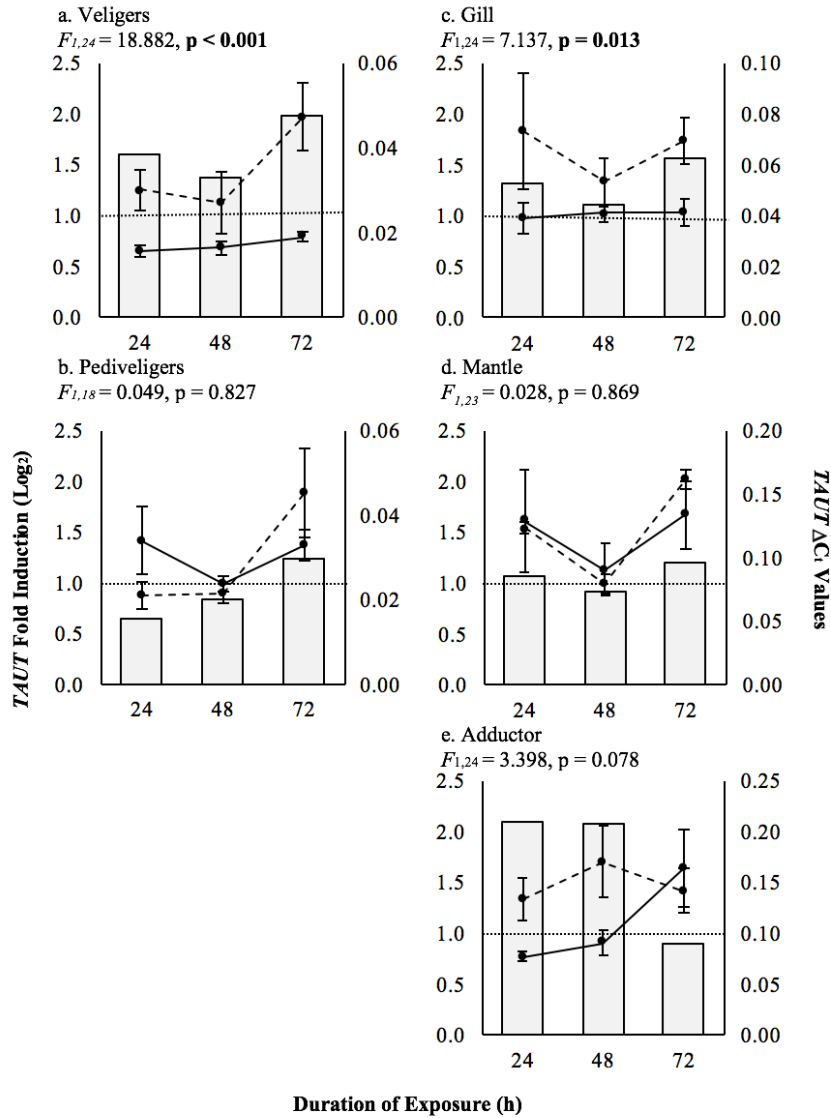


Figure 4.3. *TAUT* expression in *M. edulis* during low salinity exposure. *TAUT* expression is plotted as the $\Delta\Delta C_t$ (fold induction, bars) and the mean ΔC_t (\pm SE) for control (solid line) and low salinity (dashed line) treated veligers (a), pediveligers (b), and the gill (c), mantle (d), and adductor (e) tissues of juvenile mussels. The fold induction shows the \log_2 expression of treatment groups relative to controls, thus, a value of 1 (dotted line) indicates no difference in expression between groups. *TAUT* was significantly down-regulated in salinity-treated veliger larvae (a) and in the gill tissue (c) of juvenile mussels.

Stage	Tissue	Source	df	MS	F	P
Veliger		Tissue type	1	0.002	18.882	< 0.001
		Duration of exposure	2	0.000	3.137	0.062
		Tissue type x Exposure duration	2	0.000	1.719	0.201
		Error	24	0.000		
Pediveliger		Tissue type	1	6.83 x 10 ⁻⁶	0.049	0.827
		Duration of exposure	2	0.001	4.036	0.036
		Tissue type x Exposure duration	2	0.000	2.273	0.132
		Error	18	0.000		
		Tissue type	1	0.005	7.137	0.013
		Duration of exposure	2	0.000	0.386	0.684
Gill		Tissue type x Exposure duration	2	0.000	0.500	0.613
		Error	24	0.001		
		Tissue type	1	9.13 x 10 ⁻⁵	0.028	0.869
		Duration of exposure	2	0.010	3.137	0.062
Juvenile	Mantle	Tissue type x Exposure duration	2	0.001	0.336	0.718
		Error	23	0.003		
		Tissue type	1	0.011	3.398	0.078
		Duration of exposure	2	0.006	1.820	0.184
Adductor		Tissue type x Exposure duration	2	0.007	2.259	0.126
		Error	24	0.003		

Table 4.3. *TAUT* ANOVA results. The two-factor ANOVA tested the effects of low salinity treatment and duration of exposure on *TAUT* expression for veliger and pediveliger larvae and the gill, mantle, and adductor tissues of juvenile *M. edulis*.

significant ($F_{1,48} = 6.120$, $p = 0.017$) as was the length of exposure ($F_{5,48} = 4.550$, $p = 0.002$). Ammonia excretion peaked at around $70 \mu\text{g NH}_3\text{-N}\cdot\text{h}^{-1}\cdot\text{g}^{-1}$ dry tissue weight and was upwards of 7-fold higher (e.g., after 4 h exposure) in salinity-stressed mussels compared to control animals (Figure 4.4). Ammonia excretion in both groups declined in the first 4 h of exposure and values in the two groups were very similar by 72 h of exposure. O_2 consumption, on the other hand, did not differ significantly between control and treatment groups (Figure 4.5; $F_{1,43} = 2.595$, $p = 0.115$). There was a significant effect of the length of exposure on oxygen consumption ($F_{5,43} = 5.909$, $p < 0.001$), but no interaction between treatment and length of exposure ($F_{5,43} = 1.084$, $p = 0.383$).

Ammonia excretion when measured on a dry weight basis, was an order of magnitude higher in larval mussels than in juvenile mussels. In veligers, the effects of low salinity treatment ($F_{1,48} = 21.498$, $p < 0.001$), length of exposure ($F_{5,48} = 11.492$, $p < 0.001$), and their interaction ($F_{5,48} = 4.912$, $p = 0.001$) were all statistically significant. Although there was considerable variation in the rate of excretion in both groups over the first 4 h, by 24 h of exposure the rate of excretion peaked in veliger larvae at $> 1800 \mu\text{g NH}_3\text{-N}\cdot\text{h}^{-1}\cdot\text{g}^{-1}$ dry tissue weight, a rate that was eight times higher than what we observed in control larvae (Figure 4.6). However, after 48–72 h of exposure the rate of excretion was equal in control and stressed veligers. In pediveligers, the rate of NH_3 excretion was significantly greater ($F_{1,33} = 32.646$, $p < 0.001$) in animals exposed to low salinity (Figure 4.7). Ammonia excretion in the control groups was relatively constant until 72 h, while the rate of excretion for pediveligers in the low salinity treatment was 400 % higher after 1 h of exposure and decreased to levels similar to the control treatment by 24 h. This variation resulted in significant effects for the length of exposure

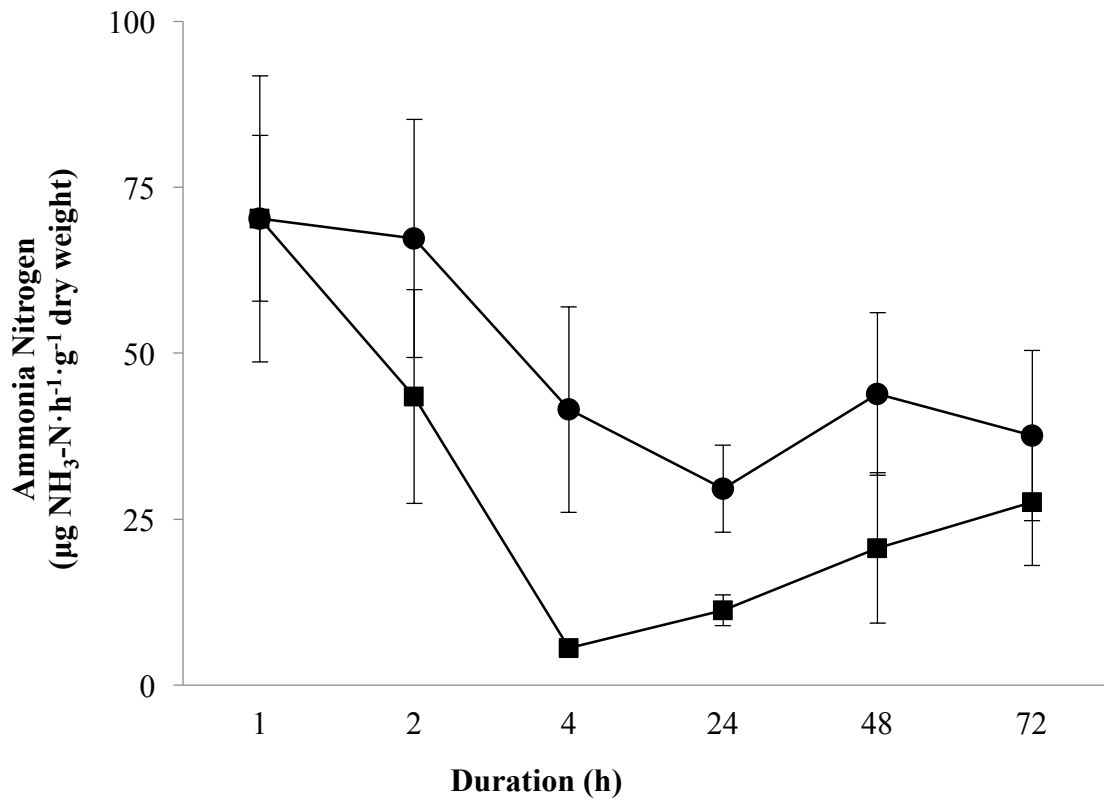


Figure 4.4. NH₃ excretion in juvenile mussels during low salinity exposure. The production of ammonia-nitrogen ($\mu\text{g NH}_3\text{-N}\cdot\text{h}^{-1}\cdot\text{g}^{-1}$ dry weight \pm SE) was significantly higher in animals exposed to low salinity (20 ppt; circles; $F_{1,48} = 6.12$, $p = 0.017$) than in the control group (squares).

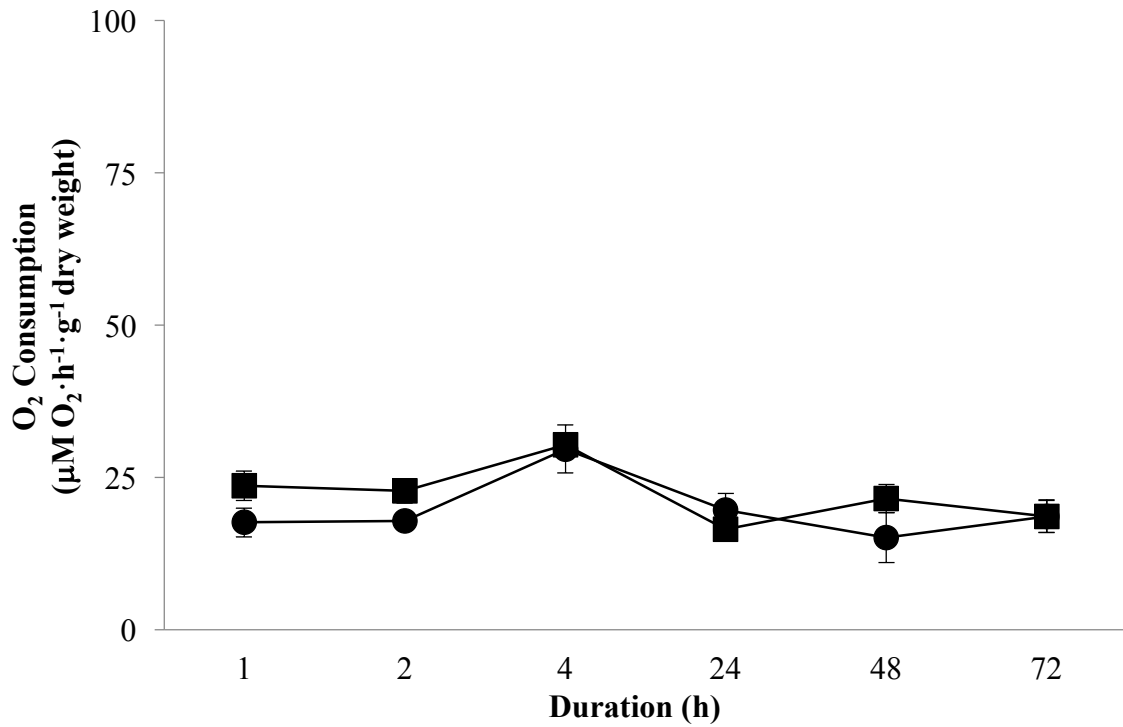


Figure 4.5. O₂ consumption in juvenile mussels during low salinity exposure. There were no significant differences in the O₂ consumption (µM O₂·h⁻¹·g⁻¹ dry weight ± SE) between mussels in the control (squares) and low salinity treatment groups (circles; $F_{1,43} = 2.595$, $p = 0.115$).

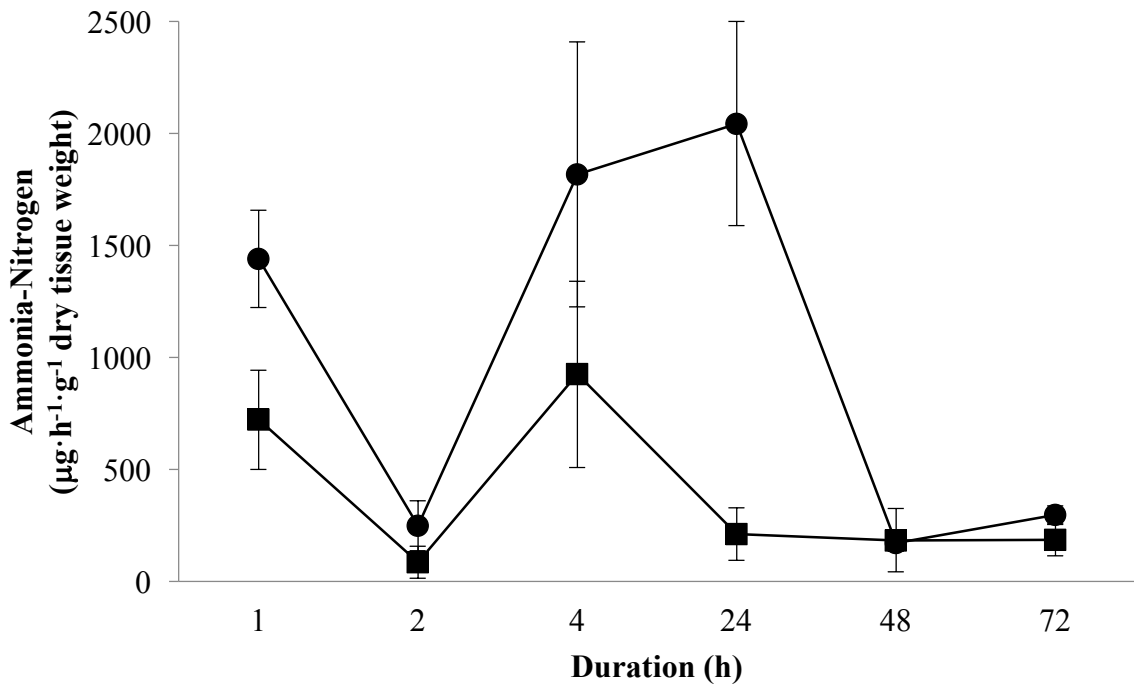


Figure 4.6. Ammonia excretion in veligers exposed to low salinity. There was a significant effect of low salinity exposure on the mean ammonia-nitrogen production ($\mu\text{g NH}_3\text{-N}\cdot\text{h}^{-1}\cdot\text{g}^{-1}$ dry weight \pm SE) in veligers ($F_{1,43} = 21.498$, $p < 0.001$). Veligers in the treatment group (circles) had higher ammonia production than the control groups (squares).

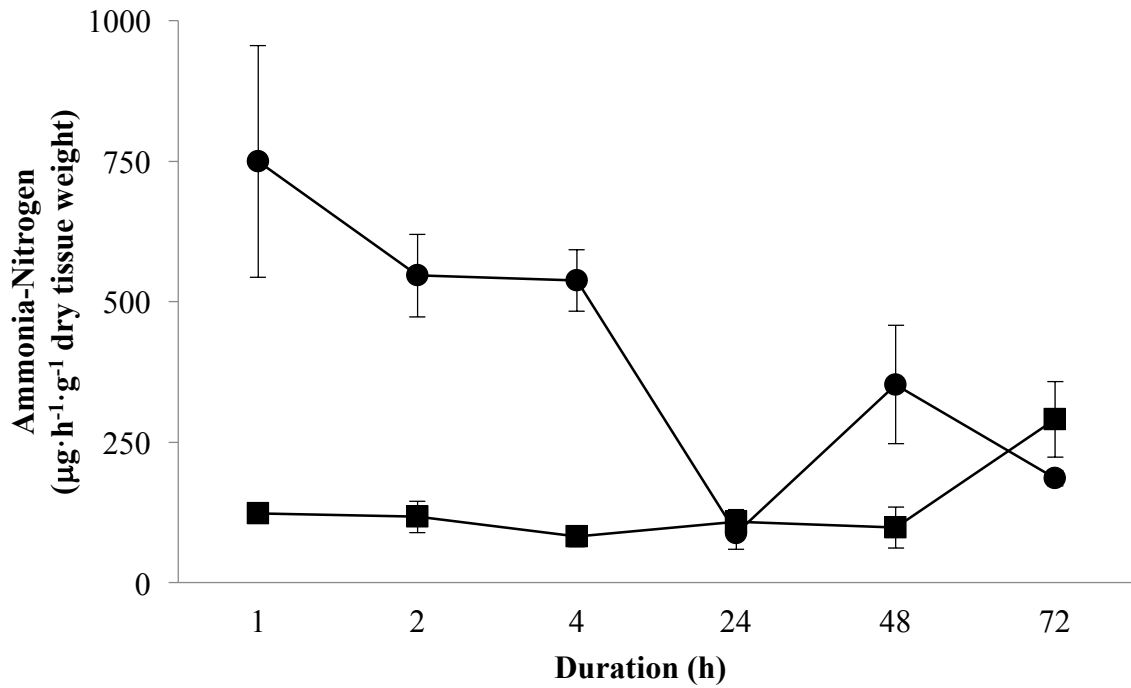


Figure 4.7. Ammonia excretion in pediveligers exposed to low salinity. Exposure to low salinity had a significant effect ($F_{1,33} = 32.646$, $p < 0.001$) on the production of ammonia in pediveliger relative. Rates of ammonia produces ($\mu\text{g NH}_3\text{-N}\cdot\text{h}^{-1}\cdot\text{g}^{-1}$ dry weight \pm SE) at 1, 2, 4, 24, 48, and 72 h of exposure to control (30 ppt; squares) or low salinity (20 ppt; circles) treatments.

($F_{5,33} = 3.399$, $p = 0.014$) and the interaction between treatment and the length of exposure ($F_{5,33} = 5.870$, $p = 0.001$) on NH_3 production.

4.5 Discussion

We employed a microarray-based approach to identify candidate genes involved in the blue mussel response to low salinity exposure. Two of the genes that appeared to be differentially expressed, particularly in comparisons between *Mytilus edulis* and *M. trossulus*, were betaine-homocysteine *S*-methyltransferase (*BHMT*) and taurine transporter (*TAUT*). These genes are involved, respectively in metabolism of betaine and transport of taurine. While our microarray data suggested that expression of *BHMT* in the gill tissue of *M. edulis* was unaffected by exposure to low salinity (Figure 4.1), we found a significant downregulation of *BHMT* in the gill of juvenile *M. edulis* using qPCR (Figure 4.2). Similarly, *TAUT* appeared to be downregulated in *M. edulis* after 32 h of low salinity in our microarray study, but was upregulated in the gill of *M. edulis* in our qPCR assays, especially after a 72-h exposure to low salinity (Figure 4.3).

These conflicting results are likely the consequence of combination of factors derived from the systematic differences of the two experiments. Both studies monitored gene expression after 24 h and 48 h of exposure to 20 ppt, although the mussels used in the microarray study were slowly acclimated to low salinity over an 8 h period whereas the mussels used in the qPCR study experienced an abrupt change in salinity. The differences in the application of the treatment may have altered the expression of *BHMT* and *TAUT*, either by shifting the expression of the genes or the timing of the response. The latter is more plausible given that we sampled in 24 h increments and the acclimation of the mussels in the microarray study may have offset the patterns of expression,

precluding measurement in the narrow window we sampled. Additionally, the mussels used in these studies were collected from separate populations and studies have shown that previous experience can impact transcriptional responses (Li et al. 2010, Lockwood et al. 2015) to low salinity treatment. Finally, the design of our microarray study, in which cDNA was hybridized to pooled samples from multiple time points, resulted in low signal resolution. This method of hybridization against an average, collective level of gene expression was employed to reduce costs, but may have masked any individual variation in expression; given such, the data from our microarray study should be interpreted with caution. In contrast, we are confident that the results from our more targeted qPCR approach generated reflect the dynamics of *BHMT* and *TAUT* expression in the gills (and other tissues) of *M. edulis* under this low-salinity exposure regime.

4.5.1. Transcriptional Response to Low Salinity

The regulation of *BHMT* in *M. edulis* was significantly affected by exposure to low salinity, although this response was not consistent across tissues or developmental stages. We observed a significant downregulation of *BHMT* in the gill tissue of salinity-challenged juvenile mussels, but minimal changes in expression in other tissues (Figure 4.2). In humans, *BHMT* codes for a betaine-homocysteine methyltransferase, which catalyzes the methylation of homocysteine from betaine to create methionine (Li et al. 2008) and may be involved in protein-protein interactions (Pajares and Pérez-Sala 2006). During low salinity exposure, we would expect an upregulation of *BHMT* as a mechanism of controlling intracellular betaine concentrations, as has been observed for *BHMT* in rats (Schäfer et al. 2007) and fish (Qian and Song 2011). In rats, induction of *BHMT* seems to be triggered by a decrease in betaine (Schäfer et al. 2007); a similar

mechanism is thought to drive regulation of the BHMT protein in the cyanobacterium, *Aphanothece halophytica* (Incharoensakdi and Waditt 2000), and in the gills of ayu, *Plecoglossus altivelis* (Lu et al. 2010), during salinity stress.

While we had expected to see an upregulation of *BHMT* in our experiment, when evaluated in the context of the cellular level response, our findings are perhaps not surprising. In a related experiment (see Chapter 3), we did not observe measureable or consistent effects of low salinity treatment on the concentration of betaine in the gill, mantle, and adductor muscle of juvenile mussels or in mussel larvae. If, as in other species, intracellular betaine concentrations are an important driver of *BHMT* expression in *M. edulis*, then the relative steady-state concentration of betaine under low salinity exposure is unlikely to trigger increases in transcription.

Instead, we observed subtle downregulation of *BHMT* in the gill and mantle tissue of juvenile mussels. Although our previous study on osmolyte concentrations in *M. edulis* under low salinity stress found an apparent increase in betaine concentration, this was mostly due to corresponding decreases in the concentrations of betaine seen in the control groups and may reflect an experimental artifact. Betaine counterbalances the negative impacts changes in intracellular ion concentrations resulting from osmotic pressure changes (Bowlus and Somero 1979), so high concentrations are beneficial, particularly during short-term low salinity exposure. The downregulation of *BHMT* in larval and juvenile blue mussels, which would result in decreases in betaine concentration, is likely the cell acting to selectively maintain betaine to offset damaging changes in the internal milieu (Somero 1986). Alternatively, transcription of the gene may be regulated by

changes in methionine metabolism or other downstream pathways, as has been suggested by Zhang et al. (2015).

At the same time, we have an incomplete picture of the function of *BHMT* in blue mussels, for which an annotated genome is presently unavailable. There have been no detailed studies linking *BHMT* expression with protein function or with cellular-level effects, so we can only assume that the role of *BHMT* in *M. edulis* is similar to other species. The 780 base pairs of sequence information we gathered in *M. edulis* (Appendix B) only covers a portion of the gene, and BLAST searches against the *C. gigas* database identify the sequence as a paralog of *BHMT*, *BHMT2*. In humans, *BHMT2* has 73% sequence homology to *BHMT* and lacks a portion of the C-terminus and has a small deletion near the N-terminus (Li et al. 2008, Szegedi et al. 2008). The regulation of human *BHMT2* does not respond to betaine concentrations and instead acts on S-methylmethionine to methylate homocysteine in the same pathway (Szegedi et al. 2008). It is possible that the gene we targeted in this study is *BHMT2* and, that as in humans, is unaffected by the presence of betaine. However, the *BHMT* sequence from *M. edulis* has only 32% sequence homology to human *BHMT* or *BHMT2*, so it is difficult to say whether both paralogs occur in the mussel genome, which paralog our gene codes for, or what the function of the enzyme is in *M. edulis*. Additional studies should be conducted to characterize this gene and its role, if any, in hypoosmotic stress in blue mussels.

The taurine transporter gene, on the other hand, has been extensively characterized in *M. galloprovincialis* by Hosoi et al. (2005). We observed significant increases in *TAUT* expression in the gill tissue and in veligers (Figure 4.3), large, but inconsistent, increases in expression in the adductor muscle, and slight downregulation in

the mantle and pediveligers under the same conditions. The taurine transporter is in the solute carrier 6 family of transporters and is responsible for the Cl⁻-dependent uptake of taurine and other amino acids (Toyohara et al. 2005, Koito et al. 2010). Given its role in uptake of taurine, it may seem surprising to see an upregulation of *TAUT* during exposure to low salinity, when the cell decreases the FAA concentrations to remain isosmotic to the external environment. However, similar to our findings, Hosoi and colleagues observed an upregulation of *TAUT* in the mantle tissues of *M. galloprovincialis* (Hosoi et al. 2005) and *C. gigas* (Hosoi et al. 2007) during hypoosmotic exposure. Taurine, like betaine, acts as a counterbalancing solute so decreases in intracellular taurine trigger an induction of *TAUT* (Hosoi et al. 2005, Hosoi et al. 2007), which Toyohara et al. (2005) suggest is transcribed into a smaller molecular weight transporter to provide for increased uptake and counteract losses of taurine to the environment. The response of *TAUT* to low salinity may change during periods of prolonged exposure when the cell shifts to using taurine as the predominant osmolyte (Pierce and Warren 2001, Meng et al. 2013).

Consistent with this proposed role for *TAUT* in stabilizing intracellular taurine concentrations, we observed little change in taurine abundance during the 72-h exposure to low salinity (see Chapter 3). There was an apparent increase in taurine concentrations in the gill and mantle of mussels held at low salinity for 48 h. As we observed with betaine, however, this change was predominately due to an unexpected drop in taurine concentration in the control mussels at 48 h, rather than from decreased salinity, per se. Overall, the patterns of *TAUT* expression appear unrelated to changes in the intracellular concentrations of taurine, at least over the time frame covered in this study. Perhaps *TAUT* acts over longer time scales, its post-translational activity is regulated by other

means, or these differences reflect tissue- or stage-specific differences in metabolism, as we reported in Chapter 3.

4.5.2. Organismal Reponse to Low Salinity

Decreases in the FAA pool associated with low salinity exposure can result from the catabolism of FAA or transport of the FAAs out of the cell (Bishop 1976, Hoyaux et al. 1976, Shumway et al. 1977, Livingstone et al. 1979). The increased metabolism of FAAs is often manifested at the organismal level through increases in excretion of NH_3 and O_2 consumption in salinity-treated individuals. Increases in NH_3 excretion have been reported in *M. edulis* as soon as 1 h of exposure to low salinity (Sadok et al. 1997), with high excretion rates persisting for up to 8 d (Livingstone et al. 1979). We did not observe appreciable differences in the excretion of NH_3 until 4 h among juvenile mussels (Figure 4.4), and by 48 h excretion had returned to near-control conditions. Concomitant decreases in the concentration of FAAs in juveniles occurred from 24 through 72 h (see Chapter 3), suggesting both increased FAA leakage and catabolism are responsible for osmolyte declines during hypoosmotic stress.

Surprisingly, we found no evidence that O_2 consumption was impacted by salinity exposure in this study (Figure 4.5). Previous studies have found that O_2 consumption nearly doubled in low salinity conditions (Stickle and Sabourin 1979) to match the O_2 demands from increased amino acid catabolism. It is possible that NH_3 production occurred via anaerobic pathways (Zurbug and De Zwaan 1981), which would explain the increase in NH_3 without a corresponding decrease in O_2 . Alternatively, the mussels from both groups may have been consuming enough oxygen to meet the metabolic demands from increased amino acid catabolism and transport, so there was not an

observed increase in the treatment group. The mussels appeared to be actively pumping so it is doubtful that these responses were from shell-closures.

In larval mussels, NH_3 excretion was over an order of magnitude greater than in juveniles and similar to excretion levels in larval *Perna perna* reported by Lemos et al. (2003). In veligers, there were small increases in NH_3 excretion during short-term exposure and a spike in production at 24 h (Figure 4.6). Declines in FAA concentrations during osmotic exposure were relatively consistent through time, so the increases in excretion at 24 h may have resulted from unrelated metabolic degradation pathways, such as the purine cycle or serine dehydrase (Bishop 1976). Similarly, pediveligers increased their rates of excretion during short-term exposure (Figure 4.7), when there were no observable decreases in the concentrations of FAAs (Table C.2). These findings support the hypothesis that greater reductions in FAA concentrations in larvae result from their highly permeable tissues and inability to exhibit shell closing behavior for any considerable length of time. In both cases, it seems likely that rapid turnover of osmolytes not measured in this study or an increase protein catabolism cause an increase in NH_3 excretion that is not reflected in declines in FAAs.

Overall, variation in transcription, composition of the FAA pools, and excretion suggests that larval responses to low salinity differ from those of juvenile *M. edulis*. In juveniles, we saw a consistent response at the organismal level that may be explained by decreases in glycine at the cellular level (see Chapter 3). While we did not monitor expression of genes related to glycine metabolism using qPCR, we can use information from the microarray study to look for upregulation of genes involved in glycine metabolism or transport. In studies of *Modiolus demissus* (Ellis et al. 1985) and *C. gigas*

(Meng et al. 2013) decreases in glycine during hypoosmotic exposure were attributed to increased glycine metabolism through dehydrogenation to serine. We did not observe differences in expression of serine hydroxymethyl-transferase, but did see increases in expression of glycine transaminase and in Na⁺-dependent glycine transporters (Table B.1), again indicating that both transport and metabolism (possibly via incorporation into glutamate), are likely responsible for reductions in glycine and that these changes are regulated at the transcriptomic level.

The variation we observed in gene expression likely indicates tissue- or stage-specific differences in metabolism. In juvenile mussels, retention of taurine and betaine may be linked to expression of *TAUT* and *BHMT*, respectively, but that these responses are tissue-specific. So, while the tissues responded similarly on a cellular level during exposure to low salinity, they differed in patterns of gene expression. Often, transcriptomic studies focus on a single tissue or a single time point, although the expression of some genes, like *TAUT* and *BHMT* may be dynamically changing in both space and time. Given the variability in the response of these genes to low salinity exposure, it is difficult to make predictions about the role of transcriptional regulation during the stress responses without looking more closely at the changes in expression within each tissue.

In larval mussels, excretion of NH₃ only occurs during short-term exposure, which might indicate that this stage acclimates to environmental change relatively quickly (Bartberger and Pierce 1976). However, analysis of the changes in the FAA composition during stress (see Chapter 3) contradicts this hypothesis and instead suggests that larvae depend heavily on transport of amino acids, rather than catabolism. If loss of

osmolytes is occurring at high rates in larval mussels, then larvae must either risk substantial loss of FAAs or mount a response to combat these cellular-level changes. Given the transcriptional patterns of *BHMT* and *TAUT* in larvae, it is likely that decreases of betaine and taurine, respectively, regulated changes in expression. With respect to *BHMT*, betaine decreased slightly during low salinity exposure, which may have triggered a downregulation of *BHMT* to slow betaine metabolism and limit overall losses that occur through transport. The same was observed in the relationship of taurine and *TAUT*. In veligers, declines in taurine were accompanied by an upregulation of *TAUT* at all time points. Pediveligers downregulated the expression of *TAUT* and experienced a drop in intracellular taurine at 24 h; however, by 48 h taurine began to stabilize, without increases in *TAUT* expression. This result suggests that veligers may be actively transporting taurine into the cells to counteract loss, but because of metabolic differences between the stages (as per Sprung and Widdows 1986), pediveligers may have relied on taurine synthesis (Welborn and Manahan 1995) rather than uptake to restore taurine levels within the cell.

This study highlights developmental and tissue-specific variability in the response to low salinity stress in *M. edulis*. Larval-specific morphology and metabolism may lead to increased susceptibility to osmotic stress and require that larval mussels increase energy expenditures to offset environmental change. Our results demonstrate that stage-specific differences in the response do occur and elucidating larval responses is important for a thorough understanding how the mussel populations, and the species as a whole, respond to increasing runoff and the freshening of coastal waters. We have also observed important tissue-level differences in the response to osmotic stress in *M. edulis*, again

associated with morphology and metabolism of the tissue, demonstrating that a focus on a single tissue limits our understanding of the response to environmental stress and that broader, more comparative approaches are more appropriate and inclusive.

CHAPTER 5

UNDERSTANDING THE ROLE OF CALMODULIN AND OTHER CALMODULIN-LIKE GENES IN THE ACUTE HYPOOSMOTIC STRESS RESPONSE OF THE BLUE MUSSEL, *MYTILUS EDULIS*

5.1 Abstract

Our preliminary microarray studies on the transcriptomic responses of blue mussels (*Mytilus edulis*) during hypoosmotic exposure have suggested the calmodulin (*CaM*) and two calmodulin-like genes (*CAML1* and *CAML2*) are upregulated in response to low salinity treatment. CaM is an important calcium-binding molecule that plays a role in numerous cell-signaling pathways and, along with CaM-like proteins, is involved in cellular stress responses. The role of CaM and CaM-like proteins in the osmotic stress response of blue mussels remains largely under investigated. This study was undertaken to improve our understanding of expression of *CaM* and *CAML* genes in *M. edulis* during low salinity exposure, as well as to look at variation in their spatial expression within various tissues and across developmental stages. We used structural analysis of the *CaM*, *CAML1*, and *CAML2* genes, as well as variation in the temporal and spatial distribution of these genes, to gain a better understanding of the putative protein function. Additionally, we used real-time quantitative PCR (qPCR) to monitor the dynamics of expression during short-term, hypoosmotic exposure. This is the first study to identify calmodulin-like genes in *M. edulis* and the first to examine variation in the expression of *CaM* and other related genes across developmental stages as well as

during low salinity treatment. We found evidence for stage- and tissue-specific patterns of expression in *CaM* and *CAML* genes in salinity-challenged mussels and in those acclimated to control conditions. These findings implicate *CaM* and closely related genes in decreased salinity tolerance of early-life history stages of the blue mussel.

5.2 Introduction

Blue mussels (*Mytilus edulis*) are an ecologically important species in the Gulf of Maine and inhabit both estuarine and marine intertidal and subtidal habitats. As such, mussel populations are periodically exposed to salinity fluctuations caused by an interplay between terrestrial runoff, precipitation, and tidal changes. When faced with changes in environmental salinity, mussels regulate intracellular inorganic ionic and organic osmolyte concentrations to remain isosmotic to the external environment without extensive cellular damage (Lange 1963, Davenport 1979). The ability to tolerate these changes in salinity by both larval and juvenile mussels determines their distributions along salinity gradients (Qiu et al. 2002, Westerbom et al. 2002). Human-induced changes to global climate are predicted to alter nearshore salinity (Antonov et al. 2002, Durack et al. 2012), so understanding the capacity of blue mussels to respond to hypoosmotic exposure at all developmental stages is important for predicting how local mussel communities will be affected by climate-induced salinity variations.

The physiological response of mussels to salinity perturbations has been extensively studied over the past several decades (e.g. Lange 1963, Costa and Pritchard 1978, Deaton et al. 1985, Garnder and Thompson 2001, Qiu et al. 2002). However, the genetic mechanisms that underlie salinity tolerance in blue mussels have received far less attention. Comparative transcriptomic studies can be used to evaluate patterns of

divergence between closely related species in order to provide information on the evolutionary underpinnings of tolerance and the capacity for the evolution of tolerance in mytilids (Lockwood and Somero 2011). Previous studies by Qui et al. (2002) and Westerbomb et al. (2002) have suggested that *M. edulis* is less adapted to low salinity stress than its congener *M. trossulus* and that these differences in salinity tolerance have impacts on the distributions of these two species. We conducted a microarray-based study to investigate species-specific differences in the transcriptional response of these two species when exposed to an acute hypoosmotic stress (Chapter 4). We found that during low salinity treatment, calmodulin (*CaM*) and two calmodulin-related genes (*CAML1* and *CAML2*) were upregulated in *M. edulis* but not in *M. trossulus*.

Calmodulin (calcium-modulated protein) is the predominant calcium-binding protein in Eukaryotes. It functions as a cellular signaling molecule and through protein-protein interactions plays a role in growth, metabolism, and various other cellular functions (Cheung 1980, Klee et al. 1980, Vogel 1994, Zielinski 1998, Chin and Means 2000). Because of its importance in regulating cellular processes, the structure of CaM is highly conserved (Zielinski 1998); CaM contains four EF hand domains (helix-loop-helix structures) that allow it to bind up to four Ca^{2+} in a highly-regulated manner (Finn and Forsén 1995, Lewit-Bentley and Réty 2000). Calmodulin proteins also contain conserved protein-binding sites that allow complexation with over 50 other proteins (Klee et al. 1980, Méhul et al. 2000). Several studies, spanning a broad range of species, have shown that CaM is also functionally important in cellular stress responses (Snedden and Fromm 2000, Calabrese et al. 2010). CaM is suspected to play a role in the osmotic stress response in humans (Falktoft and Lambert 2004), plants (Perochon et al. 2011), and

mollusks (Pierce et al. 1989, Pierce and Warren 2001), where it mediates efflux of taurine from the cells.

In many plant and animal species, there are also numerous calmodulin-like proteins, named because of structural similarity to calmodulin (Snedden and Fromm 1998, Perochon et al. 2011). Calmodulin-like proteins are relatively common among plant taxa where their function may differ from calmodulin due to structural changes that affect calcium-binding (Snedden and Fromm 1998, Perochon et al. 2011). Although they are not as widely characterized in animals, recent studies have shown that calmodulin-like proteins may be common in both vertebrate (Rhyner et al. 1992, Méhul et al. 2000) and invertebrate systems (Li et al. 2005, Jackson et al. 2007, Ren et al. 2013). The calmodulin-like proteins characterized in these studies are thought to have novel roles and are often localized in a specific tissue or cell type, and some may be involved in salinity stress responses (Reddy et al. 2011, Zeng et al. 2015).

The purpose of this study was to evaluate the expression of *CaM* and two, novel calmodulin-like genes, *CAML1* and *CAML2*, during short-term, hypoosmotic exposure. Our preliminary microarray study was limited in that we were unable to capture transcriptional changes that occurred during the early- and intermediate- response to low salinity stress and we only evaluated the response in the gill tissue of juveniles (see Chapter 3). Qui et al. (2002) have shown that larvae are more susceptible to low salinity exposure than are juveniles, so we have expanded our investigation of the dynamics of expression during salinity stress to include multiple tissues and several life-history stages. Given the functional importance of *CaM* within the cell and its potential role in amino

acid efflux and osmoregulation, we predicted that the expression of *CaM* would increase in low salinity-challenged *M. edulis* as we observed in our microarray study.

We also analyzed the temporal variation in the expression of *CaM* along with the novel calmodulin-like genes, *CAML1* and *CAML2*, that were identified in the microarray study. Finally, we used information from the nucleotide sequences of *CaM*, *CAML1*, and *CAML2* to analyze the secondary structure of the predicted protein products with gene expression data. We also used an *in situ* hybridization approach to assess the spatial distributions of these genes within the gill tissue of *M. edulis* and to explore the potential functional significance of these genes in developmental and tissue-specific processes.

5.3 Methods

5.3.1 Sequencing and Marker Development

We developed primers to target calmodulin (*CaM*) and two calmodulin-like genes, *CAML1* and *CAML2* in *M. edulis* using information from our microarray study and the *M. californianus* EST database. These primers were used with complementary DNA (cDNA) isolated from *M. edulis* to generate PCR products for direct sequencing. The sequence information supported the development of internal primers and the use of 5' and 3' Rapid Amplification of cDNA Ends (RACE) to obtain full-length coding sequence information for *CaM*, *CAML1*, and *CAML2*. More details on the marker development can be found in Appendix B. Gene sequences from other species homologous to *CaM* in *M. edulis* were identified through BLAST (Basic Local Alignment Search Tool) against the NCBI (National Center for Biotechnology Information) nucleotide database. The retrieved sequences were aligned with our *CaM* sequence from *M. edulis* using the Clustal Omega Multiple Sequence Alignment Tool (EMBL-EBI). We analyzed the

sequences to identify base-pair substitutions that may provide insight into functional changes that occur at the level of the protein and modeled these changes using the UCSF ChimeraX Molecular Modeling System and MODELLER programs. A similar approach was used to develop sequence alignments and model changes in the predicated protein structure for *M. edulis* *CAML1* and *CAML2*.

Sequence information for *M. edulis* *CaM*, *CAML1*, and *CAML2* was also used to design primer sets for gene expression analysis using real-time quantitative polymerase chain reaction (qPCR) and for cloning reactions used in mRNA *in situ* hybridizations. Given regions of high sequence similarity between *CaM* and *CAML* genes, the qPCR primers were designed to target areas where the nucleotide sequences diverged among paralogs, and the polymerase chain reaction (PCR) products were sequenced to ensure that we were only amplifying our gene of interest and not other *CAML*-genes. The complete list of primers for sequencing is given in Table B.6.

5.3.2 Salinity Challenge Experiments

Larval and juvenile *M. edulis* were exposed to acute, low salinity treatment to evaluate the response of *CaM*, *CAML1*, and *CAML2* during osmotic stress. Larvae were exposed to control (32 ppt) or low salinity (20 ppt) UV-sterilized, filtered seawater (UV-FSW at 13.5 °C) for 1, 2, or 4 h at either the veliger or pediveliger stage, as described in Section 4.3.4. and sampled for gene expression studies. In another experiment, juvenile mussels were similarly exposed to 20 ppt or 32 ppt artificial seawater for 1, 2, or 4 h before the gill, mantle, and adductor muscle tissues were removed and frozen as described in Section 4.3.3. The gill, mantle, and adductor samples were used to evaluate tissue-specific differences in the expression of *CaM* and *CAML*-genes.

5.3.3 Gene Expression Studies

Using a small portion of each tissue sample or a subset of each larval pool, we extracted RNA and synthesized cDNA templates (Section 4.3.6) for qPCR amplification. Expression of *CaM* and *CAML2* during low salinity treatment was monitored in veliger and pediveliger mussels following the protocol in Section 4.3.6, using our *CaM*- and *CAML2*-targeted qPCR primers (Table 5.1). Preliminary studies indicated that *CAML1* was not expressed in larval mussels; we conducted standard PCR reactions using the *CAML1* qPCR primer sets and larval cDNA for 40 cycles at a 60 °C annealing temperature to confirm this observation. The reactions were analyzed for presence or absence of *CAML1* products using agarose gel electrophoresis. In the tissue samples of juvenile *M. edulis*, qPCR assays were run for *CaM*, *CAML1*, and *CAML2*, except for the adductor muscle tissues from 1 h treatment because of poor RNA recoveries. Expression of *CaM* and the two *CAML* genes were normalized to our reference genes 40S ribosomal subunit (*40 S*) and elongation factor 1a (*EF1a*) and analyzed using the ΔC_t method (Bustin et al. 2009).

5.3.4 *In Situ* Hybridizations

We developed digoxigenin (DIG)-labeled RNA probes to evaluate spatial patterns of expression of *CaM*, *CAML1*, and *CAML2* using *in situ* hybridization in the gill tissue of juvenile *M. edulis*. Probes for each gene were developed by initial PCR amplifications with gene specific primers (see Table 5.1); the standard PCR reactions were run for 30 cycles using a 52 °C annealing temperature (see Section B.2. for more detailed analysis of the PCR protocol). The resulting PCR products were purified using PureLink® PCR Purification Kit (Life Technologies™) following the manufacturer's protocol. Purified

Gene Name	Symbol	Function	Primer	Sequence (5' to 3')	Size (bp)	T _m (°C)
40S Ribosomal Subunit	<i>40S</i>	Normalizing Gene	40S RBP-F5 40S RBP-R4	TACCGCTGACAGTCTTGGTG ACATCCACGGACTGACTTCC	193	56.8
Elongation Factor 1 α	<i>EF1a</i>	Normalizing Gene	EF1a Q1F EF1a Q1R	ACCCAAAGGAGGCCAAAAGTT TGTC AACGATACCAGCATCC	211	54.8
Calmodulin	<i>CaM</i>	Target	CAM Q1F CAM Q1R	ATGGCTGATCAGCTGACAGAAGA TCGTAACCTCATCCTCATTTGTCAC	260	54.4
Calmodulin-like 1	<i>CAML1</i>	Target	CAML1 QF1 CAML1 QR1	GAGGAGTGTGTTAGAGGGGG TGCTTTTCTGTGCATACCATATCCT	266	50.9
Calmodulin-like 2	<i>CAML2</i>	Target	CAM2 Q1F CAM2 Q1R	AACGCAGACCAGGTGATAGC CGAAGTTCTTCTTCACTATCAGTG	269	53.2

Table 5.1. Primer sets used in the *CaM* and *CAML* qPCR assays. The primer names, 5' to 3' oligonucleotide sequences, expected product size (in base pairs, bp), and annealing temperature (T_m in °C) are listed for each of the four genes used in the qPCR assays. The 40S ribosomal subunit (*40S*) and elongation factor 1a (*EF1a*) were used as reference genes to normalize the expression of the target genes, calmodulin (*CaM*), calmodulin-like 1 (*CAML1*), and calmodulin-like 2 (*CAML2*).

products were ligated into pGEM®-T Easy Vector (Promega Corporation) by mixing 5 µl 2X ligation buffer, 1 µl T Easy vector, 2 µl purified PCR product, 1 µl T4 DNA ligase, and 1 µl nuclease-free H₂O and allowing the reaction to run overnight at 4 °C.

Recombinant plasmids (2 µl of the ligation reaction) were used to transform 25 µl One Shot® TOP10 Chemically Competent *E. coli* (Invitrogen™) cells. The transformation reaction was kept on ice for 20 m and heat shocked for 45 s at 42 °C before we added 950 µl S.O.C. medium, incubated the reaction at 37 °C for 90 m, and plated 100 µl of the transformed cells on LB plates containing 500 µg ampicillin, 10 µmoles of isopropyl β-D-1-thiogalactopyranoside (IPTG), and 1 mg X-Gal. Colonies were permitted to grow at 37 °C for 24 h before being held at 4 °C for an additional 24 h. We transferred a single blue colony (indicating that transformation had occurred) into 1.5 ml LB broth with ampicillin (100 µg/ml) and incubated at 37 °C overnight. The clones were checked by PCR amplification using the vector-specific M13 forward and reverse primers and sequencing the purified PCR product at the University of Maine DNA Sequencing Facility (Orono, ME).

The cloned PCR products were used to develop gene-specific DIG-labeled RNA probes. For each gene, additional primers were designed that matched the original PCR primers but to which we added sequences for the T7 RNA polymerase promoter region to the 5' end (Table 5.2). These modified primers were paired with unmodified primers to amplify PCR products corresponding to the sense and antisense strands of each gene using the gene-specific plasmid DNA as the template. PCR products for the sense and antisense strands were purified using the PureLink® PCR Purification Kit (Life Technologies™). The DIG-labeled probe was generated by mixing 2 µl of 10X DIG

Target	Primer	Sequence (5' to 3')	Size (bp)	T _m (°C)	Strand
Calmodulin (<i>CaM</i>)	CAM FOR	ATGGCTGATCAGCTGACA	458	51.4	Sense
	CAM REV	CGTTGTTTTCATTATTGTCATCAT			Antisense
Calmodulin-like 1 (<i>CAML1</i>)	CAML1 QF1	GAGGAGTGTGTTAGAGGCCGG	378	51.5	Antisense
	CAML1 REV3	ATGGATACAAATAGATCATAATTTCCGC			Sense
Calmodulin-like 2 (<i>CAML2</i>)	CAM2 4L	TTCATCTACGATACAGCCATG	533	52.0	Antisense
	CAM2 4R	TGGCCGTCATCATTTGTCAC			Sense

Table 5.2. Primer sets used to target genes for *in situ* hybridizations. These primer sets were used to amplify *CaM*, *CAML1*, and *CAML2* for the cloning reactions and were then modified by attaching the T7 promotor region (5' TAA TAC GAC TCA CTA TAG GG 3') to the 5' end of the primer. For each primer set, we were then able to amplify a sense and antisense stranding using the T7-modified primer and the corresponding unmodified primer (i.e. CAM FOR-T7 and CAM REV amplified the CAM antisense strand).

RNA labeling mix, 2 μ l 10X transcription buffer, 2 μ l T7 RNA polymerase, and 1 μ l RNase Inhibitor (Roche Diagnostics) with 200 ng purified PCR product in 20 μ l reaction. Following a 2 h incubation at 37 °C, we added 2 μ l DNase I and incubated for an additional 15 m at 37 °C before stopping the reaction with 2 μ l 0.2 M EDTA. The probe was precipitated by incubating the product in 2 μ l LiCl and 75 μ l pure EtOH at -80 °C, centrifuging the mix at 13,200 rpm for 10 m, and washing the pellet with 70 % EtOH. The RNA pellet was resuspended in 10 ml nuclease-free H₂O and incubated at 37 °C for 10 m before the probe concentrations were determined using a NanoDrop 2000 UV-Vis Spectrophotometer.

We used longitudinal sections through the gill tissue for *in situ* hybridizations. A section of gill tissue was dissected from juvenile *M. edulis* and fixed in 0.1 M PBS with 4 % formaldehyde. Prior to embedding, the tissue was dehydrated and cleared by 3 x 10 m washes in 0.1 M PBS, 3 x 5 m exchanges in 50 % EtOH, 3 x 5 m in 70 % EtOH, 3 x 5 m in 95 % EtOH, 2 x 5 m in 100 % EtOH, 1.5 h in 100 % EtOH, and 2 x 10 m in xylene. The cleared tissue was infiltrated with paraffin by soaking 3 x 10 m in paraffin baths. We then took 7 μ m sections through the block on a rotary microtome and adhered sections to nuclease-free SuperBlock microscope slides.

Slides were prepared for hybridization by deparaffinization in 3 x 10 m toluene washes, rehydrated through an EtOH series, rinsed in water, and transitioned into 0.1 M phosphate buffered saline (PBS) solution. The slides were post-fixed in 0.1 M PBS with 0.1 % TWEEN® 20 (PBS-T) and 4 % formaldehyde for 25 m and rinsed 4 x 5 m washes in PBS-T, 1 x 5 m wash in PBS-T with 10 μ g/ml Proteinase K, and 4 additional 5 m washes in PBS-T at room temperature. The slides were transitioned into hybridization

buffer (5X SCC buffer, 50 % formamide, 0.1 mg/ml salmon testes DNA, and 0.1 % TWEEN® 20) in a series of incubations at 55 °C. For each *in situ* hybridization, individual RNA probes were added to the hybridization buffer (500 ng/ml) and denatured at 80 °C for 2 m before being applied to the slides. All hybridizations were incubated overnight at 55 °C.

The following day, the probe was removed and the tissue sections were rinsed in hybridization buffer (2 x 30 m) and 0.1 M PBS-T (4 x 5 m). We used the DIG Wash and Block Buffer Set following the manufacturer's protocol to prepare the slides for DIG detection. We applied a 1:300 dilution of the Anti-Digoxen antibody (Roche Diagnostics) in 1X Blocking solution and incubated overnight at 4 °C. The antibody was removed and the pH of the slides adjusted using the 1X detection buffer before bathing the slides in 1-Step™ NBT/BCIP (Thermo Scientific) for 5 – 60 m until color developed. We stopped the reaction by rinsing the slides in TE buffer and immediately mounted a coverslip using Permount Mounting Medium. The slides were imaged on an Olympus BX41 compound microscope with a ZEISS Axiocam ERc 5s camera at 100X.

5.3.5 Data Analysis

Gene expression data were analyzed in SSPS Statistics 22.0 (IBM Corporation). Tissue- or stage-specific differences in the expression of *CaM*, *CAML1*, and *CAML2* were tested using a series of two-factor ANOVAs. In each model, we used normalized gene expression values from our control groups of each experiment (ΔC_i) and evaluated the effects of tissue (which included larval stage) and a time component on expression. These were tested as main effects with an interaction term. We tested pairwise comparisons using Fisher's Least Significant Difference (LSD) post-hoc analyses to

distinguish the effects of each tissue from one another. To test for the effects of low-salinity treatment on expression of *CaM*, *CAML1*, and *CAML2*, we ran an additional two-factor ANOVA model. Each gene was run as the dependent variable, with treatment and duration of exposure as main effects. These, along with an interaction term, were tested against a Type III Sum of Squares model with $\alpha = 0.05$ for each developmental stage or tissue.

Images taken of the *in situ* hybridizations were examined in ImageJ (Schneider et al. 2012) to investigate whether there were differences in the color development between the sense and antisense hybridizations. Briefly, we created a stack containing a comparable grayscale image of the sense and antisense strands and used the threshold function in Image J to determine areas in the antisense strands containing digoxigenin stain (see Figure 5.6d for an example). Given the preliminary nature of the *in situ* hybridization experiment, no statistical analyses were conducted.

5.4 Results

5.4.1 Structural Analysis of *CaM* and *CAML* genes

We identified and sequenced calmodulin (*CaM*) and two calmodulin-like genes (named *CAML1* and *CAML2*) in *Mytilus edulis*. Like calmodulin in other species, *CaM* is 149 amino acids in length and contains four EF hand domains that function in Ca^{2+} binding (Figure 5.1). The amino acid sequence for *CaM* in *M. edulis* is highly conserved in mytilid congeners (Figure 5.2) and has 91.9 % sequence similarity with humans (Figure 5.1) and 93.2 % similarity to *CaMs* from other invertebrate species (Figure 5.3). For *M. edulis*, we observed five amino acid substitutions in the central alpha helix domain between EF-Hand domains two and three. We also detected several substitutions

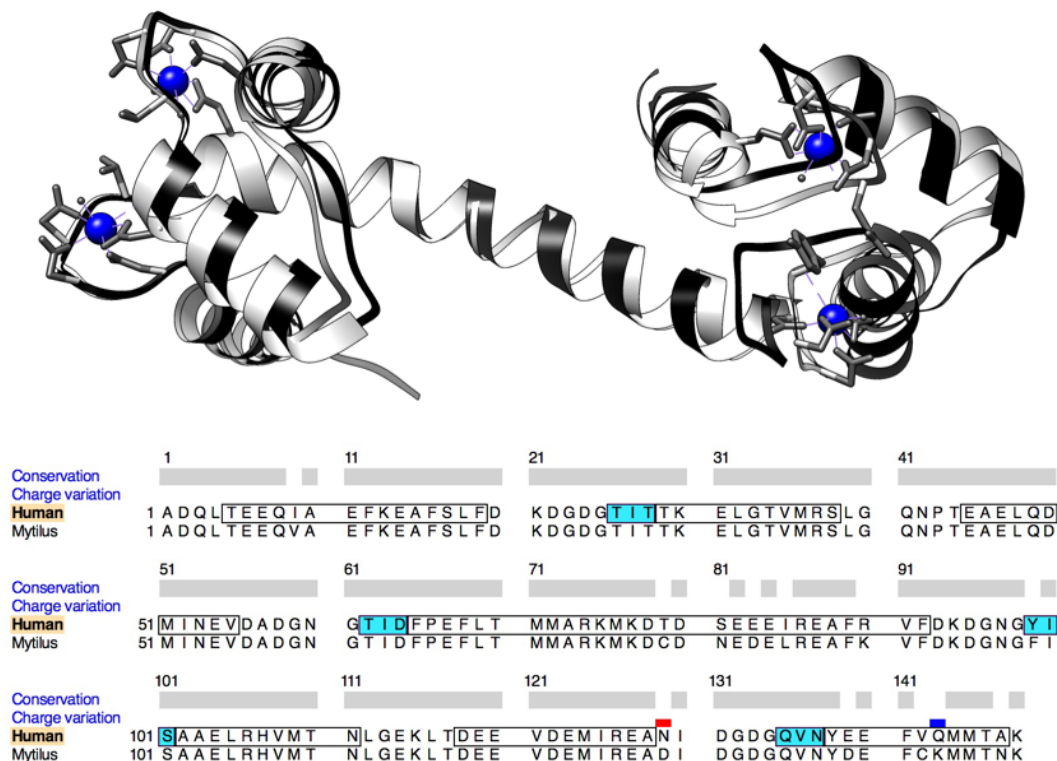


Figure 5.1. Comparison of *M. edulis* and human calmodulin. The predicted protein structure for *M. edulis* (black ribbon) is overlain on the structure in humans (white ribbon). Calmodulin is highly conserved, with 91.89 % sequence similarity between the two species; regions of overlap are indicated by the gray bar above the sequence alignment. CaM contains four EF-hand domains (positions 19–25, 56–61, 93–98, 128–134) each containing a calcium-binding domain, which are demonstrated visually in the protein model surrounding the blue Ca^{2+} ions. The alignment shows the predicted secondary structure, with helices (white bar) and beta sheets (teal bar) of CaM, and depicts where amino acid substitutions result in a positive (red) or negative (blue) charge variation.

```

M. edulis          1  MADQLTEEQVAEFKEAFSLFDKDGDTITTKELGTVMRSLGQNPTEAELQDMINEVDADG
M. trossulus     1  .....
M. galloprovincialis 1  .....
M. californianus  1  .....

M. edulis          61  NGTIDFPEFLTMMARKMKDCDNEDELREAFKVFDDKDGNGFISAAELRHVMTNLGEKLTDE
M. trossulus     61  .....
M. galloprovincialis 61  .....
M. californianus  61  .....

M. edulis          121  EVDEMIREADIDGGQVNYDEFCKMMTNK
M. trossulus     121  .....
M. galloprovincialis 121  .....-----
M. californianus  121  .....

```

Figure 5.2. Multiple sequence alignment of Mytilid *CaM*. The sequence alignment shows the high homology among the four species in the Mytilid species complex, *M. edulis*, *M. trossulus*, *M. galloprovincialis*, and *M. californianus*. Sequence information for *M. galloprovincialis* was incomplete, but otherwise, there are no amino acid substitutions among the four congeners.

Mytilus	1	MADQLTEEQIAEFKEAFSLFDKGDGTITTKELGTVMRS LGQNPTAEELQDMINEVDADG
Ciona	1
Lottia	1
Acropora	1
Metridium	1
Haliotis	1
Pinctada	1
Lumbricus	1
Aplysia	1
Strongylocentrotus	1
Acartia	1
Balanus	1
Mytilus	61	NGTIDFPEFLTMMARKMKDCNEDELREAFKVFDDKGNFISAAELRHVMTNLGEKLTDE
Ciona	61T.S.E.I...R.....
Lottia	61T.S.E.I...R.....
Acropora	61T.S.E.I...R.....
Metridium	61T.S.E.I...R.....
Haliotis	61T.S.E.I...R.....
Pinctada	61T.S.E.I...R.....
Lumbricus	61T.S.E.I...R.....
Aplysia	61T.S.E.I...R.....
Strongylocentrotus	61T.S.E.I...R.....
Acartia	61T.S.E.I...R.....
Balanus	61T.S.E.I...R.....
Mytilus	121	EVDEMIREADIDGGQVNYDEFCKMMTNK
Ciona	121V.....E..VN.....
Lottia	121L.....E..V...S.
Acropora	121E..V...S.
Metridium	121E..V...S.
Haliotis	121E..V...S.
Pinctada	121E..V...MS.
Lumbricus	121E..VT..MS.
Aplysia	121E..VT...S.
Strongylocentrotus	121E..VT...S.
Acartia	121E..VT...S.
Balanus	121E..VT...S.

Figure 5.3. Multiple sequence alignment of invertebrate calmodulins. The amino acid sequence of *CaM* identified in *M. edulis* has > 93 % homology with 11 other invertebrate species. In the alignment, a dot indicates that there is no change in amino acid between species, while a letter indicates a change in the amino acid sequence between *M. edulis* and another species.

at the 3' end of the gene. Although these substitutions are unique to *Mytilus*, our modeling efforts indicate these changes are unlikely to disrupt the protein tertiary structure common to CaM.

The predicted structure for *CAML1* and *CAML2* are strikingly different from *CaM* in *M. edulis*. *CAML1* is 150 amino acid residues and only shares 30.9 % sequence homology with *M. edulis CaM*; there are numerous amino acid substitutions that resulted in charge variations in the secondary structure and very few regions that are conserved between the two genes (Figure 5.4). Even so, modelling suggests that at least three of the EF hand domains in *CAML1* are intact. *CAML2* was more similar to *CaM* than was *CAML1* (Figure 5.5), with 87.9 % similarity at the amino acid level. The EF hand domains and calcium binding sites were intact in *CAML2*, although there are some amino acid substitutions and charge differences within these functional domains. Interestingly, there is a substitution in *CAML2* that may act as an alternate start codon and result in a protein that is 23 amino acids longer than *CaM* at the N-terminus.

5.4.2 Baseline Expression of *CaM* and *CAML* genes

We evaluated the spatial distribution of *CaM*, *CAML1*, and *CAML2* transcripts within the gill tissue of juvenile *M. edulis* using digoxigenin-labeled mRNA *in situ* hybridizations. *CaM* was highly expressed and had a relatively broad distribution within the gill tissue (Figure 5.6). The abundance of *CaM* mRNA appeared to be higher in the cytoplasm compared to the nuclei and was concentrated near the membranes of the cells. We did not see high levels of *CaM* expression in the cilia or in cartilaginous regions near the basement membranes of the epithelial cells. The expression of *CAML1* and *CAML2* was much lower than that of *CaM* in the gill and the distribution of mRNA for these

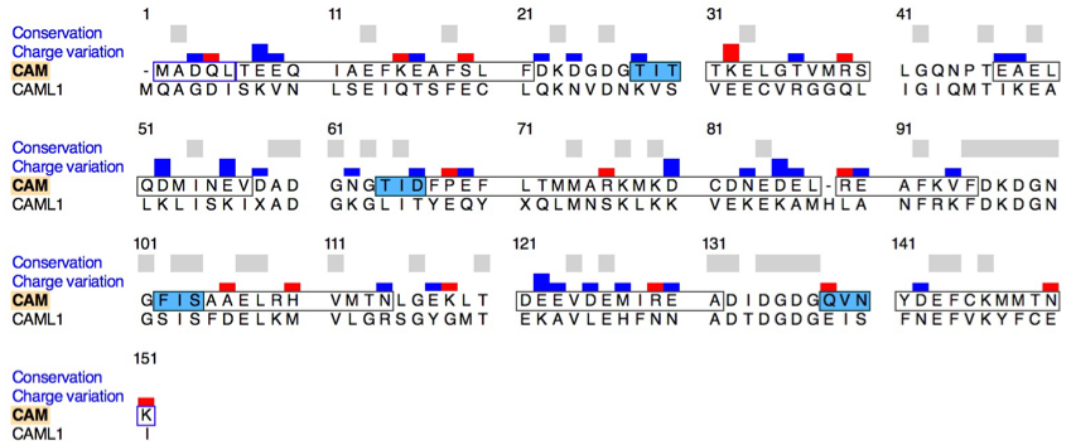
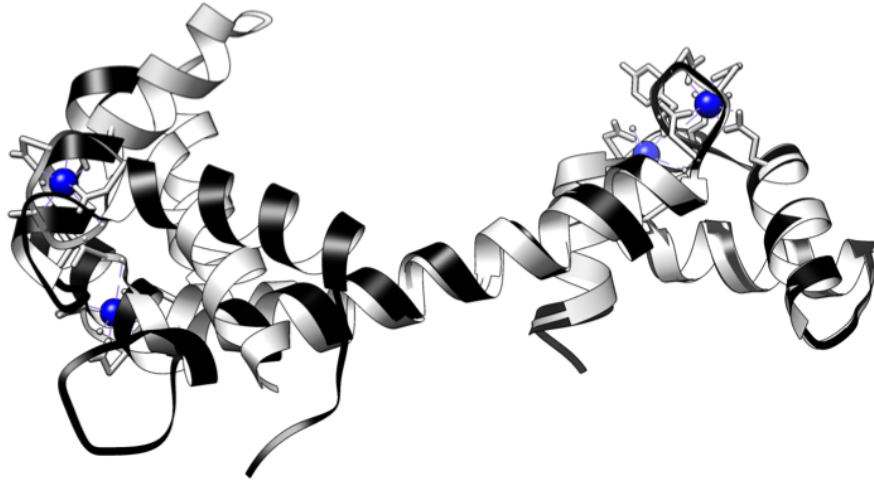
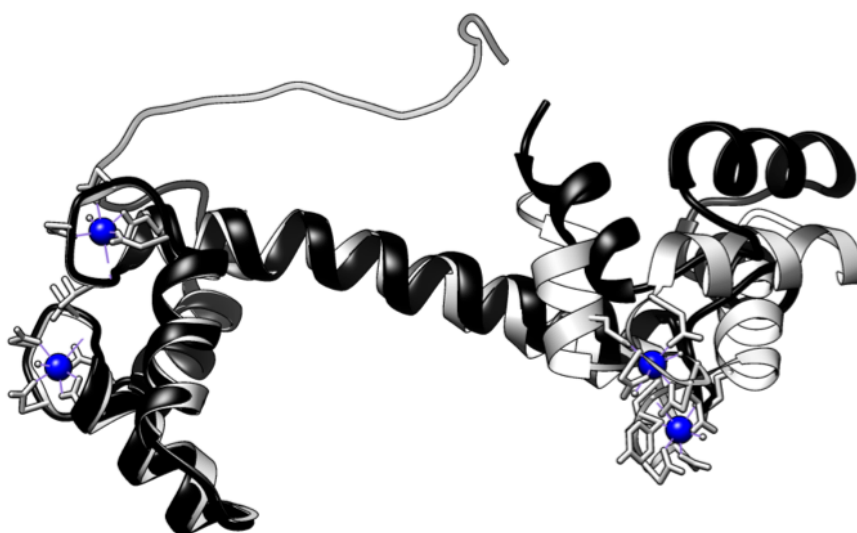


Figure 5.4. Comparison of *M. edulis* CaM and CAML1 predicted proteins. *CAML1* (black ribbon) shares only 30.2 % sequence homology with *CaM* (white ribbon) and likely only has three functioning EF-hand domains (regions before the teal highlight). As indicated by the gray bars, there are very few regions where the amino acid sequences are similar between these two genes, and many places where amino acid substitutions result in charge variation (red and blue bars) that will affect protein stability and folding.



	1	11	21	31	41
Conservation	[Gray bars]				
Charge variation	[Blue bars]				
CAM	-----	-----	---MADQLTE	EQVAEFKEAF	SLFDKDGDT
CAML2	MKKAKQKNKA	HMDDIVYLKI	NADQVIALTE	EQVAEFKEAF	SLFDKDGDT
	51	61	71	81	91
Conservation	[Gray bars]				
Charge variation	[Red bars]				
CAM	ITTKELGTVM	RS LGQNP T[EA	ELQDMINEVD	ADGNGTIDFP	EFLTMMARKM
CAML2	ITTSELGTVM	RS LGQNPTEA	ELQDMINEVD	ADGNGTIDFE	EFLLMARKM
	101	111	121	131	141
Conservation	[Gray bars]				
Charge variation	[Blue bars]				
CAM	KDCDNEDEL R	EAFKVF DDKDG	NGFISAAEL R	HVMTN LGEKL	TDEEVDEMIR
CAML2	KDTDSEEL R	EAFRVFDKDG	NGFISAAEL R	HVMTN LGEKL	TDEEVDEMIK
	151	161	171		
Conservation	[Gray bars]				
Charge variation	[Red bars]				
CAM	[EA]D I DGDGQV	NYDEFCKMMT	NK		
CAML2	EADLDGDGLV	NYEEFVTMMT	AK		

Figure 5.5. Comparison of *M. edulis* CaM and CAML2 predicted proteins. There is 87.9 % sequence homology between *CaM* (white ribbon) and *CAML2* (black ribbon), with most of the Ca^{2+} -binding (teal highlighted area) and EF hand domains conserved between proteins. It is unclear where CAML2 is initiated, as there are two start codons within the first 20 amino acids. Conserved regions are highlighted in gray, while charge differences in the amino acid sequence are shown in red or blue.

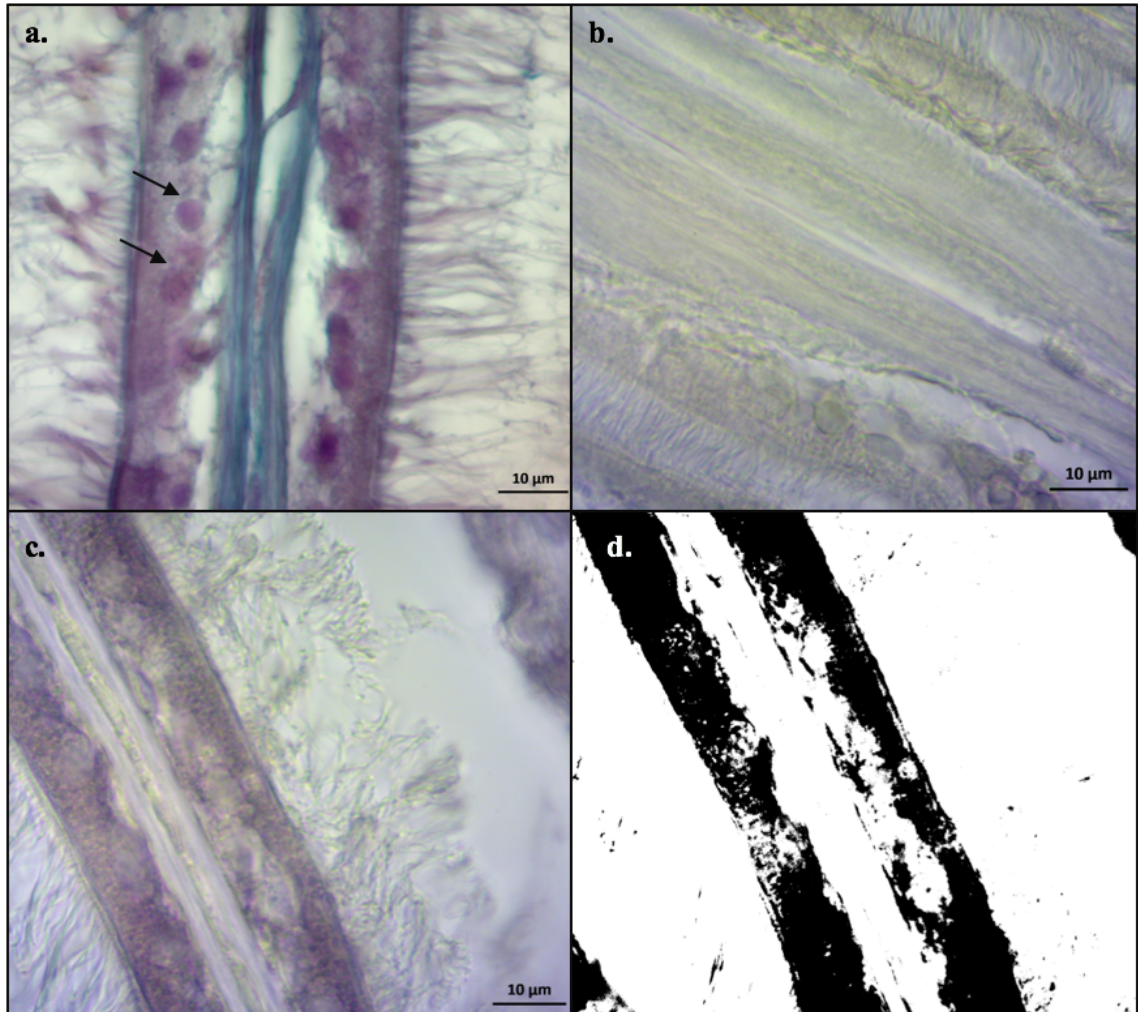


Figure 5.6. Visualization of *CaM* expression in the gills of *M. edulis*. An example of background staining in the sense strand (b) is shown in contrast to the dark staining seen in the antisense strand (c). The widespread distribution of *CaM* found in the cytoplasm of the gill cells is depicted in the binary image (d). For reference, image a shows the longitudinal section of the gill filament (running from the apex of the gill to the branchial axis), with nuclei stained dark purple with hematoxylin (arrow) and the collagenous matrix lining the epithelial cells of the gill stained with alcian blue. All micrographs were imaged at 100 X.

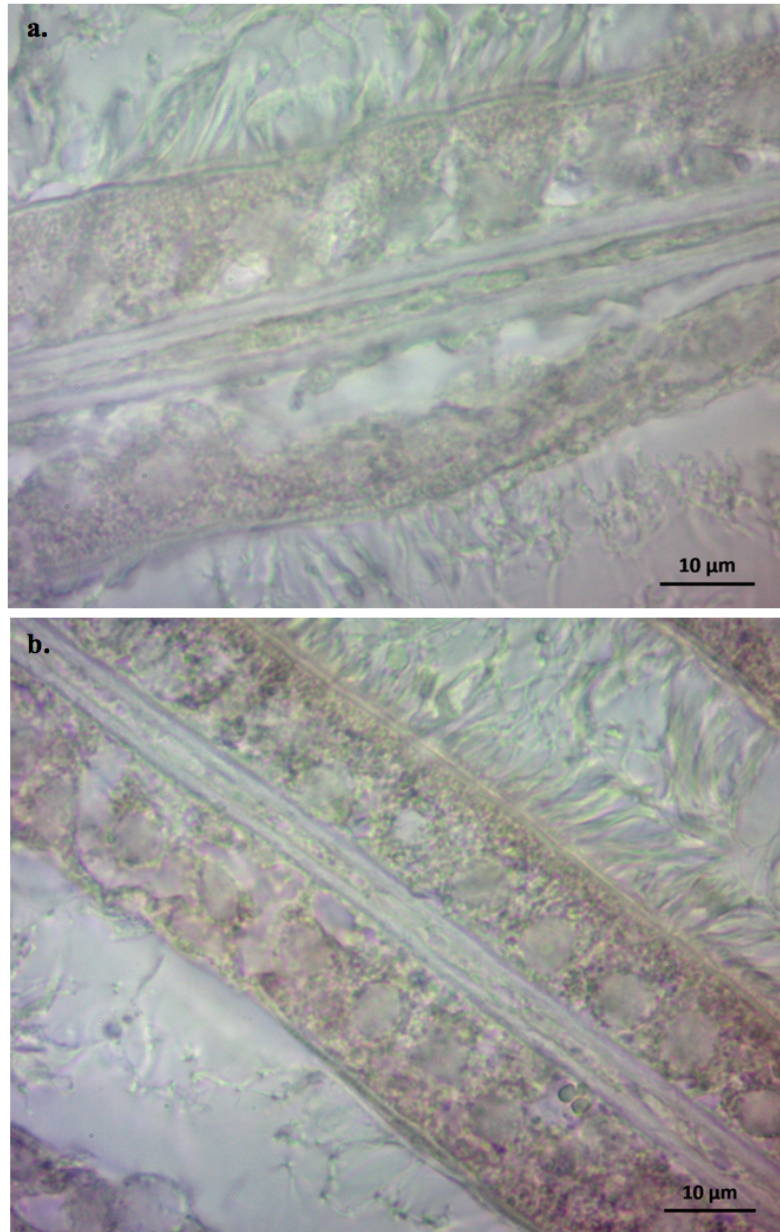


Figure 5.7. Visualization of *CAML1* in *M. edulis* gill tissue. Expression of digoxigenin-labeled *CAML1* can be seen by the faint purple spots within the epithelial cells in the antisense strand (b); the sense strand (a) is shown for reference. Gene expression studies indicate that expression of this gene is low in the gill tissue and is not as widespread as that of *CaM* (Figure 5.6).

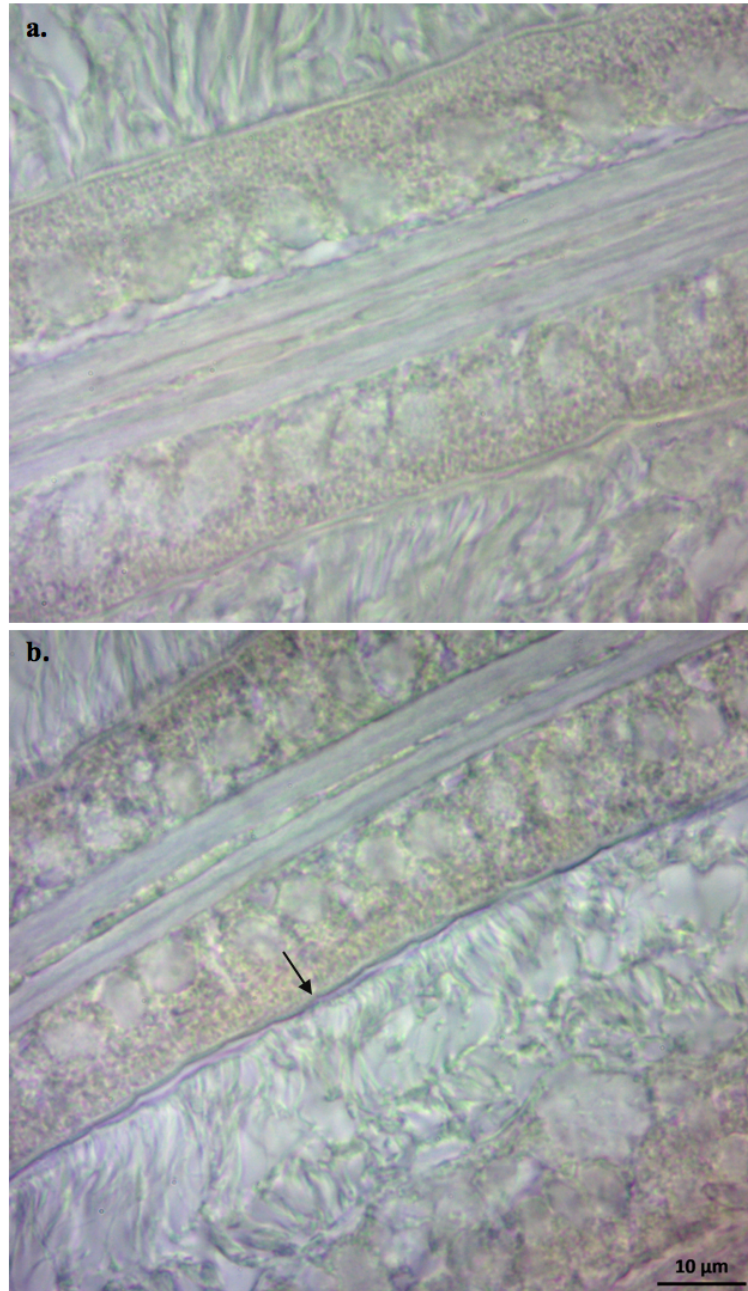


Figure 5.8. Visualization of *CAML2* in *M. edulis* gill tissue. Expression of digoxigenin-labeled *CAML2* can be seen by the purple areas that line the membranes of the epithelial cells marked by the arrow in the antisense strand (b); the sense strand (a) is shown for reference. Gene expression of *CAML2* is low in the gill and is not as widespread as that of *CaM* (Figure 5.6).

genes was more localized. *CAML1*, which had the lowest levels of expression, only appeared in dense pockets surrounding the nuclei within the cytoplasm of epithelial cells (Figure 5.7), while *CAML2* expression tended to localize at the perimeter of the cells (Figure 5.8). Overall, staining was light due to low baseline expression of both genes, making it difficult to draw firm conclusions about the patterns of expression. However, it was apparent that neither gene is expressed at the same high level as *CaM*.

There were similar trends in the copy number of each gene in our qPCR studies. Evaluation of the baseline gene expression data indicated that there was stage- and tissue-specific patterns of expression under normal conditions for *CaM*, *CAML1*, and *CAML2*. *CaM* expression was significantly lower in larval mussels compared to juveniles (Figure 5.9), although expression did not vary between veligers and pediveligers. Within the juvenile, *CaM* expression in the adductor differed from the copy numbers observed in the mantle or gill tissue. *CAML1* appears to be developmentally regulated, as we were unable to amplify the gene in veliger or pediveliger mussels. Within juvenile mussels, *CAML1* expression varied significantly (Figure 5.10) among all three tissues, being highest in the gill. *CAML2* also showed stage- and tissue-specific patterns of expression, but most of these differences stemmed from relatively high rates of expression in the adductor muscle (Figure 5.11).

5.4.3 *CaM* and *CAML* expression during hypoosmotic exposure

We observed stage-specific and tissue-specific patterns of *CaM*, *CAML1*, and *CAML2* expression for larval and juvenile mussels exposed to acute, low salinity treatment. In veliger mussels, *CaM* expression decreased slightly over a 4 h exposure to low salinity relative to the controls, although the effect of treatment was not significant

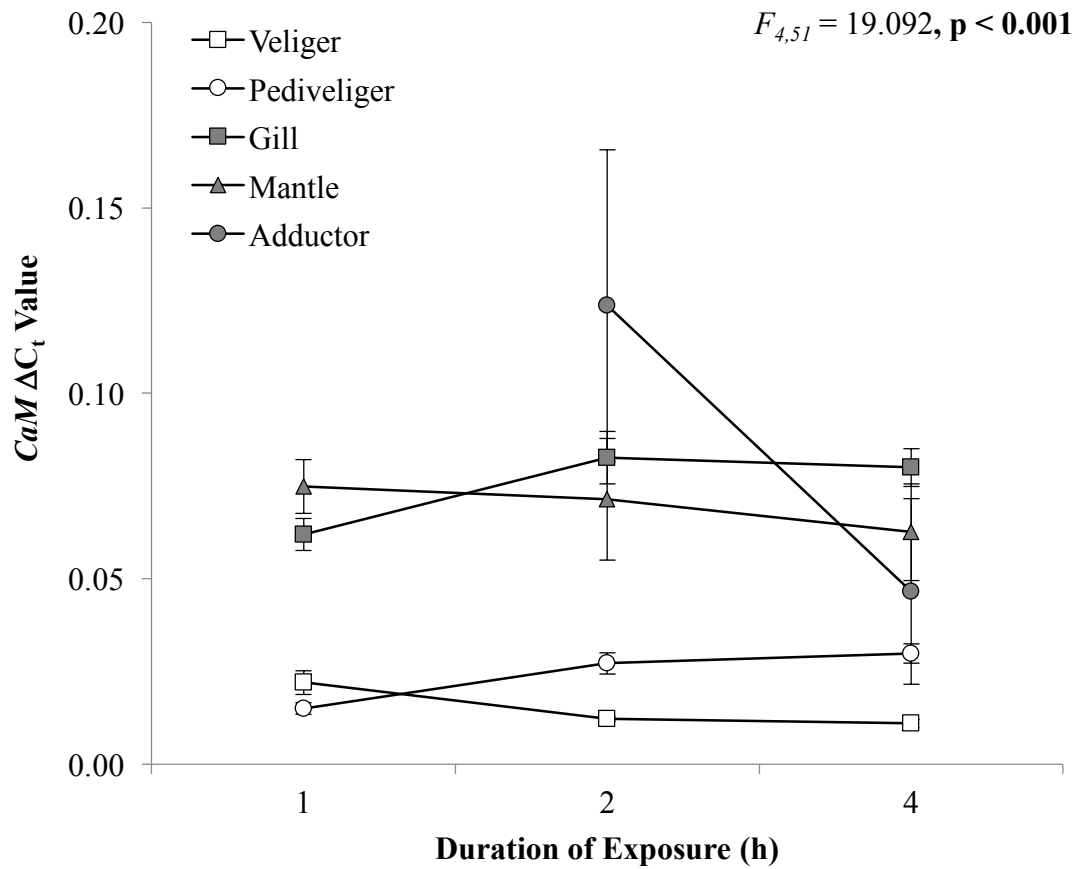


Figure 5.9. Baseline *CaM* expression in *M. edulis*. The mean ΔC_t values (\pm SE) for the control veliger (open squares) and pediveliger (open circles) larvae were significantly lower than what we observed in the gill (closed squares), mantle (closed triangles), or adductor (closed circles) tissues of juvenile *M. edulis*.

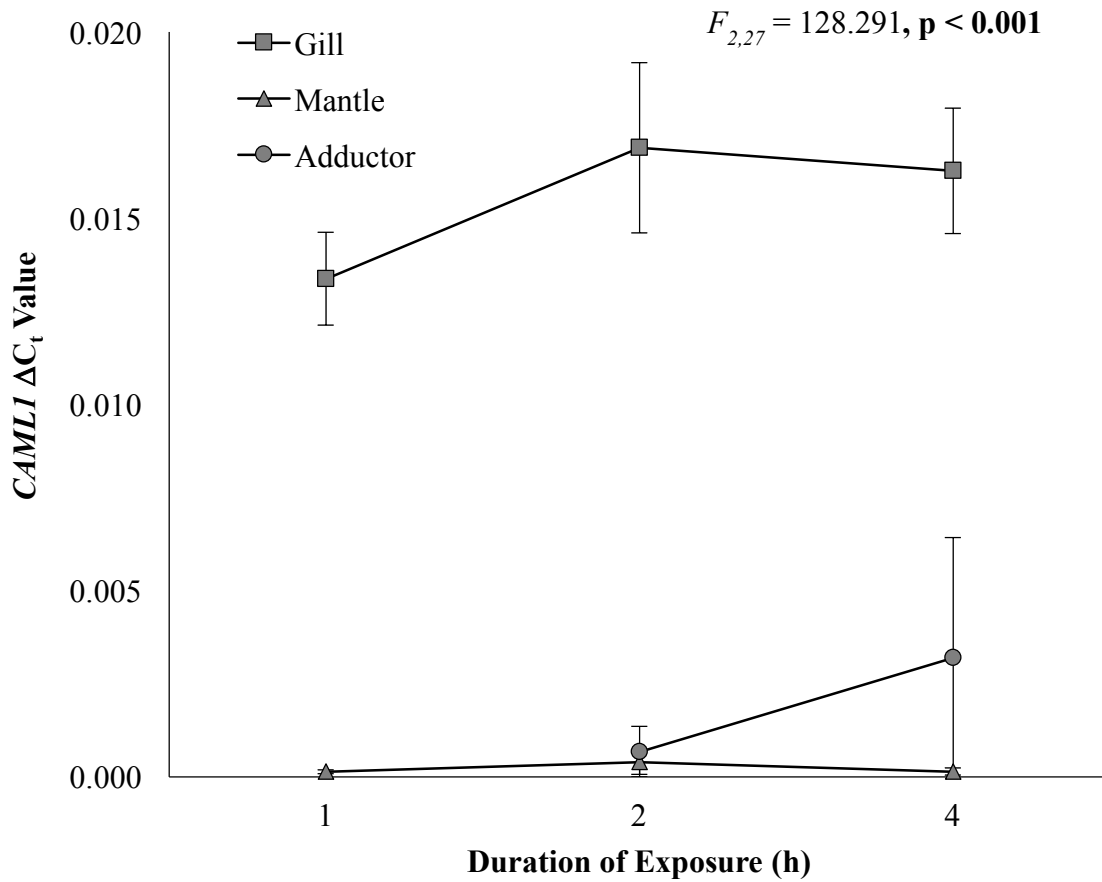


Figure 5.10. Baseline *CAML1* expression in juvenile mussels. The mean ΔC_t values (\pm SE) for *CAML1* expression in juvenile mussels was significantly higher in the gill tissue (closed squares) than in the mantle (closed triangles) or adductor (closed circles) tissues. This gene was not expressed in larval mussels.

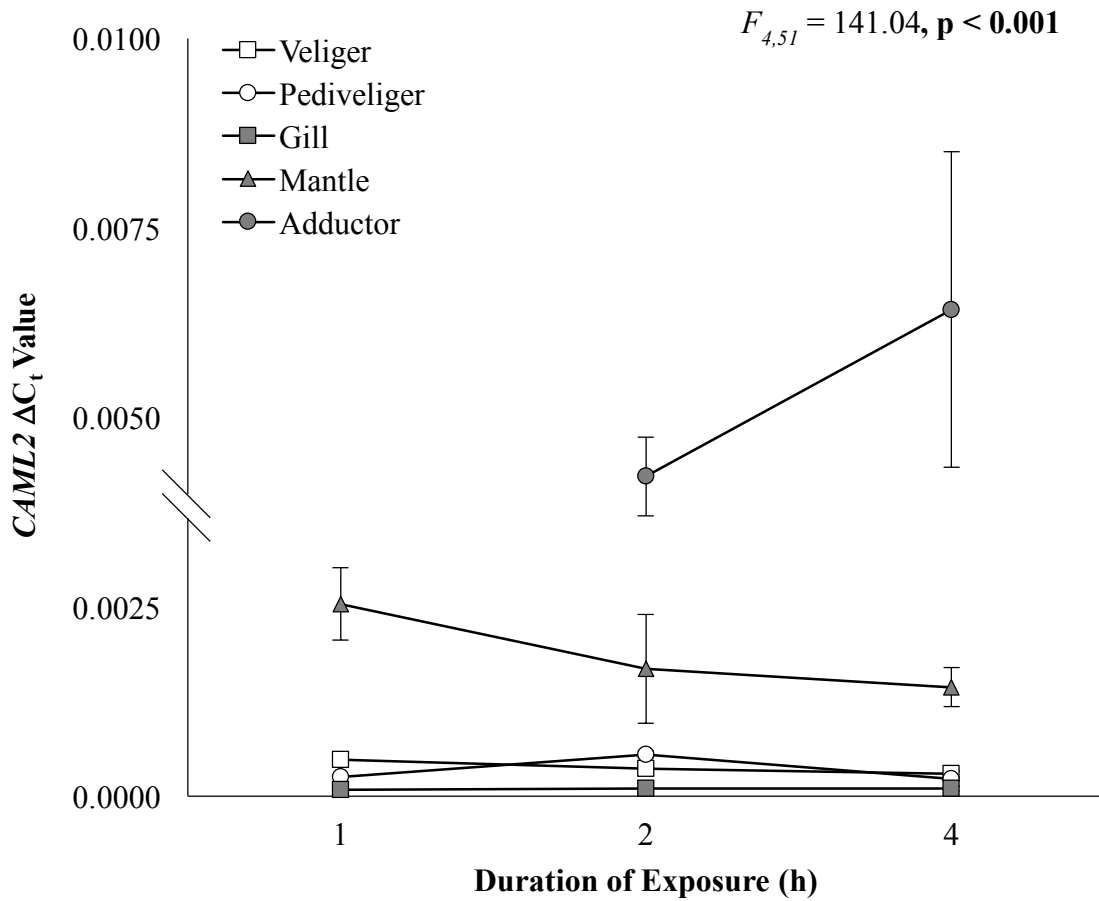


Figure 5.11. Baseline *CAML2* expression in *M. edulis*. The mean ΔC_t *CAML2* expression (\pm SE) was low in veligers (open squares), pediveligers (open circles), and the gill tissue (closed squares) relative to the mantle (closed triangles) and the adductor muscle (closed circles). There was a significant effect of stage or tissue type on *CAML2* expression, as well as an effect of time ($F_{2,51} = 4.231, p = 0.020$) and from the interaction term ($F_{7,51} = 3.488, p = 0.004$), resulting from the large increase in copy number in the adductor muscle of juvenile *M. edulis*.

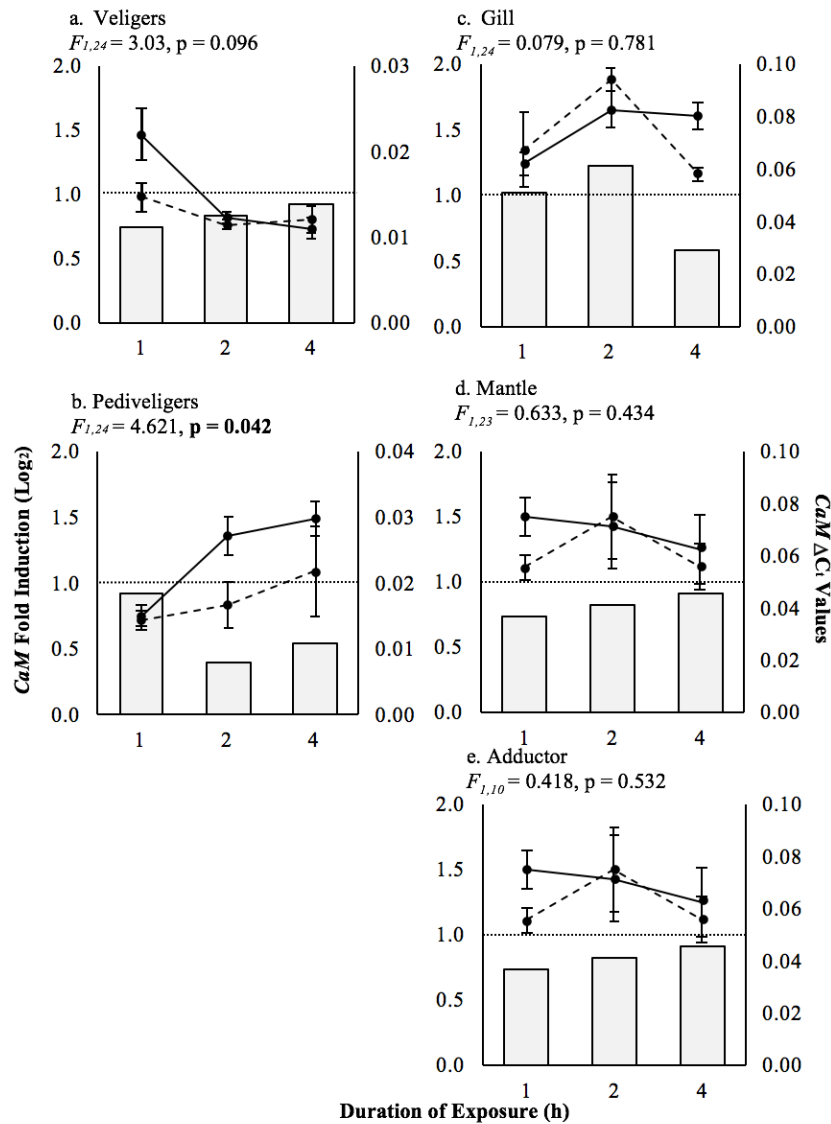


Figure 5.12. *CaM* expression in *M. edulis* during low-salinity exposure. *CaM* was significantly downregulated in pediveligers (b), but not in veliger (a) larvae or in the gill (c), mantle (d), or adductor (e) tissues of juvenile *M. edulis*. Gene expression is plotted as the fold induction of *CaM* during low-salinity exposure, relative to the controls, on a log₂ scale (bars), where the dotted line at 1 indicates that there was no change in expression and a value of greater than 1 represents an upregulation of the gene. The normalized mean ΔC_t values (± SE) for *CaM* that are used to calculate the fold induction and for statistical analyses are shown on the secondary axis for the control (solid line) and low-salinity treatment (dashed line) groups over the 4 h duration of the experiment.

(Figure 5.12a). The duration of exposure ($F_{2,24} = 10.264$, $p = 0.001$) and the interaction of treatment and duration of exposure ($F_{2,24} = 3.400$, $p = 0.050$) significantly affected *CaM* expression in veliger mussels, as the expression in the control groups at 1 h was reduced compared to the other time points. In pediveligers, we observed a significant downregulation of *CaM* in the low salinity treatment (Figure 5.12b), as well as a significant effect from the duration of exposure ($F_{2,24} = 4.488$, $p = 0.017$). In this case, expression of the gene declined in both the control and treatment groups over the 4 h course of the experiment. There was no interaction effect on *CaM* in pediveligers.

CaM expression was unaffected by low salinity treatment in any of the tissues examined in juvenile mussels. In the gill tissue (Figure 5.12c), *CaM* expression was variable and ranged from a slight upregulation at 2 h to an approximately 1-fold downregulation in the treatment group at 4 h. This resulted in a significant effect from duration of exposure on *CaM* expression ($F_{2,24} = 5.894$, $p = 0.008$); there was no interaction effect. In the mantle tissue, *CaM* showed an initial downregulation and began to increase in the treatment groups as the length of exposure increased (Figure 5.12d). This pattern was more extreme in the adductor muscle (Figure 5.12e), where we observed a downregulation at 2 h followed by an upregulation at 4 h. *CaM* expression in the mantle and adductor muscle were unaffected by length of exposure and there the interaction term was not significant in either tissue.

There was no evidence of changes in the abundance of *CAMLI* mRNA in juvenile mussels during low salinity exposure. *CAMLI* was slightly upregulated over the first 2 h of low salinity exposure and then began to decrease in the gill tissue, while the opposite trend was observed in the mantle and adductor muscle (Figure 5.13). We found no

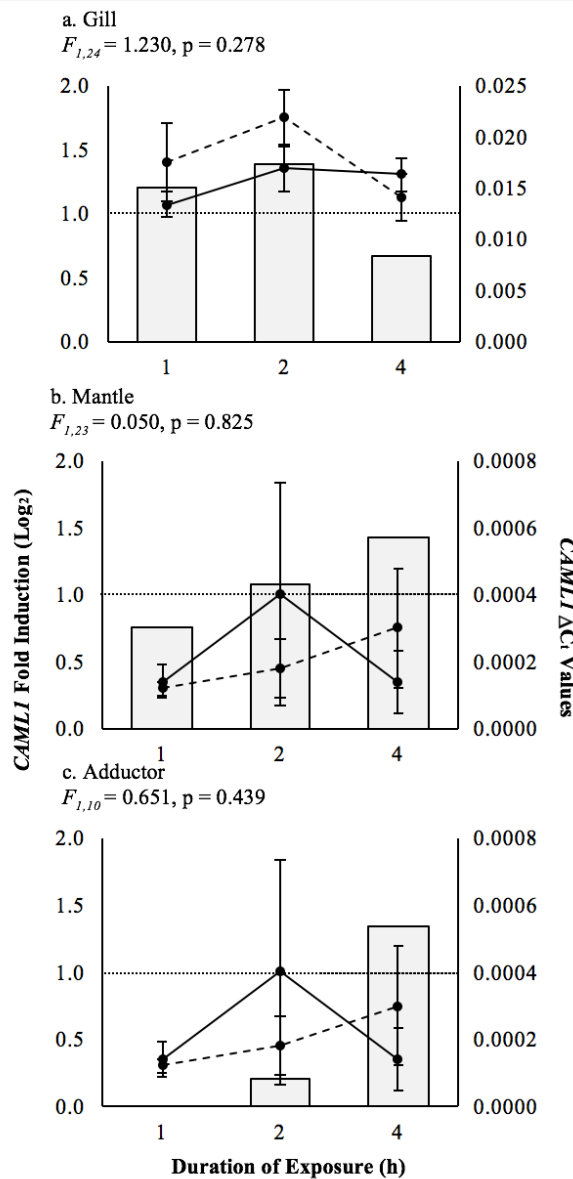


Figure 5.13. *CAML1* expression in *M. edulis* during low-salinity exposure. Expression of the calmodulin-like gene, *CAML1* was not affected by low-salinity treatment in the gill (a), mantle (b), or adductor muscle (c) of juvenile *M. edulis*. Each plot shows the fold induction of *CAML1* during low-salinity exposure, relative to the controls, on a log₂ scale (bars); the dotted line at 1 indicates that there was no change in expression, where a value of greater than 1 represents an upregulation of the gene. The normalized mean ΔC_t values (\pm SE) for *CAML1* are shown on the secondary axis for the control (solid line) and low-salinity treatment (dashed line) groups over the 4 h duration of the experiment. We were unable to measure expression of this gene in the 1 h adductor samples because of poor RNA recoveries.

significant effects of treatment, duration of exposure, or the interaction of the two on expression of *CAML1* in the gill or mantle tissue. We did, however, find that duration of exposure significantly affected *CAML1* expression in the adductor muscle, where expression in both the treatment and control groups decreased from 2 to 4 h.

The expression of *CAML2* was significantly affected by low salinity treatment, although this effect varied among stages and tissues of *M. edulis*. In veligers, *CAML2* expression was slightly downregulated at all time points sampled (Figure 5.14a), but this was not significant. We did not observe differences in *CAML2* expression in veligers from the duration of exposure or the interaction term. *CAML2* expression was significantly decreased in pediveligers during hypoosmotic exposure, especially at 2 h (Figure 5.14b). We observed a significant effect from the duration of exposure ($F_{2,24} = 5.869$, $p = 0.008$), but not the interaction of the two, resulting from an increase in expression of *CAML2* in the control group at 2 h.

An upregulation of *CAML2* was also observed in the gill tissue of low-salinity treated juvenile mussels (Figure 5.14c). In addition to a treatment effect, expression of *CAML2* was significantly affected by the duration of exposure ($F_{2,24} = 4.636$, $p = 0.020$) and the interaction of duration and treatment ($F_{2,24} = 3.463$, $p = 0.048$). The raw expression values in the treatment group varied over the course of the experiment, as can be seen by the 2-fold increase in expression at 2 h. In the mantle tissue, *CAML2* varied with duration of exposure and was downregulated more than 1-fold at 2 h but then upregulated by 4 h (Figure 5.14d). However, the expression was unaffected by treatment, duration of exposure, or the interaction term. In the adductor muscle, expression of

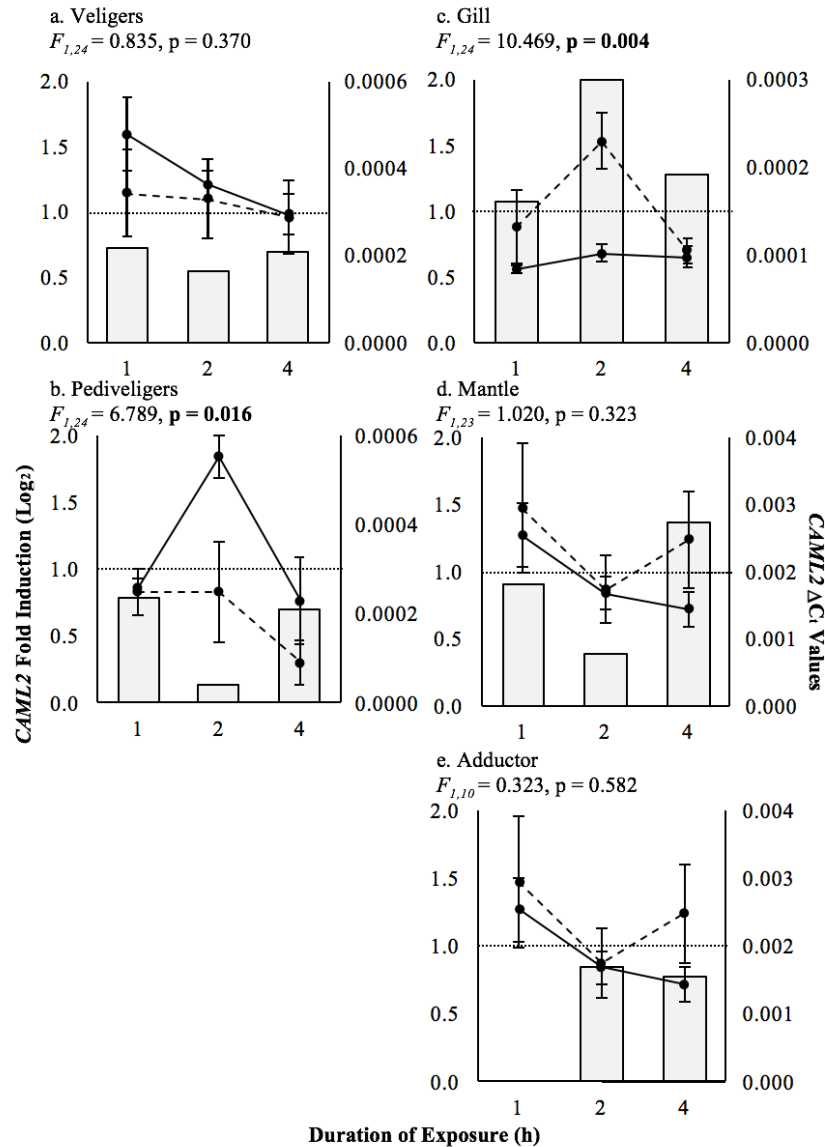


Figure 5.14. *CAML2* expression in *M. edulis* during low-salinity exposure. We observed a significant upregulation of *CAML2* in pediveligers (b) and in the gill tissue (c) of juveniles exposed to low salinity. *CAML2* expression was unaffected by salinity treatment in veligers (a) or in the mantle (d) or adductor (e) tissues of juveniles. We were unable to monitor expression of *CAML2* in the 1 h adductor samples because of difficulties with RNA extraction. Each plot shows the fold induction of *CAML2* during low-salinity exposure, relative to the controls, on a log₂ scale (bars); the dotted line at 1 indicates that there was no change in expression, where a value of greater than 1 represents an upregulation of the gene. The normalized mean ΔC_t values (\pm SE) for *CAML2* are also shown on the secondary axis for the control (solid line) and low-salinity treatment (dashed line) groups over the 4 h duration of the experiment.

CAML2 in the treatment groups was similar to that of the controls (Figure 5.14e) and was not significantly affected by treatment, duration of exposure, or the interaction of the two.

5.5 Discussion

To our knowledge, this is the first study to provide the complete coding sequence for calmodulin (*CaM*) from *Mytilus edulis*. Mussel *CaM* has high sequence homology to other invertebrate calmodulins (Figure 5.3) and, like other invertebrate *CaMs*, the predicted protein is 149 amino acids in length and only contains one tyrosine residue (Jamieson et al. 1980, Toda et al. 1981, Swanson et al. 1990, Li et al. 2004, Chen et al. 2012a, Chen et al. 2012b, Ren et al. 2013). In contrast, while most invertebrate calmodulins vary from human *CaM* by three residues (Simpson et al. 2005), we observed 11 residues that varied between *M. edulis* and human *CaM* (Figure 5.1) and from 9 to 11 that varied between *M. edulis* and other invertebrate species (Figure 5.3). Cysteine residues typically are rare in mature *CaM* proteins; however, we observed a substitution of cysteine for threonine at residue 79 and a valine to cysteine substitution at residue 142 that is conserved among all mytilid species (Figure 5.2). These substitutions have not been reported in vertebrate or invertebrate calmodulins (Li et al. 2004). The substitution from a tyrosine in human *CaM* at residue 99 (which acts as a phosphorylation site) to phenylalanine in *Mytilus* was also observed in the freshwater mussel *Hyriopsis cumingii*; Ren et al. (2013) suggested this substitution may alter the translational regulation of *CaM* in *H. cumingii*. Like other calmodulins, *M. edulis CaM* does not contain tryptophan (Li et al. 2004).

In other species, calmodulin is widely distributed in the nucleus and cytoplasm of cells and can constitute up to 0.1 % of the total protein pool (Chin and Means 2000,

Perochon et al. 2011). *CaM* mRNA expression in the gills of *M. edulis*, as observed from *in situ* hybridization (Figure 5.6), show similar patterns of widespread distribution in the cytoplasm and relatively lower expression in the nuclei. Interestingly, Strommel et al. (1983) estimated that CaM constituted 0.4 % of the protein pool within the cilia of *Aequipecten irradians* and Reed and Satir (1980) found calmodulin played an important role in regulating ciliary activity in the *Elliptio* sp. gills. We did not find any evidence for expression in the cilia of gills, although it is possible that the protein is translocated into the cilia from the cytoplasm following translation (Toutenhoofd and Strehler 2000). Although we did not have an opportunity to examine the distribution of *CaM* expression in the mantle tissue or adductor mussel, our qPCR-based evaluation of the copy number of *CaM* transcripts suggests that expression of this gene in the mantle tissue and adductor muscle is similar to what was observed in the gill. This is contrary to what Sailer et al. (1990) reported on the distribution of calmodulin proteins in *M. edulis*, although there is evidence that *CaM* transcripts in vertebrates may remain stable in the cytoplasm and that tissue-specific regulation of translation modulates intracellular CaM pools (Toutenhoofd and Strehler 2000).

We did, however, detect a significant decrease in the copy number of *CaM* transcripts in larval blue mussels relative to the juvenile tissue samples (Figure 5.9). Ontogenetic regulation of *CaM* expression has been reported in other species, such as the polychaete *Hydroides elegans* (Weinman et al. 1991, Yang et al. 1998, Jackson et al. 2007, Chen et al. 2012a, 2012b), and, as we observed in *M. edulis*, generally results in lower abundance of *CaM* mRNA in precompetent and competent larval worms relative to juveniles (Chen et al. 2012b). Bassim et al. (2014) reported developmental regulation of

numerous ‘calmodulin’ genes in *M. edulis* in their RNAseq-based study. However, the high sequence homology among small partial reads, common in RNAseq data, makes it difficult to determine clearly how many of the transcripts they detected code for calmodulin versus calmodulin-like genes. Several previous studies have shown that *CaM* may be important in regulating developmental transitions (Chen et al. 2012a), as well as playing a role in shell secretion (Jackson et al. 2007), detection of settlement cues, and in regulating calcium stores in larvae (Chen et al. 2012b). It is somewhat surprising then, that a gene with such a crucial role in the cell would be found in lower abundance in developing larvae than in post-metamorphic juveniles.

The calmodulin-like gene *CAML1* is also developmentally regulated in *M. edulis* and was not detected in veliger or pediveliger larvae. In comparison to the predicted protein sequence for mussel CaM, *CAML1* has very low sequence homology to CaM (Figure 5.4). Even so, three of the four EF-hand domains have minimal substitutions. Jamieson et al. (1980) suggested that the glycine residues within the EF-hand domains help form the helical structure where calcium-binding occurs and those within the *CAML1* EF-hand domains 2-4 are unaltered (residues 58-63, 96-101, and 132-137; Figure 5.4). Our modeling work suggests the EF-hand domains of *CAML1* maintain their structure and may still function to bind calcium, although the affinity to Ca^{2+} may be altered. It is unlikely, however, that this protein is involved in protein-protein interactions to the same extent as CaM. We found substitutions in methionine at residue 126 and toward the C-terminus, which in mammalian systems are the sites of CaM-protein interactions (Chin and Means 2002). *CAML1* was more locally distributed in the gill cells of *M. edulis* compared to *CaM* and was less abundant (Figure 5.7). These differences,

together with the lack of expression in larvae, suggest that this protein is functionally distinct from calmodulin and plays a novel, but perhaps less extensive, roll in cellular function or signaling.

CAML2 has higher sequence homology to *CaM* (Figure 5.5) than does *CAML1* and structural analysis suggests that all four EF-hand domains in *CAML2* are functional. Furthermore, there were no substitutions of the methionine residues that may facilitate interaction with calcium-binding proteins (Chin and Means 2000). The major structural difference between *CaM* and *CAML2* is an insertion at the 5' end of the gene that extends the open reading frame by 36 to 69 base pairs (Figure 5.5) and results in an elongation of the protein at the N-terminus, prior to the first EF-hand domain. In *CaM*, the N-terminal may interact with other proteins when Ca^{2+} is not bound because of the structural flexibility in this region (Chin and Means 2000); undoubtedly, this insertion will impact the stability of the protein and the protein-protein interactions that may occur at this site.

As with *CaM* and *CAML1*, we observed both tissue- and stage-specific differences in the baseline expression *CAML2*. *In situ* hybridization suggested that the expression of *CAML2* was lower than *CaM* in the gill tissue and appeared to be localized around the perimeter of the gill cells and within regions of the cytoplasm (Figure 5.8). Copy-number analysis indicated that while expression within the gill tissue was relatively low, on average *CAML2* expression increased by 16-fold in the mantle tissue and by over 100-fold in the adductor muscle. We also found higher baseline expression of *CAML2* in veliger and pediveliger larvae relative to the gill tissue. Given the patterns of expression observed from *in situ* hybridization and in qPCR studies, it is likely that *CAML2* is involved in a calcium-mediated role that may be more targeted than that of *CaM*. In

other mollusk species, some *CAML* genes are thought to play a role in shell formation (Jackson et al. 2007, Ren et al. 2013). Further studies are needed to determine the function of *CAML1* and *CAML2* in *M. edulis*, although it is unlikely that either of these genes is involved in biomineralization.

Data from our previous microarray study (Chapter 4), suggested that expression of *CaM*, *CAML1*, and *CAML2* may be induced by low salinity exposure in blue mussels (Figure 4.1). During hypoosmotic exposure, calmodulin is thought to help regulate taurine efflux from cells and, therefore, maintenance of osmotic balance (Pierce et al. 1989, Pierce and Warren 2001, Falktoft and Lambert 2004) and its upregulation has been observed during short-term hypoosmotic stress in *M. trossulus* and *M. galloprovincialis* (Lockwood and Somero 2011). Calmodulin-like proteins are also known to have a role in plants response to osmotic stress, where they function in cell signaling pathways and regulation of transcription factors (Snedden and Fromm 1998, Perochon et al. 2011, Reddy et al. 2011, Zeng et al. 2015).

It was somewhat surprising, then, to find that *CaM*, *CAML1*, and *CAML2* were generally downregulated in *M. edulis* during low salinity exposure. In juvenile *M. edulis*, we observed distinct gene- and tissue-specific patterns of expression. Overall, expression of *CaM* was reduced in all tissue of juvenile mussels, except the adductor muscle after 4 h of exposure (Figure 5.12). In the adductor muscle, an increase in *CaM* expression may aid in the behavioral response of mussels to hypoosmotic stress, helping to isolate the mussel from the external environment through closure of the valves (Sailer et al. 1990). As a cellular signaling molecule, *CaM* may play a role in osmosensing and early signal transduction pathways (Kültz 2005, Zhao et al. 2012) in other tissues. As such, we

expected that our qPCR results from this study would support our observations from a microarray study (Figure 4.1) and from preliminary qPCR studies in the gill tissue (Figure C.5). However, it is possible that *CaM* upregulation only occurs during longer term salinity exposure (e.g., greater than 4 h) or that translational regulation controls the response of *CaM* (Toutenhoofd and Strehler 2000). Zhao et al. (2012) found that oysters decreased *CaM* expression during low salinity exposure in the gill tissue as a response to declines in intracellular calcium concentrations, but this would not explain why *CaM* expression in *M. edulis* varied among our different gene expression studies.

Unlike *CaM*, we found significant increases in the expression of *CAML2* in the gill tissue of juvenile *M. edulis* and decreases in expression in the adductor muscle (Figure 5.14). As discussed above, it is possible that this gene functions in calcium-binding and may play a similar role to CAML genes in plants that are involved in salt-stress related signaling pathways (Zeng et al. 2015). If so, the tissue-specific patterns in expression suggest this role may be restricted to the gill tissue. We observed marked increases in the expression of *CAML2* in the adductor muscle in control animals suggesting that *CAML2* exhibits tissue-specific functions and is not necessarily implicated in the stress response. Similarly, *CAML1* may have developed novel functions that are specific to post-metamorphic mussels. Differential patterns of expression in *CAML1* among the gill and adductor muscle (Figure 5.13) may also suggest that the role of this protein varies among tissue types.

Surprisingly, larval mussels differed from juveniles in the regulation of *CaM* and *CAML2* during low salinity exposure. We found decreases in the expression of both genes at multiple time points, stages, and tissues. In pediveligers, there was a significant

effect of treatment on the expression of *CaM* and *CAML2* (Figures 5.12 and 5.14). CaM is known to play an integral role in growth (Weinman et al. 1991), shell formation (Jackson et al. 2007), and larval settlement (Chen et al. 2012a, Chen et al. 2012b), suggesting that the role of CaM in these processes in mussel larvae is not related to increases in transcript abundance. On the other hand, bivalve larvae are known to delay metamorphosis when exposed to environmental stressors (Bayne 1965) and downregulation of genes involved in Ca_2^+ signaling may help to mediate this response. Furthermore, larvae are more sensitive to low salinity exposure than juvenile mussels and show marked reductions in growth when reared at low salinity. Variations in the expression of *CaM* and *CAML* genes during osmotic stress across developmental stages may signify a divergence in metabolic regulations pre- and post-metamorphosis that account for reduced growth and increased susceptibility in early life history stages.

To our knowledge, this study is the first to identify and sequence calmodulin-like genes in *M. edulis* and to explore tissue- and stage-specific patterns of expression during normal and low salinity conditions. It appears that blue mussels, like other species, have numerous genes that code for calmodulin-like proteins and that these genes and calmodulin may be developmentally regulated and differentially expressed among tissues of post-metamorphic mussels and during short-term hypoosmotic exposure. Despite the importance of these calcium-binding proteins in other species, we know very little about their role in the cellular function, during osmotic stress, or in larval development of blue mussels. Further research should be conducted to better understand the physiological implications of the stage- and tissue-specific patterns of *CaM*, *CAML1*, and *CAML2* expression found in this study.

CHAPTER 6

ORNITHINE METABOLISM AND THE OSMOTIC STRESS RESPONSE: A COMPARATIVE STUDY OF CONGENERIC SPECIES

6.1 Abstract

Previous studies of transcriptomic responses in blue mussels (*Mytilus* spp.) to hypoosmotic exposure have suggested differential utilization of the amino acid ornithine among congeneric species. Ornithine catabolism is used to generate glutamate or proline through the activity of ornithine aminotransferase (OAT), or to create putrescine and other polyamines through activity of ornithine decarboxylase (ODC). Variation in expression of genes involved in ornithine metabolic pathways may help to explain differences in the salinity tolerances of *M. galloprovincialis*, *M. trossulus*, and *M. edulis*. This study was undertaken to better understand the potential role of OAT and ODC in blue mussels during exposure to altered salinity, as well as to look for variation in gene expression across developmental stage and among species. We found evidence that *OAT* gene expression increases during low salinity exposure in all three species, and that in *M. edulis* increased expression manifested in increased OAT activity. We did not observe consistent changes in the expression of *ODC* during hypoosmotic exposure, although it tended to be downregulated. During hyperosmotic stress, the patterns of expression of these two genes reversed, suggesting that synthesis of proline or glutamate is important during low salinity exposure but that polyamine synthesis may be more important during hyperosmotic exposure. The three species responded similarly to osmotic stress with

respect to *ODC* and *OAT* expression, although the magnitude or timing of expression varied slightly among species.

6.2 Introduction

Blue mussels (*Mytilus* spp.) are dominant members of coastal habitats and play an important role in intertidal and subtidal community ecology by providing habitat (Arribas et al. 2014) and food (Seed 1969) for other species. Numerous studies have documented how tolerance to environmental stressors, including stress caused by changes in salinity, affects the distribution and abundance of species in this genus (e.g., Gardner and Thompson 2001, Qiu et al. 2002, Westerbom et al. 2002, Braby and Somero 2006). Climate change is predicted to cause a freshening in sea-surface salinities in the coastal regions where mussels live (Antonov et al. 2002, Durack et al. 2012), creating potential shifts in the geographic range of these species. Understanding the molecular mechanisms underlying variation in mussels' capacity to tolerate low salinity stress is important for predicting how mytilid species will be affected by climate change-associated salinity fluctuations, as well as their capacity to adapt to shifting environments (Somero 2010).

Two mytilid species, *M. edulis* and *M. trossulus*, inhabit the Gulf of Maine (Koehn 1991, Rawson et al. 2001) and these congeners are affected differently by lowered salinity (Gardner and Thompson 2001, Qiu et al. 2002). For example, the studies of Qiu et al. (2002) and Westerbom et al. (2002) suggest that *M. trossulus* is more euryhaline than *M. edulis*. Thus, comparative studies of the osmotic response in these closely related species provide a unique opportunity to evaluate the evolutionary underpinnings of the response to low salinity stress. Using a microarray-based approach (see Chapter 4), we compared how the patterns of gene expression for these two species

respond to short-term, low salinity exposure. We observed differential expression of a gene coding for ornithine aminotransferase (OAT; Figure 4.1), a key enzyme in the ornithine cycle that catalyzes the conversion of ornithine into glutamate or proline (Andrews and Reid 1971, Bishop et al. 1994; Figure 6.1). In a similar study comparing the low salinity response in of *M. trossulus* and another congener, *M. galloprovincialis*, Lockwood and Somero (2011) found evidence for differential expression for a gene coding for ornithine decarboxylase (ODC). This enzyme shunts ornithine through an alternative pathway catalyzing the decarboxylation of ornithine to produce the polyamine, putrescine (Pegg 2006). We conducted a series of follow-up experiments using quantitative real-time polymerase chain reaction (qPCR) to monitor gene expression in *M. edulis* and found that expression of *OAT* (Figure C.3) is upregulated, while that of *ODC* (Figure C.4) is downregulated at multiple time points over a 48-h exposure to reduced salinity. Together, our studies and that of Lockwood and Somero (2010) indicate there is divergence among mussels in the genus *Mytilus* with respect to the utilization of ornithine during low salinity stress.

To better understand regulation of *OAT* and *ODC* during hypoosmotic exposure, and to make direct comparisons among species, we exposed individuals of *M. edulis*, *M. trossulus*, and *M. galloprovincialis* to hypoosmotic conditions and monitored changes in expression of *OAT* and *ODC* using qPCR. As part of these studies, we investigated the variation in the regulation of *OAT* and *ODC* across developmental stages and different tissues in *M. edulis*. Typically, larval stages are more sensitive than juveniles and adults to environmental stress and thus determining capacity of larval stages to respond is essential for a thorough understanding of species-specific differences in low salinity

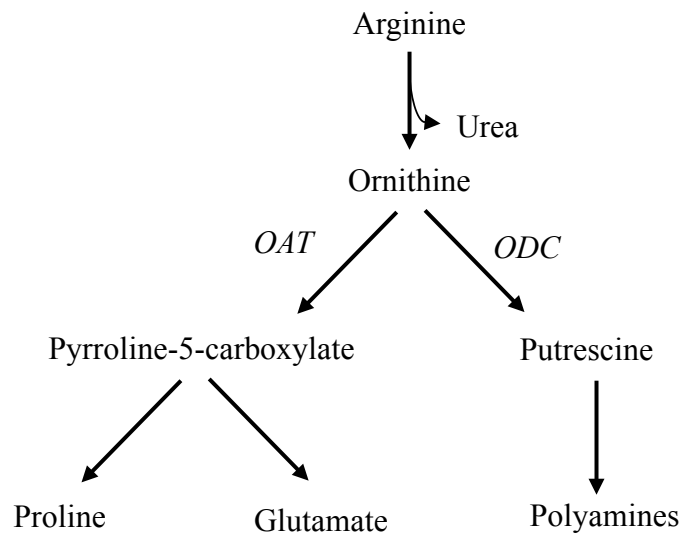


Figure 6.1. Overview of ornithine metabolism. Ornithine catabolism occurs via two pathways, through the activity of ornithine aminotransferase (OAT) which converts ornithine into proline or glutamate via pyrroline-5-carboxylate (P5C) or through ornithine decarboxylase (ODC) which breaks down ornithine into polyamines. Redrawn from Bishop et al. (1985) and Bishop et al. (1994).

tolerance (Qiu et al. 2002, Lockwood and Somero 2001). We also monitored activity of OAT using a colorimetric enzyme assay to determine if OAT activity is transcriptionally regulated in *M. edulis* and whether that regulation varies across developmental stages. Finally, we monitored *OAT* and *ODC* expression in individuals of the three species exposed to hyperosmotic stress. A primary goal of this study was to use qPCR-based assays to validate patterns of *OAT* and *ODC* expression during low salinity exposure to validate patterns observed in microarray studies (Chapter 4, Lockwood and Somero 2011). Our gene expression studies, with the use of enzyme assays, allow us to place the differential patterns of expression into a broader physiological context that will increase our understanding of how mytilid species deal with osmotic stress.

6.3 Methods

6.3.1 Hyposalinity Experiments

We examined the variation in *OAT* and *ODC* expression among larval and juvenile *M. edulis* when exposed to short-term low salinity conditions. The larvae were reared in ambient conditions (13.5 °C, 32 ppt) at the shellfish hatchery at the Darling Marine Center in Walpole, ME, as outlined in Section 2.3.1. Larvae were exposed to control (32 ppt) or low salinity treatments (20 ppt) for 24, 48, and 72 h at both the veliger and pediveliger stages, as described in Section 4.3.4. Field collected juvenile *M. edulis* were acclimated to common garden conditions (13.5 °C, 32 ppt) for 3 w before they were exposed to a similar control and experimental treatments, as detailed in Section 4.3.3. We sampled the gill, mantle, and adductor muscles from juveniles in both treatments at three different durations of exposure, 24, 48, and 72 h. We also sampled gill tissue from a separate set of *M. edulis* held in control or experimental treatments for only 4 h.

We repeated the low salinity experiments using *M. galloprovincialis* and *M. trossulus*. *M. galloprovincialis* mussels were supplied by Catalina Sea Ranch, CA, a mussel culture facility located on the San Pedro Shelf. The mussels were shipped overnight to the University of Maine, Orono, ME, in September 2016 and acclimated to control conditions (13.5 °C, 32 ppt) in a recirculating seawater system for 3 w, during which they were fed an approximately 3 % ration of Shellfish Diet 1800 (Reed Mariculture, Inc.). One day prior to the salinity-challenge experiments, we inserted a small spacer (slit airline tubing) between the valves of the mussels to prop them open and ensure that they were bathed in the external medium for the duration of the experiment. Individual mussels were placed into 1 l beakers containing treatment (20 ppt) or control (32 ppt) seawater and held at 13.5 °C for 4, 24, or 48 h before they were dissected; the gill and mantle tissues were flash frozen in liquid N₂ and stored at -80 °C.

The adult specimens of *M. trossulus* used in this experiment were part of a previous project that were obtained from the underside of a dock in Newport, OR, in February 2012. The mussels were shipped overnight to the University of Maine, Orono, ME, acclimated to control conditions (32 ppt, 12 °C), and fed for 3 w prior to low salinity treatments, similar to the culture of *M. edulis* and *M. galloprovincialis* described above. The *M. trossulus* mussels were exposed to a low salinity (20 ppt) or control (32 ppt) treatment for 24 or 48 h, but rather than shocking the mussels by direct salinity transfer, we slowly lowered the salinity by 1.25 ppm h⁻¹ to allow the mussels to adjust to the treatment conditions. Following each experiment, the gill tissue was removed, flash frozen in liquid N₂, and stored at -80 °C.

6.3.2 Hypersalinity Experiments

Mussels from all three species were also exposed to high salinity conditions for 4 and 24 h. For this experiment, the *M. galloprovincialis* and the *M. edulis* were from the same population samples described above, while a new sample of *M. trossulus* was obtained from Newport, OR, in 2017. All mussels were acclimated to control conditions (13.5 °C, 30 ppt) in a recirculating system at the University of Maine. Prior to experimentation, we inserted plastic spacers into the *M. galloprovincialis* and *M. trossulus*, but not *M. edulis*, to prop open the valves during treatment. The mussels were then placed into 1 l beakers containing control (30 ppt) or high salinity treatment (40 ppt) seawater (Crystal Sea®, Marine Enterprises, LLC) and held at 13.5 °C for 4 and 24 h. The gills from each mussel were dissected, flash frozen in liquid N₂, and stored at -80 °C.

6.3.3 Gene Expression Studies

We used qPCR to monitor the expression of two genes involved in ornithine metabolism, ornithine aminotransferase (*OAT*) and ornithine decarboxylase (*ODC*), during low salinity treatment. Primers for qPCR analysis of *OAT* and *ODC* expression were designed from expressed sequence tags (ESTs) identified from our microarray study (Appendix B). A portion of the tissue from each sample was used to extract total RNA; the methods for the sample preparation, including the RNA extraction, cDNA synthesis, and the qPCR assays can be found in Section 4.3.6. Due to sequence divergence among the congeners at the *OAT* gene, an alternative reverse primer was used for the *OAT* qPCR assays with *M. galloprovincialis* and *M. trossulus* (Table 6.1). Expression of *OAT* and *ODC* was normalized to 40 S ribosomal protein (*40S*) and elongation factor 1a (*EF1a*) and analyzed using the ΔC_t method (Bustin et al. 2009).

Gene Name	Symbol	Function	Primer	Sequence (5' to 3')	Size (bp)	T _m (°C)
40S Ribosomal Subunit	40S	Normalizing Gene	40S RBP-F5	TACCCGCTGACAGTCTTGGTG	193	56.8
			40S RBP-R5	ACATCCACCGGACTGACTTCC		
Elongation Factor 1 α	<i>EF1α</i>	Normalizing Gene	EF1 α Q1F	ACCCAAGGGAGCCAAAAGTT	211	54.8
			EF1 α Q1R	TGTCAACGATACCAGCATCC		
			OAT Q3F	CATTGTCATCCAAAGATTGTC AAGGC		
Ornithine aminotransferase	<i>OAT</i>	<i>M. edulis</i> Target	OAT Q2R	ACCAGCAGCAAAACACAATCT	252	55.2
			OAT Q3F	CATTGTCATCCAAAGATTGTC AAGGC		
			OAT Q1R	TCCTGGCTAATTTACAGGCTGT		
Ornithine decarboxylase	<i>ODC</i>	Congener Target	ODC Q1F	AATGGCATGCCAGCACCAA	191	56.1
			ODC Q1R	TTGGGTTAAACTTCAGGGTTTC		

Table 6.1. Primer sets used in the *OAT* and *ODC* qPCR assays. The primer names, 5' to 3' oligonucleotide sequences, expected product size (in base pairs, bp), and annealing temperature (T_m in °C) are listed for each of the four genes used in the qPCR assays. The 40S ribosomal subunit (*40S*) and elongation factor 1 α (*EF1 α*) were used as reference genes to normalize the expression of the target genes, ornithine aminotransferase (*OAT*) and ornithine decarboxylase (*ODC*). For *OAT*, an alternate reverse primer (OAT Q1R) was used in the assays for *M. galloprovincialis* and *M. trostulus* because of substitutions between species in the priming region.

6.3.4 Ornithine Aminotransferase Activity Assays

We used a modified end-point colorimetric assay, described by Peraino and Pitot (1963) to monitor the activity of ornithine aminotransferase (via production of pyrroline-5-carboxylic acid, P5C; Figure 6.1) during low salinity exposure in larval and juvenile *M. edulis*. Proteins were extracted from a subset of each tissue sample or pool of larvae by placing roughly 50 mg of wet tissue into a 1.5 ml tube containing 200 μ l of homogenization buffer (25 mM HEPES, 5 mM EDTA, 10% glycerol, 1% Triton X, 4 μ g/ml pyrroline phosphate, 1X PMSF, and cOmplete™ EDTA-free (Roche Diagnostics) Protease Inhibitors) and manually grinding with a pestle. The homogenized samples were spun at 13,200 g for 10 m at 4 °C and the supernatants were removed and stored at -80 °C. Protein concentrations were determined against a standard bovine serum albumin (BSA) curve using the Bradford Protein Assay (Bradford 1976).

The ornithine aminotransferase assay was run by combining 200 ng of total protein with the enzyme assay mixture, which contained 7.5 μ l 1M KPO₄ buffer, 24 μ l 150 mM ornithine, 2.5 μ l 200 mM aminobenzaldehyde, and 2 μ l α -ketoglutarate. For each sample, we ran two replicate reactions as well as two control reactions that contained H₂O instead of the enzyme substrate, α -ketoglutarate. The reactions were incubated at 20 °C for 2 h before the reaction was terminated by heat shock at 95 °C for 10 m. The absorbance of the 100- μ l sample was read at 440 nm on a UV-3100PC Scanning Spectrophotometer (VWR®) for the juvenile tissue samples and a DU-640 UV-VIS Spectrophotometer (Beckman Coulter, Inc.) for the larval samples. We also ran a ‘control’ protein sample with each assay that allowed us to standardize absorbance values and control for run-to-run variability. We quantified OAT activity with respect with

respect to the increase in P5C as a function of the total mass of protein added to each assay ($\mu\text{moles P5C}\cdot\text{g}^{-1}\cdot\text{protein h}^{-1}$); activity estimates included adjusting the absorbance of our positive (containing α -ketoglutarate) reactions to that of the controls, multiplied the molar extinction coefficient of P5C (2.71×10^3 ; Herzfeld and Knox 1968), and adjusted for the duration of the incubation and total protein added.

6.3.5 Data Analysis

All statistical analyses were performed in SSPS Statistics 22.0 (IBM Corporation). For the *M. edulis* qPCR data, the effects of low-salinity treatment on the ΔC_t expression of *OAT* and *ODC* were tested using a two-factor ANOVA, with treatment and duration of exposure as the main effects, with an interaction term. We were also interested in understanding differences in the expression of these genes among closely related species, so we also ran a two-factor ANOVA for the 4, 24, and 48 h data with salinity treatment and species as the main effects, as well as the interaction of these variables. For the hypersalinity experiments, we designed a similar model to evaluate the effects of high-salinity treatment on the species-specific patterns of *OAT* and *ODC* expression. We ran two-factor ANOVAs for the 4 h and 24 h exposure data with high salinity treatment and species as main effects and an interaction term. All statistics for the qPCR data were run on the normalized ΔC_t values and the hypotheses for each model were tested using a Type III Sum of Squares with an overall $\alpha = 0.05$. The effects of low-salinity treatment on ornithine aminotransferase activity in larval and juvenile *M. edulis* were also tested using a two-factor ANOVA. For each stage, we tested the low-salinity treatment and duration of exposure main effects on enzyme activity against a Type III Sum of Squares model with $\alpha = 0.05$. For the models comparing responses among

species, we ran Fisher's Least Significant Difference (LSD) post-hoc analyses to discern which species diverged in their regulation of *OAT* and *ODC*.

6.4 Results

6.4.1 Regulation of Ornithine in Hyposaline-Challenged *M. edulis*

The regulation of ornithine aminotransferase (*OAT*) and ornithine decarboxylase (*ODC*) is significantly affected by exposure to low salinity in larval and juvenile *M. edulis*. In veliger larvae, we observed a significant two- to four-fold increase in *OAT* expression (Figure 6.2a) and a one- to three-fold decrease in *ODC* expression (Figure 6.3a) during low salinity exposure, as well as a significant decline in *ODC* expression in both control and treatment groups with prolonged exposure ($F_{2,24} = 8.296$, $p = 0.002$). *OAT* expression was unaffected by duration of exposure and, for both *OAT* and *ODC*, there were no significant interactions between treatment and duration of exposure in veligers. Ornithine aminotransferase enzyme activity mirrored *OAT* expression and was significantly higher in veligers from the low salinity treatment group (Figure 6.4a). Pediveligers also upregulated expression of *OAT* (Figure 6.2b) and increased *OAT* activity (Figure 6.4b) during low salinity treatment, although the expression of *ODC* was not significantly altered in treated pediveligers (Figure 6.3b). Neither length of exposure nor interaction between treatment and exposure affected the expression of *OAT* or *ODC*, or the activity of *OAT* in pediveligers.

In juvenile mussels, the regulation of *OAT* and *ODC* during low salinity exposure was similar to larval mussels, although there were slight variations among tissues. The expression of *OAT* was significantly upregulated in the gills of treated mussels (Figures 6.2c) and increased over 4-fold during low salinity exposure. This corresponded to an

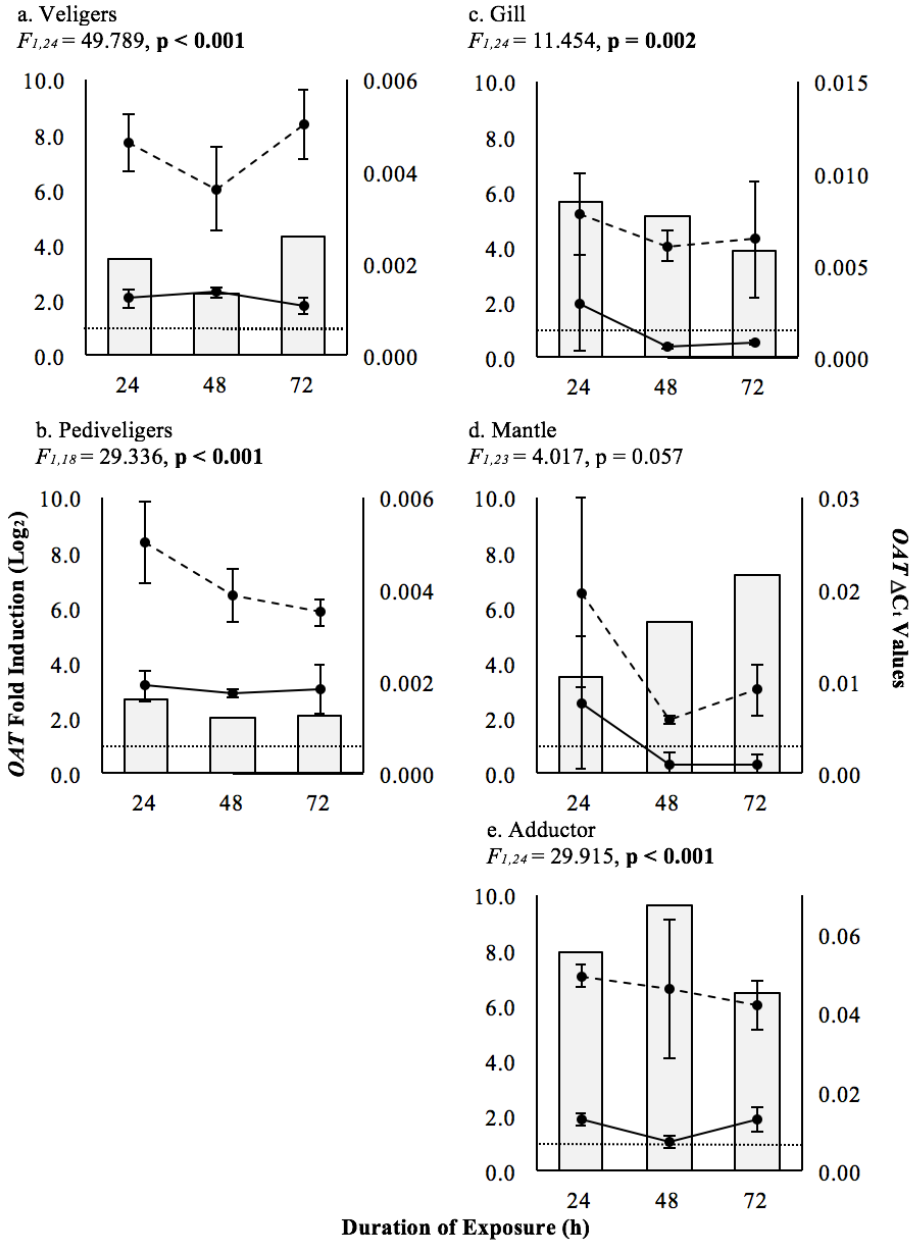


Figure 6.2. *OAT* expression in hyposalinity-challenged *M. edulis*. *OAT* was upregulated more than 2-fold in veliger (a) and pediveliger (b) larvae, and greater than 4-fold in the gill (c), mantle (d), and adductor tissues (e) of juvenile mussels exposed to low salinity. *OAT* expression is displayed as the fold induction on the primary y-axis, where the expression of the salinity treated groups is plotted relative to the controls on a log₂ scale (bars) and the dotted line at 1 indicates no change in expression between treatments. The secondary y-axis shows the normalized ΔC_t expression values for the control (solid line) and the low salinity (dashed line) treatments (\pm SE).

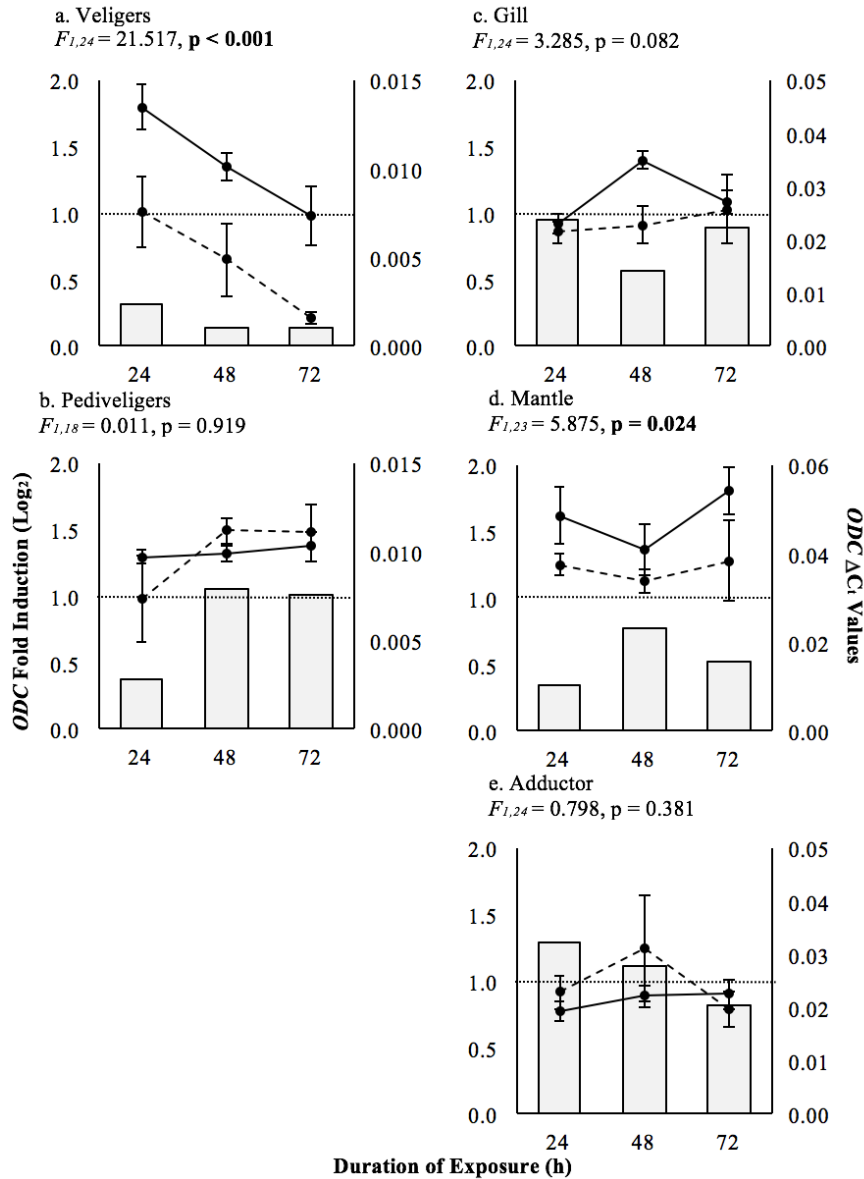


Figure 6.3. *ODC* Expression in *M. edulis* during low-salinity exposure. In veligers (a) and in the mantle tissue (d), *ODC* expression was significantly downregulated, but in pediveligers (b) and the gill (c) and adductor tissues (e) of juvenile mussels, *ODC* expression was unaffected by low salinity exposure. *ODC* expression is displayed as the fold induction on the primary y-axis, where the expression of the salinity treated groups is plotted relative to the controls on a \log_2 scale (bars) and the dotted line at 1 indicates no change in expression between treatments. The secondary y-axis shows the normalized ΔC_t expression values for the control (solid line) and the low salinity (dashed line) treatments (\pm SE).

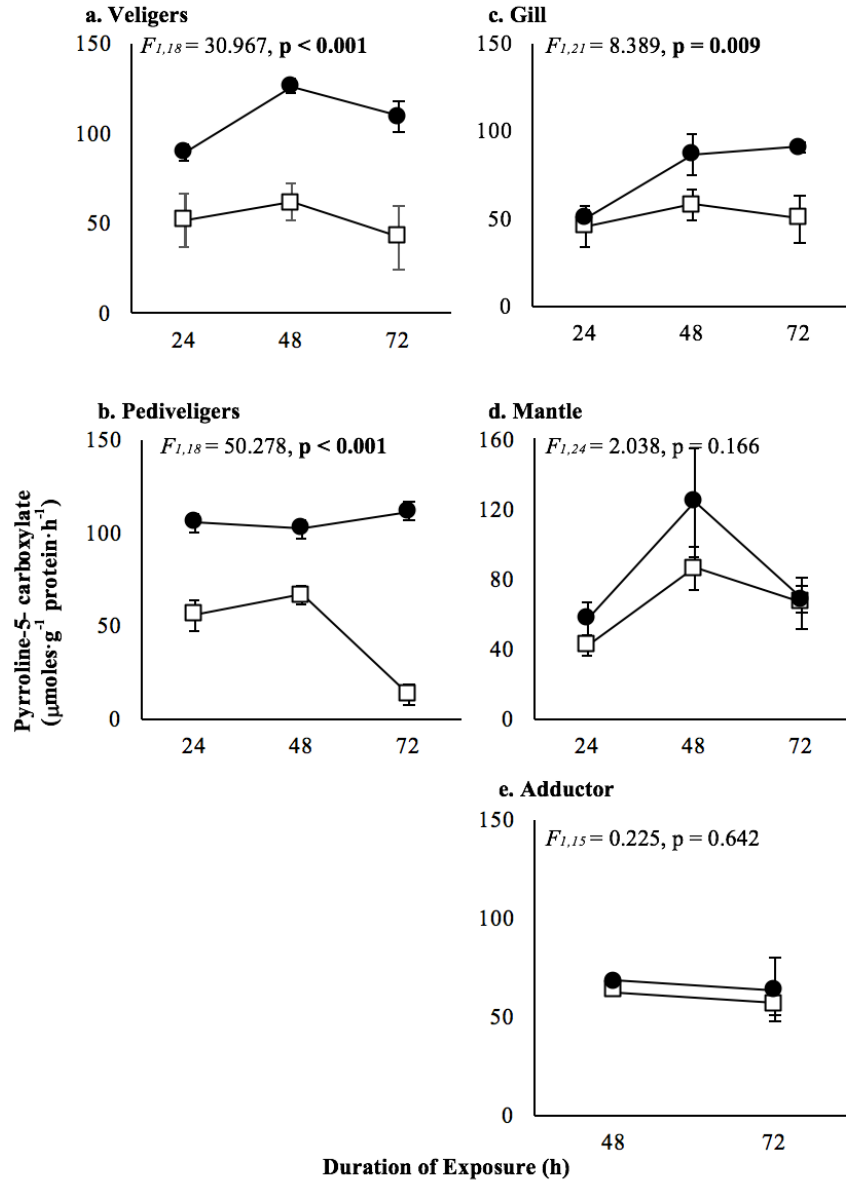


Figure 6.4. Ornithine aminotransferase activity in *M. edulis*. OAT activity was measured as the production of pyrroline-5-carboxylate (P5C) in $\mu\text{moles}\cdot\text{g}^{-1}\text{ protein}\cdot\text{h}^{-1} \pm \text{SE}$. OAT activity was significantly increased in the veliger (a) and pediveliger (b) larvae and in the gill tissue (c) of juvenile mussels from the low salinity treatment (closed circles) relative the control groups (open squares). We did not observe increased OAT activity in the mantle (d) or adductor tissues (e) of low salinity-treated juveniles. Due to limited tissue availability from the 24 h exposure, OAT activity was only measured at 48 and 72 h in the adductor muscle.

increase in the OAT enzyme activity in the gill tissue (Figure 6.4c), which we observed at 48 and 72 h of low-salinity exposure, resulting in a significant effect of the duration of exposure ($F_{2,21} = 3.574$, $p = 0.046$). The expression of *ODC* was not significantly different in the gills of treated animals relative to the controls (Figure 6.3c) and did not differ among the time points sampled.

In the mantle tissue, we observed an upregulation of *OAT* during low-salinity exposure (Figure 6.2d), as well as a significant decrease in the expression of *ODC* (Figure 6.3d). There was no effect of duration of exposure or an interaction between treatment and duration of exposure on the expression of either gene. While we did observe a 3.5- to 7-fold increase in the expression of *OAT* in the mantle, the activity of the enzyme was not significantly increased in the treatment group (Figure 6.4d). There was no effect of duration of exposure nor the interaction between treatment and duration on the expression of *OAT* or *ODC* in the mantle tissue of juvenile *M. edulis*.

We observed slightly different patterns in the expression of *OAT* and *ODC* in the adductor muscle. *OAT* was strongly upregulated during low-salinity treatment (Figure 6.2e), with almost a 10-fold increase in expression at 48 h. Expression of *ODC*, on the other hand, was not significantly affected by low salinity exposure, although there was a slight upregulation at 24 h, which was not observed in the other tissues (Figure 6.3). There was no effect of duration of exposure or the interaction between treatment and length of exposure on *OAT* or *ODC* expression in the adductor. As observed in the mantle, increases in *OAT* gene expression did not correspond to increased activity of the OAT enzyme (Figure 6.4e). However, we were unable to measure OAT activity in the adductor after 24 h low salinity exposure because of limited tissue quantities. Overall, our

data indicate that *OAT* gene expression and OAT activity in *M. edulis* are generally increased during low salinity exposure, while *ODC* expression tends to be downregulated in the same individuals.

6.4.2. Ornithine Regulation in Congeners Exposed to Low Salinity

We compared patterns of gene expression for *OAT* and *ODC* among the gill tissue of three mytilid congeners, *M. edulis*, *M. trossulus*, and *M. galloprovincialis* after 4, 24, and 48 h of low salinity treatment (Figures 6.5 and 6.6). For both genes, we observed significant differences in expression within the gill tissue of the three species, regardless of salinity treatment. At 4 h, we were unable to measure gene expression in *M. trossulus*, but found that *OAT* expression significantly differed between *M. edulis* and *M. galloprovincialis* (Figure 6.5a). In both species, low-salinity treatment results in a significant increase in *OAT* expression ($F_{1,16} = 28.724$, $p < 0.001$), although the magnitude of the response in *M. galloprovincialis* was 4 times greater than in *M. edulis*, which is reflected in the significant interaction term in the ANOVA between species and treatment ($F_{1,16} = 18.102$, $p = 0.001$). *ODC* was downregulated in treated *M. edulis* at 4 h, but not in *M. galloprovincialis* (Figure 6.6a), however, the effect of low salinity on expression in the two species was not significant ($F_{1,16} = 1.002$, $p = 0.332$).

At 24 h of low-salinity exposure, there were also species-specific differences in *OAT* expression in the gill tissue (Figure 6.5), stemming from variation in the magnitude of the response to salinity treatment. *OAT* expression in *M. galloprovincialis* increased almost 20-fold (Figure 6.6b) during low salinity treatment, and to a lesser extent in the other species ($F_{1,22} = 22.600$, $p < 0.001$) leading to a significant interaction effect ($F_{2,22} = 11.572$, $p < 0.001$) on *OAT* expression at 24 h. *ODC* expression also varied among

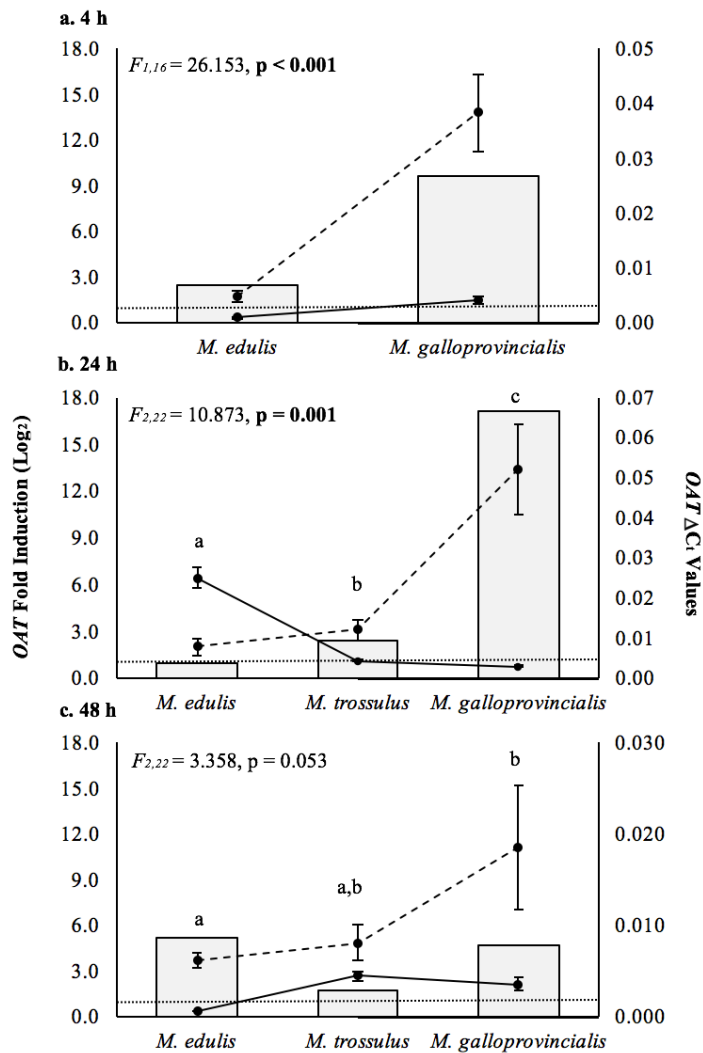


Figure 6.5. *OAT* expression in the gill of congeneric mussels exposed to low salinity. At 4 (a) and 24 h (b) of exposure, there were species-specific patterns of expression of *OAT* during low salinity stress. The F statistic and p values for each time point indicate differences in the response among species and not the effect of low salinity treatment. At 4, 24, and 48 h (c) or low salinity treatment, we observed a significant effect of treatment on *OAT* expression relative the control groups. Gene expression is graphed as the relative *OAT* fold induction (bars) for the low-salinity treatment (dashed line) relative to the controls (solid line). The fold induction is plotted on a \log_2 scale, where the dotted line at 1 indicates that there is no change in expression during low salinity exposure. The ΔC_t values are the mean, normalized expression (\pm SE) for each species; letters indicate significant differences in expression among species at $\alpha = 0.05$.

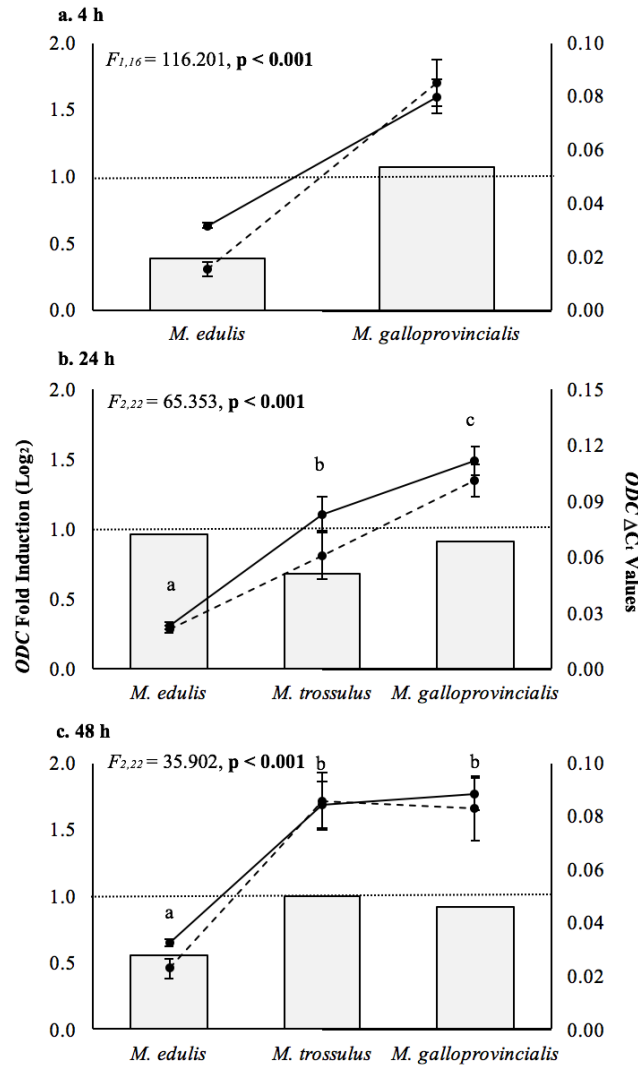


Figure 6.6. *ODC* expression in the gill of congeneric mussels exposed to low salinity. The expression of *ODC* during 4 h (a), 24 h (b), and 48 h (c) low salinity exposure was significantly different among species, although the effects of low salinity treatment on expression were not significant. *M. edulis* showed slight down-regulations of the gene (approximately 1-fold) at 4 and 48 h of exposure, while the other two species did not alter *ODC* expression during low salinity treatment. The *F* statistic and *p* values for each time point indicate differences in the response among species and not the effect of low-salinity treatment. Gene expression is graphed as the relative *ODC* fold induction (bars) for the low salinity treatment (dashed line) relative to the controls (solid line). The fold induction is plotted on a \log_2 scale, where the dotted line at 1 indicates that there is no change in expression. The ΔC_t values are the mean, normalized expression (\pm SE) for each species; the letters indicate significant differences in expression among species at $\alpha = 0.05$.

species at 24 h, resulting from increases in the copy number of *ODC* in both control and treated *M. galloprovincialis* relative to the other two species and not from low salinity treatment ($F_{1,22} = 3.407$, $p = 0.078$). In all three species, the expression of *ODC* in the low salinity treatment was similar to that of the controls.

As the length of exposure increased to 48 h, we observed a shift in the response among the three species, with respect to *OAT* expression (Figure 6.5c). At 4 and 24 h of exposure, *OAT* expression was significantly increased in *M. galloprovincialis* relative to the other two species, yet at 48 h the three species were more similar in their regulation of the gene during low salinity treatment. There was a significant effect of low-salinity exposure on expression of *OAT* among the three species ($F_{1,22} = 10.023$, $p = 0.004$). As was observed at 24 h, there was no effect of low salinity treatment on *ODC* expression in the three species, but a significant species-effect (Figure 6.6c) resulting from fewer copies of *ODC* in both control and treated *M. edulis*. The tendency to upregulate *OAT* and downregulate *ODC* during low salinity exposure was similar across species, although the timing and magnitude of gene regulation did vary, especially between *M. galloprovincialis* and the two other species.

6.4.3. Ornithine Regulation During Hypersalinity Exposure

During high salinity exposure, the regulation of *OAT* and *ODC* appeared to be opposite of what we observed during low salinity exposure in *M. edulis*, *M. trossulus*, and *M. galloprovincialis*. There were significant differences in the patterns of *OAT* and *ODC* expression among species. After 4 h at 40 ppt, there was a slight, but non-significant, decrease in *OAT* expression ($F_{1,24} = 3.810$, $p = 0.068$) in all three species (Figure 6.7a). At the same time, *ODC* expression was increased in *M. galloprovincialis*, decreased in

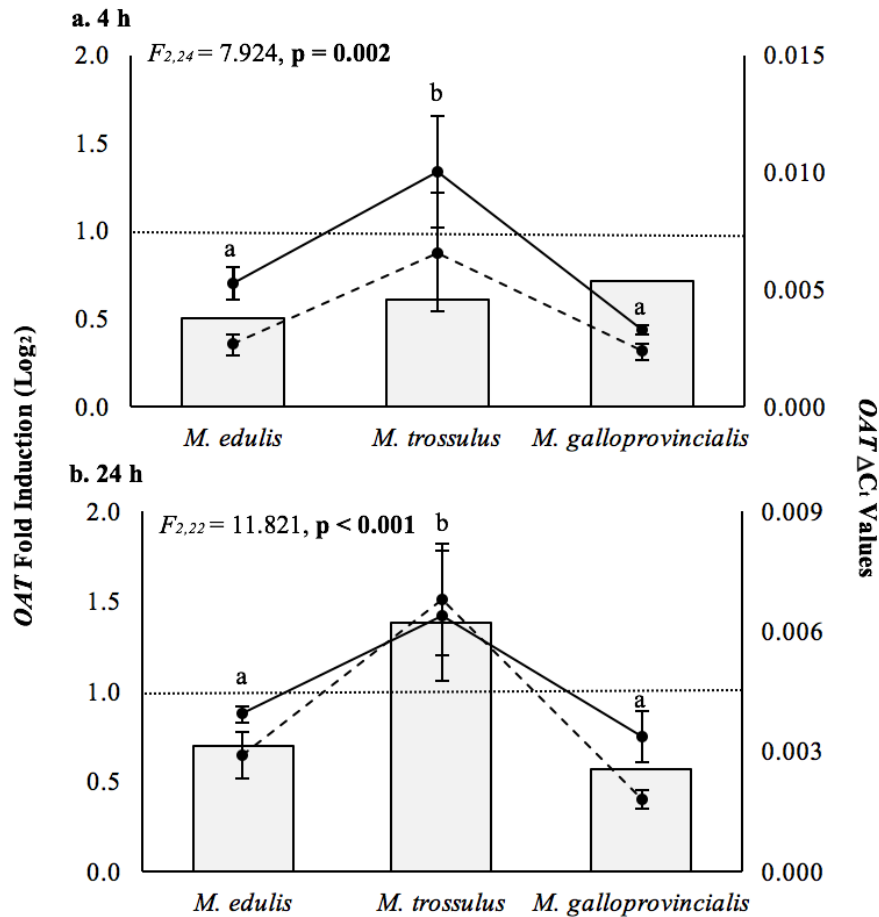


Figure 6.7. *OAT* expression in the gill of congeneric mussels exposed to high salinity. Expression of *OAT* differed among the three species, but was not significantly affected by high salinity exposure. *OAT* regulation was significantly different in *M. trossulus* compared to the other species and showed patterns of upregulation at 24 h (b), but had reduced copy numbers compared to the other two species, regardless of treatment at 4 h (a). *OAT* expression is displayed as the fold induction on the primary y-axis, where the expression of the salinity treated groups is plotted relative to the controls on a log₂ scale (bars) and the dotted line indicate at 1 indicates no change in expression between treatments. The secondary axis shows the normalized ΔC_t expression values for the control (solid line) and the low salinity (dashed line) treatments (± SE).

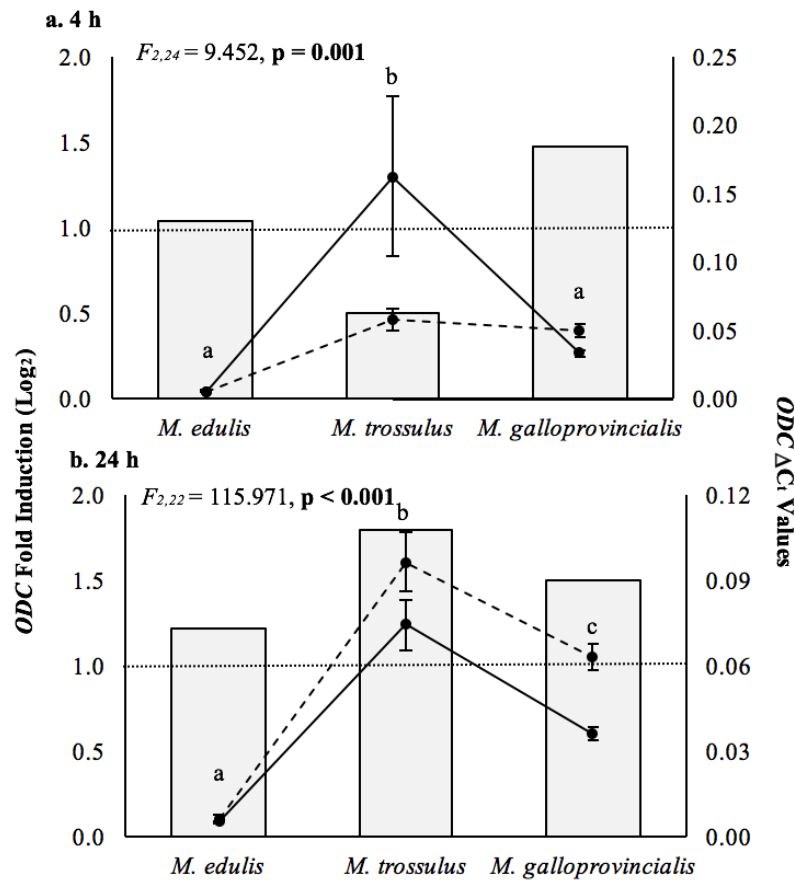


Figure 6.8. *ODC* expression in the gill of congeneric mussels exposed to high salinity. There were species-specific patterns of expression of *ODC* at 4 h (a) and 24 (h) of high salinity exposure, indicating that the copy number of *ODC* varies between species, with *M. trrossulus* varying from the other two. There was also a significant effect of treatment at 4 h, where *ODC* was upregulated in response to high salinity conditions. *ODC* expression is displayed as the fold induction on the primary y-axis, where the expression of the salinity treated groups is plotted relative to the controls on a log₂ scale (bars) and the dotted line indicate at 1 indicates no change in expression between treatments. The secondary axis shows the normalized ΔCt expression values for the control (solid line) and the low salinity (dashed line) treatments (± SE).

M. trossulus, and showed no difference among the treatment and control groups in *M. edulis* (Figure 6.8a; $F_{1,24} = 2.208$, $p = 0.150$). We also observed a significant interaction effect from treatment and species on the expression of *ODC*. Overall, expression of *OAT* and *ODC* was greater in *M. trossulus* compared to its congeners at 4 h, regardless of salinity treatment.

After 24 h in hypersalinity conditions, the species-specific *OAT* and *ODC* expression patterns became more apparent. In *M. edulis* and *M. galloprovincialis* exposed to 40 ppt seawater, *OAT* expression decreased relative to the controls, while it increased after the same exposure in *M. trossulus* (Figure 6.7b). The effects of treatment and the interaction of treatment and species were not significantly different for *OAT* expression in these three species. With respect to *ODC* expression, we observed significant increases in expression resulting from low salinity treatment ($F_{1,22} = 15.823$, $p = 0.001$), with the largest increase in *M. galloprovincialis* and the lowest in *M. edulis* (Figure 6.8b), and a significant interaction between species and salinity treatment ($F_{2,22} = 3.727$, $p = 0.040$). As seen in our other experiments, all three species differed in the copy number of *ODC* regardless of treatment, with the lowest mRNA abundance in *M. edulis* and the highest in *M. trossulus*. However, many of the *M. trossulus* specimens in the control and treatment groups spawned during the experiment, so these results need to be interpreted with caution.

6.5 Discussion

We found that *OAT* is typically upregulated when blue mussels (*Mytilus* spp.) are acutely exposed to low salinity, while *ODC* is downregulated. Our findings suggest that changes in ornithine metabolism are an important part of the osmotic stress response in blue mussels, although the exact role of ornithine metabolism in invertebrates during

hypoosmotic exposure is not well understood. Lockwood and Somero (2011) suggested that an increase in *ODC* expression in *M. galloprovincialis* after 4 h at low salinity could potentially be important for maintaining cell volume through pathways involved in polyamine synthesis. In other species, Lovett and Watts (1995) noted declines in polyamine levels in the blue crab, *Callinectes sapidus*, while Watts et al. (1996) found increased activity of ODC in brine shrimp, *Artemia franciscana*. In both studies, the authors speculated that inhibition of Na⁺, K⁺ ATPase activity by putrescine may be important during hypoosmotic stress, but were undecided on whether the response would be beneficial or harmful to the cell (Lovett and Watts 1995, Watts et al. 1996). In mammals, increases in polyamine levels during cellular hypoosmotic stress are thought to regulate ion concentrations through control of ion and membrane channels (Rhee et al. 2007, Miller-Fleming et al. 2015). In plants polyamines can serve as osmolytes (Groppa and Benavides 2008, Tiburcio et al. 2014) and in other species are thought to help maintain cellular homeostasis (Hird 1986, Kournoutou et al. 2014).

The role of *OAT* in the response to osmotic stress has received more attention. Meng et al. (2013) attributed an increase in *OAT* and proline dehydrogenase expression in the oyster, *Crassostrea gigas*, to the importance of proline catabolism during low salinity exposure. On the other hand, during hyperosmotic exposure, there is more evidence that *OAT* activity may be important for combatting cellular stress. In studies of the ribbed mussel *Geukensia demissa*, *OAT* activity during hypersalinity exposure led to increased concentrations of proline (Greenwalt and Bishop 1980, Bishop et al. 1981), which help maintain osmotic balance. A similar response is well documented in plants (Delauney and Verma 1993, Kishor et al. 2005, Liang et al. 2013), where proline accumulation not

only serves a role in intracellular isosmotic regulation but also in stabilizing the cells and as a source of energy. However, there is also evidence that polyamine accumulations occur in plants during hyperosmotic stress, by acting as osmolytes and helping to stabilize the cell from osmotically-induced damage (Groppa and Benavides 2008, Tiburcio et al. 2014). It is possible that utilization of ornithine through both pathways is a necessary component of osmotic stress responses.

The increased expression of *OAT* and decreased expression of *ODC* in larval and juvenile *M. edulis*, suggests that conversion of ornithine into glutamate or proline and not the alternative decarboxylase pathway leading to polyamine production, is utilized by this species during hypoosmotic exposure. We observed a significant upregulation of *OAT* over a 1–3 d exposure to low salinity in veliger and pediveliger larvae and within the gill and adductor muscle of juveniles (Figure 6.2), as well as an increase in OAT enzyme activity in larvae and in the gill tissue of juveniles (Figure 6.4). Interestingly, we did not observe increases in OAT activity in the adductor and mantle tissue, despite these tissues heavily upregulating *OAT* gene expression during low salinity treatment. It is possible that regulation of ornithine aminotransferase differs across developmental stage (i.e. transcriptionally regulated in larvae and not in juveniles) or among various tissues, as has been reported in rats (Meuckler et al. 1984). Alternatively, these observations may be the result of a time lag between increases in gene expression and protein concentrations. In our preliminary study, we found that larvae upregulated *OAT* after only 2 h of low salinity exposure, while the response was somewhat delayed in the gill tissue of juveniles (Figure C.3). There is evidence for rapid turnover of OAT enzyme in rats (Swick et al. 1968), so a lack of enzyme activity during low salinity treatment may have stemmed

from increased turnover that had not been compensated for by changes in gene expression until after 48 h. In either case, there is strong support that OAT plays an important role during hypoosmotic exposure in *M. edulis*.

The physiological significance of these findings, however, is difficult to predict, because either glutamate or proline can be synthesized by activity of OAT (Figure 6.1). We were unable to reliably quantify the abundance of proline or glutamate via NMR-based metabolomics (Chapter 3), indicating that the concentrations of both were relatively low in our larval and juvenile *M. edulis* samples. Even so, glutamate may be rapidly utilized under hypoosmotic conditions as glutamate catabolism through glutamate dehydrogenase (GDH) activity is a means of reducing intracellular osmolyte concentrations while generating energy (Livingstone et al. 1979, Burcham et al. 1983, Moyes et al. 1985). Similarly, the standing stock of proline may be low as it can be incorporated into collagens (Hird 1986) or used as an intermediate to be shunted into the Krebs cycle (Bishop et al. 1994). Additional studies need to be conducted to determine the broader implications of OAT activity during hypoosmotic stress.

The expression of *ODC* during low salinity exposure in *M. edulis* was more variable than that of *OAT*. In veligers and the mantle tissue of juveniles, we observed a significant downregulation of the gene, but no effect of treatment in pediveligers, the gill, or adductor muscle (Figure 6.3). For the most part, *ODC* expression did not change relative to the controls or expression declined during low salinity treatment. Ornithine decarboxylase is highly regulated in mammals at the level of transcription and translation, as well as by changes in the abundance and activity of the ornithine decarboxylase antizyme (Pegg 2006). Although we did not observe changes in expression

of the ODC antizyme (unpublished microarray data), it is difficult to make firm conclusions about whether variation in *ODC* expression during low salinity stress has an impact on polyamine concentrations in *M. edulis*.

The response of *OAT* and *ODC* expression to low salinity exposure within the gill tissue of *M. edulis* is similar to what we observed in other mytilids species. There was a significant effect of low salinity treatment on *OAT* expression among the three species, as *OAT* was upregulated 1.5- to 2.5-fold in *M. trossulus* and 4- to 17-fold in *M. galloprovincialis* (Figure 6.6). *ODC* expression, on the other hand, was largely unaffected by low salinity exposure in *M. trossulus* and *M. galloprovincialis* (Figure 6.7), contradictory to the findings of Lockwood and Somero (2011). Together, these studies suggest that all three species of mussels rely on the conversion of OAT-mediated conversion of ornithine to glutamate or proline rather than ODC-mediated production of polyamines during low salinity exposure, mytilids, as has been observed in oysters (Meng et al. 2013). These patterns of expression were reversed during high salinity exposure in all three species.

Interestingly, we found that the baseline expression of *ODC* was generally higher in *M. galloprovincialis* compared to *M. edulis* or *M. trossulus*, regardless of salinity exposure (Figure 6.6). Lockwood and Somero (2011) found that there were relatively few changes in the transcriptomic response to low salinity between *M. galloprovincialis* and *M. trossulus*, although gene expression values are always normalized to controls. It is possible that differential expression does not occur because there are already adequate mRNA stores to serve as templates for effector proteins. Alternatively, higher levels *ODC* expression in *M. galloprovincialis* compared to *M. edulis* or *M. trossulus* may

indicate that polyamine levels are higher in this species. An abundance of polyamines may play a role in the success of *M. galloprovincialis* at invading new habitats or may lower their tolerance to low salinity by necessitating greater increases in *OAT* expression to mount the same osmotic response as *M. edulis* and *M. trossulus*.

Overall, our results indicate that utilization of ornithine during osmotic stress may be an adaptive response in mytilids congeners. We have provided evidence that during low salinity exposure, the activity of ornithine aminotransferase increases the production of either glutamate or proline and that this response decreases during hyperosmotic exposure. The activity of ornithine decarboxylase may be inversely related to the changes observed in *OAT*, suggesting a coordinated shift in the fate of ornithine from hypo- to hyper-osmotic conditions. However, given the complexity of *ODC* regulation, further studies should be conducted to determine the role of polyamines in the osmotic stress responses of mytilid mussels.

CHAPTER 7

SUMMARY AND CONCLUSIONS

Low salinity exposure affects larval and juvenile mussels at all levels of biological organization. At the organismal level, we have shown that exposure to low salinity conditions early in development carries through metamorphosis and negatively impacts the size at metamorphosis and the size of early post-settlement juvenile mussels. Larval exposure to low salinity also affects post-metamorphic mussels' tolerance to low salinity conditions, although it appears this effect depends on when larval stress is incurred. Mussels that were exposed to low salinity as veligers and as juveniles had reduced growth rates relative to other treatment groups, while those treated as pediveligers and juveniles had higher growth rates, suggesting that previous exposure, in some cases, may help condition mussels for repeated low salinity events (Chapter 2). The varying effects of low salinity exposure on veliger and pediveliger larvae likely results from metabolic differences and variation in the developmental complexity among these stages. Interestingly, we found that pediveligers share more metabolites with juvenile mussels than veligers do, suggesting that the pediveliger stage is a morphological and metabolic transition between veligers and juveniles.

Our comparisons of metabolite baselines under ambient conditions indicates there are appreciable the stage- and tissue-specific differences in osmolyte concentrations in the cells of blue mussels. Likewise, gene copy number variation among stages and tissues was notable; establishing the inherent variability that exists at these levels. These studies provided us with an appropriate physiological context for interpreting the transcriptomic

responses we observed during hypoosmotic exposure. Not surprisingly, many of the differences we observed in the composition of the free amino acid pools seem to reflect variation in function and morphology of the different stages or various tissues (Chapter 3). In some cases, this trend was also observed in patterns of expression for genes that likely play a role in maintaining cellular homeostasis (Chapter 4). There were other instances where analysis of baseline expression provided insight as to why larval stages are more susceptible to low salinity exposure than juvenile mussels (Chapter 5) or why a species is less tolerant to low salinity than its congeners (Chapter 6). These results highlight the need for more comprehensive baseline studies of the cellular and molecular mechanisms of blue mussel physiology, especially at early life history stages.

We are just beginning to scratch the surface in our understanding of how blue mussels respond to short-term, low-salinity exposure. Previous studies of the hypoosmotic stress response in blue mussels provided limited information because they focused on a single tissue, a single time point, or evaluated a single process. By using comparative and integrative approaches, we have found evidence that the osmotic stress response in blue mussels is developmentally, spatially, and temporally dynamic and incorporates levels of complexity that cannot be observed or appreciated without a broader context. For instance, we observed that both larval and juvenile blue mussels utilize glycine as the predominant osmolyte during low salinity exposure, suggesting that the response of these stages is similar. However, further analysis of excretion rates, the magnitude of glycine efflux, other changes in the free amino acid pools, and gene expression data suggest that juveniles may be much better at regulating intracellular osmolytes. Larvae, on the other hand, may have to expend more energy to combat

leakage of important osmolytes from their cells because of increased surface area to volume ratios and the absence of a behavioral avoidance to low salinity (Chapter 3). We also observed differences in the regulation of calmodulin and calmodulin-like genes during low salinity exposure (Chapter 5), as well as in the expression and activity of genes involved in ornithine catabolism (Chapter 6) in early life history stages. Collectively, our findings suggest that larval mussels do not have the same capacity to respond to low salinity exposure as their post-metamorphic counterparts.

A common goal of ecophysiological studies is to improve our understanding of how the physiology of a species might permit acclimation and even adaptation to climate change-induced shifts in their natural environment. This includes identifying the ‘weak links’ in the system where physiological limits are reached, and increasing knowledge of the mechanisms that control these limits. While we are far from forecasting what the effects of decreased salinity will have on blue mussel populations, it is apparent that the vulnerability of blue mussel larvae will be a critical factor for making these predictions. Without further consideration of how larval stages respond to environmental stress, we will never be able to fully understand the effects of climate change on the resilience of *M. edulis*.

REFERENCES

- Allen, K. and J. Awapara. 1960. Metabolism of sulfur amino acids in *Mytilus edulis* and *Rangia cuneata*. *Biological Bulletin* 118: 173-182
- Almada-Villela, P.C. 1984. The effects of reduced salinity on the shell growth of small *Mytilus edulis*. *Journal of the Marine Biological Association of the United Kingdom* 64: 171-182
- Anderson, C.L., J.L. Jensen, and T.F. Orntoft. 2004. Normalization of real-time quantitative reverse transcription-PCR data: a model-based variance estimation approach to identify genes suited for normalization, applied to bladder and colon cancer data sets. *Cancer Research* 64: 5245-5250
- Andrews, T.R. and R.G.B. Reid. 1971. Ornithine cycle and uricolytic enzymes in four bivalve molluscs. *Comparative Biochemistry and Physiology* 42B: 475-491
- Antonov, J.I., S. Levitus, and T.P. Boyer. 2002. Steric sea level variations during 1957 – 1994: importance of salinity. *Journal of Geophysical Research* 107: 8013
- Arribas, L.P., L. Donnarumma, M. Gabriela Palomo, and R.A. Scrosati. 2014. Intertidal mussels as ecosystem engineers: their associated invertebrate biodiversity under contrasting wave exposures. *Marine Biodiversity* 44: 203-211
- Bacon, P.R. 1971. The maintenance of a resident population of *Balanus eburneus* (Gould) in relation to salinity fluctuations in a Trinidad mangrove swamp. *Journal of Experimental Marine Biology and Ecology* 6: 187-198
- Babarro, J.M.F. and M.J. Fernández-Reiriz. 2006. Variability of taurine concentrations in *Mytilus galloprovincialis* as a function of body size and specific tissue. *Comparative Biochemistry and Physiology, Part B* 145: 94-100
- Bartberger, C.A. and S.K. Pierce. 1976. Relationship between ammonia excretion rates and hemolymph nitrogenous compounds of a euryhaline bivalve during low salinity acclimation, *Biological Bulletin* 150: 1-14
- Bashevkin, S.M. and J.A. Pechenik. 2015. The interactive influence of temperature and salinity on larval and juvenile growth in the gastropod *Crepidula fornicata* (L.). *Journal of Experimental Marine Biology and Ecology* 470: 78-91
- Bassim, S., A. Tanguy, B. Genard, D. Moraga, and R. Tremblay. 2014. Identification of *Mytilus edulis* genetic regulators during early development. *Gene* 551: 65-78
- Bayne, B.L. 1965. Growth and the delay of metamorphosis of the larvae of *Mytilus edulis* (L.). *Ophelia* 2: 1-47

- Bayne, B.L. 1973. Aspects of the metabolism of *Mytilus edulis* during starvation. *Netherlands Journal of Sea Research* 7: 399-410
- Bayne, B.L., P.A. Gabbott, and J. Widdows. 1975. Some effects of stress in the adult on the eggs and larvae of *Mytilus edulis* L. *Journal of the Marine Biological Association of the United Kingdom* 55: 675-689
- Bertram, D.F. and R.R. Strathmann. 1998. Effects of maternal and larval nutrition on growth and form of planktotrophic larvae. *Ecology* 79: 315-327
- Bharti, S.K. and R. Roy. 2012. Quantitative ^1H NMR spectroscopy. *Trends in Analytical Chemistry* 35: 5-26
- Bishop, S.H. 1976. Nitrogen metabolism and excretion: regulation of intracellular amino acid concentrations *In* M. Witey (ed.), *Estuarine Processes* Vol 1: 414-431. Academic Press, New York
- Bishop, S.H., D.E. Greenwalt, and J.M. Burcham. 1981. Amino acid cycling in ribbed mussel tissues subjected to hyperosmotic shock. *Journal of Experimental Zoology* 215: 277-287
- Bishop, S.H., L.L. Ellis, and J.M. Burcham. 1983. 6. Amino acid metabolism in molluscs *In* P.W. Hochachka (ed.), *The Mollusca* Vol 1: 275-279. Academic Press, New York
- Bøhle, B. 1972. Effects of adaptation to reduced salinity on filtration activity and growth of mussels (*Mytilus edulis* L.). *Journal of Experimental Marine Biology and Ecology* 10: 41-47
- Bower, C.E. and T. Holm-Hansen. 1980. A salicylate-hypochlorite method for determining ammonia in seawater. *Canadian Journal of Fisheries and Aquatic Sciences* 37: 794-798
- Bowlus, R.D. and G.N. Somero. 1979. Solute compatibility with enzyme function and structure: rationales for the selection of osmotic agents and end-products of anaerobic metabolism in marine invertebrates. *Journal of Experimental Zoology* 208: 137-152
- Braby, C.E. and G.N. Somero. 2006. Following the heart: temperature and salinity effects on heart rate in native and invasive species of blue mussels (genus *Mytilus*). *Journal of Experimental Biology* 209: 2554-2566
- Bradford, M.M. 1976. A rapid and sensitive method for the quantitation of microgram quantities of protein utilizing the principle of protein-dye binding. *Analytical Biochemistry* 72: 248-254

- Bricteux-Grégoire, S., Gh. Duchâteau-Bosson, Ch. Jeuniaux, and M. Florkin. 1964. Constituants osmotiquement actifs des muscles adducteurs de *Mytilus edulis* adaptée a l'eau de mer ou a l'eau saumâtre. Archives Internationales de Physiologie et de Biochimie 72: 116-123
- Buckley, B.A., M.-E. Owen, and G.E. Hofmann. 2001. Adjusting the thermostat: the threshold induction temperature for the heat-shock response in intertidal mussels (genus *Mytilus*) changes as a function of thermal history. Journal of Experimental Biology 204: 3571-3579
- Burcham, J.M., K.T. Paynter, and S.H. Bishop. 1983. Coupled mitochondria from oyster gill tissue. Marine Biology Letters 4: 349-356
- Burg, M.B., E.D. Kwon, and D. Kültz. 1996. Osmotic regulation of gene expression. The FASEB Journal 10: 1598-1606
- Bussell, J.A., E.A. Gidman, D.R. Causton, D. Gwynn-Jones, S.K. Malham, M.L.M. Jones, B. Reynolds, and R. Seed. 2008. Changes in the immune response and metabolic fingerprint of the mussel, *Mytilus edulis* (Linnaeus) in response to lowered salinity and physical stress. Journal of Experimental Marine Biology and Ecology 358: 78-85
- Bustin, S.A., V. Benes, J.A. Garson, J. Hellermans, J. Huggett, M. Kubista, R. Mueller, T. Nolan, M.W. Pfaffl, G.L. Shipley, J. Vandesompele, and C.T. Wittwer. 2009. The MIQE guidelines: Minimum Information for publication of Quantitative real-time PCR Experiments. Clinical Chemistry 55: 611-622
- Calabrese, V., C. Cornelius, A.T. Dinkova-Kostova, E.J. Calabrese, and M.P. Mattson. 2010. Cellular stress responses, the hormesis paradigm, and vitagenes: Novel targets for therapeutic intervention in neurodegenerative disorders. Antioxidants and Redox Signaling 13: 1763-1811
- Cameron, R.C., E.J. Duncan, and P.D. Dearden. 2013. Biased gene expression in early honeybee larval development. BMC Genomics 14: 903
- Capello, T., A. Mauceri, C. Corsaro, M. Maisano, V. Parrino, G. Lo Paro, G. Messina, and S. Fasulo. 2013. Impact of environmental pollution on caged mussels *Mytilus galloprovincialis* using NMR-based metabolomics. Marine Pollution Bulletin 77: 132-139
- Caponera, J.A. and P.D. Rawson. 2008. Highly divergent duplicate mannose-6-phosphate isomerase (*Mpi*) genes in the blue mussel, *Mytilus edulis*. Marine Genomics 1: 47-53

- Chen, Z.-F., H. Want, K. Matsumura, and P.-Y. Qian. 2012a. Expression of calmodulin and myosin light chain kinase during larval settlement of the barnacle *Balanus amphitrite*. *Plos One* 7: e31337
- Chen, Z.-F., H. Want, and P.-Y. Qian. 2012b. Characterization and expression of calmodulin gene during larval settlement and metamorphosis of the polychaete *Hydroides elegans*. *Comparative Biochemistry and Physiology, Part B* 162: 113-119
- Cheung, W.Y. 1980. Calmodulin plays a pivotal role in cellular regulation. *Science* 207: 19-27
- Chin, D. and A.R. Means. 2000. Calmodulin: a prototypical calcium sensor. *Trends in Cell Biology* 10: 322 – 328
- Conesa, A., S. Götz, J.M. García-Gómez, J. Terol, M. Talón, and M. Robles. 2005. Blast2GO: a universal tool for annotation, visualization and analysis in functional genomics research. *Bioinformatics* 21: 3674-3776
- Costa, C.J. and A.W. Pritchard. 1978. The response of *Mytilus edulis* to short duration hypoosmotic stress. *Comparative Biochemistry and Physiology* 61A: 149-155
- Crawford, C.C. and K.L. Webb. 1968. Amino acid flux in an estuary. *Science* 159: 1463-1464
- Crisp, D.J. 1976. The role of the pelagic larva *In* P. Spencer Davies (ed.), *Perspectives in Environmental Zoology* Vol 1: 145-153. Pergamon Press, Oxford and New York
- Cubero-Leon, E., C.M. Ciocan, C. Minier, J.M. Rotchell. 2012. Reference gene selection for qPCR in mussel, *Mytilus edulis*, during gametogenesis and exogenous estrogen exposure. *Environmental Science and Pollution Research* 19: 2728-2733
- Davenport, J. 1979. Is *Mytilus edulis* a short term osmoregulator? *Comparative Biochemistry and Physiology* 64A: 91-95
- Deaton, L.E. 2001. Hyperosmotic volume regulation in the gills of the ribbed mussel, *Geukensia demissa*: rapid accumulation of betaine and alanine. *Journal of Experimental Marine Biology and Ecology* 260: 185-197
- Deaton, L.E., T.J. Hilbish, and R.K. Koehn. 1985. Hyperosmotic volume regulation in the tissues of the mussel *Mytilus edulis*. *Comparative Biochemistry and Physiology* 80A: 571-574
- Delauney, A.J. and D.P.S. Verma. 1993. Proline biosynthesis and osmoregulation in plants. *The Plant Journal* 4: 215-213

- Diederich, C.M., J.N. Jarrett, O.R. Chaparro, C.J. Segura, S.M. Arellano, and J.A. Pechenik. 2001. Low salinity stress experienced by larvae does not affect post-metamorphic growth or survival in three calyptraeid gastropods. *Journal of Experimental Marine Biology and Ecology* 397: 94-105
- Dineshram, R., V. Thiyagarajan, A. Lane, Y. Ziniu, S. Xiao, and P.T.Y. Leung. 2013. Elevated CO₂ alters larval proteome and its phosphorylation status in the commercial oyster, *Crassostrea hongkongensis*. *Marine Biology* 160: 2189-2205
- Dona, A.C., M. Kyriakides, F. Scott, E.A. Shephard, D. Varshavi, K. Veselkov, and J.R. Everett. 2016. A guide to the identification of metabolites in NMR-based metabonomics/metabolomics experiments. *Computational and Structural Biotechnology Journal* 14: 135-153
- Doney, S.C., M. Ruckelshaus, J.E. Duffy, J.P. Barry, F. Chan, C.A. English, H.M. Galindo, J.M. Grebmeier, A.B. Hollowed, N. Knowlton, J. Polovina, N.N. Rabalais, W.J. Sydeman, and L.D. Talley. 2012. Climate change impacts of marine ecosystems. *Annual Review of Marine Science* 4: 11-37
- Durack, P.J., S.E. Wijffels, and R.J. Matear. 2012. Ocean salinities reveal strong global water cycle intensification during 1950 to 2000. *Science* 336: 455-458
- Ellis, L.L, J.M. Burcham, K.T. Paytner, and S.H. Bishop. 1985. Amino acid metabolism in euryhaline bivalves: regulation of glycine accumulation in ribbed mussel gills. *Journal of Experimental Zoology* 233: 347-358
- Ellis, R.P., J.I. Spicer, J.J. Byrne, U. Sommer, M.R. Viant, D.A. White, and S. Widdicombe. 2014. ¹H NMR metabolomics reveals contrasting response by male and female mussels exposed to reduced seawater pH, increased temperature, and a pathogen. *Environmental Science and Technology* 48: 7044-7052
- Emllet, R.B. and S.S. Sadro. 2006. Linking stages of life history: how larval quality translates into juvenile performance for an intertidal barnacle (*Balanus glandula*). *Integrative and Comparative Biology* 46: 334-346
- Evans, T.G. and G.N. Somero. 2010. Phosphorylation events catalyzed by major cell signaling proteins differ in response to thermal and osmotic stress among native (*Mytilus californianus* and *Mytilus trossulus*) and invasive (*Mytilus galloprovincialis*) species of mussels. *Physiological and Biochemical Zoology* 83: 984-996
- Falktoft, B. and I.H. Lambert. 2004. Ca²⁺-mediated potentiation of the swelling-induced taurine efflux from HeLa cells: On the roll of calmodulin and novel protein kinase C isoforms. *Journal of Membrane Biology* 201: 59-75

- Finn, B.E. and S. Forsén. 1995. The evolving model of calmodulin structure, function, and activation. *Structure* 3: 7-11
- Fischer, J. and N.E. Phillips. 2014. Carry-over effects of multiple stressors on benthic embryos are mediated by larval exposure to elevated UVB and temperature. *Global Change Biology* 20: 2108-2116
- Fisher, R.A. 1921. Some remarks on the methods formulated in a recent article on “the quantitative analysis of plant growth”. *Annals of Applied Biology* 7: 345-430
- Fuller, S.C. and R.A. Lutz. 1988. Early shell mineralogy, microstructure, and surface sculpture in five mytilid species. *Malacologia* 29: 363-371
- Gardner, J.P.A. and R.J. Thompson. 2001. The effects of coastal and estuarine conditions on the physiology and survivorship of the mussels *Mytilus edulis*, *M. trossulus*, and their hybrids. *Journal of Experimental Marine Biology and Ecology* 265: 119-140
- Gasteiger, E.L., P.C. Haake, and J.A. Gergen. 1960. An investigation of the distribution and function of homarine (*N*-methyl picolinic acid). *Annals of the New York Academy of Sciences* 90: 622-636
- Gazeau, F., J.-P. Gattuso, C. Dawber, A.E. Pronker, F. Peene, C.H.R. Heip, and J.J. Middleburg. 2010. Effect of ocean acidification on the early life stages of the blue mussel *Mytilus edulis*. *Biogeosciences* 7: 2051-2060
- Gilles, R. 1972. Osmoregulation in three molluscs: *Acanthochitona discrepans* (Brown), *Glycymeris glycymeris* (L.), and *Mytilus edulis* (L.). *Biological Bulletin* 142: 25-35
- Goldberg, E.D. 1975. The mussel watch—a first step in global marine monitoring. *Marine Pollution Bulletin* 6: 111
- Gracey, A.Y., M.L. Chaney, J.P. Boomhower, W.R. Tyburczy, K. Connor, and G.N. Somero. 2008. Rhythms of gene expression in a fluctuating intertidal environment. *Current Biology* 18: 1501-1507
- Greenwalt, D.E. and S.H. Bishop. 1980. Effect of aminotransferase inhibitors on the pattern of free amino acid accumulation in isolated mussel hearts subjected to hyperosmotic stress. *Physiological Zoology* 53: 262-269
- Groppa, M.D. and M.P. Benavides. Polyamines and abiotic stress: recent advances. *Amino Acids* 34: 35-45
- Grosberg, R.K. and D.R. Levitan. 1992. For adults only? Supply-side ecology and the history of larval biology. *Trends in Ecology and Evolution* 7: 130-133

- Helm, M.M., N. Bourne, and A. Lovatelli. 2004. Hatchery culture of bivalves: A practical manual. FAO Fisheries Technical Paper 471, Rome. 177 p.
- Herzfeld, A. and W.E. Knox. 1968. The properties, developmental formation, and estrogen induction of ornithine aminotransferase in rat tissues. *Journal of Biological Chemistry* 243: 3327-3332
- Hettinger, A., E. Sanford, T.M. Hill, A.D. Russell, K.N.S. Sato, J. Hoey, M. Forsch, H.N. Page, and B. Gaylord. 2012. Persistent carry-over effects of planktonic exposure to ocean acidification in the Olympia oyster. *Ecology* 93: 2758-2768
- Hines, A., G. S. Oladiran, J.P. Bignell, G.D. Stentiford, and M.R. Viant. 2007. Direct sampling of organisms from the field and knowledge of their phenotype: key recommendations for environmental metabolomics. *Environmental Science and Technology* 41: 3375-3381
- Hird, F.J.R. 1986. The importance of arginine in evolution. *Comparative Biochemistry and Physiology* 85B: 285-288
- His, E., R. Robert, and A. Dinet. 1989. Combined effects of temperature and salinity on fed and starved larvae of the Mediterranean mussel *Mytilus galloprovincialis* and the Japanese oyster *Crassostrea gigas*. *Marine Biology* 100: 455-463
- Hosoi, M., K. Takeuchi, H. Sawada, and H. Toyohara. 2005. Expression and functional analysis of mussel taurine transporter, as a key molecule in cellular osmoconforming. *Journal of Experimental Biology* 208: 4203-4211
- Hosoi, M., C. Shinzato, M. Takagi, S. Hosoi-Tanabe, H. Sawada, E. Terasawa, and H. Toyohara. 2007. Taurine transporter from the giant Pacific oyster *Crassostrea gigas*: function and expression in response to hyper- and hypo-osmotic stress. *Fisheries Science* 73: 385-394
- Hoyaux, J., R. Gilles, and Ch. Jeuniaux. 1976. Osmoregulation in molluscs of the intertidal zone. *Comparative Biochemistry and Physiology* 53A: 361-365
- Hrs-Brenko, M. and A. Calabrese. 1969. The combined effects of salinity and temperature on larvae of the mussel *Mytilus edulis*. *Marine Biology* 4: 224-226
- Huxtable, R.J. 1992. Physiological actions of taurine. *Physiological Reviews* 72: 101-163
- Incharoensaki, A. and R. Waditt. 2000. Degradation of glycine betaine by betaine-homocysteine methyltransferase in *Aphanothece halophytica*: effect of salt downshock and starvation. *Current Microbiology* 41: 227-231
- Innes, D.J. and L.E. Haley. 1977. Genetic aspects of larval growth under reduced salinity in *Mytilus edulis*. *Biological Bulletin* 153: 312-321

- Jackson, D.J., G. Wörheide, and B.M. Degnan. 2007. Dynamic expression of ancient and novel molluscan shell genes during ecological transitions. *BMC Evolutionary Biology* 7:160
- Jones, O.A.H., F. Dondero, A. Viarengo, and J.L. Griffin. 2008. Metabolic profiling of *Mytilus galloprovincialis* and its potential applications for pollution assessment. *Marine Ecology Progress Series* 369: 169-179
- Jones, S.J., F.P. Lima and D.S. Wetthey. 2010. Rising environmental temperatures and biogeography: poleward range contraction of the blue mussel, *Mytilus edulis* L., in the western Atlantic. *Journal of Biogeography* 37:2243-2259
- Kasschau, M.R., C.M. Skisak, J.P. Cook, and W.R. Mills. 1984. β -Alanine metabolism and high salinity stress in the sea anemone, *Bundosoma cavernata*. *Journal of Comparative Physiology B* 154: 181-186
- Kishor, P.B.K, S. Sangam, R.N. Amrutha, P.S. Laxmi, K.R. Naidu, K.R.S.S. Rao, S. Rao, K.J. Reddy, P. Theriappan, and N. Sreenivasulu. 2005. Regulation of proline biosynthesis, degradation, uptake and transport in higher plants: its implications in plant growth and abiotic stress tolerance. *Current Science* 88: 424-438
- Klee, C.B., T.H. Crouch, and P.G. Richman. 1980. Calmodulin. *Annual Reviews of Biochemistry* 49: 489-515
- Kluytmans, J.H., D.I. Zandee, W. Zurburg, and H. Pieters. 1980. The influence of seasonal changes on energy metabolism in *Mytilus edulis* (L.) – III. Anaerobic energy metabolism. *Comparative Biochemistry and Physiology* 67B: 307-315
- Koehn, R.K. 1991. The genetics and taxonomy of species in the genus *Mytilus*. *Aquaculture* 94: 125-145
- Koito, T., I. Nakamura-Kusakabe, T. Yoshida, T. Maruyama, T. Omata, N. Miyazaki, and K. Inoue. 2010. Effects of long-term exposure to sulfides on taurine transporter gene expression in the gill of the deep-sea mussel *Bathymodiolus platifrons*, which harbors a methanotrophic symbiont. *Fisheries Science* 76: 381-388
- Kournoutou, G.G., S. Pytharopoulou, M. Leotsinidis, and D.L. Kalpxis. 2014. Changes of polyamine pattern in digestive glands of mussel *Mytilus galloprovincialis* under exposure to cadmium. *Comparative Biochemistry and Physiology, Part C* 165: 1-8
- Kültz, D. 2005. Molecular and evolutionary basis of the cellular stress response. *Annual Reviews of Physiology* 67: 225-257

- Kültz, D., D. Fiol, N. Valkova, S. Gomez-Jimenez, S.Y. Chan, and J. Lee. 2007. Functional genomics and proteomics of the cellular osmotic stress response in 'non-model' organisms. *Journal of Experimental Biology* 210: 1593-1601
- Lacroix, C., V. Coquillé, J. Guyomarch, M. Auffret, and D. Moraga. 2014. A selection of reference genes and early-warning mRNA biomarkers for environmental monitoring using *Mytilus* spp. as sentinel species. *Marine Pollution Bulletin* 86: 304-313
- Landes, A., P. Dolmer, L.K. Poulsen, J.K. Pettersen, and B. Vismann. 2015. Growth and respiration in blue mussels (*Mytilus* spp.) from different salinity regimes. *Journal of Shellfish Research* 34: 373-382
- Lange, R. 1963. The osmotic function of amino acids and taurine in the mussel, *Mytilus edulis*. *Comparative Biochemistry and Physiology* 10: 173-179
- Lemos, D., R.L.V. Jorge, and V.N. Phan. 2003. Simultaneous measurements of oxygen consumption and ammonia-N excretion in embryos and larvae of marine invertebrates. *Comparative Biochemistry and Physiology Part A: Molecular and Integrative Physiology* 136: 321-328
- Lesser, M.P. 2016. Climate change stressors cause metabolic depression in the blue mussel, *Mytilus edulis*, from the Gulf of Maine. *Limnology and Oceanography* 61: 1705-1717
- Lewis, P.R. 1952. The free amino-acid of invertebrate nerve. *Biochemical Journal* 52:330-338
- Lewit-Bentley, A. and S. Réty. 2000. EF-hand calcium binding proteins. *Current Opinion in Structural Biology* 10: 637-643
- Li, F., Q. Feng, C. Lee, S. Wang, L.L. Pelleymounter, I. Moon, B.W. Eckloff, E.D. Wieben, D.J. Schaid, V. Yee, and R.M. Weinshilboum. 2008. Human betaine-homocysteine methyltransferase (BHMT) and BHMT2: common gene sequence variation and functional characterization. *Molecular Genetics and Metabolism* 94: 326-335
- Li, H., P. Venier, M. Prado-Alvárez, C. Gestal, M. Toubiana, R. Quartesan, F. Borghesan, B. Novoa, A. Figueras, and P. Roch. 2010. Expression of *Mytilus* immune genes in response to experimental challenges varied according to the site of collection. *Fish and Shellfish Immunology* 28: 640-648
- Li, S. L. Xie, C. Zhang, Y. Zhang, M. Gu and R. Zhang. 2004. Cloning and expression of a pivotal calcium metabolism regulator: calmodulin involved in shell formation from pearl oyster (*Pinctada fucata*). *Comparative Biochemistry and Physiology, Part B* 138: 235-243

- Li, S., L. Xie, Z. Ma, and R. Zhang. 2005. cDNA cloning and characterization of a novel calmodulin-like protein from pearl oyster *Pinctada fucata*. FEBS Journal 272: 4899-4910
- Liang, X., L. Zhang, S.K. Natarajan, and D.F. Becker. 2013. Proline mechanisms of stress survival. Antioxidants and Redox Signaling 19: 998-1011
- Lin, C.Y., H. Wu, R.S. Tjeerdema, and M.R. Viant. 2007. Evaluation of metabolite extraction strategies from tissue samples using NMR metabolomics. Metabolomics 3: 55-67
- Livingstone, D.R., J. Widdows, and P. Fieth. 1979. Aspects of nitrogen metabolism of the common mussel *Mytilus edulis*: adaptation to abrupt and fluctuating changes in salinity. Marine Biology 53: 41-55
- Lockwood, B.L. and G.N. Somero. 2011. Transcriptomic responses to salinity stress in invasive and native blue mussels (genus *Mytilus*). Molecular Ecology 20: 517-529
- Lockwood, B.L., K.M. Connor, and A.Y. Gracey. 2015. The environmentally tuned transcriptomics of *Mytilus* mussels. Journal of Experimental Biology 218: 1822-1833
- Lovett, D.L. and S.A. Watts. 1995. Changes in polyamine levels in response to acclimation salinity in gills of the blue crab *Callinectes sapidus* Rathbun. Comparative Biochemistry and Physiology 110B: 115-119
- Lowy, J. 1953. Contraction and relaxation in the adductor muscles of *Mytilus edulis*. The Journal of Physiology 120: 129-140
- Lu, X.J., J. Chen, Z.A. Huang, Y.H. Shi, and F. Wang. 2010. Proteomic analysis on the alteration of protein expression in gills of ayu (*Plecoglossus altivelis*) associated with salinity change. Comparative Biochemistry and Physiology, Part D 5: 185-189
- Maltby, L. 1999. Studying stress: the importance of organism-level responses. Ecological Adaptations 9: 431-440
- Manahan, D.T. 1983. The uptake and metabolism of dissolved amino acids by bivalve larvae. Biological Bulletin 164: 236-250
- Manahan, D.T. 1989. Amino acid fluxes to and from seawater in axenic veliger larvae of a bivalve (*Crassostrea gigas*). Marine Ecology Progress Series 53: 247-255
- Marshall, D.J. and S.G. Morgan. 2011. Ecological and evolutionary consequences of linked life-history stages in the sea. Current Biology 21: R718-R725

- Martel, A.L., R. Tremblay, N. Toupoint, F. Olivier, and B. Myrand. 2014. Veliger size at metamorphosis and temporal variability in prodissoconch II morphometry in the blue mussel (*Mytilus edulis*): potential impact for recruitment. *Journal of Shellfish Research* 33: 442-455
- Méhul, B., D. Bernard, L. Simonetti, M.A. Bernard, and R. Schmidt. 2000. Identification and cloning of a new calmodulin-like protein from human epidermis. *Journal of Biological Chemistry* 275:12841-12847
- Meng, J., Q. Zhu, L. Zhang, C. Li, L. Li, Z. She, B. Huang, and G. Zhang. 2013. Genome and transcriptome analyses provide insight into the euryhaline adaptation mechanism of *Crassostrea gigas*. *Plos One* 8: e58563
- Miller-Fleming, L., V. Olin-Sandoval, K. Campbell, and M. Rasler. 2015. Remaining mysteries of molecular biology: the role of polyamines in the cell. *Journal of Molecular Biology* 427: 3389-3406
- Mitta, G., F. Hubert, E.A. Dyrzynda, P. Boudry, and P. Roch. 2000. Mytilin B and MGD2, two antimicrobial peptides of marine mussels: gene structure and expression analysis. *Developmental and Comparative Immunology* 24: 381-393
- Moyes, C.D., T.W. Moon, and J.S. Ballantyne. 1985. Glutamate catabolism in mitochondria from *Mya arenaria* mantle: effects of pH on the role of glutamate dehydrogenase. *Journal of Experimental Zoology* 236: 293-301
- Mueckler, M.M., S. Moran, and H.C. Pitot. 1984. Transcriptional control of ornithine aminotransferase synthesis in rat kidney by estrogen and thyroid hormone. *Journal of Biological Chemistry* 259: 2302-2305
- Nasrolahi, A., C. Pansch, M. Lenz, and M. Wahl. 2012. Being young in a changing world: how temperature and salinity changes interactively modify the performance of larval stages of the barnacle *Amphibalanus improvisus*. *Marine Biology* 159: 331-340
- Netherton, J.C. and S. Gurin. 1982. Biosynthesis and physiological role of homarine in marine shrimp. *The Journal of Biological Chemistry* 257: 11971-11975
- Neufeld, D.S. and S.H. Wright. 1995. Basolateral transport of taurine in the epithelial cells of isolated, perfused *Mytilus californianus* gills. *Journal of Experimental Biology* 198: 465-473
- Newell, R.I.E. 1989. Species profiles: Life histories and environmental requirements of coastal fishes and invertebrates (North and Mid-Atlantic) – blue mussel. US Fish and Wildlife Service Biological Report 82: TR EL-82-4

- Nishitani, H., S. Kikuchi, K. Okumura, and H. Taguchi. 1995. Finding of a homarine-synthesizing enzyme in turban shell and some properties of the enzyme. *Archives of Biochemistry and Biophysics* 322: 327-332
- O'Connor, C.M., D.R. Norris, G.T. Crossin, and S.J. Cooke. 2014. Biological carryover effects: linking common concepts and mechanisms in ecology and evolution. *Ecosphere* 5: 28
- Osovitz, C.J. and G.E. Hofmann. 2007. Marine macrophysiology: studying physiological variation across large spatial scales in marine systems. *Comparative Biochemistry and Physiology A* 147: 821-827
- Padilla, D.K. and B.G. Miner. 2006. Legacies in life histories. *Integrative and Comparative Biology* 46: 217-223
- Pajares, M.A. and D. Pérez-Sala. 2006. Betaine homocysteine S-methyltransferase: just a regulator of homocysteine metabolism. *Cellular and Molecular Life Sciences* 63: 2792-2803
- Parker, L.M., W.A. O'Connor, D.A. Raftos, H-O Pörtner, and P.M. Ross. 2015. Persistence of positive carryover effects in the oyster, *Saccostrea glomerata*, following transgenerational exposure to ocean acidification. *PLOS One* 10: e0132276
- Pechenik, J.A., T. Gleason, D. Daniels, and D. Champlin. 2001. Influence of larval exposure to salinity and cadmium stress on juvenile performance of two marine invertebrates (*Capitella* sp. I and *Crepidula fornicata*). *Journal of Experimental Marine Biology and Ecology* 264: 101-114
- Pechenik, J. A. 2006. Larval experience and latent effect—metamorphosis is not a new beginning. *Integrative and Comparative Biology* 46: 323-333
- Pegg, A.E. 2006. Regulation of ornithine decarboxylase. *Journal of Biological Chemistry* 281: 14529-14532
- Péquignat, E. 1973. A kinetic and autoradiographic study of the direct assimilation of amino acids and glucose by organs of the mussel *Mytilus edulis*. *Marine Biology* 19: 227-244
- Peraino, C. and H.C. Pitot. 1963. Ornithine- δ -transaminase in the rat I. Assay and some general properties. *Biochimica et Biophysica Acta* 73: 222-231
- Perochon, A., D. Aldon, J.-P. Galadu, and B. Ranty. 2011. Calmodulin and calmodulin-like proteins in plant calcium signaling. *Biochimie* 93: 2048-2053

- Petes, L.E., M.E. Mouchka, R.H. Milston-Clements, T.S. Momoda, and B.A. Menge. 2008. Effects of environmental stress on intertidal mussels and their sea star predators. *Oecologia* 156: 671-680
- Phillips, D.J.H. and D.A. Segar. 1986. Use of bio-indicators in monitoring conservative contaminants: Programme design imperatives. *Marine Pollution Bulletin* 17: 10-17
- Phillips, N.E. 2002. Effects of nutrition-mediated larval condition on juvenile performance in a marine mussel. *Ecology* 83: 2562-2574
- Phillips, N.E. 2006. Natural variability in size and condition and settlement of 3 species of marine invertebrates. *Integrative and Comparative Biology* 46: 598-604
- Pierce, D.W., P.J. Gleckler, T.P. Barnett, B.D. Santer, and P.J. Durack. 2012. The fingerprint of human-induced changes in the ocean's salinity and temperature fields. *Geophysical Review Letters* 31: L21704
- Pierce, S.K. 1982. Invertebrate cell volume controls: a coordinated use of intracellular amino acids and inorganic ions as osmotic solute. *Biological Bulletin* 163: 405-419
- Pierce, S.K. and J.W. Warren. 2001. The taurine efflux portal used to regulate cell volume in response to hypoosmotic stress seems to be similar in many cell types: lessons to be learned from molluscan red blood cells. *American Zoologist* 41: 710-720
- Pierce, S.K., A.D. Politis, D.H. Cronkite, L.M. Rowland, and L.H. Smith, Jr. 1989. Evidence of calmodulin involvement in cell volume recovery following hypoosmotic stress. *Cell Calcium* 10: 159-169
- Qian, Y.-X. and J.-J. Song. 2011. Effects of salinity and betaine on BHMT mRNA expression in *Lateolabrax japonicus*. *Zoological Research* 32: 277-284
- Qiu, J.-W. and P.-Y. Qian. 1999. Tolerance of the barnacle *Balanus amphitrite amphitrite* to salinity and temperature stress: effects of previous experience. *Marine Ecology Progress Series* 188: 123-132
- Qiu, J.-W., R. Tremblay, and E. Bourget. 2002. Ontogenetic changes in hyposaline tolerance in the mussels *Mytilus edulis* and *M. trossulus*: implications for distributions. *Marine Ecology Progress Series* 228: 143-152
- Rawson, P.D., S. Hayhurst, and B. Vanscoyoc. 2001. Species composition of blue mussel populations in the northeastern Gulf of Maine. *Journal of Shellfish Research* 20: 31-38

- Rayssac, N., F. Pernet, O. Lacasse, and R. Tremblay. 2010. Temperature effect on survival, growth, and triacylglycerol content during the early ontogeny of *Mytilus edulis* and *M. trossulus*. *Marine Ecology Progress Series* 417: 183-191
- Reddy, A.S.N., G.S. Ali, H. Celesnik, and I.S. Day. 2011. Coping with stresses: roles of calcium- and calcium/calmodulin-regulated gene expression. *Plant Cell* 23: 2010-2032
- Reed, W. and P. Satir. 1980. Calmodulin in mussel gill epithelial cells: role in ciliary arrest. *Annals New York Academy of Sciences* 356: 423-426
- Ren, G., X. Hu, J. Tang, and Y. Wang. 2013. Characterization of cDNAs for calmodulin and calmodulin-like protein in the freshwater mussel *Hyriopsis cumingii*: Differential expression in response to environmental Ca^{2+} and calcium binding of recombinant proteins. *Comparative Biochemistry and Physiology, Part B* 165: 165-171
- Rhee, H.J., E.-J. Kim, and J.K. Lee. 2007. Physiological polyamines: simple primordial stress molecules. *Journal of Cellular and Molecular Medicine* 11: 685-703
- Rhyner, J.A., M. Koller, I. Durussel-Gerber, J.A. Cox, and E.E. Strehler. 1992. Characterization of the human calmodulin-like protein expressed in *Escherichia coli*. *Biochemistry* 31: 12826-12832
- Rice, M.A. and G.C. Stephens. 1988. Influx and transepithelial flux of amino acids in the mussel *Mytilus edulis*. *Journal of Experimental Biology* 135: 275-287
- Riisgård, H.U., L. Bøttinger, and D. Pleissner. 2012. Effect of salinity on growth of mussels, *Mytilus edulis*, with special reference to Great Belt (Denmark). *Open Journal of Marine Science* 2: 167-176
- Saeed, A.I., V. Sharov, J. White, J. Li, W. Liang, N. Bhagabati, J. Braisted, M. Klapa, T. Currier, M. Thiagarajan, A. Sturn, M. Snuffin, A. Rezantsev, D. Polov, A. Ryltsov, E. Kostukovich, I. Borisovsky, Z. Liu, A. Vinsavich, V. Trush, and J. Quackenbush. 2003. TM4: a free, open-source system for microarray data management and analysis. *Biotechniques* 34: 374-378
- Sadok, S., R.F. Uglow, and S.J. Haswell. 1997. Haemolymph and mantle fluid ammonia and ninhydrin positive substances variations in salinity-challenged mussels (*Mytilus edulis* L.). *Journal of Experimental Marine Biology and Ecology* 212: 195-212
- Sailer, M., A. Reuzel-Selke, and R.K. Achazi. 1990. The calmodulin-protein-kinase system of *Mytilus edulis* catch muscle. *Comparative Biochemistry and Physiology* 96B: 533-541

- Schäfer, C., L. Hoffmann, K. Heldt, M.R. Lornejad- Schäfer, G. Brauers, T. Gehrman, T.A. Garrow, D. Häussinger, E. Mayatepek, B.C. Schwahn, and F. Schliess. 2007. Osmotic regulation of betaine homocysteine-*S*-methyltransferase expression in H4IIE rat hepatoma cells. *American Journal of Physiology – Gastrointestinal and Liver Physiology* 292: G1089-G1098
- Schneider, C.A., W.S. Rasband, and K.W. Eliceiri. 2012. NIH Image to ImageJ: 25 years of image analysis. *Nature Methods* 9: 671-675
- Seed, R. 1969. The ecology of *Mytilus edulis* L. (Lamellibranchiata) on exposed rocky shores. II. Growth and mortality. *Oecologia* 3: 317-350
- Shick, J.M., E. Gnaiger, J. Widdows, B.L. Bayne, and A. De Zwaan. 1986. Activity and metabolism in the mussel *Mytilus edulis* L. during intertidal hypoxia and aerobic recovery. *Physiological Zoology* 59: 627-642
- Shumway, S.E., P.A. Gabbott, and A. Youngson. 1977. The effect of fluctuating salinity on the concentrations of free amino acids and ninhydrin-positive substances in the adductor muscles of eight species of bivalve molluscs. *Journal of Experimental Marine Biology and Ecology* 29: 131-150
- Silva, A.L. and S.H. Wright. 1992. Integumental taurine transport in *Mytilus* gill: short-term adaptation to reduced salinity. *Journal of Experimental Biology* 162: 265-279
- Simpson, R.J., C.S. Wilding, and J. Grahame. 2005. Intron analyses reveal multiple calmodulin copies in *Littorina*. *Journal of Molecular Evolution* 60: 505-512
- Snedden, W.A. and H. Fromm. 1998. Calmodulin, calmodulin-related proteins and plant responses to the environment. *Trends in Plant Science* 3: 299-304
- Snedden, W.A. and H. Fromm. 2000. Calmodulin as a versatile calcium signal transducer in plants. *New Phytologist* 151:35-66
- Solórzano, L. 1969. Determination of ammonia in natural waters by the phenylhypochlorite method. *Limnology and Oceanography* 14: 799-801
- Somero, G.N. 1986. Protons, osmolytes, and fitness of internal milieu for protein function. *American Journal of Physiology* 251: R197-R213
- Somero, G.N. 2010. The physiology of climate change: how potentials for acclimatization and genetic adaptation will determine ‘winners’ and ‘losers’. *The Journal of Experimental Biology* 213: 912-920
- Sprung, M. 1984. Physiological energetics of mussel larvae (*Mytilus edulis*). I. Shell growth and biomass. *Marine Ecology Progress Series* 17: 298-293

- Sprung, M. and J. Widdows. 1986. Rate of heat dissipation by gamete and larval stages of *Mytilus edulis*. *Marine Biology* 91: 41-45
- Stafford, J. 1906. XIV. On the recognition of bivalve larvae in plankton collections. *Contributions to Canadian Biology and Fisheries B*: 221-242
- Stephens, G.C. and R.A. Schinske. 1961. Uptake of amino acids by marine invertebrates. *Limnology and Oceanography* 6: 175-181
- Stickle, W.B. and T.D. Sabourin. 1979. Effects of salinity on the respiration and heart rate of the common mussel, *Mytilus edulis* L., and the black chiton, *Katherina tunicata* (Wood). *Journal of Experimental Marine Biology and Ecology* 41: 257-268
- Stommel, E.W., R.E. Stephens, H.R. Masure, and J.F. Head. 1982. Specific localization of scallop gill epithelial calmodulin in cilia. *Journal of Cell Biology* 92: 622-628
- Suchanek, T.H. 1979. The *Mytilus californianus* community: studies on the composition, structure, organization, and dynamics of a mussel bed. PhD Thesis, University of Washington, USA
- Swanson, M.E., S.F. Sturner, and J.H. Schwartz. 1990. Structure and expression of the *Aplysia californica* calmodulin gene. *Journal of Molecular Biology* 216: 545-553
- Swick, R.W., A.K. Rexroth, and J.L. Stange. 1968. The metabolism of mitochondrial proteins III. The dynamic state of rat liver mitochondria. *Journal of Biological Chemistry* 243: 3581-3587
- Szegedi, S.S., C.C. Castro, M. Koutmos, and T.A. Garrow. 2008. Betaine-homocysteine *S*-methyltransferase-2 is an *S*-methylmethionine-homocysteine methyltransferase. *Journal of Biological Chemistry* 283: 8939-8945
- Thorson, G. 1950. Reproductive and larval ecology of marine bottom invertebrates. *Biological Reviews of the Cambridge Philosophical Society* 24: 1-45
- Tiburcio, A.F., T. Altabella, M. Bitrián, and R. Alcázar. 2014. The role of polyamines during the lifespan of plants: from development to stress. *Planta* 240: 1-18
- Tikunov, A.P., C.B. Johnson, H. Lee, M.K. Stoskopf, and J.M. Macdonald. 2010. Metabolomic investigations of American oysters using ¹H-NMR spectroscopy. *Marine Drugs* 8: 2578-2596
- Toda, H., M. Yazawa, K. Kondo, T. Honma, K. Narita, and K. Yagi. 1981. Amino acid sequence of calmodulin from scallop (*Patinopecten*) adductor muscle. *Journal of Biochemistry* 90: 1493-1505

- Tomanek, L. and B. Helmuth. 2002. Physiological ecology of rocky intertidal organisms: a synergy of concepts. *Integrative and Comparative Biology* 42: 771-775
- Tomanek, L., M.J. Zuzow, L. Hitt, L. Serafini, and J.J. Valenzuela. 2012. Proteomics of hyposaline stress in blue mussel congeners (genus *Mytilus*): implications for biogeographic range limits in response to climate change. *The Journal of Experimental Biology* 215: 3905-2916
- Toutenhoofd, S.L. and E.E. Strehler. The calmodulin multigene family as a unique case of genetic redundancy: multiple levels of regulation to provide spatial and temporal control of calmodulin pools. *Cell Calcium* 28: 83-96
- Toyohara, H., M. Yoshida, M. Hosoi, and I. Hayashi. 2005. Expression of taurine transporter in response to hypo-osmotic stress in the mantle of Mediterranean blue mussel. *Fisheries Science* 71: 356-360
- Tsuchiya, M. and M. Nishihira. 1985. Islands of *Mytilus* as a habitat for small intertidal animals: effects of island size on community structure. *Marine Ecology Progress Series* 25: 71-8
- Tuffnail, W., G.A. Mills, P. Cary, and R. Greenwood. 2009. An environmental ¹H NMR metabolomics study of the exposure of the marine mussel *Mytilus edulis* to atrazine, lindane, hypoxia, and starvation. *Metabolomics* 5: 33-43
- Vogel, H.J. 1994. Calmodulin: a versatile calcium mediator protein. *Biochemistry and Cell Biology* 72: 357-376
- Watts, S.A., E.W. Yeh, and R.P. Henry. 1996. Hypoosmotic stimulation of ornithine decarboxylase activity in the brine shrimp *Artemia franciscana*. *Journal of Experimental Zoology* 274: 15-22
- Weinman, J., B.D. Gaspera, A. Dautigny, D.P. Dinh, J. Wang, H. Nojima, and S. Weinman. 1991. Developmental regulation of calmodulin gene expression in rat brain and skeletal muscle. *Cell Regulation* 2: 819-826
- Welborn, J.R. and D.T. Manahan. 1995. Taurine metabolism in larvae of marine molluscs (Bivalvia, Gastropoda). *Journal of Experimental Biology* 198: 1791-1799
- Westerbom, M. M. Kilpi, and O Mustonen. 2002. Blue mussels, *Mytilus edulis*, at the edge of the range: population structure, growth and biomass along a salinity gradient in the north-eastern Baltic Sea. *Marine Biology* 140: 991-999
- Widdows, J. 1991. Physiological ecology of mussel larvae. *Aquaculture* 94: 147-163

- Wilbur, K.M. and A.S.M. Saleuddin. 1983. Shell formation *In* A.S.M. Saleuddin and K.M. Wilbur (eds.) *The Mollusca* Vol 4: 238-239. Academic Press, New York
- Wishart, D.S., T. Jewison, A.C. Guo, M. Wilson, C. Knox, Y. Liu, Y. Djoumbou, R. Manal, F. Aziat, E. Dong, S. Bouatra, I. Sinelnikov, D. Arndt, J. Xia, P. Liu, F. Yallou, T. Bjorndahl, R. Perez-Pineiro, R. Eisner, F. Allen, V. Neveu, R. Greiner, and A. Scalbert. 2013. HMDB 3.0—The Human Metabolome Database in 2013. *Nucleic Acid Research* 41: D801-D807
- Wright, S.H. and T.W. Secomb. 1986. Epithelial amino acid transport in marine mussels: role in net exchange of taurine between gills and seawater. *Journal of Experimental Biology* 121: 251-270
- Wright, S.H., T.W. Secomb, and T.J. Bradley. 1987. Apical membrane permeability of *Mytilus* gill: influence of ultrastructure, salinity, and competitive inhibitors on amino acid fluxes. *Journal of Experimental Biology* 129: 205-230
- Wright, S.H., T.M. Wunz, and A.L. Silva. 1992. Betaine transport in the gill of a marine mussel, *Mytilus californianus*. *American Journal of Physiology – Regulatory, Integrative, and Comparative Physiology* 263: R226-R232
- Yancey, P.H. 2005. Organic osmolytes as compatible, metabolic, and counteracting cryoprotectants in high osmolarity and other stresses. *Journal of Experimental Biology* 208: 2819-2830
- Yancey, P.H., M.E. Clark, S.C. Hand, R.D. Bowlus, and G.N. Somero. 1982. Living with water stress: evolution of osmolyte systems. *Science* 217: 1214-1222
- Yang, T., S. Lev-Yadun, M. Feldman, and H. Fromm. 1998. Developmentally regulated organ-, tissue-, and cell-specific expression of calmodulin genes in common wheat. *Plant Molecular Biology* 37: 109-120
- Young, C.M. 1990. Larval ecology of marine invertebrates: a sesquicentennial history. *Ophelia* 32: 1-48
- Zandee, D.I., J.H. Kluytmans, W. Zurburg, and H. Pieters. 1980. Seasonal variations in biochemical composition of *Mytilus edulis* with reference to energy metabolism and gametogenesis. *Netherlands Journal of Sea Research* 14: 1-29
- Zeng, H., L. Xu, A. Singh, H. Wang, L. Du, and B.W. Poovaiah. 2015. Involvement of calmodulin and calmodulin-like proteins in plant responses to abiotic stress. *Frontiers in Plant Science* 6: 600

- Zhang, Y., J. Sun, H. Mu, J. Li, Y. Zhang, F. Xu, Z. Xiang, P.-Y. Qian, J.W. Qiu, and Z. Yu. 2015. Proteomic basis of stress responses in the gills of the Pacific oyster *Crassostrea gigas*. *Journal of Proteomic Research* 14: 304-317
- Zhao, X., H. Yu, L. Kong, and Q. Li. 2012. Transcriptomic responses to salinity stress in the Pacific Oyster *Crassostrea gigas*. *Plos One* 7: e46244
- Zielinski, R.E. 1998. Calmodulin and calmodulin-binding proteins in plants. *Annual Review of Plant Physiology and Plant Molecular Biology* 49: 697-725
- Zurburg, W. and A. De Zwaan. 1981. The role of amino acids in anaerobiosis and osmoregulation in bivalves. *Journal of Experimental Zoology* 215: 315-325
- Zwaan, A. de and T.C.M. Wijsman. 1976. Anaerobic metabolism in Bivalvia (Mollusca): Characteristics of anaerobic metabolism. *Comparative Biochemistry and Physiology* 54B: 313-324

APPENDIX A: SUPPLEMENTAL MATERIAL FOR CHAPTER 2

Table A.1. Supplemental table containing complete dataset for peaks identified in *M. edulis*. The peaks listed here indicate the chemical shift (in ppm, relative to TSP) for each metabolite observed using 2D-TOCSY (Figure 3.2), as well as the multiplicity for each peak when it could be determined (s = singlet, d = doublet, dd = doublet of doublets, t = triplet, and m = multiplet), as a continuation from Table 3.2. When appropriate, the possible identity for the metabolite is included and the tissue or sample from which the metabolite was identified (P = pediveliger, G = gill, M = mantle, A = adductor).

No	Chemical Shift (ppm)	Possible Identity
Veliger-specific metabolites		
27	1.33, 1.57	
28	1.73, 4.18	
29	2.14, 2.23	
30	2.70, 3.58	Sarcosine
31	2.74, 3.27, 3.44	
32	2.97, 4.30	
33	3.02, 4.19	
34	3.09, 3.57	
35	4.13, 4.18	
36	4.36, 5.97, 7.95	
37	4.39, 4.49, 6.13	
38	4.43, 6.68	
Pediveliger-specific metabolites		
39	1.4 (d)	
40	1.78, 3.12	
41	2.22, 2.24	
42	2.72, 3.46	
43	3.60, 5.39	
44	3.61, 3.84	
45	3.63, 3.96	
46	3.75, 4.65	

Table A.1, continued...

No	Chemical Shift (ppm)	Possible Identity
Pediveliger-specific metabolites, cont.		
47	3.90, 4.10	
48	4.17, 4.28	
49	4.27, 4.58	
50	5.32, 7.03	
51	7.85 (m)	
Other larval-specific metabolites		
52	3.37, 4.44	
53	3.79, 3.90	
Gill-specific metabolites		
54	1.86, 3.70	
55	2.35 (m)	
56	3.23, 4.65	
57	3.38, 3.43	
58	3.41, 3.69	
59	3.42, 3.80	
60	3.46, 3.71	
61	3.46, 4.64	
62	3.52, 3.70, 3.82, 5.22	Glucose
63	3.69, 3.72	
64	4.48, 5.13	
65	6.90	
66	7.19 (m)	
Mantle-specific metabolites		
67	1.47, 1.90	
68	3.07, 3.19	
69	3.11, 3.41	
70	3.17	
71	3.34, 4.02	
72	3.48 (dd), 3.68 (dd)	Cysteine-S-sulfate
73	3.90, 3.96	
74	5.23, 5.30	
75	7.31	

Table A.1, continued...

No	Chemical Shift (ppm)	Possible Identity	
Adductor-specific metabolites			
76	0.95 (m)		
77	1.08, 1.13		
78	1.19		
79	1.49, 3.70		
80	2.46, 3.41		
81	2.68, 2.73	Citric acid	
82	2.76, 2.81		
83	2.86, 3.44, 3.59, 3.80	Unknown #3 ¹	
84	3.13, 3.24		
85	3.18, 3.22		
86	3.23, 3.75		
87	3.9 (m)		
No	Chemical Shift (ppm)	Possible Identity	Source of Metabolite
Juvenile-specific metabolites			
88	2.25, 3.88, 4.12, 4.64		M, A
89	6.59		G, M
90	7.39 (m)		G, M
Other metabolites			
91	5.21 (d)	α -glucose	P, A
92	5.38 (d)	Allantoin	P, A
93	6.54 (s)		P, A
94	3.08, 3.41		P, G
95	4.11, 4.38		P, G
96	4.49, 6.14		P, G
97	3.06 (m)		P, G, M
98	8.29 (m)		P, G, A
99	8.33 (m)		P, G, M

APPENDIX B:
SUPPLEMENTAL MATERIAL FOR GENE EXPRESSION STUDIES

B1. Microarray Analysis

There were 10,241 putative genes where we observed signal from 3 or more of the probes for the *M. edulis* dataset and 10,448 in the *M. trossulus* dataset, resulting in a total of 10,880 genes. A subset of these genes was selected from each dataset in which there was a greater than 1-fold change in expression between the treatment and control groups at 8 or 32 h of exposure to 20 ppt. This refined the number of genes of interest to 4,697 from *M. edulis* and 5,055 from *M. trossulus*, for a total of 5,817 genes. We then identified 416 that were differentially expressed between the two species (Table B.1) and looked at the functional annotation to determine which of these may play an important role in the cellular response to salinity stress. Of the 62 genes of interest (Figure 4.1), we selected a small subset, including betaine-homocysteine *S*-methyltransferase, taurine transporter, ornithine aminotransferase, and calmodulin, to study further using a more targeted qPCR approach.

B2. Marker Development

Markers were developed using sequence information in the *M. californianus* EST database, targeting those that showed differential expression in the microarray study. Primer sets were tested by amplification using the polymerase chain reaction (PCR), in a 25- μ l reaction. The PCR master mix contained 2.5 μ l 10X PCR buffer, 0.75 μ l MgCl₂, 0.5 μ l 10 mM dNTP mix, 0.25 μ l of the reverse and forward primers, 0.2 μ l Taq-DNA polymerase (Invitrogen), and 19.6 μ l nuclease-free water. For each reaction, we added 1

μ L of cDNA template to 24 μ l mix and ran the PCR in an Eppendorf 5333 MasterCycler thermal cycler. PCR amplifications followed a standard protocol, with a denaturing step at 94 °C for 2 m, 30 cycles consisting of 20 s denaturing step at 94 °C, 30 s annealing at 50 °C, and 2 m elongation at 72 °C, followed with a final incubation at 72 °C for 5 m. Products were run on a 2 % agarose gel containing ethidium bromide at 75 V for 45 m and visualized with UV-light.

cDNA samples that were used for sequencing and PCR amplifications were prepared by the protocol outlined in Section 4.3.6. We used tissue samples from adult *M. edulis* and *M. trossulus* that had been collected for other studies; some of the animals were untreated, while others had been exposed to varying degrees of low salinity exposure. We attempted to obtain sequence data from multiple individuals of each species to develop primer sets and to ensure that we were confident that the sequences we were amplifying were coming only from our gene of interest.

We also used 3' and 5' RACE (rapid amplification of cDNA ends) to obtain full sequence information for many of our genes of interest. For the 3' RACE reactions, we mixed 20 units RNase Inhibitor, 1 μ g of total RNA, and 12 mM CDSP1 Oligo dT primer (5' AAGCAGTGGTATCAACGCAGA 3') in 64 μ l nuclease-free H₂O, incubated the reaction for 10 m at 65 °C, and cooled to 42 °C. We then added 20 μ M 5X First Strand Buffer (Invitrogen), 2 μ l 0.1 M DTT, 10 μ l 10 μ M dNTPs, and 0.5 μ l RNase Inhibitor and continued to incubate at 42 °C for 2 m. Finally, we added 2 ml of Superscript II Reverse Transcriptase (Invitrogen), incubated for 90 m at 42 °C, before inactivating the reaction by heating to 85 °C for 15 m. The product was cleaned up using a PCR purification kit (Promega Corporation) and eluted in 40 μ l. The first strand cDNA was

amplified using Touchdown PCR. The master mix for the reaction is described above and used a gene specific primer with a PII upstream adaptor primer (5' AAG CAG TGG TAT CAA C 3'). The cycling protocol for the touchdown PCR is as follows: 1 m at 94 °C, 10 cycles of 94 °C for 30 s, 60 °C for 30 s, with a 1 °C decrease every cycle, followed by 2 m at 72 °C, 30 cycles of 94 °C for 30 s, 50 °C for 30 s and 72 °C for 2 m, and a final incubation at 72 °C for 5 m. We then performed a nested PCR amplification using 1:100 dilution from the 1st strand amplification as template, a PII short adapter primer (5' GGT ATC AAC GCA GAG T 3'), and an internal gene specific primer. Products were cleaned up using the Wizard Gel Purification Kit (Promega Corporation) and sequenced by the DNA Sequencing Facility at the University of Maine (Orono, ME).

The 5' RACE reactions were performed following the 3' RACE protocol, with the following modifications to the initial reverse transcriptase reactions. We mixed 1 µg total RNA with 1 µL of 12 µM gene specific primer, 1 µl 12 µM PRS IIA adapter primer (5' AAG CAG TGG TAT CAA CGC AGA GTA CC 3') and 0.5 µl RNase OUT in a 5 µl reaction and incubated at 65 °C for 2 m. The reaction was cooled to 42 °C and then we added 5 µl of 5X ImProm-II Reaction Buffer (Promega Corporation), 1 µL 0.1 M DTT, and 1 µl ImProm II Reverse Transcriptase (Promega Corporation). The reaction was incubated at 42 °C for 1 h and then heated to 65 °C for 10 m. We then added 40 µl of nuclease-free water to the reaction before proceeding to the 1st strand cDNA synthesis.

Betaine-homocysteine S-methyltransferase

Primers were designed using sequence information from the *M. californianus* EST that corresponded to our analysis of the microarray study (ES402453; Table B.1). Using BHMT FOR2 and BHMT REV 2 (Table B.2), we obtained 750 bp of sequence

information from both *M. edulis* and *M. trossulus*. We targeted areas conserved between the two species to develop qPCR for *BHMT*. There is 99% homology between our sequence, which covers the middle portion of the coding region, and *Crassostrea gigas* (EKC27615.1; Figure B.1). Our sequence data, as well as the position of the primers we developed can be found in Figure B.2.

Taurine Transporter

The taurine transporter gene has been described in *M. galloprovincialis* by Hosoi et al. (2005). We used sequence data available from *M. galloprovincialis* (GenBank AB190909) to design qPCR primer sets (Table B.2). The position of the qPCR primers can be found in Figure B.3. Amplification of this gene using genomic DNA can also be used as a marker for species identification between *M. edulis* and *M. trossulus* because of variations in introns between the congeners.

40S Ribosomal Protein

We used ES387615 from the *M. californianus* database to develop primers targeting the 40S Ribosomal Protein (Figure B.4). This gene was targeted as a normalizing or reference gene for qPCR; the primer sets are listed in Table B.3.

Ornithine Aminotransferase

Ornithine aminotransferase (ES398776) was upregulated over 2-fold in *M. edulis* after 24 and 48 h low salinity exposure, while showed less of an upregulation in *M. trossulus* at the same time points (Table B.1). Primers were developed to target *OAT* in *M. edulis* (Table B.4) and to obtain sequence information for developing qPCR primers. The sequence for *OAT*, as well as the position of the primers can be found in Figure B.5.

Ornithine Decarboxylase

Ornithine decarboxylase was identified by Lockwood and Somero (2011) in a similar microarray study using *M. trossulus* and *M. galloprovincialis*. Because *ODC* also functions in ornithine metabolism, opposite of *OAT*, we designed primers to look at the role of this pathway in the stress response out the of *M. californianus* database targeting ES390663 (Table B.5). There are two other ESTs that BLAST as *ODC* in the *M. californianus* database and it is probable that there are two genes, although we were unsuccessful in amplifying the other targets. The partial sequence information for *ODC* with position of the primers can be found in Figure B.6.

Calmodulin

We identified calmodulin in the *M. californianus* database (ES394383) by sequence homology to *CaM* in other species. Initially, we designed CaM For to amplify with one of the reverse primers for *CAML2* (Table B.7). We also used 3' RACE to obtain sequence for the entire gene and then designed our qPCR primers. The sequence information is in Chapter 5, but the position of the primers within the sequence are in Figure B.8. Our primer sets were designed in areas of dissimilarity between the *CaM*-like genes to ensure we were targeting calmodulin and not a similar gene. Calmodulin was differentially expressed in the microarray study and was downregulated in *M. trossulus* and upregulated in *M. edulis* (Table B.1).

Calmodulin-like 1

CAML1 was initially identified from the microarray (Table B.1) because it was differentially expressed between *M. edulis* and *M. trossulus* during low salinity exposure. The EST from the microarray (ES392136) was identified as calmodulin using the Basic Local Alignment Search Tool (BLAST®, National Library of Medicine) because of

overlap in the EF-hand domains, although there is only 31% sequence homology between *CaM* and *CAML1*. We developed a series of primer sets (Table B.6, Figure B.8) using PCR amplifications and 3' RACE to obtain sequence information, which is detailed in Chapter 5. These primer sets do not amplify a gene in larval samples; using 3' RACE three bands of approximately 1000, 650, and 200 bp would amplify but the sequences do not contain an open reading frame. We were not able to obtain full sequence information from *M. trossulus* because there seemed to be a lot of variability in the *CAML1* sequence between the two species.

Calmodulin-like 2

To identify another *CaM*-like gene in *M. edulis*, we aligned all of the *CAML* sequences in *M. californianus* and chose one EST that had the most sequence homology to *CaM* (ES406016). We called this gene calmodulin-like 2 and then designed primers to obtain sequence information (Table B.6). We used PCR amplifications using our primer sets as well as 3' and 5' RACE to sequence the entire *CAML2* gene (Figure B.9). Our qPCR primers were designed to target areas that differed in sequence from *CaM* to ensure we were amplifying the appropriate gene of interest.

Dermatopontin

Dermatopontin (*DPT*) was initially chosen as a gene of interest because of its differential expression between *M. edulis* and *M. trossulus* in the microarray study (Table B.1). We designed primers (Table B.7) from *M. californianus* using ES737940. We had trouble amplifying more than 100 bp in either *M. edulis* or *M. trossulus* and decided not to continue developing the marker. The sequence for *DPT* can be found in Figure B.10.

Sarcoplasmic Calcium Binding Protein

Sarcoplasmic calcium binding protein or *SCBP* was also differentially expressed between *M. edulis* and *M. trossulus* (Figure B.1). We were interested in this gene because of its role in calcium signaling and buffering, so we developed primers using an EST from *M. californianus* (ES390981, reverse complement sequence; Table B.7). We developed qPCR assays for this gene and we able to obtain roughly 300 bp of sequence information from *M. edulis*. We ran some preliminary qPCR studies of *SCBP* expression in larval mussels and it was upregulated after 24 and 48 h of exposure. However, we did not use this marker in our more recent studies and further assays should be run to determine the role of *SCBP* during low salinity exposure. The sequences for *M. edulis* and *M. trossulus* was not very similar, so primer sets only target *M. edulis* (Figure B.11).

T-complex Testes-specific Protein 1

T-complex testis-expressed-1 (*TCTEX*) is a dynein light chain protein involved in cytoskeletal reorganization. This gene was strongly upregulated in *M. edulis* during low salinity exposure (Figure B.1) so we used information from the microarray (ES738040) to develop species-specific primer sets (Table B.7). We have most of the gene sequenced (Figure B.12) and ran some preliminary qPCR assays using the primers we developed. The gene was upregulated in larvae after 48 h of exposure to low salinity, but the marker was never used in other qPCR assays.

Table B.1. Differentially expressed genes in salinity challenged *M. edulis* and *M. trossulus* from the 2009 microarray study. The median change in expression is listed for *M. edulis* and *M. trossulus* following an initial 8 h acclimation to 20 ppt (t = 8 h) and then a 24 and 48 h exposure (t = 32 h and 56 h, respectively). The annotations were determined in Blast2GO using BLASTx against the NCBI online database using the associated EST.

Gene Annotation	EST	<i>M. trossulus</i>				<i>M. edulis</i>			
		8 h	32 h	56 h	8 h	32 h	56 h		
2-5-oligodenylylate synthetase 1	ES391532	0.05	-1.99	0.08	0.46	-0.82	0.63		
26S proteasome non-ATPase regulatory subunit 2	ES401603	-0.52	0.24	0.59	0.14	-1.06	-0.12		
28S ribosomal protein mitochondrial isoform	ES393902	0.05	-1.13	-0.77	0.37	-0.70	-0.48		
3-ketocacyl-CoA thiolase	ES391835	0.28	-0.81	-0.07	1.29	-0.80	0.21		
3-oxoacyl-[acyl-carrier-protein] reductase-like	ES389019	0.19	-1.23	-0.30					
39S ribosomal protein mitochondrial-like	ES397466	-0.19	-0.37	-0.59	-0.19	-1.69	-0.53		
60 kDa SS-A/Ro ribonucleoprotein	ES391689	0.21	0.01	-0.14	0.41	1.84	0.87		
Adenylylate kinase 8-like	ES736420	1.37	-1.45	-0.89	1.17	-1.30	0.32		
Adenylylate kinase isoenzyme 5	ES738667	-0.26	-0.05	1.33	0.25	-1.17	-0.18		
Akirin 2	ES405710	0.63	-0.23	-0.58	0.30	1.45	1.62		
Ala-tRNA(Pro) Hydrolase	ES406590	2.66	1.00	-0.07	-0.81	1.17	0.08		
Alcohol dehydrogenase class-3-like	ES403093	0.49	-0.79	-0.27	-0.02	-1.11	0.60		
Aldehyde dehydrogenase, mitochondrial-like	ES738788	0.02	-1.79	-0.12	0.11	2.02	1.14		
Allantoinase 1	ES393810	0.43	-1.27	0.34	-0.12	-0.48	-0.81		
α -ketoglutarate-dependent dioxygenase alkB homolog 2 isoform 1	ES393273	0.16	-1.11	0.22	0.37	0.00	-0.07		
α/β hydrolase domain-containing 14-like	ES391181	0.71	-1.04	-0.48	0.18	0.22	-0.86		
Alternative oxidase, mitochondrial-like	ES402065	0.36	-0.14	-0.02	0.03	1.52	1.34		
Amidase-like isoform	ES402424	0.12	-0.83	-1.41	1.12	-1.91	-2.50		
AN1-type zinc finger protein 6	ES389689	0.48	-0.56	1.02	-0.06	1.92	-0.64		
Anaphase-promoting complex subunit 2-like	ES403430	0.65	-0.08	0.15	-0.50	1.42	1.74		
Ankyrin repeat domain-containing 34B-like	ES407054	-0.20	-1.34	-1.32	-0.04	-1.36	-0.55		
Ankyrin repeat domain-containing protein 54-like	ES402657	0.41	-1.20	-0.29	0.28	-0.14	-0.04		
Ankyrin repeat protein	ES388750	0.88	0.33	0.46	-1.08	0.35	0.79		
Ankyrin repeat protein	ES404574	0.68	-0.07	-0.21	1.46	0.27	-0.95		
Ankyrin-3	ES393668	0.83	-0.10	-0.98	-1.53	0.39	0.82		
AP-1 complex subunit μ -1-like	ES398779	0.28	-1.29	-0.10	0.70	-0.50	0.61		

Gene Annotation	EST	<i>Δ M. trossulus</i>				<i>Δ M. edulis</i>			
		8 h	32 h	56 h	8 h	32 h	56 h		
Arachidonate 5-lipoxygenase-like	ES394263	-0.13	0.64	-4.97	-0.46	5.05	2.20		
Arginine N-methyltransferase 1	ES392825	0.14	-0.04	0.31	1.28	-1.28	2.23		
Arginine N-methyltransferase 3	ES387484	0.25	-1.61	-0.85	0.04	-1.32	-1.08		
Arginine serine-rich PNISR isoform	ES392316	-0.92	0.12	0.47	1.09	-2.42	-1.45		
Ariadne-1-like protein	ES390725	2.30	0.15	-0.31	-0.17	-0.18	-2.32		
Arnadillo repeat-containing protein 4	ES398293	-0.89	-0.70	-0.32	0.19	-1.24	-0.25		
Arrestin domain-containing protein 2-like	ES389784	-0.53	-0.30	-0.07	1.06	-0.96	0.26		
Arylsulfatase B	ES737591	1.07	-0.84	-0.25	0.30	0.73	-0.15		
ATP-binding cassette sub-family A member 5	ES737682	-0.38	2.58	0.58	0.66	0.62	0.58		
ATPase ASNA1 homolog	ES397688	0.94	0.82	0.87	1.09	-0.22	-1.14		
B-cell lymphoma/leukemia 10-like	ES738377	0.28	-1.61	-1.28	-0.17	2.41	0.22		
Baculoviral IAP repeat-containing 2-like	ES396930	1.30	0.20	-0.17	-0.17	0.26	-0.04		
Baculoviral IAP repeat-containing protein 3	ES390299	0.42	-0.55	0.17	1.99	-0.55	-2.93		
Basic leucine zipper and W2 domain-containing 1	ES389942	0.04	1.00	0.62	0.91	-1.22	0.48		
Beclin 1 isoform	ES398053	-0.09	-1.41	-0.53	0.50	-0.97	-0.74		
β-taxilin	ES390377	0.09	-1.31	-0.67	-0.15	0.91	-0.45		
Betaine-homocysteine S-methyltransferase	ES402453	-0.21	-2.46	-1.66	-0.43	0.17	0.00		
Bombesin receptor-activated protein C6orf89-like	ES398214	0.27	-1.60	-0.15	0.19	-0.52	-0.02		
BTB POZ domain-containing protein 17-like	ES408009	0.36	-0.59	-0.22	0.94	-1.45	0.60		
BTB POZ domain-containing protein 6	ES736388	2.22	-0.32	-0.28	-0.42	-0.29	-0.78		
BTG1 protein, partial	ES737473	0.24	-1.20	-1.08	0.25	0.09	0.60		
C-type lectin 6	ES394431				1.08	-1.98	-0.19		
C-type lectin domain family 10A isoform 1	ES738863	0.39	-0.05	0.87	-1.74	0.32	1.19		
Cadherin EGF LAG seven-pass G-type receptor 1	ES403150	0.17	0.51	0.61	0.08	-1.60	-0.06		
Calcium responsive transcription factor-like	ES399649	1.46	-1.06	0.09	0.66	0.82	1.40		
Calmodulin	ES394383	-0.66	-1.23	-0.61	0.23	1.49	-0.24		
Calmodulin-like 1 (CAML1)	ES392136	0.26	-1.70	-1.08	-0.28	0.99	-0.47		

Gene Annotation	EST	<i>ΔM. trossulus</i>			<i>ΔM. edulis</i>		
		8 h	32 h	56 h	8 h	32 h	56 h
Calmodulin-like 2 (CAML2)	ES406016	-0.61	0.12	0.61	0.08	0.18	-0.19
Caltractin-like	ES391686	0.11	-1.43	-0.06	1.08	-1.16	-0.05
Caltractin-like	ES736826	-0.08	-0.82	-0.60	0.33	-1.36	-0.20
Carbohydrate sulfotransferase 15	ES391143	-0.14	-0.12	-0.62	0.90	-1.45	-0.95
Carbonyl reductase [NADPH] 1-like	ES400716	-0.22	-0.14	-0.21	-0.66	1.86	1.48
Cartilage matrix protein	ES398875				-0.15	2.95	0.03
Caspase 8	ES391951	0.18	0.68	0.60	1.68	0.21	0.88
Catenin β-like isoform	ES395666	0.86	-0.13	-1.18	-0.06	2.23	1.31
Cathepsin L	ES395998	-1.61	-3.23	-1.54	-1.46	0.37	1.40
CD63 antigen	ES392720	-0.18	-0.28	-0.33	-0.61	1.21	1.26
Cell division control protein 42 homolog	ES398967	1.21	0.52	-0.23	-0.95	1.31	1.77
Cell division cycle 16 homolog	ES401190	0.84	-1.35	-0.79	0.33	-0.68	0.16
Cell division cycle 5-like	ES407204	-0.03	0.16	0.64	-0.40	-2.26	-0.28
Centrosomal protein of 104 kDa	ES393021	-0.08	-0.17	0.23	1.71	-0.71	0.04
Centrosomal protein of 63 kDa	ES389482	0.60	-1.30	-0.31	0.48	-1.15	1.32
Cholecystokinin receptor type A	ES402938	0.59	-1.15	-0.46	0.03	0.17	0.41
Chromosome 3 open reading frame 33-like	ES399544	-0.63	1.06	0.60			
Chromosome 8 open reading frame 74	ES397317	0.09	-0.31	-0.92	0.14	-1.11	-0.28
Cilia- and flagella-associated protein 20	ES736869	0.55	-1.05	-0.66	-0.28	0.64	0.62
Cingulin-like protein	ES387604	0.24	-1.75	-1.16	0.05	0.09	0.21
Cleavage and polyadenylation specificity factor subunit 5	ES738225	0.15	-1.28	-0.77	-0.21	0.75	0.23
Coactosin-like protein	ES403739	0.65	1.68	-0.10	0.67	0.25	0.16
Coiled-coil domain-containing 42A	ES404863	-0.60	-0.54	-0.85	-0.08	-1.25	0.52
Coiled-coil domain-containing protein 180-like	ES389679	1.18	1.17	0.51	0.73	-1.21	0.38
Coiled-coil domain-containing protein 92	ES393326	-1.36	0.22	-0.18	0.22	-0.08	0.04

Gene Annotation	EST	<i>Δ M. trossulus</i>			<i>Δ M. edulis</i>		
		8 h	32 h	56 h	8 h	32 h	56 h
Coiled-coil domain-containing protein KIAA1407	ES392865	-0.17	-0.52	0.41	0.31	-1.48	0.05
homolog	ES396905	-0.07	0.08	-0.17	0.13	-1.37	-0.33
Collagen α-5(VI) chain	ES396420				-1.11	-0.14	0.03
Collagen matrix protein	ES395514	1.16	-0.06	0.76	-0.22	-0.49	1.36
Collagen-like protein	ES388689	-0.78	0.25	-1.05	1.60	-0.71	0.06
Collagen, type XII, α 1	ES387923	4.16	-2.49	-0.91	-3.97	3.53	5.97
CREBRF homolog	ES400633				-1.31	1.75	1.85
Cubilin	ES402236	1.74	-1.08	-2.19	-1.15	1.35	1.50
Cytochrome P450 family 4	ES390213	-0.42	-1.80	-0.77	-0.21	1.05	-0.52
Cytosolic non-specific dipeptidase-like	ES407828	0.50	-1.91	-0.92	1.02	-1.10	0.70
DC-STAMP domain-containing protein 2	ES407446	-0.86	-0.60	-0.76	0.04	-1.38	0.66
Decaprenyl-diphosphate synthase subunit 2	ES406294				-0.42	-1.75	-0.33
Denticleless-like protein, partial	ES404886	0.95	2.33	1.30	0.20	-0.54	-1.00
Dermatopontin-like	ES737940	-0.34	0.64	-0.27	-0.18	2.56	-0.64
Dihydroliponamide dehydrogenase, mitochondrial	ES402318	-0.50	-0.57	-0.69	2.15	-0.15	0.74
Dipeptidyl peptidase 1	ES407270	0.11	-1.24	-0.57	0.66	0.91	1.75
Disks large-associated 4-like	ES401550	-0.01	0.70	1.05	-0.30	1.24	1.00
Disrupted in renal carcinoma protein 2-like	ES403934	0.38	-0.51	-0.09	-0.04	1.49	0.63
Disulfide Bond Formation Protein A	ES388967	0.51	0.07	-0.49	0.83	-1.03	0.06
DNA ligase 1	ES387991	0.45	1.75	0.52	-0.72	-0.19	-0.60
DNA polymerase delta subunit 3-like	ES405265	0.14	-0.05	-0.16	-0.05	-1.47	0.37
DNA-directed RNA polymerase III subunit RPC2	ES405893	-0.26	0.00	0.56	-0.38	-2.88	-0.59
DNA-directed RNA polymerases and III subunit RPABC5	ES392430	0.49	1.06	0.84	-0.59	1.15	0.50
DNAJ homolog subfamily C member 2	ES400455	0.26	0.06	-0.19	0.15	-1.16	-0.29
DNAJ homolog subfamily C member 28	ES403031	0.51	-0.03	-0.05	0.30	-1.58	0.05

Table B.1, cont.

Gene Annotation	EST	<i>Δ M. trrossulus</i>			<i>Δ M. edulis</i>		
		8 h	32 h	56 h	8 h	32 h	56 h
DNAJ-like protein subfamily B member 1	ES736575	0.62	-1.07	-0.23	0.10	-0.36	0.20
DNAJ-like protein subfamily B member 5	ES391035	1.21	-0.28	0.24	0.13	-0.38	-0.20
Dual specificity phosphatase 10	ES404209	1.97	-0.25	-0.06	-0.20	3.09	3.20
Dynein heavy chain axonemal-like	ES402972	0.46	0.06	-0.60	-0.20	-1.32	-0.26
Dynein intermediate chain 3, ciliary	ES396543	0.60	-1.62	-0.24	1.12	-0.39	-0.36
E3 ubiquitin-protein ligase TRIM33-like	ES737581				-0.16	1.50	1.16
E3 ubiquitin-protein ligase TRIM71-like	ES406092	0.20	0.37	0.66	-0.46	1.78	0.46
Ectonucleoside triphosphate diphosphohydrolase 3	ES398424	0.14	-0.11	-0.15	0.90	2.16	0.60
EF-hand domain containing family C2-like	ES403376	0.92	-2.29	-1.16	2.25	1.29	1.29
EH domain-containing protein 1	ES736195	-0.26	1.01	1.33	0.20	-1.72	0.41
Electron transfer flavoprotein subunit β	ES736201	0.28	-1.06	-0.63	0.44	-1.41	-0.15
Elongation factor 2	ES396413	1.04	1.04	0.70	-0.57	1.97	-0.06
Embryonic protein UVS isoform	ES392558	1.11	-0.26	-0.83			
Endo-1,4-β-glucanase	ES388612	-0.06	-1.29	1.48	-0.04	-0.75	0.31
Endoglucanase 4-like isoform	ES736810	0.40	-1.97	-0.11	0.57	-1.57	0.76
Enkurin	ES400756	-0.34	-1.51	-0.91	0.51	-1.04	0.34
Enoyl-CoA Hydratase 1	ES389454	0.17	-1.56	-0.85	-0.80	-0.28	-0.35
Ephrin type-A receptor 4-like	ES393341	-1.18	0.30	0.36	0.39	-2.62	-0.32
ESF1 homolog	ES404544	0.19	1.03	-0.55	0.20	-1.85	-0.37
ETS-related transcription factor Elf-3	ES391882	0.04	0.18	-0.62	-1.53	1.78	1.14
ETS-related transcription factor Elf-5	ES396917	-0.59	-0.13	-0.80	-1.15	1.33	0.65
Eukaryotic peptide chain release factor subunit 1	ES406217	1.07	0.70	0.40	-0.31	1.25	1.20
Eukaryotic translation initiation factor 3 subunit M	ES389519	-0.09	-0.27	-0.19	1.09	-0.14	-0.09
Exonuclease 3-5 domain-containing protein 1	ES389400	1.25	-0.72	0.09	-0.45	0.48	0.77
FACT complex subunit SSRP1-like	ES408118	-0.47	-0.34	-0.21	-0.43	-1.51	-0.11
FAD-linked oxidoreductase	ES388864	-0.09	0.17	-0.28	-1.16	0.25	-0.15
FAD/FMN-containing dehydrogenase	ES396002				-0.47	1.08	0.37

Gene Annotation	EST	<i>Δ M. crossiius</i>				<i>Δ M. edulis</i>			
		8 h	32 h	56 h		8 h	32 h	56 h	
FAM195A-like	ES738750	0.70	0.65	-0.32	-0.20	1.18	1.36		
FAM50A-like	ES401633	0.26	-0.21	-0.42	0.90	-2.55	0.15		
Fascin-like	ES399121	-0.29	-0.35	-0.10	1.01	-1.26	-0.98		
Fatty acid synthase	ES390199	1.97	-0.68	-1.66	-0.61	2.02	1.96		
FERM domain-containing 4A	ES397369	-0.53	0.21	0.33	0.37	-1.69	-0.11		
FGFR1 oncogene partner	ES391567	-2.47	-0.69	-0.66					
Fibrillin 2	ES400512	0.99	1.81	-1.82	-0.06	-1.18	-0.26		
Fibrinogen-related protein	ES388989	0.51	-1.02	-0.08	-0.71	-0.73	-0.62		
Fibrinogen-related protein 1	ES398931	2.14	0.41	-0.22	-1.51	-0.71	1.38		
FK506-binding protein	ES397774	0.53	0.74	-0.35	0.57	-1.39	0.31		
Fructose-bisphosphate aldolase	ES392199	-0.53	-0.68	0.06	1.29	0.03	0.51		
Glucosidase 2 subunit β	ES401553	-1.29	-0.57	0.76		0.69	-1.90		
Glutamate dehydrogenase, mitochondrial-like	ES401129	1.07	-0.19	-0.39	0.48	-0.62	0.46		
Glutaminyl-peptide cyclotransferase-like	ES395573	0.22	-1.30	-0.68	0.86	-0.62	-0.36		
Glutaminyl-tRNA synthetase	ES405047	0.53	-0.03	0.12	-0.14	-1.13	-0.06		
Glutathione peroxidase-like	ES737852	0.05	-1.51	-0.77	-0.35	-0.66	-0.26		
Glutathione S-transferase A	ES392983	0.01	-1.03	-0.32	-0.10	0.74	0.24		
Glycine amidinotransferase	ES389028	-0.66	-1.23	-0.61	0.23	1.49	-0.24		
Glycine N-acyltransferase-like	ES737323	1.96	-0.12	0.04	-0.42	1.52	0.53		
Glycogen phosphorylase, muscle form-like	ES402939	-0.19	-0.20	0.03	0.26	-2.11	1.55		
Glycogenin 1-like	ES401240	-0.53	0.06	0.15	0.28	-1.72	-0.13		
Glycosyl-phosphatidylinositol-linked carbonic anhydrase	ES390880	0.70	-0.20	-0.50	1.92	-1.71	-1.32		
Golgi to ER traffic protein 4 homolog	ES405790	0.47	0.15	-0.13	-0.10	1.91	1.11		
Growth arrest-specific protein 8	ES736616	-0.04	-1.23	-0.49	1.47	-1.28	0.05		
GTP-binding protein 128up-like	ES402518	-0.16	-0.63	-0.15	0.62	-1.01	-0.05		
GTP-binding protein 6	ES393211	-0.12	-0.50	0.11	1.06	-2.02	-2.20		

Table B.1, cont.

Gene Annotation	EST	<i>Δ M. rossius</i>			<i>Δ M. edulis</i>		
		8 h	32 h	56 h	8 h	32 h	56 h
GTP-binding protein SAR1b-like	ES401081	0.61	0.60	-0.71	0.15	1.50	2.41
GTPase IMAP family member 4	ES399752	3.33	-3.17	-3.64	1.25	0.23	-0.23
GTPase IMAP family member 4	ES736699	-1.04	1.09	0.85	-0.96	2.90	-0.30
GTPase IMAP family member 4-like	ES408072	-3.32	-4.18	0.18	-0.25	-3.04	-0.30
GTPase IMAP family member 7	ES737905	1.16	0.48	-0.41	0.94	3.08	2.24
HAUS augmin-like complex subunit 5	ES402242	0.37	-0.25	-0.48	0.34	-1.37	-0.30
HBS 1-like protein	ES390820	0.66	-0.70	-0.24	1.16	-0.48	0.36
Heat shock 22 kDa	ES737901	0.84	2.31	0.15	-0.33	3.84	3.73
Heat shock 70 kDa 12A	ES387872	0.39	-1.36	-0.86	-0.93	0.13	0.27
Heat shock 70 kDa 12A	ES394247	-0.39	-0.11	-1.08	1.31	-0.55	-0.49
Heat shock 70 kDa 12A	ES395102	1.24	-0.49	-0.20	0.74	0.14	-1.51
Heat shock 70 kDa 12A	ES402304	0.89	-1.77	-0.62	0.68	0.52	0.02
Heat shock 70 kDa 12A	ES404729	-0.17	-1.45	-0.85	-0.70	-0.43	-0.46
Heat shock 70 kDa 12B	ES396901	-0.15	-0.22	0.84	-0.03	1.43	0.69
Hepatic lectin-like	ES736490	2.12	-0.38	-4.49	-0.15	-0.89	0.04
Hexokinase-like	ES399106	0.31	0.14	0.11	-1.03	0.97	1.75
Histone deacetylase 1	ES395086	-0.30	-0.48	-0.17	1.20	-1.74	0.07
Histone deacetylase 11-like	ES390061	0.32	0.03	-0.06	0.77	-1.21	0.19
Histone deacetylase 2	ES396807	-0.15	1.12	0.92		-1.77	-0.25
Histone variant H2A.X	ES406464	-1.47	0.23	0.35	-0.09	0.28	1.12
Histone-lysine N-methyltransferase SMYD3-like	ES407929	0.69	0.81	0.01	-0.41	2.04	-0.31
HSP70-binding 1-like	ES738082	-0.34	1.39	0.32	-1.34	0.84	0.70
Hypothetical protein AC249_AIPGENE16517	ES402375	0.09	-0.24	-0.18	0.23	-1.61	0.19
Hypothetical protein JURDEDRRAFT_76257	ES736373	-0.17	-1.03	1.22	-0.76	1.49	0.08
Hypothetical protein CGI_10001623	ES391133	1.32	-0.83	-0.43	0.29	0.85	0.52
Hypothetical protein CGI_10002430	ES401558	1.35	-0.87	-0.67	-0.23	0.06	-0.04
Hypothetical protein CGI_10002666	ES406426	-0.34	-0.25	-0.25	0.53	-1.41	0.06

Gene Annotation	EST	$\Delta M. trossulus$				$\Delta M. edulis$			
		8 h	32 h	56 h	8 h	32 h	56 h		
Hypothetical protein CGI_10004737	ES404698	0.04	-0.55	-0.21	1.20	-1.92	-0.65		
Hypothetical protein CGI_10012213	ES738688	1.04	-1.11	-1.80	-1.91	1.50	1.71		
Hypothetical protein CGI_10015862	ES404684	0.37	0.54	0.00	-0.68	3.02	0.27		
Hypothetical protein CGI_10020519	ES392818	0.36	-0.27	0.33	-0.14	1.41	1.44		
Hypothetical protein CGI_10021274	ES390596	0.19	-0.64	-0.17	1.51	-1.83	-1.19		
Hypothetical protein CGI_10021607	ES394793				0.19	1.87	0.80		
Hypothetical protein CGI_10025483	ES390047				-0.46	1.50	-0.01		
Hypothetical protein CGI_10025670	ES401039	0.06	0.83	-0.14	-0.55	1.15	1.23		
Hypothetical protein CGI_10026086	ES737010	4.97	0.38	-0.30	-2.97		1.96		
Hypothetical protein CGI_10026724	ES400708	0.15	1.44	-0.78	0.11	-0.26	-1.75		
Hypothetical protein CGI_10027067	ES398521	-0.05	1.13	0.03	0.21	4.49	-0.17		
Hypothetical protein CGI_10028227	ES396575	1.34	0.22	-0.41	0.46	1.16	0.39		
Hypothetical protein LOTGIDRAFT_153720	ES392900	0.83	-0.39	0.48	-0.98	2.34	0.97		
Hypothetical protein LOTGIDRAFT_235629	ES736096	-0.31	-1.90	0.76					
Hypothetical protein NEMVEDRAFT_v1g223877	ES738512	1.04	-1.28	-0.77	0.19	1.12	0.88		
IgGfC-binding protein	ES395834	1.34	0.02	0.11	-0.37	0.05	1.22		
Immediate early response gene 5	ES398927	2.97	0.37	-0.33	-3.02	3.20	3.49		
Immediate early response gene 5	ES403261	2.15	0.40	0.43	-2.14	2.88	2.46		
Inhibitor of nuclear factor kappa-B kinase-2	ES737837	0.35	0.46	0.07	-0.72	2.35	1.67		
Inositol oxygenase-like	ES390575	2.44	0.87	1.62	-0.58	1.55	1.19		
Inositol-3-phosphate synthase 1-A-like	ES389624	1.22	1.23	0.62	-0.56	1.34	-0.25		
Integrator complex subunit 9-like	ES398773	0.33	-1.13	-0.35	-0.86	0.20	-0.03		
Interferon-induced helicase C domain containing 1	ES405654	0.04	-0.27	-0.87	0.41	1.44	0.01		
Interferon-induced protein 44-like	ES387521	1.03	-1.14	-0.70	2.43	-0.22	-0.73		
Interferon-induced protein 44-like	ES403777	0.53	1.11	0.17	1.93	-1.30	-1.94		
Interferon-induced protein 44-like	ES388783	0.06	-1.30	0.38					
Interferon-induced protein 44-like protein	ES392312	0.34	-1.46	-0.47	0.00	0.75	-0.13		

Table B.1, cont.

Gene Annotation	EST	<i>Δ M. trossulus</i>			<i>Δ M. edulis</i>		
		8 h	32 h	56 h	8 h	32 h	56 h
Interleukin-1 receptor-associated kinase 4	ES392643	0.17	-0.15	-0.83	-0.70	1.10	-0.12
Interleukin-1 receptor-associated kinase 4	ES396220	0.23	-0.36	-0.66	-1.23	2.02	1.17
Intraflagellar transport 52 homolog	ES403499	-0.21	-1.78	-0.29	0.58	-0.01	0.95
Kaplin-like	ES388522	0.20	-1.37	-1.45	-0.17	-1.36	0.44
Katatin p60 ATPase-containing subunit a-like 1	ES736003	-0.05	-0.09	-0.33	1.07	-1.36	-0.13
Kelch repeat and BTB domain containing 3	ES391287	0.25	-0.54	-0.38	-0.23	2.22	1.76
Kelch-like 24	ES398279	-0.18	-1.21	-1.39	-0.42	0.82	0.04
Kelch-like 24	ES393429	-0.18	0.10	-0.41	-0.28	2.62	1.18
Kruempel-like factor 5	ES400854	0.68	0.21	-1.49	-1.45	3.39	1.36
Kruempel-like factor 5	ES401242	0.77	0.32	-0.63	-1.01	3.28	3.38
L-threonine 3-dehydrogenase	ES404164	0.80	-1.31	-2.23	0.37	0.11	-1.10
Lactadherin	ES395418	1.32	-0.76	-0.24	-0.55	-0.68	1.08
Legumain-like	ES405286	0.15	0.44	0.19	0.17	1.79	2.14
Leucine-rich repeat-containing protein 1	ES391185	0.90	-1.07	-0.56	0.41	0.18	0.41
Leucine-rich repeat-containing protein 71-like	ES736082	-0.93	-0.20	0.70	1.88	-2.07	-0.36
LIM homeobox Awh-like	ES403037	0.29	-0.05	1.29	-0.78	1.53	2.04
Lipoma HMGIC fusion partner-like 3	ES396379	0.49	-0.16	-0.02	0.09	2.12	1.54
Lipoma HMGIC fusion partner-like 3	ES738711	-0.43	-0.14	-0.23	0.16	1.19	1.59
LPS-induced TNF- α factor	ES391212	1.24	-0.85	-1.30	-0.98	1.77	1.31
Lysyl oxidase-like	ES399301	0.07	-1.25	0.29			
Macrophage erythroblast attacher-like	ES395617	1.65	0.09	-0.25	0.20	-0.65	1.95
Macrophage migration inhibitory factor	ES389608	-0.51	-0.81	-0.91	-0.36	1.29	0.56
MAM and LDL-receptor class A domain-containing	ES401645	0.46	-1.56	0.06	-0.44	-1.23	0.86
Mammalian ependymin-related protein 1-like	ES399530	-0.29	-0.15	-1.35	-0.17	1.20	0.38
MAP kinase kinase 7-like	ES737087	0.64	-0.04	-0.45	-0.98	1.57	1.48
MAP kinase-interacting serine threonine-kinase 1	ES403802	0.35	-1.59	-0.11	-0.79	1.31	2.79

Gene Annotation	EST	<i>Δ M. trossulus</i>			<i>Δ M. edulis</i>		
		8 h	32 h	56 h	8 h	32 h	56 h
Neuropeptide FF receptor 2-like	ES736479	-0.22	0.35	0.33	-0.76	1.91	1.17
Neuropilin and tolloid-like protein 2	ES398585	0.29	-1.37	-1.07	-0.14	1.13	0.76
Neutral sphingomyelinase-like	ES406969	0.66	-0.78	-0.27	0.13	-2.13	-0.06
Nifu-like protein	ES405028	0.79	-0.15	-0.20	-0.07	1.55	1.15
Nuclear receptor coactivator 4	ES393648	0.17	-1.00	-0.01	1.00	-1.19	1.08
Nudix hydrolase 20, chloroplastic-like	ES403204	1.03	0.72	0.44	-0.77	2.22	1.30
O-Linked N-Acetylglucosamine (GlcNAc) transferase	ES388345	1.33	-0.81	-0.23	0.17	-0.42	0.38
Omega-amidase NIT2	ES406630	-0.03	-0.85	-2.60	-0.28	2.80	2.90
Organic cation transporter	ES397240	1.24	0.23	-0.09	-0.98	2.26	2.81
Ornithine aminotransferase	ES398776	0.68	1.43	0.26	-0.03	2.01	2.53
Ornithine decarboxylase	ES390663	0.12	-0.36	-0.05	0.01	-0.17	-0.11
Otoancorin	ES405413	0.43	0.02	-0.45	-0.10	-1.69	-0.13
Paired box Pax-6	ES737413	0.20	0.29	0.05	0.12	1.26	1.50
Paramyosin isoform	ES393486	0.85	-2.75	-0.12	-0.17	0.41	2.01
Peptidyl-prolyl cis-trans isomerase-like 4	ES400295	1.00	0.10	0.30	0.39	-1.29	-0.13
Peritrophin-1-like	ES736365	0.82	-0.39	-0.57	-0.49	3.31	2.01
Peroxisomal sarcosine oxidase	ES398370	1.12	-2.12	-0.43	0.11	0.20	1.21
Peroxisomal sarcosine oxidase-like	ES403913	1.02	-1.59	-0.45	1.10	-0.55	1.40
Peroxisomal sarcosine oxidase-like	ES405841	0.72	-0.20	-0.12	0.05	1.73	-0.44
Peroxisomal targeting signal 2 receptor-like	ES403315	0.86	-0.03	-0.05	-1.18	0.95	-0.05
Phosphatidylinositol-4-phosphate 5-kinase type-1 α -like	ES407462				0.03	1.30	-1.08
Phosphoenolpyruvate carboxykinase, cytosolic							
GTP	ES406074	1.02	-0.09	-0.11	-0.24	2.84	2.57
Phospholipase A2	ES388244	0.33	-0.81	-0.20	-0.90	-3.13	2.10
Plasma α -L-fucosidase	ES390967	0.05	-0.72	-0.33	-0.95	1.42	1.50

Table B.1, cont

Gene Annotation	EST	<i>Δ M. trossulus</i>			<i>Δ M. edulis</i>		
		8 h	32 h	56 h	8 h	32 h	56 h
Poly [ADP-ribose] polymerase 14	ES736599	1.25	-0.53	0.04	0.42	0.48	2.25
Poly [ADP-ribose] polymerase 15	ES395571	-1.10	-0.31	-0.30	-0.41	-0.33	0.45
Predicted uncharacterized LOC105328279	ES406213	0.52	-1.14	-0.43	0.15	-1.14	-0.50
Predicted: uncharacterized Clorf228-like	ES736398	0.64	-1.56	-1.17	0.52	-0.74	0.75
Predicted: uncharacterized LOC107332276	ES396006	0.35	-1.22	-0.10	-0.21	-2.93	1.45
Predicted: uncharacterized LOC585101	ES401884	-0.38	-1.51	-0.04	0.03	-0.30	1.10
Probable chitinase 3	ES393634	-0.30	0.17	0.51	-0.35	1.40	-0.54
Probable thiopurine S-methyltransferase	ES736764	0.56	-1.67	-0.75	-0.41	0.60	0.34
Probable tRNA N6-adenosine threonylcarbamoyltransferase	ES399685	-0.01	-1.84	-0.75	0.33	-0.32	-0.75
Profilin-2	ES387473	-0.27	0.47	1.31	0.75	-1.55	0.51
Prohormone-4-like	ES408019	0.10	-1.02	-0.03	-0.06	-0.15	-0.20
Proline iminopeptidase	ES394580	0.40	-0.68	-0.56	-0.07	1.74	0.65
Proteasome subunit β type-3	ES405577	0.09	-1.12	-0.75	0.21	0.07	-0.63
Protein FAM167A-like	ES395136	1.28	-1.23	0.48	0.13	-0.96	0.35
Protein odd-skipped related 2-like	ES394208	-0.45	-0.35	-0.59	-0.23	1.23	0.47
Protein-glutamine γ-glutamyltransferase K-like	ES397288	-0.61	-1.60	-1.48	0.64	-0.79	-0.62
Protein-glutamine γ-glutamyltransferase K-like	ES400107	-0.37	-1.44	-0.64	0.09	-0.91	-0.24
Protocadherin Fat 4	ES392101				-0.49	1.62	0.51
Putative C1q domain containing protein Mgc1q14	ES738896	1.24	-1.79	-0.86	0.29	0.75	0.88
Putative C1q domain containing protein Mgc1q18	ES737266	0.93	-1.32	2.00	0.61	0.41	0.26
Putative C1q domain containing protein Mgc1q31	ES389205	2.54	-0.03	-1.64	-0.53	-0.43	1.46
Putative Chondroitin 6-sulfotransferase	ES390801	0.49	-1.28	-0.74	-0.06	-0.19	-1.03
Putative flocculation protein FLO10	ES395754	0.65	0.24	-0.19	0.63	1.99	0.61
Putative fucosyltransferase A-like	ES736832	1.50	-0.18	0.17	0.37	0.59	-0.33
Putative period clock protein	ES407115	-0.86	-3.28	-0.72	1.24	-0.25	2.21
Putative transcription factor PML	ES393617	1.16	-2.19	1.09	-0.59	1.06	-0.73

Gene Annotation	EST	<i>Δ M. trossulus</i>			<i>Δ M. edulis</i>		
		8 h	32 h	56 h	8 h	32 h	56 h
MAX dimerization protein 1-like	ES390391	-1.30	-0.29	0.51	0.40	-0.82	0.43
Mediator of RNA polymerase II transcription subunit 15	ES390948	0.62	0.00	-0.20	-0.19	-1.91	-0.43
Mediator of RNA polymerase II transcription subunit 8	ES395088	-1.34	-0.29	-0.53	-0.31	0.68	-0.38
Meprin A subunit β	ES736080	-1.36	-4.55	-1.88	-0.09	0.84	1.16
Methylosome subunit pICln-like	ES391770	1.39	0.16	0.35	-0.70	1.04	0.42
Microfibril-associated glycoprotein 4-like	ES405313	0.10	0.35	0.10	-2.77	0.91	0.78
Mfmi-chromosome maintenance complex-binding	ES401829	0.51	0.25	0.38	0.45	-1.81	0.45
Mitochondrial-processing peptidase subunit β	ES389068	0.52	-1.13	-1.40	1.03	-0.97	0.37
Molluscan insulin-related peptide 5	ES403241	0.00	0.56	-1.45	-0.31	1.96	-0.07
Monocarboxylate transporter 5	ES399555	-0.40	-1.61	-0.22	-0.01	-1.04	-0.56
Monocarboxylate transporter 9	ES399317	0.40	0.50	0.56	-0.35	1.39	0.62
Monocarboxylate transporter 9	ES399930	0.32	-0.07	-0.02	-0.70	3.12	0.74
Muscarinic acetylcholine receptor M3	ES405934	-1.33	0.19	-0.09	-0.70	3.12	0.74
Myeloid differentiation primary response 88	ES397477	1.22	0.15	-1.35	-1.01	2.67	1.64
Myosin heavy chain kinase B-like	ES390014	0.29	1.39	-0.52	-1.34	0.03	3.52
Myosin light chain smooth muscle	ES403089	0.55	-0.04	0.06	-0.85	1.17	0.32
Nacre protein	ES736092	0.33	-3.41	0.27	0.53	-1.56	0.39
NAD-dependent deacetylase Sirtuin-6-like	ES407031	0.72	-0.04	0.26	-0.07	1.90	0.46
NADH dehydrogenase [ubiquinone] iron-sulfur 2, mitochondria	ES387576	-0.93	-0.59	-0.01	1.14	-1.47	-0.07
NC-domain containing protein	ES388358	1.24	-0.51	-0.47	-1.01	1.23	1.79
NC-domain containing protein	ES387918	0.19	-1.34	-0.22	0.48	-0.24	0.24
Neuromedin-U receptor 2-like	ES395902	0.13	0.33	-0.10	-1.25	2.60	1.51
Neuromedin-U receptor 2-like	ES399934	0.92	-0.70	0.20	0.03	1.72	1.69
Neuromedin-U receptor 2-like	ES404599	0.11	-1.07	-0.70			

Gene Annotation	EST	<i>Δ M. trossulus</i>			<i>Δ M. edulis</i>		
		8 h	32 h	56 h	8 h	32 h	56 h
Putative upstream transcription factor 2/L-myc-2	ES396847	0.12	-2.53	0.11	0.61	-0.10	2.59
Pyridoxal phosphate phosphatase PHOSPHO2-like	ES403565	-0.02	-1.06	-1.32	0.15	-1.21	-0.94
Rab9 effector protein with kelch motifs	ES394899	0.18	1.68	0.53	0.47	-0.97	0.40
Radial spoke head 10 homolog B	ES393948	-0.07	-1.24	-0.90	0.38	-0.83	-0.87
Radial spoke head 14 homolog	ES393888	0.63	-1.23	-0.19	0.85	0.41	0.56
Radial spoke head protein 4 homolog A-like	ES399619	0.18	-1.49	-0.35	0.79	-0.40	0.43
Radial spoke head protein 4 homolog A-like	ES399903	0.42	-1.11	-0.38		0.88	0.65
Ras-related C3 botulinum toxin substrate 1	ES398459	-0.36	-0.45	-0.08	-0.06	2.15	0.06
Ras-related RAB-21-like	ES401061	0.02	-0.21	-0.52	0.59	1.59	1.51
Repressor of yield of DENV protein homolog	ES389185	0.55	-0.28	-0.95	1.16	-1.36	-0.17
Retinol dehydrogenase 13-like	ES737513	0.25	-1.36	-0.36	-0.04	0.94	-0.69
Rho GTPase	ES397042	0.04	1.15	0.59	-1.00	1.05	0.30
Rho-related GTP binding protein	ES389122	0.29	-0.02	-0.07	0.56	1.88	0.10
Ribosomal RNA processing protein 1 homolog B	ES401948	-0.25	0.51	0.66	-0.05	-1.44	-0.22
Ribosomal RNA-processing 8	ES408031	1.45	0.28	-0.60	-0.32	0.19	0.87
RING finger 207-like	ES737107	1.19	-0.50	-0.16	1.09	3.04	3.27
RNA polymerase II-associated factor 1 homolog	ES407877	0.46	-1.27	-0.13	0.54	0.39	0.10
RNA-binding protein 8A	ES396869	0.13	-1.75	-0.25	-0.76	-0.35	0.01
Sarcoplasmic calcium-binding protein	ES390981	-0.48	2.54	1.49	-2.78	2.83	1.09
Selenocysteine insertion sequence-binding protein	ES392827	0.13	-1.00	0.15	-0.79	-2.42	-0.40
Selenocysteine insertion sequence-binding protein	ES395733	-0.09	0.20	-1.02	-0.28	-1.55	-0.34
Septin 11-like	ES390789	-0.01	-1.39	-0.64	-0.38	-0.06	0.62
Serine arginine repetitive matrix 1	ES387568	-0.01	0.40	-0.07	-0.40	1.44	-0.28
Serine threonine-protein phosphatase 2A 65 kDa regulatory subunit A α isoform-like	ES399457	-0.14	-1.28	-0.06			

Gene Annotation	EST	$\Delta M. trossulus$			$\Delta M. edulis$		
		8 h	32 h	56 h	8 h	32 h	56 h
Serine threonine-protein phosphatase 2A catalytic subunit β isoform	ESS393345	-0.07	-0.74	-0.40	1.61	-1.65	1.14
Serine threonine-protein phosphatase 2A regulatory subunit B subunit α -like	ES399943	0.57	-1.07	0.16	-0.26	-0.53	0.13
Serine-threonine kinase receptor-associated Serine/threonine-protein kinase PIM-1	ESS395470	-0.07	-1.31	-0.72	0.78	-0.91	-0.08
Serrate RNA effector molecule homolog	ES400777	1.36	-0.88	-0.46	-0.41	1.31	1.54
Serum response factor-binding protein 1	ESS387933	-0.12	-1.21	-0.75	-0.41	-1.03	-0.86
SH3 domain-containing 19-like	ES394037	1.18	0.34	0.18	0.05	1.71	-0.33
Shell fibrous prismatic pertucin-like protein 1	ESS392325	-0.17	0.01	-0.77	1.12	-2.09	-0.26
Short-chain collagen C4-like	ES393785	0.82	-0.46	-0.42	-1.26	0.08	1.04
Sodium- and chloride-dependent glycine transporter 2	ES393629	-0.57	-0.74	0.05	-1.83	-0.14	-0.28
Sodium- and chloride-dependent glycine transporter 2	ES392996	-0.09	-0.95	0.44	-0.31	2.23	1.06
Sodium-coupled monocarboxylate transporter 2	ES406746	0.19	0.25	-1.64	-0.13	-2.57	1.31
Sodium-coupled monophosphate transport 2C	ES406210	0.07	0.33	0.33	0.12	1.31	0.49
Sodium-dependent phosphate transport 2C	ES405063	0.91	0.26	0.45	-1.66	2.09	1.13
Sperm associated antigen 6	ESS390965	1.47	-1.49	-0.13	1.15	-0.43	1.26
Spermatogenesis-associated protein 17-like	ES736540	0.06	1.76	-1.02	0.86	0.04	0.37
Steroid 21-hydroxylase-like	ESS392824	-0.55	-1.72	-0.02	-0.24	-0.23	0.36
Structure-specific endonuclease subunit SLX1-like	ES394284	-0.69	1.10	0.17	0.11	-0.40	0.54
Succinyl-CoA ligase subunit α , mitochondrial	ES407882	0.10	-0.44	-0.31	1.46	0.40	0.18
Sulfatase-modifying factor 1	ES401926	0.08	0.48	0.51	1.29	-0.85	-0.76
Sulfate transporter-like	ES402542	-0.40	-0.60	-0.26	0.12	-2.16	0.12
Suppressor of cytokine signaling 2	ES389869	1.10	-0.88	-1.22	-1.34	2.03	1.44
Sushi, von Willebrand factor type A, EGF and pentraxin-domain-containing 1	ESS394376	0.38	0.17	-0.11	-0.58	1.02	1.21

Gene Annotation	EST	<i>ΔM. trossulus</i>			<i>ΔM. edulis</i>		
		8 h	32 h	56 h	8 h	32 h	56 h
T-box transcription factor TBX20	ES391202	0.45	0.50	-0.20	1.36	-0.52	0.10
T-complex 1 subunit β	ES394536	0.56	-1.06	-0.71	0.18	-0.52	0.23
T-complex 1 subunit γ	ES396475	0.44	-0.91	-0.81	0.26	-1.25	-0.32
T-complex-associated testis-expressed protein 1	ES392233	0.81	-1.19	-0.24	1.34	-0.70	-0.15
Taurine transporter	ES389919	-0.11	-0.19	0.80	-0.13	-1.13	0.75
Tax1-binding protein 1-like protein B	ES406310	0.36	1.04	-0.43	-0.58	-3.61	1.58
TCTEX1 domain-containing protein 1-like	ES738040	1.79	-2.37	-1.36		2.82	2.92
Tektin 1	ES387718	1.30	-1.70	-0.44	1.69	-0.01	0.40
Tektin 3-like	ES391485	0.37	-1.20	0.27	0.49	0.51	0.90
TenA family transcriptional regulator	ES394888	-0.55	-0.26	0.98	1.04	0.64	-0.36
Testis-specific serine threonine-protein kinase 4	ES405351	0.19	-0.08	-0.16	-0.65	-1.82	1.21
Tetrahicopeptide repeat protein 29	ES390818	1.43	-1.49	-0.34	-0.34	-1.03	0.23
Thioredoxin domain-containing protein 6	ES737884	0.01	-0.52	0.13	-0.03	-1.87	-0.56
Tissue inhibitor of matrix metalloproteases	ES735948	0.06	-0.71	0.20	1.92	-0.13	0.04
TKL protein kinase	ES394880	1.47	-0.95	1.65	0.76	4.05	1.42
Toll-like receptor 1	ES392193	0.38	-0.09	0.09	0.23	-2.74	-0.88
Toll-like receptor 4	ES395520	0.59	0.33	-1.15	-0.38	1.48	0.34
Toll-like receptor N precursor	ES401264	1.75	-0.51	0.43	-1.01	0.78	-0.04
Trafficking protein particle complex subunit 3-like	ES737617	1.27	0.02	-0.34	-0.37	0.10	0.27
Transcription elongation factor B polypeptide 2	ES736552	0.37	-0.22	0.75	0.18	1.81	0.24
Transcription factor AP-1-like	ES398057	1.15	0.08	-0.17	-1.90	1.59	1.61
Transcription factor SOX-11-like	ES402468	-0.29	0.39	0.41	0.20	1.62	1.60
Transcription factor SPT20 homolog	ES390404	0.52	-1.16	-0.72	0.19	-0.90	-0.88
Transcription initiation protein SPT3 homolog	ES403797	0.32	-1.49	-1.34	1.95	-0.02	-0.12
Transforming growth factor-β-induced ig-h3	ES738897	-0.60	-3.96	-1.10	-0.54	-0.45	0.07

Table B.1, cont

Gene Annotation	EST	<i>ΔM. trossulus</i>			<i>ΔM. edulis</i>		
		8 h	32 h	56 h	8 h	32 h	56 h
Transgelin-3	ES404447	-0.44	1.22	-0.27	-0.10	1.42	-1.14
Transitional endoplasmic reticulum ATPase-like	ES736295	0.37	-1.06	-0.40	0.39	0.08	0.28
Tribbles homolog 2	ES404503	1.63	-0.31	-1.22	0.42	1.12	1.08
Tribelix transcription factor GTLL1-like	ES405853	-0.44	-1.50	-0.76	0.20	-0.53	-0.32
Tripartite motif-containing protein 2	ES392463	0.48	-0.89	-0.29	1.56	-2.35	-0.87
Tripartite motif-containing protein 2	ES398748	1.44	-0.35	0.43			
Tripartite motif-containing protein 33	ES388035	0.08	-1.14	-0.10	-0.03	-1.31	-0.11
Tripartite motif-containing protein 33	ES392912	-0.12	-0.20	0.30	-0.03	-2.68	-0.42
Tripartite motif-containing protein 33	ES394127	0.26	-0.13	-0.39	-1.15	-0.05	0.24
Tripartite motif-containing protein 45	ES390358	1.70	-0.31	-0.31	-1.95	5.94	4.93
Tripartite motif-containing protein 45	ES392512	1.67	-0.62	-0.45			
Tripartite motif-containing protein 45	ES395244	0.12	-0.17	0.25	0.33	2.51	-0.32
Tripartite motif-containing protein 45	ES398872	0.27	-0.67	0.08	1.28	-1.22	
Tripartite motif-containing protein 56	ES390324	1.33	-1.25	-1.13	0.90	2.14	1.90
Tripartite motif-containing protein 56	ES390728	1.74	-1.40	-1.19	0.61	-0.02	0.17
Tripartite motif-containing protein 56	ES736329	0.78	-1.58	-0.59	-0.64	-0.54	0.29
Twist-related protein 2	ES404061	0.04	-0.09	-0.09	-0.05	1.34	-0.17
U1 small nuclear ribonucleoprotein 70 kDa-like	ES389036	-1.08	-0.07	0.56		-0.94	-1.17
Ubiquitin-60S ribosomal L40	ES395550	-0.26	0.04	0.27	0.30	-2.61	-0.54
Ubiquitin-like modifier-activating enzyme 5	ES397693	0.70	0.57	0.03	-0.13	1.76	1.30
Ubiquitin-like modifier-activating enzyme ATG7	ES396673	0.02	1.12	0.20	-0.43	0.48	-0.32
UBX domain-containing 1	ES735895	-1.17	-0.53	0.19	-0.22	-1.07	0.41
Uncharacterized protein APZ42_034416	ES392254	0.42	-1.92	0.21	1.40	0.54	0.73
UPF0488 C8orf33 homolog	ES401368	0.62	-0.55	-1.00	0.15	-1.80	-0.30
UPF0686 c11orf1 homolog	ES404324	0.51	-1.37	-1.20	0.08	0.42	-0.03
V-type proton ATPase subunit B	ES389258	0.18	-1.15	-0.89	-0.05	1.58	1.74
Vasohibin-1-like	ES407681	1.35	-0.89	-0.28	-0.19	0.75	0.88

Table B.1, cont

Gene Annotation	EST	<i>Δ M. trossulus</i>			<i>Δ M. edulis</i>		
		8 h	32 h	56 h	8 h	32 h	56 h
Vitelline membrane outer layer 1 homolog	ES736708	0.73	2.69	-0.04	0.13	-5.41	0.28
Vitelline membrane outer layer protein 1 homolog	ES390800	0.17	-1.17	-0.01	-0.29	-0.46	-0.88
Von Willebrand factor A domain-containing	ES405319	0.75	-1.49	-0.09	-0.08	-0.78	0.89
WD repeat-containing protein	ES406101	-0.22	-0.46	-0.65	-0.47	-1.75	-0.76
WW domain-containing oxidoreductase	ES737613	0.36	-0.52	-0.35	1.51	0.35	0.22
YEPF4-like	ES405101	0.56	0.20	-0.52	-0.78	1.40	0.12
Zinc transporter ZIP1	ES395192	1.43	-0.98	-0.85	0.19	-0.56	0.67
Zygoter arrest protein 1	ES398848	0.93	-0.05	-0.09	0.18	1.98	0.76

Gene	Primer Name	Sequence (5' - 3')	T _m (°C)	Comments
<i>BHMT</i>	BHMT FOR1	GAACGTTTGAAGAATGGAGAG	51.4	Worked better in <i>M. edulis</i>
	BHMT FOR2	GCTGAGGGTTACATGTGGAA	57.1	
	BHMT FOR3	TCAAGGAACAAGTAGAATGGGC	54.9	Did not work with BHMT REV3
	BHMT REV1	TTCTGGTCCCAATAATGACTG	52.2	
	BHMT REV2	TGCCAACTGTCGAATGTCTGAAC	57.5	qPCR reverse primer
	BHMT REV3	GCACTACTGGACCCTG	55.3	
	BHMT Q1F	CGTCGTCTTGAAGAGGCTGG	57.9	qPCR forward primer
<i>TAUT</i>	BHMT Q1R	AGCGGGTACACCAATTGCCG	60.7	Not for pairing with BHMT Q1F
	TAUT FOR	TTTCAGGGCATAGGATTTGC	53.1	
	TAUT FOR2	TATAGGAATGGAGGAGGACATT	55.0	
	TAUT FOR3	CAGGGAGGTGTCAGTGCTTG	58.1	
	TAUT FOR4	AGAGGGCGGAATGTAITATTTC	54.7	
	TAUT FOR5	GGCGATCTTCACTCCCCCTTT	57.4	qPCR forward primer
	TAUT REV	TCCTCAACGTCCTGCAGTGAC	57.1	
	TAUT REV2	ACGTCCTGCAGTGACGTTGGC	60.6	
	TAUT REV3	AGAGGGCTAGGTCCCACTTGAT	59.6	
	TAUT REV4	GAACCTTAAGGCCAATATCCCAACC	53.8	qPCR reverse primer
	TAUT REV5	CTTGCAAGCGTGGCATGTG	58.0	
	TAUT REV6	GTTTCCTGCCTGGGTAAGAATG	55.9	
	TAUT REV7	GCTGTGGATAGATCTTTACC	52.5	

Table B.2. Table of primers developed for *BHMT* and *TAUT*. Sequencing and qPCR primers used to obtain sequence in *M. edulis* for betaine-homocysteine methyltransferase (*BHMT*) and taurine transporter (*TAUT*) are listed with comments and the corresponding annealing temperature (T_m).

Gene	Primer Name	Sequence (5' – 3')	T _m (°C)	Comments
	40S RBP F1	GGAAGTCAGTCCCGTGGATGT	60.0	
	40S RBP F2	GACCAAGGAGGACTGGTGAA	60.1	
	40S RBP F3	TCACGAGGATCAGCATGAAG	59.9	
	40S RBP F4	ACAAGCAAGGATTCCCAATG	59.9	
	40S RBP F5	TACCGCTGACAGTCTTGGTG	59.9	qPCR forward primer
40S	40S RBP R1	TTTCACCTGCAAGTGGTCTGC	60.0	
	40S RBP R2	CATTGGGAATCCTTGCCTGT	59.9	
	40S RBP R3	AAGGCCCTGGGATGTCTTTT	59.9	
	40S RBP R4	ACATCCACCGGACTGACTTCC	60.0	qPCR reverse primer

Table B.3. Table of primers developed for 40S. The qPCR and sequencing primers for 40 S ribosomal protein (40S) are listed with the corresponding annealing temperature (T_m).

Gene	Primer Name	Sequence (5' – 3')	T _m (°C)	Comments
	OAT FOR1	GTCAGAACCAATCGCCACACA	55.6	
	OAT FOR2	GCTCATAATTATCACCCTTACC	43.4	
	OAT REV1	GTATGTCCCAAAGCCAGCAT	55.4	
	OAT REV2	CAGCATAACTAGGAAGGCTGT	53.9	
	OAT Q1F	TGTCATCCAAAGATTGTCAAGC	53.5	
<i>OAT</i>	OAT Q2F	CAAGGACATTGTCAATCCAAAGA	53.1	
	OAT Q3F	CATTGTCATCCAAAGATTGTCAAGGC	56.8	qPCR forward primer
	OAT Q4F	AGAGCATTTCTACAATGATGTTGGG	57.2	
	OAT Q1R	TCCTGGCTAATTTACAGGCTGT	56.1	Used for <i>M. galloprovincialis</i> qPCR
	OAT Q2R	ACCAGCAGCAAACACAATCT	55.2	qPCR reverse primer

Table B.4. Table of primers developed for *OAT*. The qPCR and sequencing primers for ornithine aminotransferase (*OAT*) are listed with the corresponding annealing temperature (T_m).

Gene	Primer Name	Sequence (5' – 3')	T _m (°C)	Comments
<i>ODC</i>	ODC 1L	GATATATGAATATGGAATTTGG	44.4	
	ODC 2L	CTATAGGCAACCTTGGTGA	51.4	
	ODC 3L	CGATATACCAAGAGAAAACCAACC	53.6	
	ODC 4L	TGAATATGGATTTGGAAAACAACA	51.4	
	ODC 5L	GACTGTGCAAGTAAAGGCTG	53.6	
	ODC 6L	AATATGCTGCTGATAATGGAGTC	52.8	
	ODC 7L	GTTCCGATGTCACCCG	53.0	
	ODC 8L	GGAAAGTGGCTGTTTAGAAGC	53.7	
	ODC 1R	AATCCCCCACCAGATGTC	54.4	
	ODC 2R	CGGGTGACATCCGAACTT	54.8	
	ODC 3R	CCCACCGATGTCAAGGAT	54.5	
	ODC 4R	GCTAGCAGTCTAATTACAGGATA	51.5	
	ODC 5R	AGTGACTCCATTATCAGCAGC	54.6	
	ODC 6R	CATCCGAACCTTCTCCCCA	54.4	
	ODC 7R	CGTCTTGACTGCTCTATCG	52.5	
	ODC1 11L	GCTGTTTAGAAGCCGG	50.4	
	ODC1 12L	ACGTGTATTTGATTTAGGCCCTCTC	54.9	
	ODC 6L2	GATGAAAATTGTAAAAGGTCAAAAGC	50.7	
ODC 9L	GACCAACATGTGACG	46.9		
ODC 10L	CATGCCAGAAATGTAACCTTC	49.3		
ODC 3R1	CGTCACATGTTGGTCCCCAT	57.7		
ODC 3R2	GTGTGTAGGCTCCCATGTCT	56.6		
ODC Q1F	AATGGCATGCCAGCACCAA	58.5	qPCR forward primer	
ODC Q1R	TTCGGGTTAAACTTCAGGGTTTC	55.3	qPCR reverse primer	

Table B.5. Table of primers developed for *ODC*. These primer sets target multiple ESTs out of the *M. californianus* database. Primer 6L2, 9L, 10L, 3R1, and 3R2 were used to obtain sequence information and match the EST used by Lockwood and Somero (2011).

Gene	Primer Name	Sequence (5' - 3')	T _m (°C)	Comments
<i>CaM</i>	CAM FOR	ATGGCTGATCAGCTGACA	53.8	Used for <i>in situ</i> hybridization
	CAM REV	CGTTGTTTTCATTTATTTGTCATCAT	51.4	Used for <i>in situ</i> hybridization
	CAM Q1F	ATGGCTGATCAGCTGACAGAAGA	58.1	qPCR forward primer
	CAM Q1R	TCGTAACTCATCCCTCATTTGTCAC	54.4	qPCR reverse primer
<i>CAML1</i>	CAML1 FOR1	GCTGAGGAGTGTGTTAGAGCGGGAA	63.8	
	CAML1 FOR2	GAGAACCGCTATGCATCTGGCCAA	59.6	
	CAML1 REV1	TTCCGTCATACCATATCCCTGGCCGAC	61.8	
	CAML1 REV2	TGTCGCTCACCATCTGTGTCTGC	61.2	
	CAML1 FOR3	TGACCATTGAAAAAACCATGCAAGC	57.0	
	CAML1 FOR4	GCAGGTGATATATCGAAAAGTCAA	52.6	Missing a thiamine residue
	CAML1 QF1	GAGGAGTGTGTTAGAGCGCG	56.6	qPCR forward primer; <i>in situ</i> primer
	CAML1 QR1	TGCTTTTCTGTCCATACCATACTCT	50.9	qPCR reverse primer
	CAML1 REV3	ATGGATACAAAATAGATCATATTTCCG	51.5	Used for <i>in situ</i> hybridization
	CAM DEG1F	GACGGAAATGGAACARIMGATTT	53.5	
CAM DEG2F	GTRRRYGAATAAGGATGTAATGG	52.2		
CAM2 1R	TTCTGCCCGCACTTATAAATCC	53.0		
CAM2 1L	TGGACGGAAAATGGAACAG	52.3		
CAM2 2L	GCCTATGATGGCAAGGAAAAATG	54.5		
CAM2 NR	CATTTTCATCTACTTCTTCGTCCG	53.4		
CAM2 F	TTTGACCAAAAGATGGCGGATGG	53.5	Overlap in <i>CaM</i>	
CAM2 3L	AAAAGCTCATATGGACGATATAGT	51.1		
CAM2 3R	CTTCATTTGGCCGTCATCAT	53.3		
CAM2 4L	TTTCATCTACGATACAGCCATG	52.0	Used for <i>in situ</i> hybridization	
CAM2 5L	AAACAGAAAAAACCAAAAGCTCATATG	50.5		
CAM2 4R	TGGCCGTCATCATTTGTCAC	56.5	Used for <i>in situ</i> hybridization	
CAM2 Q1F	AACGCAGACCAGGTGATAGC	57.3	qPCR forward primer	
CAM2 Q1R	CGAAGTTCCTTCTTCACTATCAAGTG	53.2	qPCR reverse primer	

Table B.6. Table of primers developed for *CaM*, *CAML1*, and *CAML2*. The sequencing primers, two degenerate primers, and the

qPCR primers are listed for calmodulin (*CaM*) and the two calmodulin-like genes, *CAML1* and *CAML2*. The annealing temperature

(T_m) for each of the oligonucleotide sequences are reported, as well as any comments on the primers.

```

1                                     50
C. gigas      ~~~MATKGLV ERLKNGEDIL IAEGYMWELE RRGYLTAGGF IPEIVLDNPE
M. edulis    ~~~~~
M. californianus MKKMSTRGLV ERLKNGE CIL NAEGYMWEFE RRGYLKAGAF IPEVVLEKPE

51                                     100
C. gigas      VVRALHMEFI HAGTDVIEAF TYYGHREKLR TIGREDDLEK LNRVALQMAK
M. edulis    FIRQMHLEFV HAGTDVVEAF TYYGHREKLR LIGREDDLEK LNRIALKIAR
M. californianus LIRQMHLEFV HAGTDVVEAF TYYGHREKLR LIGREDDLEK LNRIALKIAR

101                                    150
C. gigas      EVARENGKLL AGGICNSGIY DPQDESTFAA VTAMFKEQIE WAVEYEVVDYI
M. edulis    EVADETGTLM AGGICNTGIY VVGDEEASNK IREMFKEQVE WAVEEKADFI
M. californianus EVADETGTLM AGGICNTGIY VAGDEEASDK IRAMFKEQVE WAVEEKADFI

151                                    200
C. gigas      IAETFNDLGE AMLALKAIQQ YGKGVPAVIT MTAYIPDMMT DDVPFPEACR
M. edulis    IGETFNDLGE GLLALEAIKK YGNGVPAVIT LTPYIPDETT DDVPFPEACR
M. californianus IGETFNDLGE GLLALEAIKK YGNGVPAVIT LTPYIPDETT DDVPLPEACR

201                                    250
C. gigas      RLEEAGAAVV GVNCGRGPRT MLPLVKEIKK VCKGPVAMPL VTFRCRDNCR
M. edulis    RLEEAGADV V GINCGRGPRT MIPLLREIKK VCQGPVAAMP VPFRTTDDHR
M. californianus RLEEAGADV V GINCGRGPRS MLPLLREIKK VCQGPVAXMP VPFRTTDDHR

251                                    300
C. gigas      TFQSLRDPET GKYLSPARLS SRKPLYPTDL EAARCSRSDI RSWAEEAKAA
M. edulis    TFQSLLDPET G~~~~~
M. californianus TFQSLLDPET GK..... ..SLYPLDL ACAMCXRSDI RQFATEAKEN

301                                    350
C. gigas      GINYIGLCCG NASFYFRELA EAYGRKPPTS KYTPNVGLSH VFGKTSEADK
M. edulis    ~~~~~
M. californianus GIEYIGLCWR NAPNYFRELP QXMEERTIK .VFPRLSQSF ILGEKLI...

351                                    367
C. gigas      YKRSTKIKEF MIGKDNA
M. edulis    ~~~~~
M. californianus .....KIF Q~~~~~

```

Figure B.1. Multiple sequence alignment of *BHMT* in bivalves. The sequence alignment shows the similarity of *BHMT* in *M. californianus* and *C. gigas*, as well as the overlap for the 260 amino acids that we have sequenced in *M. edulis*. Areas where we observed differences in the amino acid sequence are shown; changes in *C. gigas* are shown in blue, while the variation between *M. edulis* and *M. californianus* are shown in orange and red, respectively. There is a conserved metal binding domain that is highlighted in gray. The sequences highlighted in blue are areas we targeted from probe development in *M. californianus*.

Gene	Primer Name	Sequence (5' – 3')	T _m (°C)	Comments
<i>DPT</i>	DPT FOR1	GAGGACAGAAAGATTCCAGGTTTAATG	53.9	
	DPT FOR2	ACTGGTATAAACCAGCATCCATGACAA	56.5	
	DPT REV1	GAATGTGTACTGGAAACACCCTCT	54.7	
	DPT REV2	CCAGCTGTATTGTGATCTTC	53.2	Used to obtain sequence information
<i>SCBP</i>	SCBP FOR1	TACCCCTATGCCGACGAA	55.5	
	SCBP FOR2	GAGTTCTTGCAGGAAAAAATG	49.7	
	SCBP REV1	GCCCTCGTTGTCATGACC	53.4	qPCR reverse primer
	SCBP REV2	CCCAGCCTTGTATGTTTC	50.7	
<i>TCTEX</i>	SCBP Q1F	GGAGCATGGTGGAGAAATACA	59.6	qPCR forward primer
	SCBP Q1R	AGTCTTGTCTGTATCCAGAATGC	54.5	
	TCTEX FOR1	GTCGAGGCACCTAAAGCAGCATCA	59.5	
	TCTEX FOR2	GAACCCAGCAGCCAAAGTGTACAGTA	56.5	qPCR forward primer
<i>TCTEX</i>	TCTEX REV1	ATATCCCAATTCTTTCACACAGTT	52.6	
	TCTEX REV2	GTTTGTCCCAATCATAACATTACAGA	52.0	
	TCTX Q1F	TCTCAGGAACCTTCATTAGGCCGC	59.0	Did not amplify with Q1R
	TCTX Q1R	TGTTTCGCACACAATTTCTGATC	54.2	qPCR reverse primer

Table B.7. Sequencing and qPCR primers for *DPT*, *SCBP*, and *TCTEX*. For each gene, the name of the primer, the 5' to 3' oligonucleotide sequence, and the annealing temperature (T_m) are listed. For sarcoplasmic binding protein (*SCBP*) and T-complex testes specific protein (*TCTEX*) the qPCR primers are listed, as well as any comments about the function of the primers.

159
aggtttaa atgcaacaattatggcatagtagttggtatgcagatcctccatcaccacat
R F K C N N Y G I V V G M Q I L H H H H

219
ttggaggacagaagattcaggtttaa atgcaacaattatggattcatagttggtatgcag
L E D R R F R F K C N N Y G F I V G M Q

279
agcatccatcacaaccactatgaggacagaagattcagatttaa atgttgctcaattgct
S I H H N H Y E D R R F R F K C C S I A

339
ggaaaggatccttagtcagtggtcataaaaccttcaggaatcagtttgacaaaccaataca
G K D L S Q C H K T F R N Q F D K P N T

399
gtgcatgtaccaactggttccggttgtaaga
V H V P T G S V V R

Figure B.10. Partial nucleotide and amino acid sequence for *DPT* in *M. edulis*. The nucleotide and amino acid sequence of *DPT* only covers a portion of the gene from nucleotide 159-429, which is roughly 530 bp in *Haliotis diversicolor*. There is very low sequence homology between our sequence and *DPT* in other invertebrates.

405
atcacacgtgctgacggttgattacacactcaagaaattccctcttgtagaaggcataagc
I T R A D V D Y T L K K F P L V E G I S

465
aaatctaagggaaagttggaatgcgctaaaatagaagcatggtgggagaaatataatcctt
K S K G K L E C A K I E A W W E K Y I L

505
aaagggaaataataaaattaccaaggttgacctcttaaaagatttagagaaagggatatacc
K G N N K I T K V D L L K D L E K G Y T

565
gaaaacaagaaaaacttwatcgcaaaaatgaaagccttgtgtgaagacattatgtgatt
E N K K N X I A K M K A L C E D I I C I

615
ctggatacagacaagactaaaatgatttcactggataactacgtcaaggcatataaggta
L D T D K T K M I S L D N Y V K A Y K V

675
tatggtcatgcaacgaggcc
Y G H A T R

Figure B.11. Partial nucleotide and amino acid sequence for *SCBP* in *M. edulis*. The nucleotide and amino acid sequence of *SCBP* only covers a portion of the gene from nucleotide 405-607; the predicted *SCBP* in *C. gigas* is roughly 500 bp. There is high homology between the *M. californianus* and *M. edulis* sequences but <40% similarity at the amino acid level in other species.

201
tctagaacgagtatctcaggaacttcattagggcgccaaacttgtgataccagtcaaaata
S R T S I S G T S L G A K L V I P V K I

261
caaaacacgtatagactagaacctcaacaaacggagaaatttaacgcagaatcggttcaa
Q N T Y R L E P Q Q T E K F N A E S V Q

321
aaaatgatgactggagttttgtcatcttattttggacggcgaagtttatgatcagaaattg
K M M T G V L S S Y L D G E V Y D Q K L

381
tgtgcgaaacattctcaagaattgtcggatgtaattaaacgtgtaaaggaattagga
C A K H S Q E L S D V I K K R V K E L G

441
tttcctaggtataaaactagtctgtaatgttatgattggacaaaacc
F P R Y K L V C N V M I G Q N

Figure B.12. Partial nucleotide and amino acid sequence for *TCTEX* in *M. edulis*. The nucleotide and amino acid sequence of *TCTEX* covers 95 amino acids of the *M. californianus* EST. This gene has 40% similarity to TCTEX1-domain containing-1, which is 173 aa long.

APPENDIX C:
PRELIMINARY HYPOOSMOTIC STRESS EXPERIMENTS

We ran a series of preliminary experiments to get a better understanding of the dynamics of gene expression in *M. edulis* during low salinity exposure. The results from these studies were used to develop the experimental design of the larval and juvenile experiments used in this dissertation. Below is a description of the experiments as well as the findings from the gene expression and NMR studies.

C1. Preliminary Larval Experiments

Adult mussel broodstock were collected from subtidal populations at Squirrel Island, Boothbay Harbor, ME, and at the Darling Marine Center, Walpole, ME in May 2014. The mussels were exposed to a thermal shock protocol to induce spawning, as described elsewhere. We fertilized the eggs of 10 female mussels with the sperm of 4 males and combined the gametes into 20 l buckets containing UV-sterilized, filtered seawater (UV-FSW; 15 °C, 30 ppt). The embryos developed to the trochophores stage before being split into 5 batches of equal densities and transferred into 350 l tanks containing UV-FSW (14 °C, 30 ppt) supplemented with probiotic bacteria (Dr. Tim's Aquatics, LLC). Larvae were fed daily mixtures of live algae and water changes were conducted every other day by hatchery staff.

At 14 dpf, mussels had developed to the veliger stage. A subset of larvae was removed from each tank and combined into a 20-l bucket to remove any tank effects. Roughly 70,000 veligers from the pooled sample were transferred into 1 l beakers containing either control (32 ppt) or low-salinity (20 ppt) UV-FSW (14.5 °C) and held for

2, 4, 6, 8, 24, or 48 h (n = 5). Five control samples were collected at the time of treatment (0 h) to get baseline measurements prior to placement in the beakers. The veligers were sampled at the end of the treatment by sieving the contents of each beaker onto an 80 μm sieve. The larvae were transferred to a sterile, 1.5 ml Eppendorf tube, flash frozen in a methanol-dry ice bath, and stored at $-80\text{ }^{\circ}\text{C}$. Larvae were starved for 12 h prior to experimentation and not fed during treatment. This experiment was replicated at 21 dpf with pediveliger larvae.

These experiments lack biological replication because embryos were pooled prior to stocking the larval tanks and the subsets of veliger and pediveliger larvae were pooled prior to treatment. While samples contained a mixture of mussels from two populations and multiple individuals per sample, we cannot be confident that genetic differences were accounted for and therefore, results from these experiments should be interpreted with caution.

C2. Preliminary Juvenile Experiments

Juvenile *M. edulis* were collected from a subtidal population near the Darling Marine Center, Walpole, ME, in August 2014 and transferred to the University of Maine, Orono, ME. The mussels were acclimated in a recirculating system to $14\text{ }^{\circ}\text{C}$ and 32 ppt and were fed a daily ration of Shellfish Diet 1800. Following a 3-w acclimation, mussels were put into 1 l beakers containing a treatment (20 ppt) or control (32 ppt) salinity and held at $14\text{ }^{\circ}\text{C}$ for 0, 2, 4, 6, 8, 24, or 48 h. Upon completion of the treatment, mussels were sacrificed, the gills were dissected out and flash frozen in liquid N_2 . The tissue samples were stored at $-80\text{ }^{\circ}\text{C}$. As with the larval experiments, juvenile mussels were starved for 12 h prior to treatment.

C3. Gene Expression Studies

We used a subset of the veliger and pediveliger samples from May 2014 to monitored for expression of *TAUT*, *ICLN* (chloride nucleotide-sensitive channel 1A), *OAT*, *BHMT*, *CaM*, *CAML2*, and *ODC* using qPCR. For the gill tissue collected from the juvenile mussels in September 2014, we ran qPCR assays targeting *TAUT*, *OAT*, *ODC*, *CaM*, *CAML1*, *CAML2*, and *BHMT*. See Appendix B for information of marker development, sequence information, and a list of primers used in the qPCR assays. The description of the sample preparation and qPCR protocols are described in detail in Section 4.3.6. Prior to analysis, all plates were set to the same threshold value (250 RFUs) and any erroneous samples were eliminated. Expression was normalized to *40S* using the ΔC_t method and the effects of low salinity treatment on expression were tested using an independent samples Student's T Test in SPSS Statistical Software (IBM Corporation). A p value < 0.017 was considered significant to reflect repeated analysis of the same sample. The normalized expression for each gene is found in Figures C.1–C.8.

C4. Flux of FAA Pools

An additional subset of the larval samples was used to monitor changes in the FAA pools using ^1H NMR spectroscopy. The FAA extractions using acetonitrile and water, sample preparation, the specifications for the 1D NMR, and the data analysis are all described in the methods section of Chapter 3. We conducted limited statistical analysis which included running an independent samples Student's T Test in SPSS Statistical Software. We analyzed the change in FAAs in all the veliger samples (Table C.1) and analyzed the pediveliger samples from time 0, 2, 4, 6, and 8 h (Table C.2). In both cases, changes in glycine were significant in the stress larvae after 6 h of exposure.

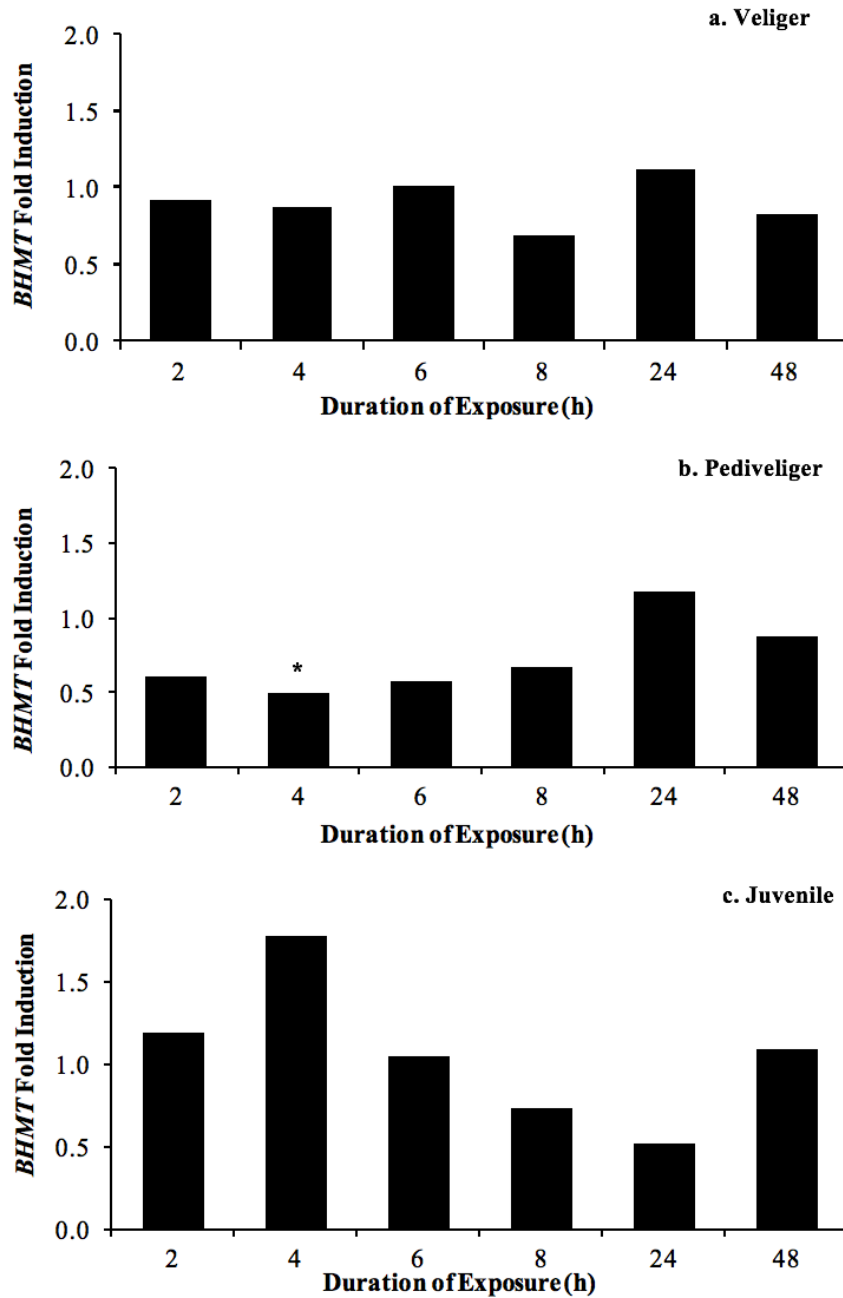


Figure C.1. Preliminary *BHMT* gene expression results. The regulation of *BHMT* expression varied at 2, 4, 6, 8, 24, and 48 h of exposure to a low salinity treatment relative to controls. There was a significant downregulation in expression in pediveligers at 4 h ($p < 0.01$, panel b), but no significant difference in expression for veligers (a) or in the gill tissue of juvenile *M. edulis* (c).

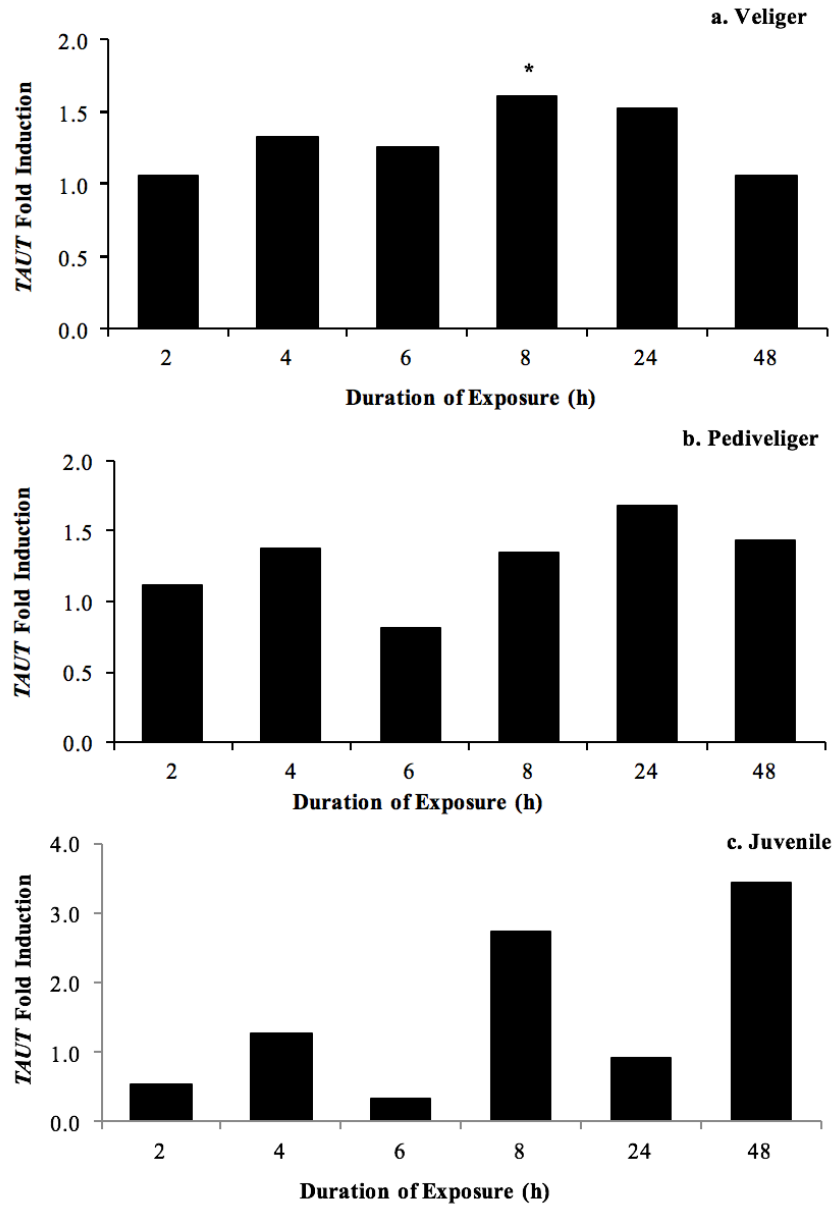


Figure C.2. Preliminary *TAUT* gene expression results. *TAUT* was significantly upregulated in veligers mussels exposed to low salinity for 8 h (a). There was a general trend toward an increase in expression during low salinity exposure in the pediveliger (b) and gill tissue of juveniles (c), although these changes in expression were not significant at $\alpha = 0.017$. Note variation in the scale for expression values between the larval and juvenile results.

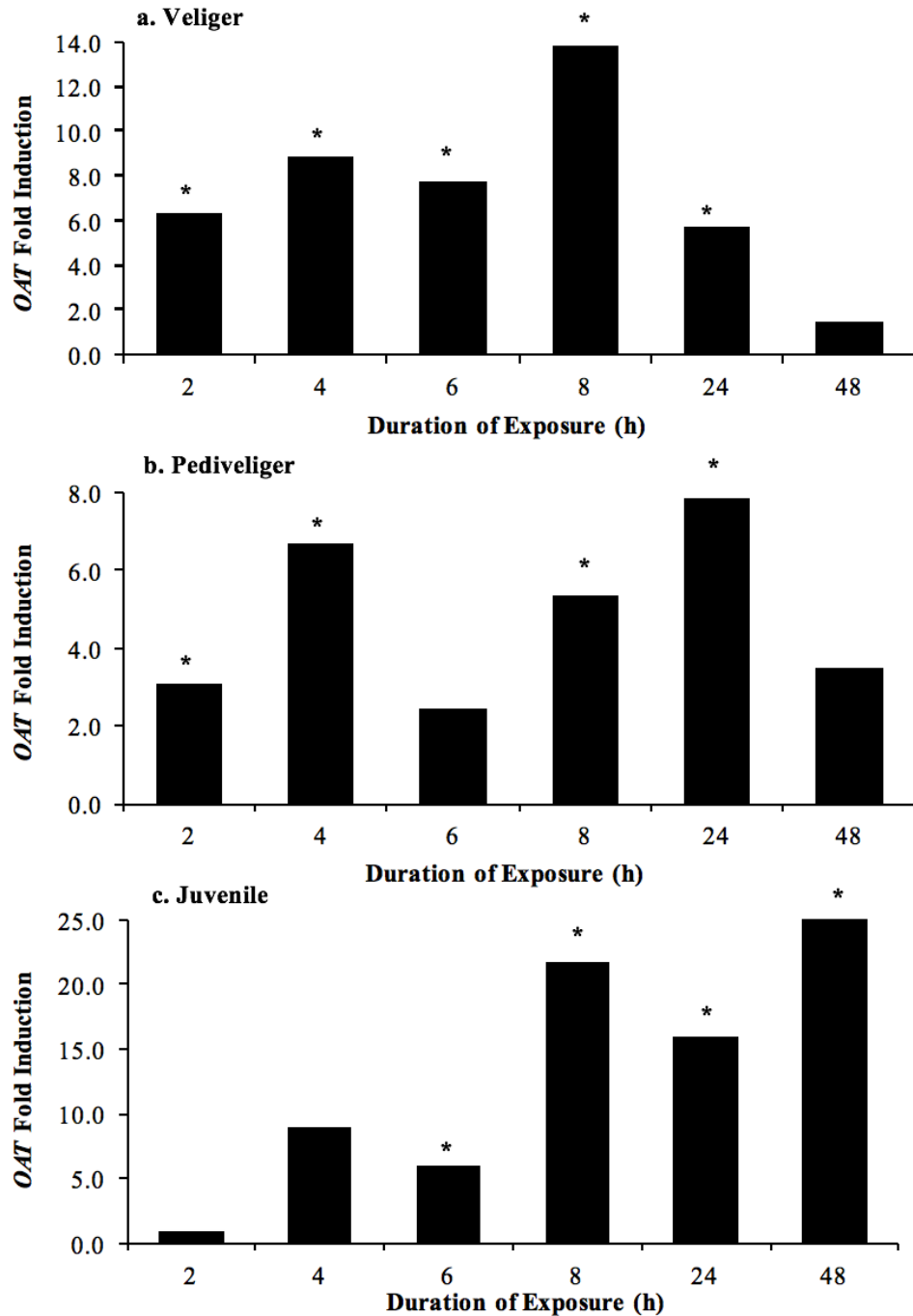


Figure C.3. Preliminary *OAT* gene expression results. *OAT* is upregulated in veliger (a), pediveliger (b), and in the gill tissue of juveniles (c) exposed to low salinity treatment. In the gill tissue of juveniles, the expression at 48 h was 76x higher in the treatment group relative to the controls, although the scale stops at 25. Asterisks indicate $p < 0.01$.

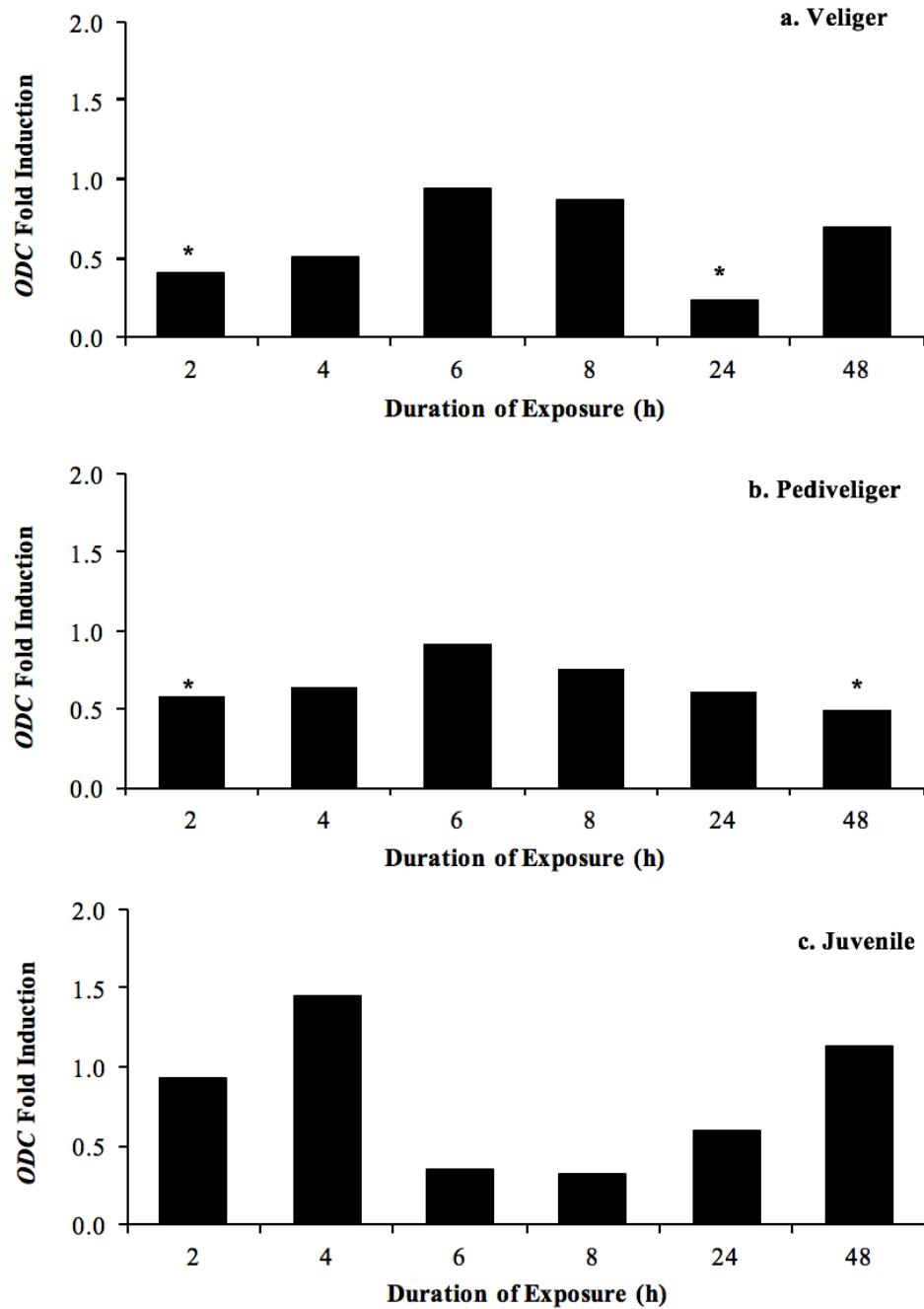


Figure C.4. Preliminary *ODC* gene expression results. Ornithine decarboxylase or *ODC* was significantly downregulated in veliger (a) and pediveliger (b) larvae exposed to low salinity. Low salinity exposure had no effect on *ODC* expression in the gill tissue of juvenile *M. edulis* (c). Asterisks indicate a p value < 0.01.

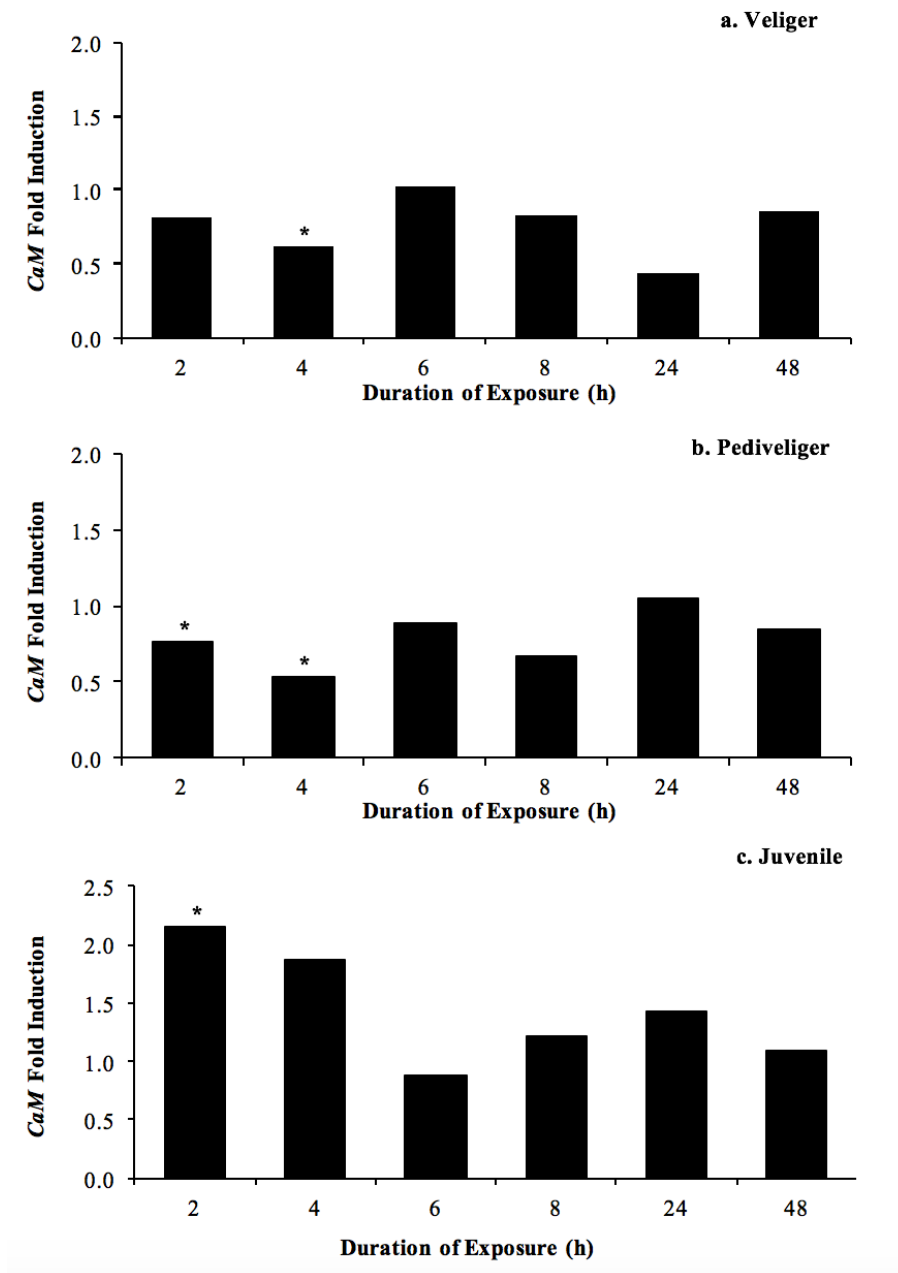


Figure C.5. Preliminary *CaM* gene expression results. Calmodulin (*CaM*) was differentially expressed after short-term exposure to low salinity stress in larval and juvenile mussels. The gene was significantly downregulated in veliger (a) and pediveliger (b) mussels, but was upregulated in the gill tissue of juvenile mussels (c) experiencing the same treatment. Asterisks indicate $p < 0.01$.

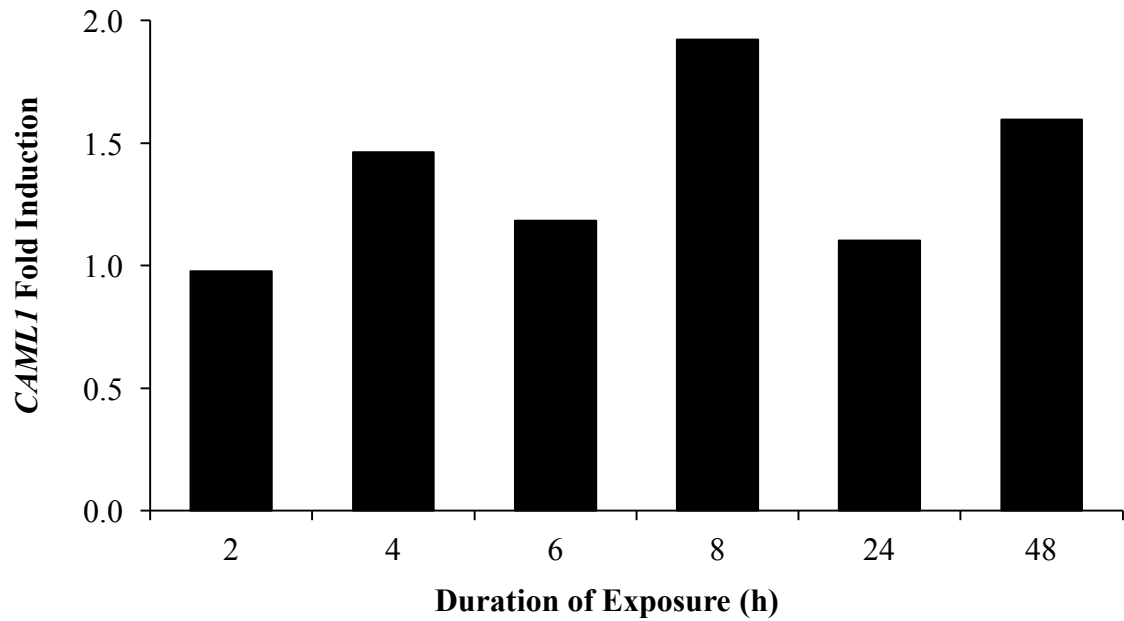


Figure C.6. Preliminary *CAMLI* gene expression in the gill of juvenile mussels. *CAMLI* tended to be upregulated during low salinity treatment, although these results were not statistically significant. This gene is not expressed in larval mussels.

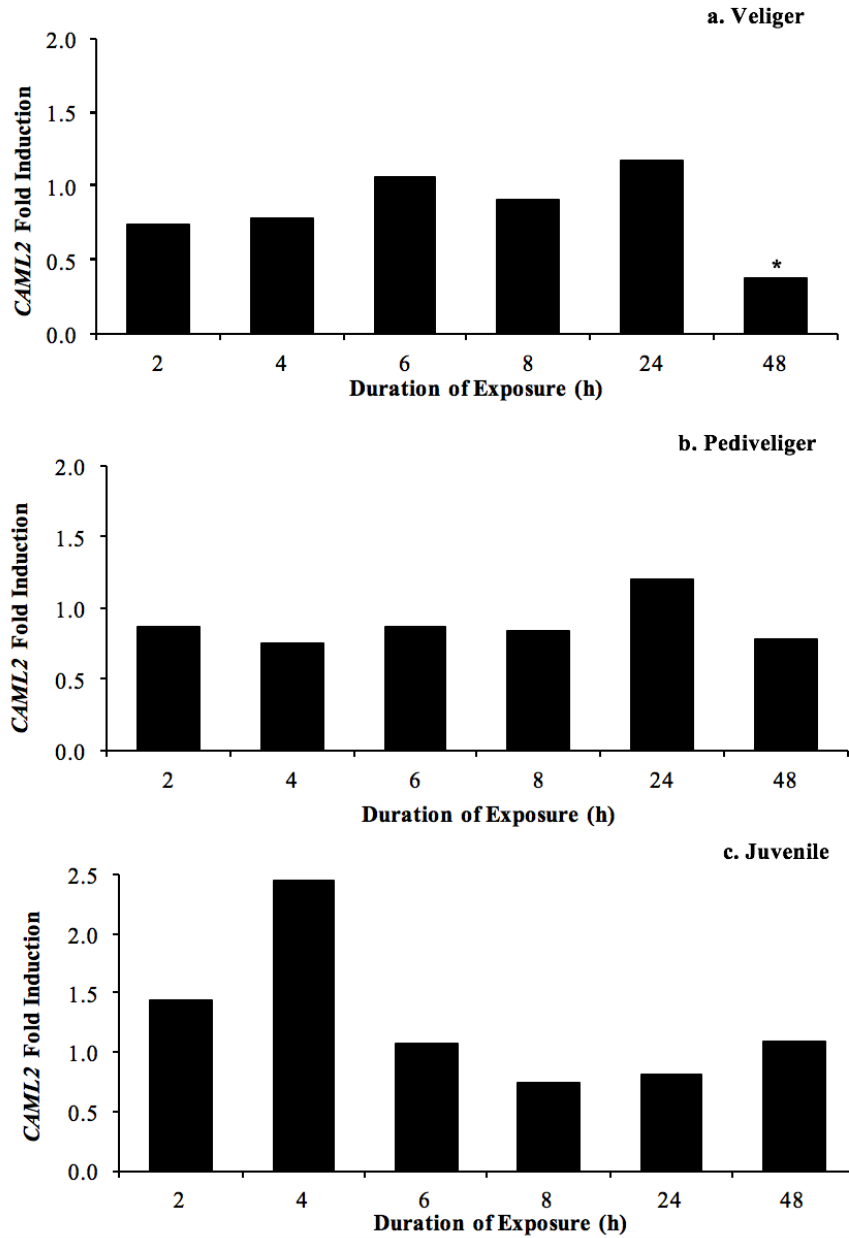


Figure C.7. Preliminary *CAML2* gene expression results. The expression of a calmodulin-like gene, *CAML2* was largely unaffected by low salinity treatment. The gene was often downregulated in veliger (a) and pediveliger (b) larvae and upregulated in the gill of juveniles (c) after short-term exposure. Its expression was significantly downregulated in veligers at 48 h, as indicated by the asterisk ($p < 0.01$).

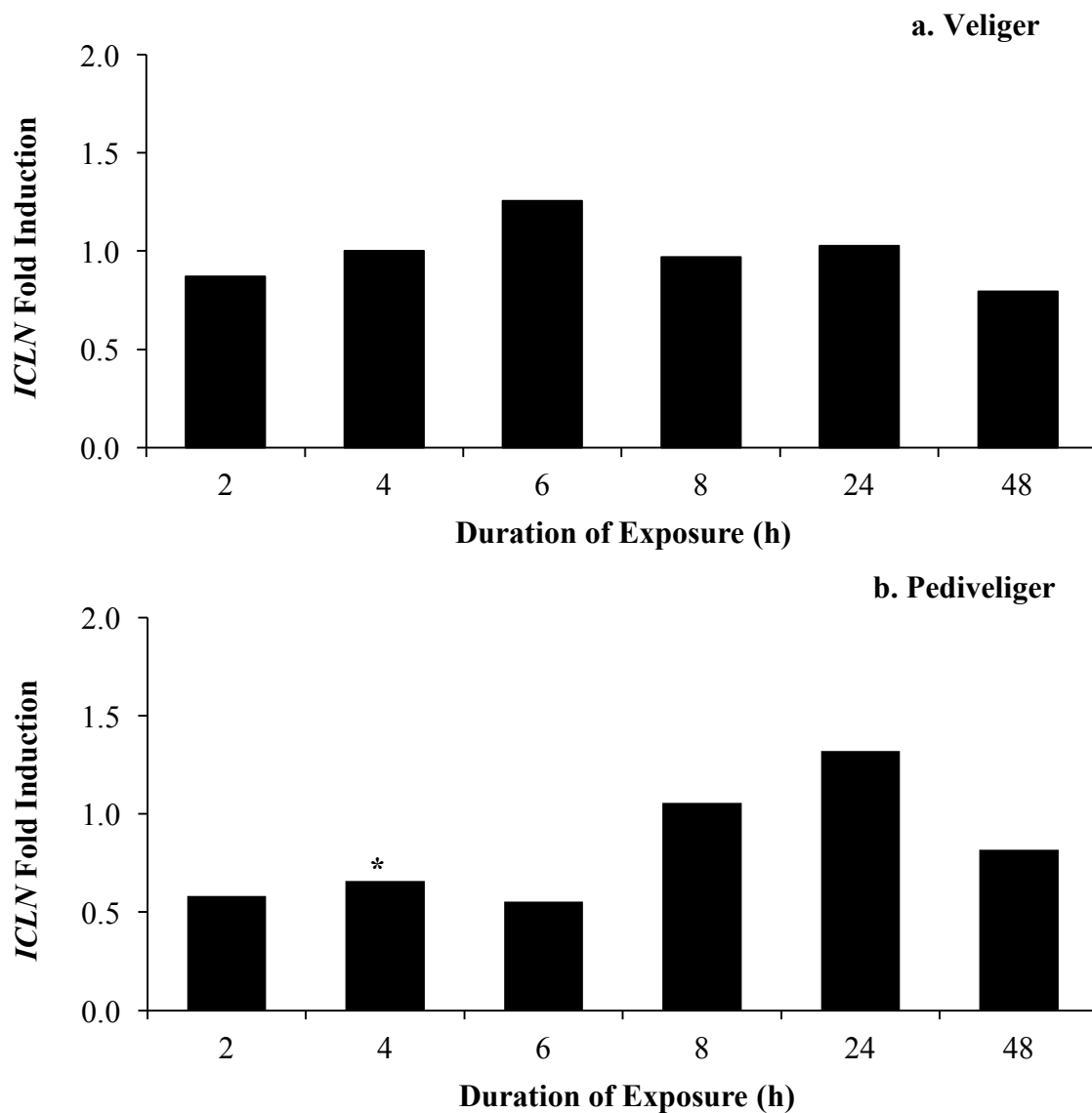


Figure C.8. Preliminary *ICLN* gene expression results. Expression of the chloride nucleotide-sensitive channel 1A gene, *ICLN*, is shown for veliger (a) and pediveliger (b) larvae. The expression in veligers was unaffected by treatment, while it was slightly downregulated after short-term exposure in pediveligers. The asterisk indicates $p < 0.01$. *ICLN* was amplified using the forward primer 5' GACGCATGGTTGTCAAAGAA 3' and 5' GCTCTGCCATGACACACAAC 3' as the reverse primer.

		Relative Concentration				
Exposure	Treatment	Taurine	Betaine	Glycine	Homarine	Alanine
2 h	30 ppt	331.6 ± 41.7	289.9 ± 36.0	227.6 ± 38.5	63.3 ± 9.4	22.1 ± 4.0
	20 ppt	386.3 ± 20.7	326.3 ± 21.3	296.6 ± 36.8	74.2 ± 3.5	17.0 ± 5.0
4 h	30 ppt	190.0 ± 11.0	159.7 ± 8.9	164.5 ± 13.3	35.5 ± 2.5	11.8 ± 1.6
	20 ppt	209.8 ± 41.3	171.4 ± 33.9	147.9 ± 17.3	36.0 ± 8.3	9.6 ± 2.7
6 h	30 ppt	270.2 ± 13.8	225.7 ± 14.6	232.9 ± 12.5	51.7 ± 4.3	17.5 ± 1.1
	20 ppt	220.2 ± 17.0	176.6 ± 12.9	144.2 ± 15.2	44.3 ± 4.0	9.4 ± 0.8
8 h	30 ppt	258.9 ± 12.0	225.8 ± 9.2	224.6 ± 12.3	52.0 ± 2.6	14.2 ± 0.7
	20 ppt	226.1 ± 10.9	219.7 ± 10.4	144.0 ± 5.9	53.7 ± 2.2	9.4 ± 2.0
24 h	30 ppt	219.0 ± 37.3	218.4 ± 26.9	218.1 ± 27.6	45.2 ± 9.2	5.1 ± 2.1
	20 ppt	283.1 ± 8.8	226.1 ± 8.2	115.0 ± 13.3	51.0 ± 4.2	7.1 ± 1.4
48 h	30 ppt	291.2 ± 35.1	245.9 ± 31.6	238.3 ± 21.8	53.7 ± 5.2	10.6 ± 3.2
	20 ppt	304.6 ± 15.0	250.7 ± 11.0	139.0 ± 8.1	54.8 ± 3.7	3.7 ± 2.3

Table C.1. Preliminary data on concentrations of FAAs in veliger mussels during low salinity treatment. The relative concentrations of taurine, betaine, glycine, alanine, and homarine ($\mu\text{mole}\cdot\text{g}^{-1}$ dry weight \pm SE) are reported for veliger *M. edulis* exposed to control (30 ppt) or low salinity treatment (20 ppt) for 2, 4, 6, 8, 24, and 48 h. The concentrations of glycine were significantly reduced in stressed animals after 6 h of exposure.

Exposure	Treatment	Relative Concentration				
		Taurine	Betaine	Glycine	Homarine	Alanine
2 h	30 ppt	369.1 ± 67.1	351.6 ± 60.3	280.9 ± 58.4	56.5 ± 8.6	19.0 ± 6.1
	20 ppt	579.5 ± 85.8	544.5 ± 75.8	459.3 ± 77.6	89.3 ± 10.4	49.2 ± 9.6
4 h	30 ppt	332.9 ± 68.3	268.9 ± 48.9	240.1 ± 46.3	50.7 ± 9.8	34.7 ± 20.3
	20 ppt	287.1 ± 8.6	251.7 ± 6.2	192.6 ± 3.9	42.0 ± 3.0	13.0 ± 2.4
6 h	30 ppt	321.0 ± 30.9	284.3 ± 27.7	252.6 ± 23.0	44.1 ± 3.6	13.6 ± 2.6
	20 ppt	289.4 ± 10.1	252.8 ± 7.5	181.3 ± 6.7	44.2 ± 2.7	11.2 ± 1.1
8 h	30 ppt	274.1 ± 20.5	243.5 ± 22.0	215.0 ± 16.6	41.5 ± 2.5	12.2 ± 3.5
	20 ppt	332.8 ± 6.5	289.6 ± 6.8	196.7 ± 12.4	53.8 ± 2.3	15.4 ± 3.4

Table C.2. Preliminary data on concentrations of FAAs in pediveliger mussels during low salinity treatment. The relative concentrations of taurine, betaine, glycine, alanine, and homarine ($\mu\text{mole}\cdot\text{g}^{-1}$ dry weight \pm SE) are reported for pediveliger *M. edulis* exposed to control (30 ppt) or low salinity treatment (20 ppt) for 2, 4, 6, and 8 h. The concentrations of glycine were significantly reduced in stressed animals after 6 h of exposure.

BIOGRAPHY OF THE AUTHOR

Melissa Anne May was born and raised in Glendale, AZ, where she first gained an appreciation for marine science. Melissa attended high school at Xavier College Preparatory in Phoenix, AZ, and went on to complete a Bachelor of Science in Zoology from Northern Arizona University in Flagstaff, AZ, in 2004. Melissa moved to San Diego, CA, after finishing her Bachelor's degree and earned her Master of Science in Marine Science from the University of San Diego in 2008, where she studied energetics of gray whale migrations. Melissa then relocated to Berkeley, CA, and worked as a Lab Coordinator and Part-time Instructor of Oceanography at Diablo Valley College. As an avid learner, Melissa decided to continue her graduate education and was accepted into the doctoral program in the School of Marine Sciences at the University of Maine, where she has studied since 2011. At the University of Maine, Melissa has been actively involved in university service as a member of SMS Social Committee, the Marine Science Professional Development Club, the Graduate Symposium Planning Committee, and the Marine Science Education Outreach Club. In her spare time, Melissa founded the University of Maine's Water Polo Club and has served as president and coach of the club since its formation in 2015. She is also a member of the Society of Integrative and Comparative Biology, the American Microscopical Society, and the American Physiological Society. Melissa will begin a postdoctoral research fellowship at California Polytechnic State University in June 2017. She is a candidate for the Doctor of Philosophy degree in Marine Biology from the University of Maine in May 2017.